Universidade de Aveiro Departamento de Engenharia Cerâmica e do Vidro
2009

Sandra Cristina de Almeida Pina

CIMENTOS DE FOSFATOS DE CÁLCIO DOPADOS PARA IMPLANTOLOGIA ÓSSEA

CEMENTS OF DOPED CALCIUM PHOSPHATES FOR BONE IMPLANTATION

Universidade de Aveiro Departamento de Engenharia Cerâmica e do Vidro
2009

Sandra Cristina de Almeida Pina

CIMENTOS DE FOSFATOS DE CÁLCIO DOPADOS PARA IMPLANTOLOGIA ÓSSEA

CEMENTS OF DOPED CALCIUM PHOSPHATES FOR BONE IMPLANTATION

Tese apresentada à Universidade de Aveiro para cumprimento dos requisitos necessários à obtenção do grau de Doutor em Ciência e Engenharia de Materiais, realizada sob a orientação científica do Doutor José Maria da Fonte Ferreira, Professor Associado com Agregação, do Departamento de Engenharia Cerâmica e do Vidro da Universidade de Aveiro.

Apoio financeiro do POCTI no âmbito do III Quadro Comunitário de Apoio.

Apoio financeiro da FCT e do FSE no âmbito do III Quadro Comunitário de Apoio.

… Aos meus pais

... Ao Betinho

o júri

presidente

Prof. Doutor Eduardo Anselmo Ferreira da Silva
professor catedrático do Departamento de Geociências da Universidade de Aveiro

Prof. Doutor Marc Bohner
professor associado do Department for Material Sciences do Federal Institute of Technology (ETH) em Lausanne, Suíça

Prof. Doutora Maria Helena Gil
professora catedrática no Departamento de Engenharia Química da Faculdade de Ciências e Tecnologia da Universidade de Coimbra

Prof. Doutora Elisabete Costa
professora auxiliar do Departamento de Engenharia Cerâmica e do Vidro da Universidade de Aveiro

Prof. Doutor Anthony W. Miles
professor catedrático do Centre for Orthopeadic Biomechanics do Departamento de Mecânica da Universidade de Bath, Inglaterra

Prof. Doutora Friedlinde Goetz-Neunheufer
professora associada do Instituto de Mineralogia, GeoZentrum Nordbayern, da Universidade de Erlangen-Nuremberg, Alemanha

Prof. Doutor José Maria da Fonte Ferreira
professor associado com agregação do Departamento de Engenharia Cerâmica e do Vidro da Universidade de Aveiro

acknowledgements

I would like to sincerely express thanks to the various people who provided me with useful and helpful assistance. Without their knowledge, care and consideration, this work would likely not have matured.

Financial support of the Portuguese Foundation for Science and Technology for the fellowship grant SFRH/BD/21761/2005 is gratefully acknowledged.

I am deeply indebted to Prof. Doutor José Maria Ferreira, my supervisor, for all his support, interest, advices and encouragement. His contributions, detailed comments and insight have been of great value to me.

To my co-supervisor Prof. Tony Miles, and Dr Sabina Gheduzzi, my honest appreciation for introducing me to injectable bone substitutes field, and for their kind assistance from the very beginning.

I am also grateful to Prof. Friedlinde Goetz-Neunhoeffer, my co-supervisor, and Prof. Neubauer, for giving me the opportunity to make part of this work in their group and for sharing their knowledge in Rietveld analysis with me.

Appreciation also goes to Dr Kannan, whose expertise and knowledge added considerably to my experience.

I wish also to thank to the group of Mineralogy from Erlangen, Germany, especially Sebastian Seufert, Christoffer Stabler and Daniel Jansen, for their warm welcome on my two visits, for always helping me with technical assistance, for the funny trips on the mountains, and good dinner moments.

Dr Paulo Rego, our personal orthopaedist, my sincere gratitude for his interest and willingness with animal experiments, and help with surgeries.

To the group of Medicina e Cirurgia Experimental from Lisbon, many thanks for their technical assistance with the animal surgeries and for great laughs.

Thanks a lot to Sandra Vieira for the attractive moments with cell experiments and for her permanent enthusiasm and good mood.

To my friends and colleagues Paula, Susana, Catarina, Ermelinda, Ashu and Bala, my genuine recognition for the friendship, encouragement and really good moments of laugh.

To Rui and Sandra Cachinho, for the never-ending support, words of advice and for always being there for me, my huge and truthful friendship.

Finally, I express many thanks and affection to my parents and brother for their continuously love, care and tolerance.

palavras-chave

cimentos de fosfatos de cálcio, iões substituídos, presa, injectabilidade, regeneração óssea, osteocondutividade, bioresorbabilidade

resumo

O principal objectivo deste estudo foi o desenvolvimento de cimentos à base de fosfatos de cálcio dopados com Mg, Sr e Zn, para aplicações clínicas.

A síntese dos pós foi obtida através de reacções de precipitação, seguido de tratamento térmico de forma a obter as fases mais apropriadas, α e β-TCP. A caracterização dos pós envolveu a quantificação de fases e o refinamento estrutural de fases através da análise de difracção de raios-X por refinamento de Rietveld, bem como, análise da área superficial por BET, e respectivos tamanhos de partícula.

Os cimentos foram preparados através da mistura dos pós com meios líquidos diferentes, usando ácido cítrico como acelerador de presa, e o polietilenoglicol (PEG) e o hidroxil propilmetilcelulose (HMPC) como agentes gelificantes. A formação da brushite foi um dos produtos resultantes obtidos da hidratação dos cimentos. Do ponto de vista de aplicação clínica, os cimentos foram caracterizados em termos de presa, injectabilidade, análise calorimétrica e resistência mecânica.

Os presentes resultados demonstraram que a incorporação de iões nos cimentos levou a uma melhoria significativa das propriedades destes quando comparados com TCP puro. Os resultados obtidos demonstraram ainda que o tempo inicial de presa tende a decrescer na presença de modificadores reológicos, uma vez que estes aumentam a viscosidade das pastas, e aumenta com o acréscimo da razão L/P, tendo sido considerada a gama de 0.30-0.34 mL g^{-1} como aceitável para manusear as pastas. As pastas cimentícias apresentaram uma boa injectabilidade, nomeadamente o seu comportamento após extrusão, com aplicação de uma força máxima de 100 N. Investigou-se ainda, com estes testes, a ausência do efeito de "filter-pressing" e que as pastas foram totalmente expelidas para uma razão L/P de 0.36 mLg^{-1}.

Os testes de calorimetria isotérmica demonstraram que as pastas apresentam reacções exotérmicas, referentes à dissolução dos pós de partida e à formação de fases intermédias; e à nucleação e crescimento da brushite.

Resistências à compressão dos cimentos estudados, após imersão numa solução de PBS durante 48h situam-se entre 1-30 MPa, valores reportados para o osso trabecular.

Testes de citotoxicidade, bioactividade e biocompatibilidade dos cimentos foram obtidos através de testes de culturas celulares, mostrando a não-toxicidade destes. A biocompatibilidade *in vivo* e a reabsorção dos cimentos foram avaliadas em estudos histológicos e histomorfométricos de secções descalcificadas obtidas através de ensaios de experimentação animal, usando o porco como modelo. Os resultados mostraram que os cimentos implantados são biocompatíveis e osteocondutivos, sem evidência de reacções infecciosas, e portanto, bons candidatos para aplicação como substitutos ósseos.

keywords calcium phosphates cements, ions substituted, self-setting, injectability, bone regeneration, osteoconductivity, bioresorbability

abstract

The main objective of this study was the development of cements based on calcium phosphates doped with Mg, Sr and Zn, for clinical applications.

Powder synthesis was obtained through precipitation reactions, followed by heat treatment in order to obtain appropriate phases, $\tilde{\alpha}$ and β-TCP.

The cements were prepared through mixing the powders with different liquids, using citric acid as setting accelerator, and polyethyleneglycol and hydroxyl propylmethylcellulose as gelling agents. Brushite was the end product of the hydration reaction. Injectability and setting behaviour were accessed through rheological measurements, extrusion, calorimetric analysis, Vicat and Gilmore needles. Phase quantification and the structural refinement of powders and cements were determined through X-ray diffraction with Rietveld refinement, as well as, BET specific surface area and particle size analysis. Mechanical strengths of wet hardened cements were evaluated.

The results obtained showed that the incorporation of ions into cements led to a significant improvement of their overall properties. Initial setting time increased in the presence of rheological modifiers due to their specific roles at the solid/liquid interface and with increasing L/P ratio. Acceptable workability pastes were obtained for L/P ratios in the range of 0.30-0.34 mL g^{-1}. The cement pastes presented good injectability even under a maximum applied force of 100 N. Filter pressing effects were absent, and all cement pastes could be fully injected for LPR > 0.36 mL g^{-1}.

Isothermal calorimetry revealed that hydration reactions produce exothermic effects due to: (i) dissolution of the starting powders and formation of intermediate phases; and (ii) nucleation and growth of brushite crystals. The intensity of the exothermic effects depended on doping element, being stronger in the case of Sr.

Wet compressive strength of the cement specimens (after immersion in PBS solution for 48 h) was in the range of values reported for trabecular bone (10-30 MPa).

Cell cultures used to evaluate citotoxicity, bioactivity and biocompatibility of cements revealed no toxic effects. The biocompatibility *in vivo* and cements resorption were evaluated using a pig model through histological and histomorphometric studies of decalcified sections. The results show that the implanted cements are biocompatible and osteoconductive, without foreign body reaction. These properties make them good candidates for applications as bone substitutes.

PREFACE

During the last century, new materials and surgical techniques have drastically changed the lives of millions of patients. Biomaterials have made an important contribution to modern health care and will expand further as musculoskeletal disorders, especially osteoporosis and fragility fractures, increase with an aging population. Each biomaterial considered for potential clinical applications has specific chemical, physical and mechanical properties, which might originate variations in host/material response. However, the biological characteristics and the anatomic site of implantation are also important for the behaviour and outcome of the implant. In surgery for fragility fractures, biomaterials are still sparsely used for bone repair. In about 10% of all reconstructive operations caused by traumatic, resectional or congenital defects, bone transplants and bone substitute materials are necessary.

The discovery in early 1980s of self-setting cements based on calcium orthophosphate (often referred to just as calcium phosphate) has opened up a new era in the medical applications of bone grafting. Synthetic bone substitutes made of calcium phosphates have chemical compositions similar to those of bone and dentine and can be fitted with bone defects. They are also particularly suited for minimally invasive surgical techniques, hardening in situ and giving stability for any defect geometry. Calcium phosphate cements (CPC) are resorbable, biocompatible and osteoconductive.
Nevertheless, the commercially available formulations still suffer from several shortcomings related to unsatisfactory levels of some properties and justify the continuous research effort that has been devoted to synthetic bone substitutes as cements.

The purpose of the present work was developing cements based on calcium phosphate, doped with several ions, to be used with minimally invasive surgical techniques with mechanical properties comparable to trabecular bone, which will

encourage new bone to grow in and remodel the bone defect. The incorporation of trace amounts of different ions on bone substitute materials is expected to have favourable effects related to the biological process, due to their occurrence in bone tissues.

This thesis is structured in four chapters. Chapter 1 is a broad literature review that ranges from bone composition and structure with particular reference to bone remodelling process, to calcium phosphate-based cements. Chapters 2 and 3 describe the preparation and characterisation of the starting calcium phosphate cement (CPC) powders doped with different ions - Mg, Zn or Sr - as well as the preparation and properties evaluation of the hardened CPC cements. Characterization was performed in terms of setting behaviour, injectability, mechanical testing and biocompatibility through *in vitro* and *in vivo* tests. In these chapters, published, accepted or submitted papers to SCI journals are presented reporting the studies that have been performed. Chapter 2 describes the CPCs doped with Mg or Sr. The evaluation of biocompatibility, resorption and new bone formation of Sr- and Zn-incorporated CPCs is presented in Chapter 3.
Finally, Chapter 4 shows the overall conclusions and some suggestions for future work.

Index

1 State of the art

1.1 Introduction

The human skeletal system is composed of various connective tissues (bone, cartilage, ligaments and tendons) with its major role providing dynamic forces to be distributed by muscle mass, as well as providing support and protection for tissues. Bone is among the body's hardest structures; only dentin and enamel in the teeth are harder. It is one of the most dynamic and metabolically active tissues in the body and remains active throughout life. A highly vascular tissue, it has an excellent capacity for self-repair and can alter its properties and configuration in response to changes in mechanical demand. For example, changes in bone density are commonly observed after periods of disuse and of greatly increased use and changes in bone shape are noted during fracture healing and after certain operations.

Many diseases and disorders have been associated with osteoporosis. For some, the underlying mechanism influencing the bone metabolism is straight-forward, whereas for others the causes are multiple or unknown. Osteoporosis is a disease of bone that leads to an increased risk of fracture. In osteoporosis the bone

mineral density is reduced, bone microarchitecture is disrupted, and the amount and variety of non-collagenous proteins in bone is altered.

Osteoporosis can be prevented with lifestyle changes and sometimes medication. Lifestyle change includes exercise and preventing falls, while medication includes calcium, vitamin D, bisphosphonates and several others. The underlying mechanism in all cases of osteoporosis is an imbalance between bone resorption and bone formation. In normal bone, there is a constant matrix remodelling of bone; up to 10% of all bone mass may be undergoing remodelling at any point in time.

In order to understand what sort of bone substitutes could be best for reconstruct large defects of normal bone, it is important first to understand the complex structure of bone and the process of bone healing. Furthermore, the best bone substitutes are naturally those with biomechanical and biological properties most closely resembling those of normal bone.

1.2 Bone anatomy

Bone is a complex, highly organised and specialised connective tissue with many functions. All bones have a mechanical function providing attachment to various muscle groups. In addition, in some parts of the body, bones provide a protective function to vital structures — skull (brain), ribs (lungs, heart) and pelvis (bladder, pelvic viscera). Some bones retain their haematopoietic function in adults — vertebrae, iliac crests, proximal parts of femur and humerus. All bones serve as a reservoir of calcium and actively participate in calcium homeostasis of the body.

1.2.1 Macrostructure of bone

The bone is composed of two types of osseous tissue: cortical (compact) (80%) and trabecular (cancellous or spongy) (20%) bones [1]. Cortical bone forms the outer shell, or cortex, of the bone and has a dense structure. It is the primary

component of the long bones of the arm and leg and other bones, where its greater strength and rigidity are needed. Trabecular bone typically occupies the interior region of bones and is composed of thin plates, or trabeculae, in a loose mesh structure. It is highly vascular and frequently contains red bone marrow where hematopoiesis, which is the production of blood cells, occurs. It has a higher surface area but is less dense, softer, weaker, and less stiff than cortical bone.

Bone can be classified as long (femur, tibia, humerus, radius), short (carpal, tarsal), flat (ribs, sternum, cranium, scapula) and irregular (vertebra). For example, it can be seen in Fig. 1.1 a schema of a long bone. It can be divided into three physiological regions, namely the epiphysis, the metaphysis and the diaphysis. The epiphysis is the rounded end of the bone. The metaphysis is the part adjacent to the epiphysis in the adult (the growth plate or physis being closed) and the diaphysis is the cylindrical shaft of the bone. Trabecular bone is found mainly in the metaphysis, while cortical bone includes the diaphysis. In the vertebral column, trabecular bone is the main constituent.

The surfaces of bone are covered by the periosteum and the endosteum as connective tissues. The periosteum covers the outer surface of bone, except the joins which are protected by articular catilage, whereas the endosteum lines the surface of the medullary cavity of long bones. The periosteum consists of an outer fibrous layer consisting of collagen fibres and fibroblasts and an inner cambium layer composed of flattened cells — the osteoprogenitor cells with the capacity to divide by mitosis and to differentiate into osteoblasts. The endosteum is composed of osteoprogenitor cells and a very small amount of connective tissue. The surfaces, periosteum and endosteum provide a continuous supply of osteoprogenitor cells or new osteoblasts for repair or growth of bone.

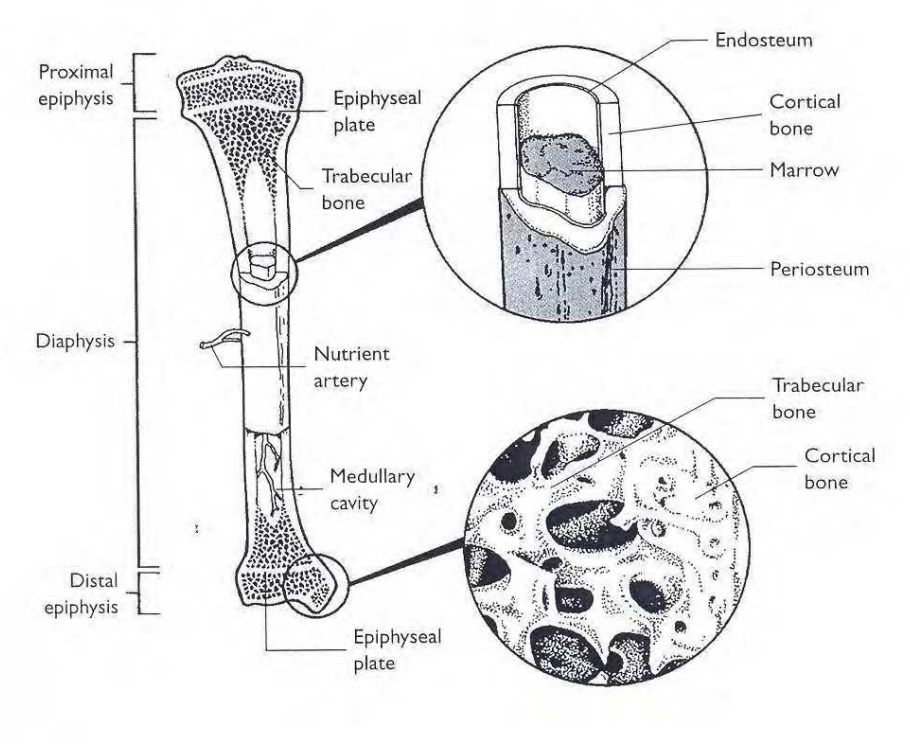

Fig. 1.1: Schema of a long bone, showing the structures of cortical and trabecular bone (adapted from [2]).

1.2.2 Microstructure of bone

1.2.2.1 Cellular components

Bone tissue is constituted by four characteristic cell types: osteoblasts, osteocytes, osteoclasts, and undifferentiated bone mesenchymal stem cells.

Osteoblasts are mononucleate bone-forming cells responsible for the synthesis and deposition on bone surfaces of the protein matrix of new intercellular material. They are located on the surface of osteoid seams and make a protein mixture known as osteoid, which mineralizes to become bone. Osteoblasts robustly produce alkaline phosphatase, an enzyme that has a role in the mineralisation of bone, as well as many matrix proteins.

Osteocytes originate from osteoblasts that have migrated into and become trapped and surrounded by bone matrix that they themselves produce and they occupy the lacunae. Osteocytes communicate with other osteocytes, as well as

with free bone surfaces by means of extensive filamentous protoplasmic extensions that occupy the canaliculi through the bone substance. Their functions include the formation of bone, matrix maintenance and calcium homeostasis. They have also been shown to act as mechano-sensory receptors—regulating the bone's response to stress and mechanical load.

Osteoclasts are large multinucleated cells responsible for bone resorption (remodelling of bone to reduce its volume) by direct chemical and enzymatic attack. Because the osteoclasts are derived from a monocyte stem-cell lineage, they are equipped with phagocytic like mechanisms similar to circulating macrophages. Osteoclasts mature and/or migrate to discrete bone surfaces. Upon arrival, active enzymes, such as tartrate resistant acid phosphatase, are secreted against the mineral substrate.

Undifferentiated mesenchymal stem cells of the bone reside in the loose connective tissue between trabeculae, along vascular channels, and in the condensed fibrous tissue covering the outside of the bone (periosteum); they give rise under appropriate stimuli to osteoblasts.

1.2.2.2 Molecular structure

On a molecular level, bone is composed of bone matrix and woven or lamellar bones. The bone matrix is where the cells are placed, representing the majority of bone. It is composed of inorganic and organic matter. The inorganic or mineral portion, which account for almost 70 wt.% of compact bone, consists mainly of small crystals of hydroxyapatite (HA, $Ca_{10}(PO_4)_6(OH)_2$) and some amorphous calcium phosphate compounds [3]. The organic phase consists of Type-I collagen fibres (approximately 95%) embedded in the ground substance containing proteoglycans and glycoproteins (5%). This organic matrix, calcified by calcium phosphate minerals, embeds bone cells, which participate in the maintenance and organization of bone. The inorganic component of bone makes the tissue hard and rigid, while the organic component gives bone its flexibility and resilience.

Depending on how the protein fibrils and osteocytes of bone are arranged, bone consists of woven or lamellar bone (Fig. 2). Woven bone, also known as ‘coarse fibred’, is considered immature bone and is characterised by the presence of randomly oriented coarse collagen fibres. It is found in the embryo, in the fracture callus and in the metaphysical region of growing bone, as well as in tumours, osteogenesis imperfecta and pagetic bone. It is also the first tissue to appear in the repair of bone (fracture healing). Lamellar is a more mature bone, since it begins to form one month after birth and actively replaces woven bone. It is characterised by the presence of collagen fibres arranged in parallel layers or sheets (lamellae).

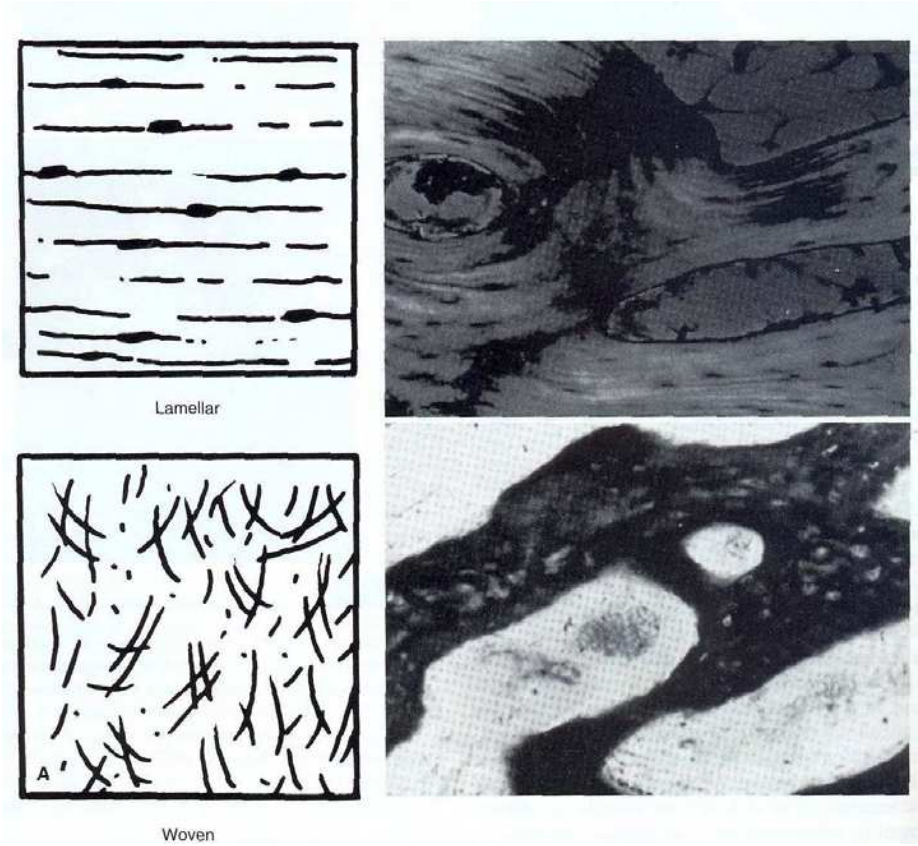

Fig. 1.2: Schematic drawing and micrographs of lamellar and woven bone (adapted from [4]).

1.2.3 Osteoconduction and bone formation

Osteoconduction is paramount to osteogenesis during the normal bone remodelling processes and is composed of three main processes: (i) migration of bone progenitor cells through a transient matrix, (ii) differentiation of the bone progenitor cells, and (iii) recruitment of functional differentiated cells to initiate the formation of new bone [5].

Osteogenesis is a result of osteoconduction and bone formation, and occurs when the first layer of bone is directly secreted onto the implant's surface [6]. During osteoconduction, pre-osteogenic cells are stimulated to migrate through a provisional matrix, which could be represented by bone grafts, implants, or a blood clot. The migrating cells then start a differentiation process that results in the secretion of the new bone matrix.

During the bone formation, differentiating osteogenic cells first secrete globular accretions of a matrix devoid of collagen called cement line. These afibrillar layers are found at the interface of secondary osteons with the surrounding tissue and may also be seen at the bone-implant interface [7]. This first layer provides nucleation sites for calcium phosphate nano-crystals, which nucleate and grow within the organic matrix. After the deposition of the cement line matrix, the osteogenic cells differentiate into osteoblasts, which elaborate the collagenous extracellular matrix assembled as fibers. Finally, the collagenous fibers undergo calcification and are separated from the underlying substratum by a calcified non-collagenous matrix [8, 9].

1.2.4 Bone remodelling

Bone has the ability to remodel, by altering its size, shape and structure to meet the mechanical demands placed on it. Bone remodelling is a dynamic, lifelong process in which old bone is removed from the skeleton and new bone is added. It consists of two distinct stages – resorption and formation – that involve the activity of special cells, as osteoclasts and osteoblasts [7]. Usually, the removal and

formation of bone are in balance and maintain skeletal strength and integrity. Fig. 3 sketches the bone remodelling process.

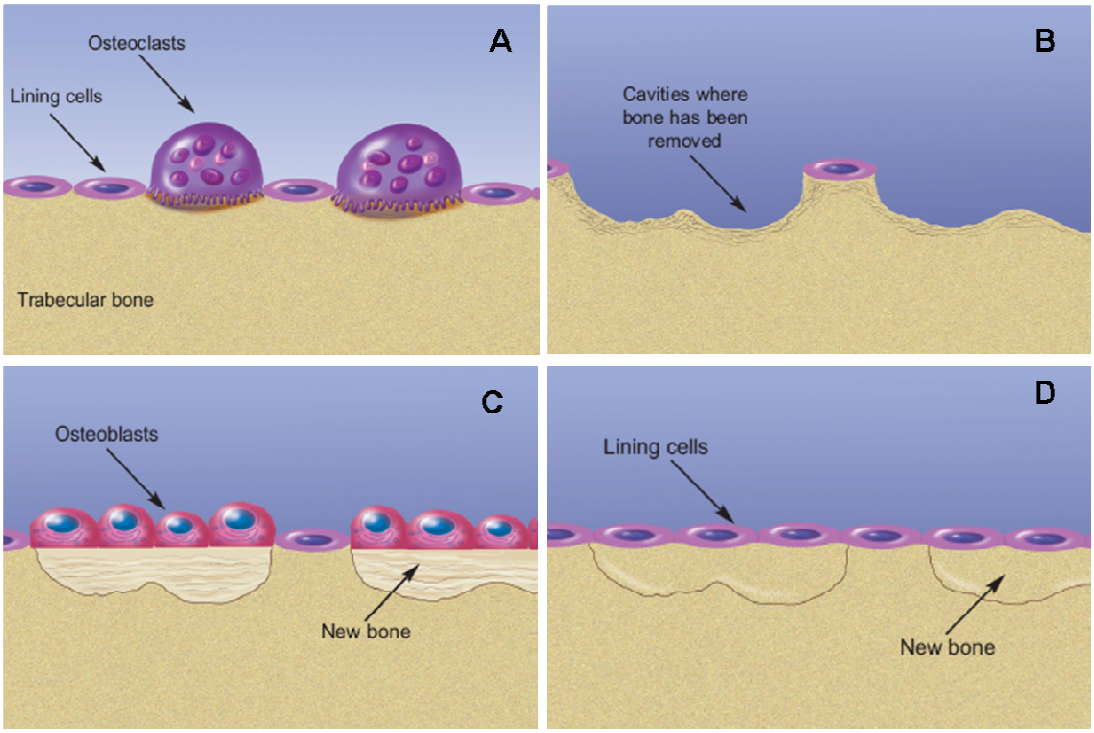

Fig. 1.3: Bone remodelling process: bone resorption (A), bone resorption complete (B), bone formation (C) and completion (D) (adapted from [4]).

Osteoclasts act on the trabecular bone surface to erode the mineral and matrix and small cavities where bone has been removed are created (Fig. 3 A and B). Osteoblasts work to repair the surface and fill the eroded cavities with new bone that then has to be mineralized (calcified) (Fig. 3 C). The bone surface is restored and covered by a layer of protective bone cells called lining cells (Fig. 3 D). The new bone is calcified and the remodelling process is completed.

During the remodelling stages, several cytokines, growth factors (IGFs, TGF-b1, FGF, BMP, EGF, PDGF, etc.) and hormones (PTH) participate in cell proliferation at remodelling sites [10].

1.3 Calcium phosphate-base bone substitutes

Bone substitutes should have a good local and systemic compatibility, the capability of being substituted by bone and of completely filling any defect. These features require osteoconductive and/or osteoinductive properties of the implant comparable to those of the natural bone.

Currently available bone substitutes show a variety of compositions and properties. Among them, compounds made of inorganic calcium phosphates (CaP) are frequently used. They are non toxic and do not cause cell death at the surrounding tissue. Biological response to these materials follows a similar cascade observed in fracture healing. This cascade includes hematoma formation, inflammation, neovascularisation, osteoclastic resorption, and new bone formation. They undergo processes of dissolution and precipitation resulting in a strong material-bone interface [11-13].

The first clinical attempt to use CaP compounds was reported by Albee in 1920, in the repair of a bony defect [14]. Only 30 years later, a second clinical report was published [15]. Levitt et al. [16] and Monroe et al. [17] suggested CaP ceramic material for bone and tooth implants. Between 1976 and 1986, serious efforts were made toward development and commercialization of CaP as biomaterials for bone repair, substitution and augmentation [18-21]. Later, tricalcium phosphate (TCP) was used to repair surgically-created infrabony defects in dogs [22] and for alveolar ridge augmentation [23], and dense hydroxyapatite (HA) cylinders were used as dental root implants after tooth extraction [24, 25].

In the past two decades, CaP biomaterials have gained acceptance in dental and orthopaedic applications, such as, repair of bone defects, tooth root replacements, ear implants, spine fusion, and coatings on orthopaedic and dental implants [18, 23, 25-28].

1.3.1 Calcium phosphates

Calcium phosphates (CaPs) are found widely in the earth crust and are characterized as white solids unless doped or containing elements that pass in the lattice structure of the respective compound. CaPs are the chemical compounds of special interest for human beings due to their similarity with the inorganic part of major normal (bones, teeth and antlers) and pathological calcified tissues of mammals [29-31]. CaPs possess remarkable biocompatibility, osteoconductivity and bioresorbability. The most relevant CaPs are presented in Table 1.1.

Table 1.1: Relevant calcium phosphates [31]

Calcium phosphate	Formula	Ca/P
Monocalcium phosphate monohydrate (MCPM)	$Ca(H_2PO_4)_2.H_2O$	0.5
Monocalcium phosphate anhydrous (MCPA)	$Ca(H_2PO_4)_2$	0.5
Dicalcium phosphate dihydrate (DCPD)	$Ca(HPO_4).2H_2O$	1.0
Dicalcium phosphate anhydrous (DCPA)	$Ca(HPO_4)$	1.0
Octacalcium phosphate (OCP)	$Ca_8(HPO_4)_2(PO_4)_4.5H_2O$	1.33
Amorphous calcium phosphate (ACP)	$Ca_xH_y(PO_4)_z.nH_2O$ n = 3 - 4.5	1.2 - 2.2
Calcium deficient hydroxyapatite (CDHA)	$Ca_9(HPO_4)(PO_4)_5(OH)$	1.5 – 1.67
α-Tricalcium phosphate (α-TCP)	α-$Ca_3(PO_4)_2$	1.5
β-Tricalcium phosphate (β-TCP)	β-$Ca_3(PO_4)_2$	1.5
Hydroxyapatite (HA)	$Ca_{10}(PO_4)_6(OH)_2$	1.67
Tetracalcium phosphate (TTCP)	$Ca_4(PO_4)_2O$	2.0

Monocalcium phosphate monohydrate (MCPM) is the most acidic CaP and the most soluble CaP at almost all pH values. Due to its acidity and solubility, MCPM is not biocompatible and thus can not be used alone as a bone substitute, but combined with several self-hardening CaPs cements [32-34]. In addition, MCPM is used as a nutrient, acidulate and mineral supplement for dry baking powders, food, feed and some beverages [35].

Dicalcium phosphate dihydrate (DCPD, or the mineral brushite) can be easily crystallized from aqueous solutions. DCPD has been detected in fracture callus, bone and kidney stones [36-38]. DCPC is biocompatible, biodegradable and osteoconductive, being easily converted into HA *in vivo* [39].

β-Tricalcium phosphate (β-TCP) is a high temperature phase of CaP, which only can be obtained by its thermal decomposition at temperatures above 800ºC. β-TCP is biodegradable and has been extensively used as bone substitute, either as granules or blocks or even, in CaP bone cements [31]. In combination with HA, β-TCP forms the biphasic CaP (BCP), being both widely used as a bone substitution bioceramics [40, 41].

α-Tricalcium phosphate (α-TCP) is usually prepared from β-TCP phase at heat treatment above 1125ºC, and quenching it prevents the reverse transformation [42]. α and β-TCP phases have exactly the same chemical composition but dissimilar crystallographic structure and solubility. α-TCP is biocompatible and more biodegradable than β-TCP, but less stable than β-phase [43]. For that reason, α-TCP is more reactive in aqueous systems, has a higher specific energy and it can be hydrolyzed to a mixture of other CaPs. It never occurs in biological ossifications but, due to its hydraulic power, is used in CaP bone cements [44, 45].

Calcium-deficient hydroxyapatite (CDHA) chemistry is very complex, because it can have a Ca/P molar ratio from 1.50 to 1.67 [46], and sometimes even outside this range [47]. CDHA is usually obtained by precipitation in an aqueous solution above a pH of 7 [48]. Their crystals are in general poorly crystalline and of submicron dimensions. The solubility of CDHA increases with a decrease of Ca/P molar ratio, crystallinity and size. CDHA decomposes on heating, above 700ºC, into β-TCP (Ca/P = 1.50), into a mixture of HA and β-TCP (1.50 < Ca/P < 1.67) or

into pure HA (Ca/P = 1.67) [41, 49]. As a first approximation, CDHA may be considered as HA with some ions missing [46]. Unsubstituted CDHA does not exist in biological systems, but the substitution of Ca^{2+} by Na^{+}, K^{+}, Mg^{2+} or Sr^{2+}; HPO_4^{2-} or PO_4^{3-} by CO_3^{2-}; OH^{-} by F^{-}, Cl^{-}, CO_3^{2-} plus some water forms biological apatite [37, 38]. Thus, CDHA is a promising compound to produce synthetic bone substitutes.

Hydroxyapatite (HA) is highly crystalline and is the most stable and least soluble CaP in an aqueous solution down to a pH of 4.2. Some impurities, as partial substitution of hydroxide by fluoride or chloride, stabilize the hexagonal structure of HA at room temperature. HA can be prepared using wet methods, such as precipitation [50-52], hydrothermal [53] and hydrolysis of other CaPs. HA can be also obtained from a solid-state reaction of, for example, MCPM, DCPA, DCPD, OCP with CaO, $Ca(OH)_2$ or $CaCO_3$, above 1200ºC. The detailed information on HA synthesis is reported and available elsewhere [54]. HA can be prepared in dense or macroporous forms, as granules or blocks [55, 56]. In addition to being used as bone substitutes, HA granules are also used as the source material for depositing coatings on commercial dental and orthopaedic implants using the plasma spray technique [19, 55-57]. Moreover, due to the very large specific surface area, HA is used in liquid chromatograpy of proteins and other biological compounds and for drug delivery purposes [58-60]. Tensile strengths for dense and porous HA are, respectively, 79 to 106 MPa, and 42 MPa [55]. The resorption of ceramic HA is believed to be slow (1 to 2% per year) and a result of surface macrophage attack, which creates a roughened surface and forms an apatitic layer similar to the biological apatite [61]. The new surface then serves as a substrate onto which bone is deposited. However, these dense materials are too brittle and degrade too slowly to be considered for orthopedic procedures.

Tetracalcium phosphate (TTCP) is the most basic and soluble CaP. It is obtained by a solid-state reaction above 1300 ºC, usually between equimolar quantities of dicalcium phosphate (DCP) and $CaCO_3$ [62]. TTCP is not very stable in aqueous solutions, since it hydrolyses to HA and $Ca(OH)_2$ [53]. Therefore, TTCP is never found in biological calcifications. TTCP is broadly used for self-setting CaP

cements preparation, such as in commercial BoneSource® and Cementek (see Table 1.3 in section 1.3.3).

Attention in the biomedical field is generally focused on MCPM, DCPD, OCP and precipitated HA (PHA), because their respective solubility products are well established [63]. It should be noted that DCP is rarely obtained by precipitation from an aqueous solution [64] at room temperature. It is usually obtained by heating DCPD at temperatures between 120ºC and 170ºC. Likewise, the hydration processes of DCP are usually effective at temperatures higher than 50ºC [65].

According to solubility, CaPs can be ranked in order of increasing the *in situ* degradation rate as: MCPM > TTCP ≈ α-TCP > DCPD > OCP > β-TCP > HA.

CaPs can be categorized into bioactive and bioresorbable materials. A bioactive biomaterial enables establishing direct chemical bonds with bone with surrounding tissues, and could provide good stabilization for materials that are subject to mechanical loading. Bioresorbable materials allow a newly formed tissue to grow into any surface irregularities but may not necessarily interface directly with the material [66-68]. Examples of bioactive materials are bioceramics made of dense HA, while porous scaffolds made of biphasic CaP, or bone grafts made of CDHA appear to be good examples of bioresorbable materials. Unfortunately, CaP biomaterials have poor mechanical properties that do not allow them to be used in load-bearing applications. For that reason, clinical applications of CaPs are focused on the production of non-load-bearing implants, such as pieces for middle ear surgery, scaffold materials for bone filling defects, or coating of dental implants and metallic prostheses [69].

Biomaterials and bioceramics of CaP are available in diverse forms, like particles, granules and blocks (dense or porous), coatings on metal implants, composites with polymers, etc. [70]. The properties of these materials depend on the conditions under which they were formed and on their inherent chemistry and final porosity. Porosity has been intentionally introduced in solid biomaterials, since a porous surface provides mechanical fixation that allows chemical bonding between biomaterials and bone. However, the presence of macroporosity leads to weaker

biomaterials and can be a rather complicated process for manufacturing. Interested readers are referred to special literature reports [71-74].

General requirements for the ideal bone grafts are: (i) pores of some 100 μm size, (ii) biodegradation rate similar to that of bone tissue formation, and (iii) enough mechanical stability.

CaP-based hydraulic cements that harden inside bone defects are other bone grafts usually used [26, 66, 75, 76]. Concept and properties of these types of materials are intensely discussed in section 1.3.3.

1.3.2 Ionic co-substitutions in calcium phosphates

It is well known that the mineral component of bone is similar to HA but contains other ions in composition, as illustrated in Table 1.2. Regarding cations, sodium (Na) has been detected as an abundant trace element next to the presence of Ca and P in natural bone and tooth mineral.

Table 1.2: Composition of inorganic phases of adult human calcified tissues

Composition (wt.%)	Bone	Enamel	Dentin
Calcium	34.8	36.5	35.1
Phosphorus	15.2	17.7	16.9
Sodium (Na)	0.9	0.50	0.60
Magnesium (Mg)	0.72	0.44	1.23
Potassium (K)	0.03	0.08	0.05
Zinc (Zn)	0.0126 - 0.0217 [77, 78]	-	-
Fluoride (F)	0.03	0.01	0.06
Chloride (Cl)	0.13	0.30	0.01
Carbonates	7.4	3.5	5.6

Each of the aforementioned elements plays an essential part in biological action course: (a) Na has a potential role in cell adhesion and in the bone metabolism and resorption processes [79, 80]; (b) Mg has its own significance in the calcification process and on bone fragility, and has indirect influence on mineral metabolism [81]; (c) K has a versatile nature in the regulation of biochemical process and also an important role in the apatite mineral nucleation process [82-84]; (d) Zn is an essential trace element for promoting osteoblast cell proliferation and differentiation [85, 86]; (e) Sr has beneficial effects in the treatment of osteoporosis due to the prevention of bone loss by mechanism of depressing bone resorption and maintaining bone formation [87-89]; (f) F is well-recognized for its potential behaviour relating to the stability of the apatite and for its prevention role in dental caries [90]; (g) Cl has the ability to develop an acidic environment on the surface of bone that activates osteoclasts in the bone resorption process [91, 92].

The presence of foreign ions into the synthetic apatites structure can alter a series of structural, physico-chemical and biological properties of CaP, such as, lattice parameters, crystallinity, solubility, dissolution, resorption and bone bonding capability [50, 93-95]. Under this perspective, a number of research results have been reported so far on the trace elemental incorporation into the synthetic apatites, such as, Mg, Sr, Zn, Na, K, F and carbonates. For example, carbonate substitution causes the formation of smaller and more soluble apatite, while fluoride incorporation has the opposite effects [96-98]. Mg incorporation in apatite is limited but causes reduction in crystallinity (smaller crystal size) and increases its extent of dissolution [99]. On the other hand, Sr causes an increase in solubility [100, 101].

It is also interesting to note, that chemical elements not found in natural bones can be intentionally incorporated into CaP biomaterials to get special properties. Examples are addition of Ag and Cu [102, 103], that have been used for imparting antimicrobial effects, while radioactive Sm-153 and Re-186 have been incorporated into HA microspheres and injected into knee joints to treat rheumatoid joint synovitis [104].

1.3.3 Calcium phosphate cements

In 1832, Ostermann prepared a CaP biomaterial in the form of a paste that set *in situ* to form a solid material. Nevertheless, Brown and Chow in 1986 [76] were the first to present this new form of CaPs, currently known as *calcium phosphate cements* (CPCs).

CPCs are made of an aqueous solution and of one or several CaPs, which upon mixing, dissolve and precipitate into a less soluble CaP and sets by the entanglement of the growth crystals, providing a mechanical rigidity to the cement. When the paste becomes sufficiently stiff, it can be placed into a defect as a substitute for the damaged part of bone, where it hardens *in situ* within the operating theatre. It hardens in generally < 20 min at body temperature (37ºC) and then displays limited solubility. The relative stability and solubility of various CaPs is the major driving force for the setting reactions that occur in CPCs. Depending upon the pH value of a cement paste, after setting, the CPCs can be denominated, according to the end product, into apatite (AP) cements and DCPD (or brushite) cements. AP is formed above pH 4.2, while brushite is preferentially formed in CPCs when pH value of the paste is < 4.2 [105], although it may grow even up to pH 6.5, due to kinetics reasons [105]. Given that water is not a reactant in the setting reaction of AP cements, a less amount of water is needed [106, 107] than when water participates in the chemical transformations such in the case of brushite cements [108].

CPCs are resorbable, osteoconductive, noncytotoxic, create chemical bonds to the host bones, restore contour and have both the chemical composition and X-ray diffraction patterns similar to those of bone [48, 108-110]. The major advantages of the CPCs include a fast setting time, excellent mouldability, outstanding biocompatibility, and easy manipulation [110, 111]; therefore, the cements are more versatile in handling characteristics than prefabricated CaP granules or blocks. Besides, like any other bioceramics, CPCs provide the opportunity for bone grafting using alloplastic materials, which are unlimited in quantity and provide no risk of infectious diseases [108].

There are a number of CPCs products available in the market that is summarized in Table 1.3.

Table 1.3: Marketed calcium phosphate cements formulations [37, 106, 112]

Company	Product	Composition	End product	Resorbable
ETEX	α-BSM®	ACP, DCPD	PHA	yes
Mitsubishi Materials	Biopex	α-TCP, TTCP, DCPD	PHA	no
Stryker	BoneSource™	TTCP, DCP	PHA	yes
	HydroSet™	DCPD, TTCP, Trisodium citrate	PHA	n.d.
Biomet	Calcibon®	α-TCP, DCP, CC, PHA	CAP	n.d.*
	Biocement D	α-TCP, DCP, CC, PHA	PHA	yes
Synthes	Norian SRS® / Norian CRS®	α-TCP, CC, MCPM	CAP	yes
	ChronOS Inject®	α-TCP, MCPM	DCPD	yes
Lorenz Surgical	Mimix	α-TCP, TTCP, HA, citric acid	PHA	n.d.*
Teknimed	Cementek	TTCP, α-TCP, MCPM	PHA	n.d.*

*n.d. = no data

Chemical reactions that take place during the setting of CPCs depend on their chemical composition. Nevertheless, it can be stated that only two major chemical types of the setting reaction are possible. The first type is an acid-base reaction that depends on the hydration rates of the acid and basic salts, followed by the neutralization of the by-products. Examples can be:

$$2Ca_4(PO_4)_2O + 2CaHPO_4 \rightarrow Ca_{10}(PO_4)_6(OH)_2 \quad (1)$$

or

$$\beta - Ca_3(PO_4)_2 + Ca(H_2PO_4)_2 H_2O + 7H_2O \rightarrow 4CaHPO_4.2H_2O \quad (2)$$

From equation (1), the basic TTCP reacts with the acidic DCPA/DCPD resulting in the formation of HA with a neutral pH. A steady state in terms of ion concentration in the solution is kept as long as the rate of dissolution of DCPA/DCPD and TTCP exceeds the rate of HA formation [113, 114]. Finally, the hardening of the cement results from the interlocking of HA crystals [109]. Several deviations from the chemical equation (1) have been studied in details [115].

The second type of the setting reaction might be defined as hydrolysis of a metastable CaP in aqueous media, e.g. when the initial and final CaPs have the same Ca/P molar ratio. Examples are cements made of α-TCP, β-TCP, ACP, TTCP plus aqueous solution, where they re-crystallize to CDHA upon contact with water. An example is expressed by the equation (3):

$$3\alpha - Ca_3(PO_4)_2 + H_2O \rightarrow Ca_9(HPO_4)(PO_4)_5OH \quad (3)$$

Experimental details on the above mentioned hydrolysis reactions are available elsewhere [116, 117].

CPCs hydration process is a slow exothermic reaction (thus preventing the attainment of high curing temperatures), during which the cement does not shrink. Previous results showed that the temperature rise arrived at the highest value of 37ºC 3 h later [118].

The liquid phases involved in the setting reaction of CPCs are aqueous solutions. As aforementioned, the systems of brushite cements, as TTCP + DCPD, harden in water, whereas other systems usually require the use of sodium phosphate solution (approximately 0.25 mol L^{-1}) as the liquid [119]. For applications requiring longer working times, glycerine or polyethylene glycol can be used [120].

As CDHA is similar to the chemical composition of bone, AP cements have been more extensively investigated and produced by several companies (Table 1.3).

Nonetheless, brushite cements have raised interest because they are resorbed *in vivo* much faster than AP cements. Although AP cements showed higher mechanical strength, they have slow *in vivo* resorption rates that interfere with the bone regeneration process [39, 121]. Moreover, brushite is metastable in physiological conditions and brushite based cements possess faster setting reactions [105, 122-124].

Brushite cements were introduced in 1987 by Mirtchi and Lemaitre, where DCPD is the major end product of the setting reaction (equation (2)). Other formulations have been already proposed, such as, β-TCP + H_3PO_4 and TTCP + MCPM + CaO. It is important to notice that β-TCP + H_3PO_4 formulations have several advantages over β-TCP + MCPM formulations, namely: (i) easier and faster preparation, (ii) a better control of the chemical composition and reactivity, and (iii) improved physico-chemical properties, such as longer setting times and larger tensile strengths due to a higher homogeneity. However, the use of H_3PO_4 might weaken the biocompatibility of the cement formulation, owing to low pH values during setting [125].

Brushite cements are acidic during setting, since DCPD can only precipitate from solutions at pH values below 6; hence the reaction is very rapid corresponding to the setting stage. Despite this initial high reactivity, the hardening stage of brushite cements typically lasts one day until completion, due to the increasing of the paste pH at the end of the setting reaction. In order to control the start of the setting reaction, inhibitors of crystal nucleation and growth, and less soluble reagents (for example, HA instead of β-TCP) can be used. Moreover, the use of monodisperse and fine powder particles is vital to provide an overall setting reaction.

Brushite cements are biocompatible and bioresorbable. In contrast to AP cements, they are faster resorbed *in vivo* and bear a rapid decrease in strength (even though strength of the healing bone increases as bone ingrowth occurs). Conversely, low mechanical strength, short setting times and the consequent rapid increase in viscosity to enable injection through hypodermic needles, prevent brushite cements from a broader clinical application. Use of chondroitin 4-sulfate [126] and glycolic acid [124] as setting retardants is an option to get more workable and less viscous pastes of brushite cements.

Brushite cements have a fast and linear degradation rate of 0.25 mm/week [127], which might lead to formation of an immature bone. Adding b-TCP granules to the cement paste could solve this problem because they act as bone anchors and encourage formation of a mature bone [127, 128].

1.3.4 Calcium phosphate cement properties

From the clinical point of view, the desirable relevant properties of CPCs are adequate flow properties, short setting times, easy injectability, mechanical properties that are comparable to those of trabecular bone and a resorption rate that is neither too fast nor too slow.

1.3.4.1 Dynamics of flow

Rheological properties have not been the subject of extensive investigations in the past. These properties are crucial in gaining understanding of the fundamentals of the dynamics of flow of an injectable CPC through the delivery system (cannula) and its subsequent interdigitation into the cancellous bone. This knowledge can also help in optimizing the design of the cannula, establishing the optimum time for injection and the optimum viscosity at the time of injection, and minimizing the risk for cement extravasations [108]. Besides, the first initial setting period, where the cements lose gradually their plasticity, can be accessed by rheological measurements as well.

The rheological behaviour of a system depends on many intrinsic factors such as the concentration of solid particles in a suspension, particle size and particle size distribution, particle shape, the pH value of the suspending media, type and amount of dispersing agents of other processing additives (binders, plasticizers, lubricants), stabilization mechanism; or on the concentration of polymer molecules in a solution, their molecular weight and molecular weight distribution; as well as on outside influences such as the ambient pressure the strength of a magnetic or an electric field, and other testing conditions including the type of load, the degree the duration of load, the temperature, etc.

The rheological behaviours can be classified as Newtonian and non-Newtonian. The shear viscosity, η, of a Newtonian fluid is independent of the intensity of the shear load. Examples of ideal viscous materials include: low molecular liquids such as water, solvents, mineral oils (without polymer additives), standard oils, pure and clean bitumen (without associative superstructures, i.e. at sufficiently high temperatures) and blood plasma. Non-Newtonian systems the evolution of viscosity as a function of shear rate, $\dot{\gamma}$, might show a decreasing (shear-thinning flow behaviour) or an increasing trend (shear-thickening flow behaviour). The overall relation between the shear stress, τ, and shear rate for systems without an (apparent) yield point can be expressed by:

$$\tau = \dot{\gamma}^n$$

For samples displaying Newtonian flow behaviour (n=1), the shear viscosity is independent on the degree of shear and the plots τ versus $\dot{\gamma}$ are straight lines passing through the origin [Fig. 1.4 (a)], while the plots η versus $\dot{\gamma}$ are straight horizontal lines [Fig. 1.4 (b)]. Fig. 1.4 (a) and (b), also show typical plots of shear-thinning (n <1), and shear-thickening (n>1) flow behaviours. In Fig. 1.4 (a), the diagram is represented with linear scale, while in Fig. 1.4 (b) a logarithmic scale was used. These last scales are recommended when the course of the curves should be visible at very low τ and $\dot{\gamma}$ values.

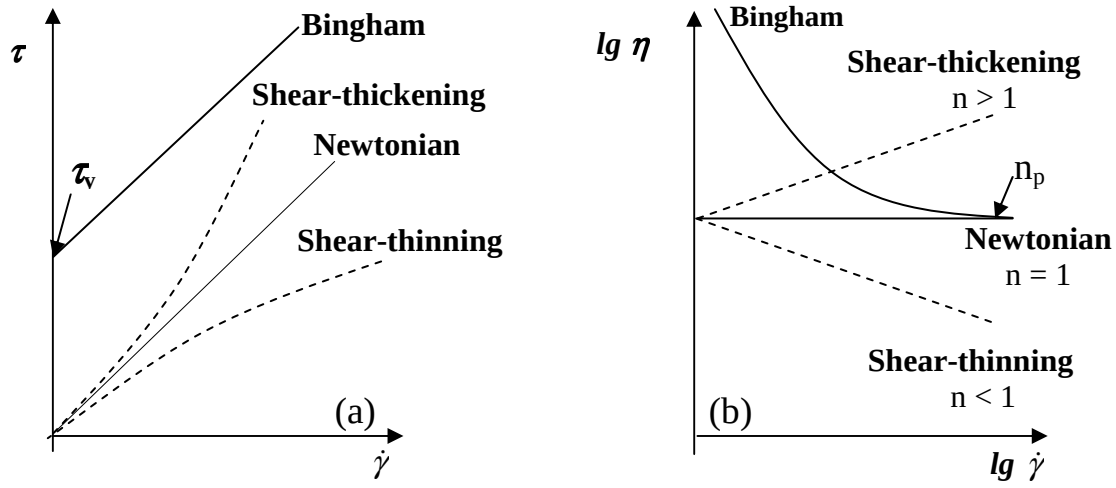

Fig. 1.4: Comparison of the flow (a) and viscosity (b) curves

Examples of shear-thickening materials include dispersions with a high concentration of solids or polymers such as ceramic suspensions, starch dispersions, etc.. The flow curve shows an increasing curve slope (Fig. 1.4 (a), i.e. η increases with increasing.

Plastic systems exhibit a yield point and “plastic flow” is the deformation process which can only occur above the yield point; below this point no or only elastic deformation occurs. The simplest or ideal plastic behaviour is the proposed by Eugen C. Bingham. At the yield point the loaded sample starts to be deformed and the rate of deformation increases linearly with the shear rate.

Inhomogeneous plastic behaviour cannot be described unequivocally using mathematics. It can only be represented using the results of empirical tests.

The terms plastic, ideal plastic, viscoplastic or elastoplastic are often used to mean different things. It is useful to understand what these terms might mean, but their use should be avoided when performing scientific rheological tests. In most cases, samples can be characterized as viscoelastic in a limited deformation range. However, when a material cannot be sheared homogeneously it is necessary to use special relative measuring systems. In this case, it is better to work with the measured raw data values (i.e. the torque, speed and deflection angle) instead of the rheological parameters (i.e. the shear stress, shear rate, deformation, viscosity and shear modulus).

Bone cements in general are considered viscoelastic materials as they change from having primarily liquid-like properties immediately after mixing to having primarily solid-like properties once cured. In general, the storage modulus (G’) corresponds to the elastic behaviour of the material and determines its inherent rigidity, thus it depends on the ability of the material to store mechanical energy. Conversely, the loss modulus (G”) corresponds to the viscous behaviour of the material and has a strong influence on its toughness and is dependent on the material’s ability to absorb and dissipate mechanical energy.

One of the first studies related to CaP paste rheology, by Bujake [129], investigated the viscosity of toothpaste-like suspensions containing DCPD, glycerine and water. These authors observed an increase of the viscosity with a

decrease of the particle size. Similar results were obtained in other studies [130-133]. Rao and Kannan [132] examined the yield stress and viscosity of HA suspensions. They observed a yield stress of 5 Pa, and a shear-thinning followed by shear-thickening behaviour. Generally, shear-thickening appears to occur at high particle loading [131, 133].

In a previous report [134], the study of the rheological behaviour of α-TCP slurries using a viscosimeter gave the possibility of looking at the effect on cement viscosity of various parameters during the initial setting, such as the particle size of the α-TCP powder, the LPR and the addition of dispersants. Also, Baroud et al. [135] studied the effects of liquid-to-powder ratio (LPR), milling of the powder particles and the presence of additives on the rheological properties of a non-reactive system. The study also demonstrated the importance of determining the rheological properties of the pastes in order to fully understand the injectability data. In addition, they recommended increasing the viscosity of the mixing liquid, to decrease the particle interactions and to decrease the particle size of the powder.

In an attempt to improve rheological properties of CPCs, the influence of several additives to the liquid phase, such as, lactic acid, glycerol, chitosan, citric acid or soluble polymers, on the injectability of CPCs have been studied by several authors [136-138]. These additives increase the viscosity of the liquid phase up to several orders of magnitude and make the cement pastes putty-like, since they improve the wetability and increase the surface charge of the cement particles due to ions adsorption at the particles' surface [139].

1.3.4.2 Setting time and reaction rate

The setting of bone cements is a continuous process that involves: (1) dissolution of reactants, (2) nucleation of new crystals, and (3) growth of crystals. After these processes, newly crystals entangle and the cement loses its viscofluid properties and transforms into a solid body [140]. Commonly, CPC should set slowly to provide enough time to a surgeon to perform implantation, by moulding or

injection, and harden fast to prevent delaying the operation, allowing the surgeon to close the defects shortly after cement placement.

The setting and hardening process of CPCs have been determined with two standardized methods, namely, Vicat needle method (ASTM C191-92) and Gilmore needles method (ASTM C266-89). Basically, both methods consist in the visual inspection of CPCs surfaces, when the test specimen bears the needles without leaving any mark on the surface. Whereas Vicat method only uses a needle to determine the final setting time (FST), Gilmore method uses two different needles to measure the initial (IST) and FST setting times of CPCs. IST is measured with a light and thick needle (113 $\pm$ 0.5 g, Ø = 2.12 $\pm$ 0.05 mm giving a static pressure of 0.3 MPa), while FST is measured with a heavy and thin needle (453.6 $\pm$ 0.5 g, Ø = 1.06 $\pm$ 0.05 mm giving a static pressure of 5 MPa) [141]. IST indicates the time during which the material must not be manipulated to avoid serious damage to the cement structure, whereas FST defines the time when the material has hardened, but maximum strength for some materials has not been achieved.

As far as clinical applications are concerned, the cement should be implanted before IST and the desired range of the setting times (in minutes) may be:

$$3 \leq IST < 8$$

$$FST \leq 15$$

These parameters are represented schematically in Fig. 1.5. In order to the surgeon has at least 1 min to apply and to mould the paste, cohesion time (CT), also called swelling time, must be at least 1 min before IST. As the mixing in a mortar is about 1 min, the shortest CT that can be allowed is about 2 min [138]. However, still have not consensus on what the ideal values of IST and FST should be. Ginebra et al. [142] have suggested that IST should be between 4 and 8 min, while FST should be between 10 and 15 min. On the other hand, Driessens et al. [143] have suggested that the cement should be injected before IST, while the wound should be closed after FST, making sure that the cement is not deformed between IST and FST otherwise cracks could be induced in it. In contrast, Sarda et al. [144] have suggested that the cement probably reaches a sufficient strength to withstand the pressure during wound closing well before FST.

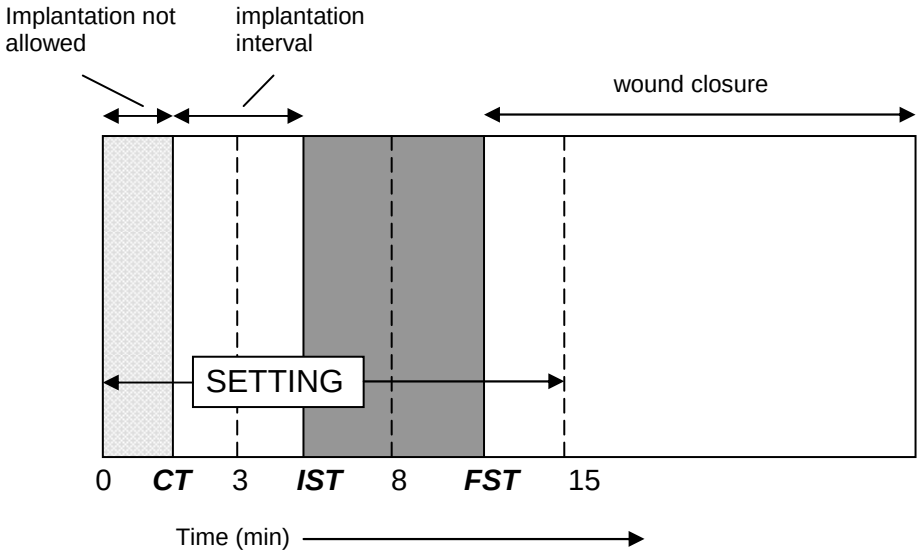

Fig. 1.5: Diagram of the setting parameters relevant for CPC. CT: cohesion time; IST: initial setting time; FST: final setting time (adapted from [143]).

Vicat and Gilmore methods have been used since the discovery of CPCs. However, these methods have not avoided criticism because of their inherent subjectivity. For this reason, some studies have been performed to record the setting process in a continuous manner and in real time by non-destructive methods, such as, isothermal calorimetry [122, 145, 146], pulse-echo ultrasound technique [147, 148] and AC impedance spectroscopy [149]. In the isothermal calorimetry method, the thermal reactions occurring during CPC setting reactions were followed as a function of time and composition. In addition, other methods have been proposed. For example, Hofmann et al. [123] followed the setting kinetics with Fourier-transform infrared (FTIR), while Grover et al. [150] used X-ray diffraction (XRD).

Accelerators and retarders are usually used to control the setting times and rheological properties, as detailed discussed in section 1.3.5.

1.3.4.3 Injectability

The viscous and cohesive properties are of major interest in the case of injectable cements. Injectability and cohesion are required for applications with limited accessibility and narrow cavities, and when there is a need for precise placement of the paste to conform to a defect area, such as periodontal bone repair and tooth root canal fillings.

As there are no standard procedures to assess injectability property, indigenous test methods were developed for the purpose [151-153], as shown in Fig. 1.6.

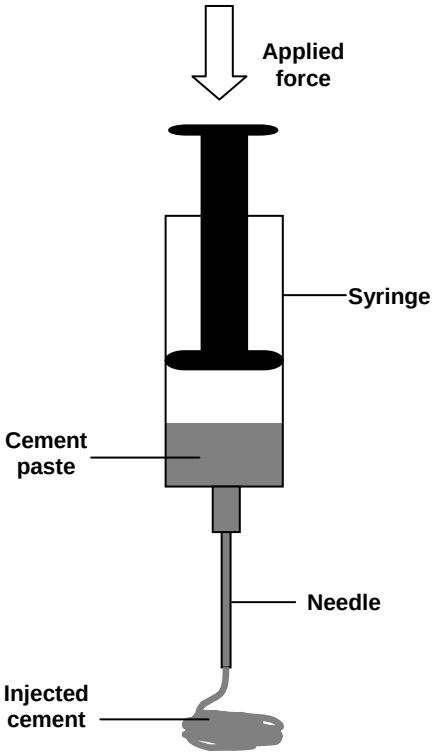

Fig. 1.6: Schematic representation of the experimental setup used to measure the injectability of CPCs.

Therefore, injectability is reported as the percentage by weight of the cement paste that could be extruded without demixing from a standard syringe, through a small hole of a long needle (usually, Ø = 2 mm and 10 cm length), pressing the

plunger manually or by applying an equivalent external force (~ 100 N) [151] (for a more detailed description, see Materials and Methods in section II.2).

Frequently, CPCs pastes show liquid-phase separation (so-called filter-pressing effect) provoked by the pressure applied to the cement paste after a certain injection pressure or after a certain injection time [75, 154]. In the case of demixing, the exact composition of the extruded part of the paste becomes unknown. For example, in 4.5 mL Norian SRS® cement paste, only ~ 3 mL of paste is injectable, while up to 1.5 mL of the cement remains in the syringe [143].

A good cohesion of the cement pastes during mixing is essential to avoid the possible occurrence of inflammatory reactions. Cohesion was reached when no disintegration of the cement paste was observed in the fluid, which can be obtained by keeping a high viscosity or using cohesion promoters (e.g., 1% aqueous solution of sodium alginate) and other chemicals [44, 112, 155].

Due to the setting process, the rheological properties of CPCs are transient and constantly changing. Combined with this is the complication that the injection process may destroy the evolving structure and thereby affect the measurements.

There are different ways to improve injectability and cohesion, such as, the injection device, LPR, particle size and particle size distribution, the plastic limit and the use of additives in the mixing liquids [151]. For example, shorter cannulas with a larger diameter favour injectability. Moreover, setting retarders, such as gelling agents, can improve injectability as well, with the presence of gelling agents and the increase of LPR increasing the setting times. Although injectability of cements is enhanced with increasing LPR [138], this approach often has a detrimental effect on the mechanical properties [156]. In addtition, α-BSM® is well injectable due to the small particle size of the powder. However, a small particle size requires a larger amount of mixing liquid, which decreases cohesion and mechanical strength [48, 145]. An indirect approach to improve injectability is to add CaP particles that act as spacers between other particles, as for the case when DCPA is added to Biocement D [48]. Another approach to improve injectability, is adding polymers to increase the viscosity and prevent filter-pressing [137, 139, 157]. Sarda et al. [157] found that the injectability of α-TCP water

mixtures was increased by 50-100% with the addition of citrate ions. Similar results were obtained for brushite and AP cements [139, 158].
The influence of all the abovementioned factors is discussed in details below in section 1.3.5.

1.3.4.4 Mechanical behaviour

As bone cements are meant to be used as bone substitutes, and because one of bone's first functions is to support the body weight, the mechanical behaviour of the cements is of a paramount importance. The mechanical strength required for cements must be at least as high as that of trabecular bone, which is close to 10 MPa.
There are two mechanical tests particularly important for implanted CPCs; compression strength (CS) (Fig. 1.7 A) that requires sample dimensions of 6.0mm diameter x 12.0mm height, whereas in the diametral compression strength (Fig. 1.7 B) cylindrical samples with dimensions of 6.0mm diameter x 3.0mm height are used.

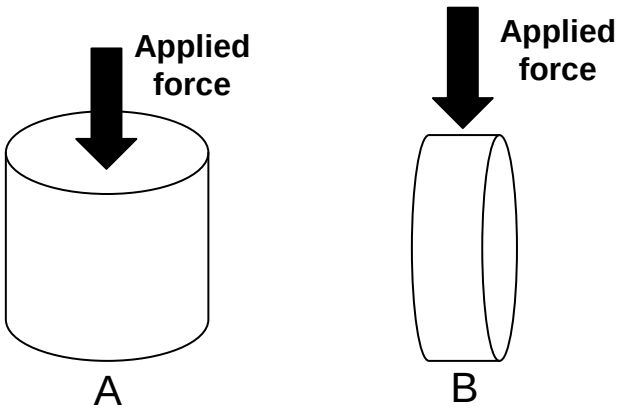

Fig. 1.7: Schematic representation of the experimental setups used to measure the (A) compression and (B) diametral compression strengths.

Diametral compression strength (frequently denominated by several authors, as diametral tensile strength, DTS), also named the Brazilian test or indirect tension

test, is routinely used for brittle materials as ceramics [159]. Direct tensile tests are rarely applied to brittle materials, since they do not deform until rupture, misalignment of the specimens may induce a tangential stress component that may lower the measured strength of the materials. Therefore, DTS test allows measurement of materials tensile strength by applying a compressive load in an experimental setup similar to the one used for axial compression, to keep simple sample shape, and to avoid the problem of mounting specimens on the universal testing machine. The advantage of this type of test is that fracture starts within the specimen and the measured value is not depending on the surface state.

CPCs are strong enough at compression which values are in the range 10-100 MPa, whereas they possess a low tensile strength (1-10 MPa) [160]. The poor mechanical properties noticeably restrict a wider clinical application of CPCs; however after 12 weeks of implantation, CS values higher than that of normal bone (60-70 MPa) have been reported [161].

Varying the crystallinity or the particle size of the materials used in the solid phase may alter the CS. Since CPC are relatively insoluble at neutral and alkaline pHs, their porosity is related to the ratios of powder to liquid used in the starting mixture. Obviously, high porosity cement would be expected to exhibit low CS.

These mechanical properties may also vary with implantation time, and animal studies have shown that mechanical properties of AP cements tend to increase continually, in contrast to those of brushite cements, which initially decrease and then increase when bone grows [161, 162]. This is the result of different porosity and bioresorption between AP and brushite cements.

To improve the mechanical properties of CPCs, incorporation of water-soluble polymers into the pastes has been attempted [163, 164]. It was observed that the strength increased mainly due to the polymers capacity to entangle. A research group reported similar results using sodium alginate and sodium polyacrylate [165]. Studies show that composites of α-BSM with polycations (polyethylenimine and polyallylamine hydrochloride) exhibited compressive strengths up to 6 times higher than that of pure α-BSM material [166].

Mechanical properties of CPCs were found to decrease exponentially with the porosity increase, since the presence of pores lead to cracks in the hardened

cement. Pressure can be applied to reduce the porosity of CPCs [156, 159, 167]. Another way to control the mechanical strength is by varying LPR in the hardening mixture. Elevated CS would be applicable in cranioplasty for regions requiring significant soft-tissue support. For smaller bone defects, such as root canal fillings, low CS cements must be used [107]. An empirical relationship between strength and porosity is reported in the literature [168].

As porosity is mainly due to an excess of water used in CPCs formulations, efforts to reduce the amount of water were made. Also, a decrease in water content leads to a strong increase in viscosity of the CPC pastes. As CPCs set at an almost constant volume, the final porosity can be predicted from the initial composition [48, 169].

Other factors affecting strength are the reagents used in the solid phase, particle sizes, incorporation of fillers into the solid phase and various liquid phases [170].

1.3.4.5 Biocompatibility and bioresorbability

Biocompatibility, osteoconductivity, and bioresorbability are all features of CPCs that make them attractive bone substitute candidates.

Biocompatibility expresses the biomaterial ability to perform with appropriate reactions in applications planned for a particular objective. Biocompatibility and bone-bonding ability of a material have been evaluated by *in vitro* and *in vivo* tests. *In vitro* biocompatibility assays are usually preceeded by mineralization tests in simulated body fluid (SBF) with ion concentrations nearly equal to those of human blood plasma [1, 171, 172] with the formation of apatite onto the materials surface. The biocompatibility screening tests include cell cultures [173] available on the market. The bone-bonding ability of a material is often evaluated. Moreover, there is a wide range of repeatable and reproducible methods, which are regulated by national and international standards for commercial use and for the scientific development of new materials and products. Detailed analysis of the surface apatite formed in SBF, by means of thin film X-ray diffraction, Fourier transform infrared spectroscopy (FTIR), scanning electron microscopy (SEM) and

transmission electron microscopy (TEM), showed that it was similar to bone mineral in its composition and structure [174]. As a result, it was speculated that osteoblasts might preferentially proliferate and differentiate to produce apatite and collagen on its surface. Thus formed apatite might bond to the surface apatite as well as to the surrounding bone. Consequently, a tight chemical bond is formed between the material and the living bone through the apatite layer. An example is β-TCP either in SBF [175, 176] or *in vivo* [177-179] environments bonding to living bone due to its high resorbability.

In vivo assessment of the biomaterials biocompatibility is a critical step in their development and implementation. While *in vitro* studies yield important fundamental interactions with biomaterials, they cannot replace *in vivo* evaluation. An animal model is an appropriate way to identify a material with *in vivo* bone bioactivity, with special attention being paid to the similarities and differences in the trabecular bone composition and architecture of human being. In this regard, pigs and sheep are suitable models because their bone structure is comparable to those from humans. CPC revealed extensive bone formation immediately after implantation without any inflammatory tissue response [158]. Bone colonization occurred much earlier and faster in CPC than in CaP ceramics [152]. Polymers [136], gelatin [33], and collagen [155] can be added to improve the biocompatibility of CPCs. Adding chitosan and citric acid improved the biocompatibility and decreased the initial inflammatory responses of self-curing CPCs [112]. Addition of 20% citric acid decreased the initial inflammatory response and enabled good bone bonding to be established.

One of the most appealing characteristics of CPCs is their resorbability *in vivo*. Upon implantation, these materials act as osteoconductive scaffolds but, in time, degrade and are replaced by bone during the remodelling process [180, 181]. The products of the cements' degradation are Ca^{+2} and PO_4^{3-} ions, which are easily excreted or recycled by the body. CPCs degradation occurs by the combination of two processes: (i) *in vivo* dissolution, which is strictly related to their composition and particle size [182], and (ii) cell-mediated resorption mainly by osteoclasts. Cell-mediated resorption is advantageous since it mimics the natural process of

bone turn-over, in which osteoclasts resorb bone and osteoblasts subsequently secrete bone matrix [183, 184]. The bioresorption process of bone substitutes obviously depends on their chemical nature, being closely related with CaPs solubility in aqueous solutions (see section 1.3.1).

A variety of characteristics may influence resorption rate. Among them are the age, sex, and general metabolic health of the host. Taking these variables into consideration, the complete resorption of CPCs may take from 3 to 36 months. Additional studies are needed in order to describe the degradability of these materials in clinical models [185].

Brushite and AP cements have an excellent bioresorbability and ability to form new bone; but AP is less bioresorbable than brushite [122]. Moreover, when the crystal size increases or the porosity decreases, the bioresorption will be longer. Norian® SRS and α-BSM® are therefore, expected to bioresorb faster than BoneSource®, Biopex and Cementek. Norian SRS was evaluated in canine tibial and femoral metaphyseal defects.

1.3.5 Influence of factors on calcium phosphate cement properties

The properties of CaP bone cements are influenced by a wide spectrum of factors, such as, the presence of additives, the powder particle size, the liquid-to-powder ratio (LPR) and the method used to mix the powder and liquid constituents of CPCs.

1.3.5.1 Additives

Additives that have been studied are fluidificants, gelling agents, reinforcing agents and antibiotics [186]. Further, radiopacifiers might be used [187]. The main requirements for additives are non-toxicity as well as the absence of inhibition of the cement setting reaction.

Fluidificants added to the liquid are aimed at enhancing the flowability of the cement pastes. An example is citric acid, which decreases the CS during initial

setting of the cement but increases its CS at saturation [157]. Moreover, citric acid also acts as setting stimulator and improves the mechanical properties of the hardened cements [188]. For several cements, mixing with sodium citrate or citric acid has resulted in some effects on the IST [139, 157], while for other cements the effect was insignificant [158].

The main role of gelling agents is to improve the workability of the pastes. These kinds of agents significantly increase the injectability, as well as the setting times. Two examples of workability-improvement agents are polysaccharides and gelatin, which lead to a reduction in total porosity and achievement of a more compact microstructure. Hidroxylpropylmethylcellulose (HPMC) is another gelling agent capable of improving the pastes cohesiveness, since HPMC is a polysaccharide able to hydrogen bond to water and form a viscous solution [189, 190].

Reinforcing agents can be added to enhance the mechanical properties of CPCs. Bohner et al. [191] used citrate, pyrophosphate and sulphate to modify the properties of CPCs. Moreover, in order to decrease CPCs brittleness, reinforcing fibres and polymers were added to cements' matrix as a part of a periodontal disease model, yielding promising results [192].

Studies have reported on the influence of additives in final CPCs properties. Wang et al. [193] showed that the addition of disodium phosphate, polyethyleneglycol (PEG 200), glycerin and citric acid influenced the injectability and the setting time of an ACP + DCPD bone substitute material. The study suggested that injectability and the setting time could be balanced and the cement could be prepared by optimizing the additives and their concentrations according to different clinical requirements. Leroux et al. [137] found that glycerol greatly improved the injectability and increased the setting time, but decreased the mechanical properties. Lactic acid reduced the setting time, increased the material toughness, but limited the dissolution rate. After injection, the cement did not present any disintegration. The effects of lactic acid were correlated with the formation of calcium complexes. Chitosan alone improved the injectability, increased the setting time, and limited the evolution of the cement by maintaining the CPC phase.

The main role of an antibiotic is to reduce infections in the body [194, 195]. However, its presence affects cement properties, as the addition of flomoxef sodium, for instance, leads to an increase in cement consistency, a decrease in DTS and an increase in the set mass porosity [196]. Both setting time and CS of a brushite CPC increased when gentamicin sulfate was added either as a powder or as an aqueous solution.

1.3.5.2 Powder particle characteristics

Powder particle characteristics include the average particle size, the particle size distribution and the specific surface area. Particle size distribution and surface area are interdependent characteristics which influence the behaviour of bone substitutes.

A reduction in particle size produces a significant decrease in both initial and final setting times, an acceleration of the rate of hardening but an unclear trend with regards to mechanical properties [111]. In a study described by Liu et al. [113], a steeper increase in pH and accelerating the dissolution of DCPA by reducing the particle size of TTCP, was observed. For instance, the commercial reagent DCPA presents a median particle size of about 1 μm, while Chow et al. [197] reported that TTCP should be ground to a median particle size of approximately 15 μm.

1.3.5.3 Liquid-to-powder ratio

The properties of CPCs are influenced by LPR, as the higher amount of mixing liquid markedly increased both IST and FST, and decreased mechanical properties [75, 151]. A decrease in LPR and the adding of reinforcing fibres, on the other hand, would decrease the cements' porosity and increase their mechanical properties [75], while injectability was found not to be affected for a LPR within the

range of 0.22 – 0.26 mL g^{-1}, but drops by nearly 100% between LPR = 0.2 and 0.22 ml g^{-1} [139].
In a study reported by Baroud et al. [135], it was found that changing LPR and the milling time significantly affected the rheological properties.

1.3.5.4 Mixing procedure

Bone cement mixing methods are categorized as manual (or hand) mixing, centrifugation, vacuum mixing, and combined mechanical mixing.
In manual mixing, the powder component is added to the liquid (which may or may not have been chilled to a temperature that is usually between 15ºC and 16ºC) in a polymeric (usually polypropylene or polyethylene) bowl. Then, these components are stirred with a, polypropylene or polyethylene, spatula with a speed of 1 or 2 Hz for 45–120 s. To be injected, the cement paste must be then transferred into a syringe. Two commercial products, Norian SRS and α-BSM, are sold with a reactant pack containing the powder and the mixing liquid, and require the use of a mixing machine and an injection gun [48]. The electrically powered mixing machine of Norian SRS mixes the cement paste within 70-80 s, and enables a fast and consistent filling of the application syringe. In spite of this kind of mixing system being very simple, it has some drawbacks. As the mixing procedure depends on the user and as the setting time of the cement is temperature dependent, the setting time varies from user to user.
In centrifugation mixing, the hand-mixed dough is immediately poured into a syringe (from which the nozzle is detached) that is then promptly placed in a centrifuge and spun with a speed of 2300–4000 rpm for 30–180 s [33, 198].
Applying vacuum to self-setting acrylic cements was first described in dentistry, but Lidgren et al. [199] studied vacuum-mixed cements as bone cements in 1984. They analyzed the mechanical strength of high- and low-viscosity gentamicin-containing cements by using three different mixing procedures: hand, vibration, and vacuum stirring. They reported that vacuum mixing improved the flexural and compression strength especially for high-viscosity cement. In another study of

Lidgren et al. [200] in 1987 it was shown that vacuum mixing improved fracture strength, maximal deflection, modulus of elasticity, and hardness when compared with hand mixing. The fatigue life was ten times longer after vacuum mixing. Vacuum mixing delayed the setting time by 1 min, and also decreased the peak temperature. Radiographic analysis showed that vacuum mixing mainly reduced not only the microporosity, but also the macroporosity. The mechanical properties deteriorated slightly after 2 months in Ringer's solution, but the differences between the mixing procedures remained unchanged [201].

1.3.6 Clinical application of CPCs

CPCs are non toxic and resorbable materials with osteoconduction, excellent biocompatibility, low exothermicity of setting reactions, but their mechanical properties are not ideal, limiting their clinical use. The main purpose of CPCs is to fill small bone defects or to increase bone volume in metaphyseal bone, thus reducing the need for bone graft. The combination of a self-setting nature, mouldability, biocompatibility and a great potential for being replaced by bone, make these materials to be used by bone remodelling cells for reconstruction of damaged parts of bones [180, 181, 202]. Besides, some formulations were found to possess an antimicrobial activity, as well as promote osteoblast cell adhesion and gene expression in vitro [117, 203].

CPCs have successfully been used for treatment of the distal radius fracture. Moreover, other successful attempts have been made to use these materials for calcaneal fractures, hip fractures, augmentation of osteoporotic vertebral bodies, tibial plateau fractures, restoration of pedicle screw fixation, reinforcement of both thoracolumbar burst fractures, cancellous bone screws, in wrist arthrodesis and for fixation of titanium implants [204, 205]. They can also be applied to reinforce osteoporotic vertebral bodies [169, 206]. Stankewich et al. [207] and Goodman et al. [208] showed augmentation of femoral neck fracture with CPC, which improved the initial stability and failure strength of the fractures.

The use of CPCs for craniofacial and maxillofacial applications has been another valuable request. TTCP + DCPA cement that showed to be efficacious in animal studies was evaluated in several medical centres for cranial defect repair as part of a US FDA-approved study in human subjects [209]. Sliindo et al. [210] reported that BoneSource^{TM} was employed to increase the supraorbital ridge in dogs, as well as in a variety of skull base defects. It was also used in 24 patients to increase or obliterate the frontal and ethmoid sinus regions and mastoid cavities. Cranial base reconstruction with CPCs has been successful for translabyrinthine, middle cranial fossa, and suboccipital craniectomy defects, as well as for extensive temporal bone fractures [211].

CPCs have been employed for dental applications too. These materials were tried as root canal fillers and for pulp capping [212, 213]. A previous study showed that a hydraulic CPC was injected as a bone filler for gaps around oral implants placed on the medial femoral condyles of 6 goats and found excellent bone formation around the graft material. However, the degradation rate of the cement appeared to be very slow and no resorption was observed [214]. In another study, researchers used a CPC for direct pulp capping and found its capability of producing a secondary dentin after 24 weeks [215].

Due to their outstanding properties (injectability, biodegradation, setting at room temperature, large surface area, and near neutral pHs [109, 110]), CPCs are very attractive candidates to be used as a delivery system for therapeutic peptides, antibiotics, anticancer drugs, anti-inflammatory drugs and bone morphogenetic protein. These drugs might be slowly released through set cement pores, after their incorporation into a liquid and a powder phase of the cements. However, it ought to be taken into account that the drugs incorporation in the cements should not affect the final CPCs properties, such as, the setting and hardening processes, rheological behaviour and injectability. Thus, the clinical performance of the drug-delivery system must be evaluated through *in vivo* tests, before application [109, 110].

The abovementioned possibility offers an attractive and efficient solution for the treatment of bone diseases such as tumours, osteoporosis or osteomyelitis [216]. In a previous study growth-factor cement (GFC) was reported [217]. A combination of bone morphogenetic protein-2, transforming growth factor β, platelet-derived growth factor, and a basic fibroblast growth factor used in a CPC for treatment of peri-implant defects in a dog model [217]. Results indicated a significant effect of GFC on increased bone-to-implant contact and amount of bone per surface area. Further examples of CPCs application as drug-delivery systems are given in the literature [109, 110, 143].

1.4 References

[1] Hench LL. Bioceramics. J Amer Ceram Soc 1998;81:1705-1728.

[2] Hall SB. The biomechanics of human bone growth and development *in Basic Biomechanics*. 5th Ed. ed. McGraw-Hill Int Ed., New York, 2006.

[3] A. Ravaglioli AKe. Bioceramics-materials, properties and applications. London: Chapman & Hall, 1992.

[4] Kaplan FS, Hayes WC, Keaveny TM. Form and function of bone. Orthopaedic Basic Science, 1994. p. 129-130.

[5] Hosseini MM. On the relationship between osteoconduction and surface texture during peri-implant osteogenesis. Institute of Biomaterials and Biomedical Engineering. University of Toronto, Toronto, 2002.

[6] McKee MD, Nanci A. Osteopontin at mineralized tissue interfaces in bone, teeth, and osseointegrated implants: ultrastructural distribution and implications for mineralized tissue formation, turnover, and repair Microsc Res Tech 1996;33:141-164.

[7] Davies JE, Nagai N, Takeshita N, Smith DC. The bone-biomaterial interface. Toronto, 1991.

[8] Davies JE. Understanding peri-implant endosseous healing. J Dent Edu 2005;8:932-949

[9] Davies JE. In vitro modeling of the bone/implant interface. Anat Rec 1996;245:426-445.

[10] Lind M. Growth factor stimulation of bone healing. Effects on osteoblasts, osteomies, and implants fixation. Acta Orthop Scand Suppl 1998;283:2-37.

[11] LeGeros RZ, Daculsi G. In vivo transformation of biphasic calcium phosphate ceramics: ultrastructural and physicochemical characterizations. Handbook of bioactive ceramics: Boca Raton: CRC Press, 1990. p. 17-28.

[12] LeGeros RZ, LeGeros JP. Bone substitute materials and their properties. Stuttgart-New York: Thieme, 1997. p. 12-18.

[13] De Bruijn JD, Klein CPAT, De Groot K. The ultrastructure of the bone-hydroxyapatite interface in vitro. J Biomed Mater Res A 1992;26:1365-1382.

[14] Albee FH. Studies in bone growth: triple CaP as a stimulus to osteogenesis. Ann Surg 1920;71:32-36.

[15] Ray RD, Ward Jr AA. A preliminary report on studies of basic CaP in bone replacement. Surg Form 1951;3:429-434.

[16] Levitt GE, Crayton PH, Monroe EA, al. e. Forming methods for apatite prosthesis. J Biomed Mater Res 1969;3:683-685.

[17] Monroe ZA, Votawa W, Base DB, al. e. New CaP ceramic material for bone and tooth implants. J Dent Res 1971;50:860-862.

[18] Aoki H, Kato K, Ogiso M, al. e. Studies on the application of apatite to dental materials. J Dent Eng 1977;18:86-89.

[19] DeGroot K. Bioceramics of CaP: Boca Raton, CRC Press, 1983.

[20] Jarcho M. Hydroxyapatite synhesis and characterization in dense polycrystalline forms. J Mater Sci 1976;11:2027-2035.

[21] Metzger DS, Driskell TD, Paulsrud JR. Tricalcium phosphate ceramic: a resorbable bone implant: review and current status. J Amer Dent Assoc 1982;105:1035-1048.

[22] Nery EB, Lynch KL, Hirthe WM, al. e. Bioceramics implants in surgically produced infrabony defects. J Periodontol 1975;63:729-735.

[23] Nery EB, Lynch KL, Pflughoeft FA, al. e. Functional loading of bioceramic augmented alveolar ridge: a pilot study. Prosthet Dent 1978;43:338-343.

[24] Denissen HW. Dental root implants of apatite ceramics experimental investigations and clinical use of dental root implants made of apatite ceramics. PhD thesis. Amsterdam: Vrije University; 1979.

[25] Denissen HW, Kalk W, Veldhuis AA, al. e. Eleven year study of hydroxyapatite implants. J Prosthet Dent 1989;61:706-712.

[26] Constantz BR, Ison IC, Fulmer MT, al. e. Coral chemistry leads to human bone repair. Science 1995;267:1796-1799.

[27] Damien CJ, Parsons JR. Bone graft and bone graft substitutes: a review of current technology and application. J Appl Biomater 1991;2:187-208.

[28] Ganeles J, Listgarten MA, Evian CL. Ultrastructure of durapatite-periodontal tissue interface in human intrabony defects. J Periodontol 1986;57:133-140.

[29] Addadi L, Weiner S. Control and design principles in biological mineralization. Angew Chem 1992;104:159-176.

[30] Bauerlein E. Biomineralization. Wiley-VHC,Weinheim, 2000.

[31] Dorozhkin SV. Calcium orthophosphates. J Mater Sci 2007;42:1061-1095.

[32] Lemaitre J, Mirtchi A, Mortier A. Calcium phosphate cements for medical use: state of the art and perspectives of development. Silicates Ind 1987;9-10:141-146.

[33] Bermudez O, Boltong MG, Driessens FCM, Planell JA. Development of Some Calcium-Phosphate Cements from Combinations of alpha-TCP, MCPM and CaO. J Mater Sci - Mater Med 1994;5:160-163.

[34] Driessens FCM, Boltong MG, Bermudez O, Planell JA, Ginebra MP, Fernandez E. Effective Formulations for the Preparation of Calcium-Phosphate Bone Cements. J Mater Sci - Mater Med 1994;5:164-170.

[35] Budavari S, O'Neil MJ, Smith A, Heckelman PE, Kinneary JF. The Merck Index: an encyclopedia of chemicals, drugs and biologicals. 12th ed ed. Chapman & Hall, 1996.

[36] Thomas J, Thomas E, Fompeydie Dea. Lithiase urinaire de brushite. Particularités cliniques, biologiques, radiologiques, évolutives et thérapeutiques. J Uro 1995;101:139-152.

[37] LeGeros RZ. Calcium Phosphates in Oral Biology and Medicine. Monographs in Oral Science: Karger, New York, 1991.

[38] LeGeros RZ. Hydroxyapatite and related materials. CRC Press, Boca Raton, 1994.

[39] Constantz BR, Ison IC, Fulmer MT, Baker J, McKinney LA, Goodman SB, Gunasekaren S, Delaney DC, Ross J, Poser R. Histological, chemical, and crystallographic analysis of four calcium phosphate cements in different rabbit osseous sites. J Biomed Mater Res Part B 1998;43:451-461.

[40] Metzger DS, Driskell TD, Paulsrud JR. Tricalcium phosphate ceramic: a resorbable bone implant. J Amer Dent Assoc 1982;105:1035-1048.

[41] Daculsi G, Laboux O, Malard O, Weiss P. Current state of the art of biphasic calcium phosphate bioceramics. Journal of Materials Science-Materials in Medicine 2003;14:195-200.

[42] Monma H, Goto M. Behavior of the α–β phase transformation in tricalcium phosphate. Yohyo-Kyokai-Shi 1983;91:473-475.

[43] Yin X, Stott MJ, Rubio A. Phys Rev B - Condens Matter Mater Phys 2003;68:205.

[44] Alves HLR, dos Santos LA, Bergmann CP. Injectability evaluation of tricalcium phosphate bone cement. Journal of Materials Science-Materials in Medicine 2008;19:2241-2246.

[45] Kim HW, Koh YH, Kong YM, Kang JG, Kim HE. Strontium substituted calcium phosphate biphasic ceramics obtained by a powder precipitation

method. Journal of Materials Science-Materials in Medicine 2004;15:1129-1134.

[46] Brown PW, Martin R. An analysis of hydroxyapatite surface layer formation. J Phys Chem B 1999;103:1671-1675.

[47] Constantz BR, Ison I, Fulmer Mea. Skeletal repair by in situ formation of the mineral phase of bone. Science 1995;267:1796-1799.

[48] Bohner M. Calcium orthophosphates in medicine: from ceramics to calcium phosphate cements. Injury-International Journal of the Care of the Injured 2000;31:37-47.

[49] Kanazawa Te. Inorganic phosphate materials. Materials Science Monographs. Tokyo, 1989.

[50] Kannan S, Ferreira JMF. Synthesis and thermal stability of hydroxyapatite-beta-tricalcium phosphate composites with cosubstituted sodium, magnesium, and fluorine. Chemistry of Materials 2006;18:198-203.

[51] Kannan S, Lemos AF, Ferreira JMF. Synthesis and mechanical performance of biological-like hydroxyapatites. Chemistry of Materials 2006;18:2181-2186.

[52] Kannan S, Lemos IAF, Rocha JHG, Ferreira JMF. Synthesis and characterization of magnesium substituted biphasic mixtures of controlled hydroxyapatite/beta-tricalcium phosphate ratios. Journal of Solid State Chemistry 2005;178:3190-3196.

[53] Elliott JC. Structure and chemistry of the apatites and other calcium orthophosphates. London: Elsevier, 1994.

[54] LeGeros RZ, LeGeros JP, Daculsi G, Kijkowska R. Encyclopedia handbook of biomaterials and bioengineering. Marcel Dekker, New York, 1995.

[55] Jarcho M. CaP ceramics as hard tissue prosthetics. Clin Orthop 1981;157:259-278.

[56] Le Geros RZ, Le Geros JP. Dense hydroxyapatite: An introduction to bioceramics. World Scientific, Singapore 1993:130-180.

[57] Bauer TW. Coating: hydroxyapatite controversies. Orthop 1995;18:885-888.

[58] Lawson MA, Xia Z, Triffitt JT, Ebetino FH, Phillips RJ, Russell RG. Refining the use of hydroxyapatite column chromatography to reveal differences in relative binding affinities of bisphosphonates Bone 2006;38:42-64.

[59] Smith GP, Gingrich TR. Hydroxyapatite chromatography of phage-display virions. Biotechniques 2005;39:879-884.

[60] Liu TY, Chen SY, Liu DM, Liou SC. J Controll Rel 2005;107:112.

[61] Moore WR, Graves SE, Bain GI. Synthetic bone graft substitutes. ANZ J Surg 2001;71:354-361.

[62] Ciesla K, Rudnicki R. Synthesis and transformation of tetracalcium phosphate in solid state. I: Synthesis of roentgenographically pure

tetracalcium phosphate from calcium dibasic phosphate and calcite. Polish J Chem 1987;61:719-727.

[63] Fernandez E, Gil FJ, Ginebra MP, Driessens FCM, Planell JA, Best SM. Production and characterization of new calcium phosphate bone cements in the CaHPO 4 -α-Ca 3 (PO 4) 2 system: pH, workability and setting times. Journal of Materials Science-Materials in Medicine 1999;10:223-230.

[64] Driessens FCM, Verbeeck RMH. Biominerals. CRC Press, Boca Raton, 1990.

[65] De Maeyere AP, Verbeeck RMH, Naessens DE. Stoichiometry of sodium(+)- and carbonate-containing apatites obtained by hydrolysis of monetite. Inorg Chem 1993;32:5709-5714.

[66] Gross KA, Berndt CC. Phosphates: geochemical, geobiological and materials importance. Mineralogical Society of America, Washington DC, 2002. p. 631-672.

[67] Cao W, Hench LL. Bioactive materials. Ceram Intern 1996;22:493-507.

[68] Neo M, Kotani S, Fujita Y, Nakamura T, Yamamuro T, Bando Y, et al. Differences in ceramic-bone interface between surface-active ceramics and resorbable ceramics: A study by scanning and transmission electron microscope. J Biomed Mater Res 1992;26:255-267.

[69] Vallet-Regi M, González-Calbet JM. Calcium phosphates as sub- stitution of bone tissues. Prog Sol Sta Chem 2004;32:1-31.

[70] Le Geros RZ, Le Geros JP. Calcium Phosphate Bioceramics: Past, Present and Future. Key Eng Mater 2003;3:240-242.

[71] Nakahira A, Murakami T, Onoki T, Hashida T, Hosoi K. Fabrication of porous hydroxyapatite using hydrothermal hot pressing and post-sintering. J Amer Ceram Soc 2005;88:1334-1336.

[72] Jones JR, Hench LL. Effect of surfactant concentration and composition on the structure and properties of sol-gel-derived bioactive glass foam scaffolds for tissue engineering. J Mater Sci 2003;38:3783-3790.

[73] Jones JR, Hench LL. Effect of porosity on the mechanical properties of bioactive foam scaffolds. Bioceramics 15 2003;240-2:209-212.

[74] Lenza RFS, Jones JR, Vasconcelos WL, Hench LL. In vitro release kinetics of proteins from bioactive foams. J Biomed Mater Res Part A 2003;67:121-129.

[75] Bohner M, Gbureck U, Barralet JE. Technological issues for the development of more efficient calcium phosphate bone cements: A critical assessment. Biomaterials 2005;26:6423-6429.

[76] Brown WE, Chow LC. A New Calcium-Phosphate Setting Cement. J Dent Res 1983;62:672-672.

[77] Otsuka M, Ohshita Y, Marunaka S, Matsuda Y, Ito A, Ichinose N, et al. Effect of controlled zinc release on bone mineral density from injectable Zn-

containing beta-tricalcium phosphate suspension in zinc-deficient diseased rats. Journal of Biomedical Materials Research Part A 2004;69:552-560.

[78] Sogo Y, Ito A, Fukasawa K, Sakurai T, Ichinose N, LeGeros RZ. Zinc-containing calcium phosphate ceramics with a (Ca+Zn)/P molar ratio of 1.67. Bioceramics 2005;17:31-34.

[79] Ginty F, Flynm A, Cashman KD. The effect of dietary sodium intake on biochemical markers of bone metabolism in young women. Br J Nutr 1998;79:343-350.

[80] Itoh R, Suyama Y. Sodium excretion in relation to calcium and hydroxyproline excretion in a healthy Japanese population. Amer J Clin Nutr 1996;63:735-740.

[81] Bigi A, Foresti E, Gandolfi M, Gazzano M, Roveri N. Isomorphous substitutions in beta-tricalcium phosphate: The different effects of zinc and strontium. Journal of Inorganic Biochemistry 1997;66:259-265.

[82] Hohling HJ, Mishima H, Kozawa Y, Daimon T, Barckhaus RH, Richter KD, et al. Microprobe analyses of the potassium calcium distribution relationship in predentin. Scan Microsc Int 1991;5:247-253.

[83] Suelter CH. Enzymes activated by monovalent cations. Science 1970;168:789-795.

[84] Wiesmann HP, Plate U, Zierold K, Hohling HJ. Potassium is involved in apatite biomineralization. J Dent Res 1998;77:1654-1657.

[85] Li X, Sogo Y, Ito A, Mutsuzaki H, Ochiai N, Kobayashi T, et al. The optimum zinc content in set calcium phosphate cement for promoting bone formation in vivo. Mater Sci and Eng 2008.

[86] Otsuka M, Marunaka S, Matsuda Y, Ito A, Layrolle P, Naito H, et al. Calcium level-responsive in vitro zinc release from zinc containing tricalcium phosphate (ZnTCP). J Biomed Mater Res 2000;52:819-824.

[87] Rokita E, Hermes C, Nolting HF, Ryczek J. Substitution of Calcium by Strontium within Selected Calcium Phosphates. J Cryst Growth 1993;130:543-552.

[88] Dahl S, Allain P, Marie P, Mauras Y, Boivin G, Ammann P, et al. Incorporation and distribution of strontium in bone. Bone 2001;28:446-453.

[89] Marie P, Ammann P, Boivin G, Rey C. Mechanisms of action and therapeutic potential of strontium in bone. Calcif Tissue Int 2001;69:121-129.

[90] Caverzasio J, Palmer G, Bonjour JP. Fluoride: mode of action. Bone 1998;22:585-589.

[91] Schlesinger PH, Blair HC, Teitalbaum SL, Edwards JC. Characterization of the Osteoclast Ruffled Border Chloride Channel and Its Role in Bone Resorption. J Biol Chem 1997;272:18636-18643.

[92] Neuman WF, Neuman MW. The chemical dynamics of bone mineral: University of Chicago Press, Chicago, 1958.

[93] Kannan S, Goetz-Neunhoeffer F, Neubauer J, Ferreira JMF. Ionic substitutions in biphasic hydroxyapatite and beta-tricalcium phosphate mixtures: Structural analysis by rietveld refinement. J Amer Ceram Soc 2008;91:1-12.

[94] Kannan S, Pina S, Ferreira JMF. Formation of strontium-stabilized α-tricalcium phosphate from calcium-deficient apatite. J Amer Ceram Soc 2006;89:3277-3280.

[95] Kannan S, Rocha JHG, Ferreira JMF. Synthesis and thermal stability of sodium, magnesium co-substituted hydroxyapatites. J Mater Chem 2006;16:286-291.

[96] Legeros RZ, Frondoza C, Lin S, Rohanizadeh R, Legeros JP. F-substituted apatites: Properties and cell responses. J Dent Res 2003;82:B36-B36.

[97] LeGeros RZ, Kijkowska R, Bautista C, Retino M, LeGeros JP. Magnesium incorporation in apatites: Effect of CO3 and F. J Dent Res 1996;75:60-60.

[98] Legeros RZ, Retino M, Mijares D, Hoshino K, Lin S, Legeros JP. Carbonate hydroxyapatite (CHA)/polymer interactions. J Dent Res 1998;77:916-916.

[99] LeGeros RZ, Gatti AM, Kijkowska R, Mijares DQ, LeGeros JP. Mg-substituted tricalcium phosphates: Formation and properties. Bioceramics 16 2004;254-2:127-130.

[100] LeGeros R, Lin S, LeGeros J, Cazalbou S, Combes C, Dupin-Roger I, et al. Strontium Ranelate Treatment Preserves Bone Crystal Characteristics and Bone Mineral Reactivity. Calcified Tissue Int 2004;74:S95-S95.

[101] LeGeros RZ. CaP in oral biology and medicine. Monographs in oral sciences: Basel, Karger, 1991.

[102] Kim TN, Feng QL, Kim JO, Wu J, Wang H, Chen GC, et al. Antimicrobial effects of metal ions (Ag+, Cu2+, Zn2+) in hydroxyapatite. J Mater Sci - Mater Med 1998;9:129-134.

[103] Li J, Li Y, Zuo Y. J Functional Mater 2006;37:635.

[104] Chinol M, Vallabhajosula S, Goldsmith SJ, Klein MJ, al e. Chemistry and biological behavior of samarium-153 and rhenium-186-labeled hydroxyapatite particles: potential radiopharmaceuticals for radiation synovectomy. J Nucl Med 1993;34:1536-1542.

[105] Gbureck U, Dembski S, Thull R, Barralet JE. Factors influencing calcium phosphate cement shelf-life. Biomaterials 2005;26:3691-3697.

[106] Schmitz JP, Hollinger JO, Milan SB. Reconstruction of bone using calcium phosphate bone cement: a critical review. J Oral Maxillof Surg 1999;57:1122-1126.

[107] Weiss DD, Sachs MA, Woodard CR. Calcium phosphate bone cements: a comprehensive review. J Long Term Eff Med Implants 2003;13:41-47.

[108] Dorozhkin SV. Calcium orthophosphates cements for biomedical application. J Mater Sci: Mater in Med 2008;43:3028-3057.

[109] Ginebra MP, Traykova T, Planell JA. Calcium phosphate cements as bone drug delivery systems: A review. Journal of Controlled Release 2006;113:102-110.

[110] Ginebra MP, Traykova T, Planell JA. Calcium phosphate cements: Competitive drug carriers for the musculoskeletal system?. Biomaterials 2006;27:2171-2177.

[111] Bohner M. Reactivity of calcium phosphate cements. J Mater Chem 2007;17:3980-3986.

[112] Khairoun I, Driessens FCM, Boltong MG, Planell JA, Wenz R. Addition of cohesion promoters to calcium phosphate cements. Biomaterials 1999;20:393-398.

[113] Liu CS, Shao HF, Chen FY, Zheng HY. Effects of the granularity of raw materials on the hydration and hardening process of calcium phosphate cement. Biomaterials 2003;24:4103-4113.

[114] Chow IC. Calcium phosphate cements: chemistry, properties, and applications. Mater Res: Soc Symp Proc 2000;599:27-37.

[115] Ishikawa K, Takagi S, Chow LC, Suzuki K. Reaction of calcium phosphate cements with different amounts of tetracalcium phosphate and dicalcium phosphate anhydrous. J Biomed Mater Res 1999;46:504-510.

[116] TenHuisen KS, Brown PW. Formation of calcium-deficient hydroxyapatite from alpha-tricalcium phosphate. Biomaterials 1998;19:2209-2217.

[117] Tsai CH, Lin RM, Ju CP, Lin JHC. Bioresorption behavior of tetracalcium phosphate-derived calcium phosphate cement implanted in femur of rabbits. Biomaterials 2008;29:984-993.

[118] Liu C, Huang Y, Chen J. The Physicochemical Properties of the Solidification of Calcium Phosphate Cement. J Biomed Mater Res B 2004;69:73-78.

[119] Takagi S, Chow LC, Ishikawa K. Formation of hydroxyapatite in new calcium phosphate cements. Biomaterials 1998;19(17):1593-1599.

[120] Xu HHK, Carey LE, Simon CG, Takagi S, Chow LC. Premixed calcium phosphate cements: Synthesis, physical properties, and cell cytotoxicity. Dent Mater 2007;23(4):433-441.

[121] Gisep A, Wieling R, Bohner M, Matter S, Schneider E, B R. Resorption patterns of calcium-phosphate cements in bone. J Biomed Mater Res Part A 2003;66:532-540.

[122] Bohner M, Gbureck U. Thermal reactions of brushite cements. Journal of Biomedical Materials Research Part B-Applied Biomaterials 2008;84:375-385.

[123] Hofmann MP, Young AM, Gbureck U, Nazhat SN, Barralet JE. FTIR-monitoring of a fast setting brushite bone cement: effect of intermediate phases. J Mater Chem 2006;16(31):3199-3206.

[124] Marino FT, Torres J, Hamdan M, Rodriguez CR, Cabarcos EL. Advantages of using glycolic acid as a retardant in a brushite forming cement. J Biomed Mater Res B - Appl Biomater 2007;83:571-579.

[125] Bohner M, vanLanduyt P, Merkle HP, Lemaitre J. Composition effects on the pH of a hydraulic calcium phosphate cement. J Mater Sci - Mater Med 1997;8:675-681.

[126] Mariño FT, Mastio J, Rueda C, Blanco L, Cabarcos EL, Marino FT. Increase of the final setting time of brushite cements by using chondroitin 4-sulfate and silica gel. J Mater Sci - Mater Med 2007;18:1195-1201.

[127] Ohura K, Bohner M, Hardouin P, Lemaitre J, Pasquier G, Flautre B. Resorption of, and bone formation from, new β-tricalcium phosphate cements: an in vivo study. J Biomed Mater Res B 1996;30 193-200.

[128] Flautre B, Maynou C, Lemaitre J, Van Landuyt P, Hardouin P. Bone colonization of β-TCP granules incorporated in brushite cements. J Biomed Mater Res - Appl Biomater 2002;63:413-417.

[129] Bujake JEJ. Rheology of concentrated dicalcium phosphate suspensions. J Pharm Sci 1965;54:1599-1604.

[130] Tian JM, Zhang Y, Guo XM, Dong LM. Preparation and characterization of hydroxyapatite suspensions for solid freeform fabrication. Ceram Int 2002;28:299-302.

[131] Olhero SM, Ferreira JMF. Influence of particle size distribution on rheology and particle packing of silica-based suspensions. Powder Technology 2004 5;139(1):69-75.

[132] Rao RR, Kannan TS. Dispersion and slip casting of hydroxyapatite. J Am Ceram Soc 2001;84:1710-1716.

133. Xu HH, Keller DS. Shear thickening behavior of concentrated calcium carbonate suspensions. Montreal, QC, Canada, 2003. p. 275-280.

[134] Friberg J, Fernandez E, Sarda S, Nilson M, Ginebra MP, Martinez S, et al. An experimental approach to the study of the rheology behaviour of synthetic bone calcium phosphate cements. Key Eng Mater 2001;192-195:777-780.

[135] Baroud G, Cayer E, Bohner M. Rheological characterization of concentrated aqueous α-tricalcium phosphate suspensions: The effect of liquid-to-powder ratio, milling time, and additives. Acta Biomater 2005;1(3):357-363.

[136] Ginebra MP, Rilliard A, Fernandez E, Elvira C, San Roman J, Planell JA. Mechanical and rheological improvement of a calcium phosphate cement by the addition of a polymeric drug. J Biomed Mater Res 2001;57:113-118.

[137] Leroux L, Hatim Z, Freche M, Lacout JL. Effects of various adjuvants (lactic acid, glycerol, and chitosan) on the injectability of a calcium phosphate cement. Bone 1999;25(2):31S-34S.

[138] Khairoun I, Boltong MG, Driessens FCM, Planell JA. Some factors controlling the injectability of calcium phosphate bone cements. J Mater Sci - Mater Med 1998;9(8):425-428.

[139] Gbureck U, Barralet JE, Spatz K, Grover LM, Thull R. Ionic modification of calcium phosphate cement viscosity. Part I: hypodermic injection and strength improvement of apatite cement. Biomaterials 2004;25:2187-2195.

[140] Ginebra MP, Fernandez E, De Maeyer EAP, Verbeeck RMH, Boltong MG, Ginebra J, et al. Setting reaction and hardening of an apatitic calcium phosphate cement. J Dent Res 1997;76:905-912.

[141] Gbureck U, Grolms O, Barralet JE, Grover LM, Thull R. Mechanical activation and cement formation of α-tricalcium phosphate. Biomaterials 2003;24(23):4123-4131.

[142] Ginebra MP, Férnandez E, Boltong MG, Bermudez O, Planell JA, Driessens FCM. Compliance of an apatitic calcium phosphate cement with the short-term clinical requirements in bone surgery, orthopaedics and dentistry. Clin Mater 1994;17:99-104.

[143] Driessens FCM, Planell JA, Boltong MG, Khairoun I, Ginebra MP. Osteotransductive bone cements. Proc Inst Mech Eng Part H - J Eng Med 1998;212:427-435.

[144] Sarda S, Fernandez E, Llorens J, Martinez S, Nilsson M, Planell JA. Rheological properties of an apatitic bone cement during initial setting. J Mater Sci-Mater Med 2001;12:905-909.

[145] Bohner M, Malsy AK, Camire CL, Gbureck U. Combining particle size distribution and isothermal calorimetry data to determine the reaction kinetics of alpha-tricalcium phosphate-water mixtures. Acta Biomater 2006;2(3):343-348.

[146] Hofmann MP, Nazhat SN, Gbureck U, Barralet JE. Real-time monitoring of the setting reaction of brushite-forming cement using isothermal differential scanning calorimetry. J Biomed Mater Res B-Appl Biomater 2006;79:360-364.

[147] Nilsson M. Injectable calcium sulphate and calcium phosphate bone substitutes: Lund University, Faculty of Medicine, Lund, Sweden; 2003.

[148] Carlson J, Nilsson M, Fernandez E, Planell JA. An ultrasonic pulse-echo technique for monitoring the setting of CaSO4-based bone cement. Biomaterials 2003;24(1):71-77.

[149] Liu C, Huang Y, Zheng H. Study of the Hydration Process of Calcium Phosphate Cement by AC Impedance Spectroscopy. J Amer Ceram Soc;82:1052 - 1057.

[150] Grover LM, Gbureck U, Young AM, Wright AJ, Barralet JE. Temperature dependent setting kinetics and mechanical properties of β-TCP–pyrophosphoric acid bone cement. J Mater Chem 2005;15:4955-4962.

[151] Bohner M, Baroud G. Injectability of calcium phosphate pastes. Biomaterials 2005;26(13):1553-1563.

[152] Burguera EF, Xu HHK, Sun LM. Injectable calcium phosphate cement: Effects of powder-to-liquid ratio and needle size 9. J Biomed Mater Res B-Appl Biomater 2008;84:493-502.

[153] Burguera EF, Xu HHK, Weir MD. Injectable and rapid-setting calcium phosphate bone cement with dicalcium phosphate dihydrate. J Biomed Mater Res B-Appl Biomater 2006;77:126-134.

[154] Habib M, Baroud G, Gitzhofer F, Bohner M. Mechanisms underlying the limited injectability of hydraulic calcium phosphate paste. Acta Biomater 2008;4:1465-1471

[155] del Valle S, Miño N, Muñoz F, González A, Planell JA, Ginebra MP. In vivo evaluation of an injectable Macroporous Calcium Phosphate Cement. J Mater Sci - Mater Med 2007;18:353-361

[156] Ishikawa K, Asoaka K. Estimation of ideal mechanical strength and critical porosity of calcium phosphate cement. J Biomed Mater Res 1995;29:1537-1543.

[157] Sarda S, Férnandez E, Nilson M, Balcells M, Planell JA. Kinetic effect of citric acid influence on calcium phosphate bone cements as water reducing agent. J Biomed Mater Res 2002;61:652-659.

[158] Barralet JE, Grover LM, Gbureck U. Ionic modification of calcium phosphate cement viscosity. Part II: hypodermic injection and strength improvement of brushite cement. Biomaterials 2004;25:2197-2203.

[159] Chow LC, Hirayama S, Takagi S, Parry E. Diametral tensile strength and compressive strength of a calcium phosphate cement: Effect of applied pressure. J Biomed Mater Res 2000;53:511-517.

[160] Ishikawa K, Takagi S, Chow LC, Ishikawa Y. Properties and mechanisms of fast-setting calcium phosphate cements. J Mater Sci: Mater Med 1995;6:528-533.

[161] Ikenaga M, Hardouin P, Lemaitre J, Andrianjatovo H, Flautre B. Biomechanical characterization of a biodegradable calcium phosphate hydraulic cement: a comparison with porous biphasic calcium phosphate ceramics. J Biomed Mater Res - Appl Biomater 1998; 40:139-144.

[162] Miyamoto Y, Ishikawa K, Fukao H, Sawada M, Nagayama M, Kon M, et al. In-Vivo Setting Behavior of Fast-Setting Calcium-Phosphate Cement. Biomaterials 1995;16:855-860.

[163] Miyazaki K, Horibe T, Anntonucci JM, Takagi S, C. CL. Polymeric calcium phosphate cements: setting reaction modifiers. Dent Mater 1993;9:46-49.

[164] Miyazaki K, Horibe T, Anntonucci JM, Takagi S, Chow LC. Polymeric calcium phosphate cements: analysis of reaction products and properties. Dent Mater 1993;9:41-45.

[165] Santos L, Oliveira L, Rigo E, Carrodeguas R, Boschi A, De Arruda A. Influence of polymeric assitives on the mechanical properties of α-tricalcium phosphate cement. Bone 1999;25:99-102.

[166] Mickiewicz R, Mayes A, Knaack D. Polymer-calcium phosphate cement composites for bone substitutes. J Biomed Mater Res 2002;61:581.

[167] Barralet E, Gaunt T, Wright AJ, Gibson IR, Knowles JC. Effect of porosity reduction by compaction on compressive strength and microstructure of calcium phosphate cement J Biomed Mater Res B 2002;63:1-9.

[168] Zhang Y, Xu H, Takagi S, Chow L. In-situ hardening hydroxyapatite-based scaffold for bone repair. J Mater Sci: Mater Med 2006;17:437-445.

[169] Bohner M. Physical and chemical aspects of calcium phosphates used in spinal surgery. Eur Spine J 2001;10 114-121.

[170] Fukase Y, Eanes ED, Takagi S, Chow LC, Brown WE. Setting Reactions and Compressive Strengths of Calcium Phosphate Cements. J Dent Res 1990;69:1852.

[171] Tas AC. Synthesis of biomimetic Ca-hydroxyapatite powders at 37 degrees C in synthetic body fluids 1. Biomaterials 2000;21(14):1429-1438.

[172] Kokubo T. Bone-bounding Biomaterials: Healthcare Communications, Leiderdrop, The Netherlands, 1992.

[173] Ueno A, Miwa Y, Miyoshi K, Horiguchi T, Inoue H, Ruspita I, et al. Constitutive expression of thrombospondin 1 in MC3T3-E1 osteoblastic cells inhibits mineralization. J Cel Phys 2006;209:322-332.

[174] Kokubo T, Takadama H. How useful is SBF in predicting in vivo bone bioactivity?. Biomaterials 2006;27:2907-2915.

[175] Ohtsuki C, Aoki Y, Kokubo T, Fujita Y, Kotani S, Yamamuro T. Bioactivity of limestone and abalone shell. Transactions of the 11th annual meeting of Jap Soc Biomater 1989; p. 12.

[176] Ohtsuki C, Kokubo T, Neo M, Kotani S, Yamamuro T, Nakamura T, et al. Bone-bonding mechanism of sintered β-3CaO-P_2O_5. Phos Res Bull 1991;1:191-196.

[177] Kotani S, Fujita Y, Kitsugi T, Nakamura T, Yamamuro T. Bone bonding mechanism of β-tricalcium phosphate. J Biomed Mater Res 1991;25:1303-1315.

[178] Neo M, Nakamura T, Ohtsuki C, Kokubo T, Yamamuro T. Apatite formation of three kinds of bioactive materials at early stage in vivo: a comparative study by transmission electron microscopy. J Biomed Mater Res 1993;27:999-1006.

[179] Fujita Y, Yamamuro T, Nakamura T, Kotani S. The bonding behavior of calcite to bone. J Biomed Mater Res 1991;25:991-1003.

[180] Apelt D, Theiss F, El-Warrak AO, Zlinszky K, Bettschart-Wolfisberger R, Bohner M, et al. In vivo behavior of three different injectable hydraulic calcium phosphate cements. Biomaterials 2004;25:1439-1451.

[181] Ooms EM, Wolke JG, van de Heuvel MT, Jeschke B, Jansen JA. Histological evaluation of the bone response to calcium phosphate cement implanted in cortical bone. Biomaterials 2003;24:989-1000.

[182] LeGeros RZ, LeGeros JP. Calcium phosphate Bioceramics: Past, present and future. Bioceramics 15 2003;240-2:3-10.

[183] Schliephake H, Gruber R, Dard M, Wenz R, Scholz S. Repair of calvarial defects in rats by prefabricated hydroxyapatite cement implants. J Biomed Mater Res A 2004;69:382-390.

[184] Yuan HP, Li YB, de Bruijn JD, de Groot K, Zhang XD. Tissue responses of calcium phosphate cement: a study in dogs. Biomaterials 2000;21:1283-1290.

[185] Ambard AJ, Mueninghoff L. Calcium phosphate cement: review of mechanical and biological properties. J Prosthodont 2006;15:321-328.

[186] Lewis G. Injectable bone cements for use in vertebroplasty and kyphoplasty: State-of-the-art review. J Biomed Mater Res B – Appl Biomater 2006;76:456-468.

[187] Wang X, Ye JD, Wang Y. Influence of a novel radiopacifier on the properties of an injectable calcium phosphate cement. Acta Biomaterialia 2007;3:757.

[188] Watanabe M, Tanaka M, Sakurai M, Maeda M. Development of calcium phosphate cement. J Eur Ceram Soc 2006;26:549-552.

[189] Carey LE, Xu HHK, Simon CG, Takagi S, Chow LC. Premixed rapid-setting calcium phosphate composites for bone repair. Biomaterials 2005;26(24):5002-5014.

[190] Xu HH, Takagi S, Quinn JB, Chow IC. Fast-setting calcium phosphate scaffolds with tailored macropore formation rates for bone regeneration. J Biomed Mater Res A 2004;68:725-734.

[191] Bohner M, Merkle HP, Lemaitre J. In vitro aging of a calcium phosphate cement. J Mater Sci -Mater Med 2000;11(3):155-162.

[192] Xu HH, Quinn JB, Takagi S, Chow LC. Processing and properties of strong and non-rigid calcium phosphate cement. J Dent Res 2002;81:219-224.

[193] Wang XP, Ye JD, Wang H. Effects of additives on the rheological properties and injectability of a calcium phosphate bone substitute material. J Biomed Mater Res B-Appl Biomater 2006;78:259-264.

[194] Kuhn K-D. Bone cements: Up-to-date comparison of physical and chemical properties of commercial materials: Springer-Verlag, Berlin, 2000.

[195] Otsuka M, Matsuda Y, Yu D, Wong J, Fox J, Higuchi W. A novel skeletal drug delivery system for anti-bacterial drugs using self-setting hydroxyapatite cement. Chem Phar Bull 1990;38:3500-3502.

[196] Takechi M, Miyamoto Y, Ishikawa K, Nagayama M, Kon M, Asaoka K, et al. Effects of added antibiotics on the basic properties of anti-washout-type fast-setting calcium phosphate cement. J Biomed Mater Res 1998;39:308-316.

[197] Chow L, Takagi S, Costantino P, Friedman C. Self-setting calcium phosphate cements. Matl Res Symp Proc 1991;179:3-24.

[198] Lemaître J. Ciments hydrauliques phospho-calciques: developpements recents et applications potentielles. Inn Tech Biol Med 1995;16:109-120.

[199] Lidgren L, Drar H, Möller J. Strength of polymethylmethacrylate increased by vacuum mixing. Acta Orthop Scand 1984;55:536-541

[200] Lidgren L, Bodelind B, Möller J. Bone cement improved by vacuum mixing and chilling. Acta Orthop Scand 1987;58:27-32.

[201] Lacout JL, Mejdoubi E, Hamad. M. Crystallization mechanisms of calcium phosphate cement for biological uses J Mater Sci - Mater Med 1996;7:371-374.

[202] Friedman CD, Costantino PD, Takagi S, Chow LC. BoneSource (TM) hydroxyapatite cement: A novel biomaterial for craniofacial skeletal tissue engineering and reconstruction. Journal of Biomedical Materials Research 1998 WIN;43(4):428-432.

[203] Bohner M, Theiss F, Apelt D, Hirsiger W, Houriet R, Rizzoli G, et al. Compositional changes of a dicalcium phosphate dihydrate cement after implantation in sheep. Biomaterials 2003 Sep;24(20):3463-3474.

[204] Higgins TF, Dodds SD, Wolfe SW. A biomechanical analysis of fixation of intra-articular distal radial fractures with calcium-phosphate bone cement. Journal of Bone and Joint Surgery-American Volume 2002;84A(9):1579-1586.

[205] Thordarson DB, Hedman T, Yetkinler DN, Eskander E, Lawrence B, Poser RD. Superior compressive strength of calcaneus fracture construct augmented with remodelable cancellous bone cement J Biomech 1998;1:3.

[206] Turner TM, Urban RM, Singh K, Hall DJ, Renner SM, Lim TH, et al. Vertebroplasty comparing injectable calcium phosphate cement compared with polymethylmethacrylate in a unique canine vertebral body large defect model. Spine Journal 2008 May-Jun;8(3):482-487.

[207] Stankewich C, Swiontkowski MF, Tencer AF, Yetkinler DN, Poser RD. Augmentation of femoral neck fracture fixation with an injectable calcium-phosphate bone mineral cement. J Orthop Res 1996;14:786.

[208] Goodman SB, Bauer TW, Carter D, Casteleyn PP, Goldstein SA, Kyle RF, et al. Norian SRS cément augmentation in hip fracture treatment. Clin Orthop 1998;348:42.

[209] Kamerer DB, Friedman CD, Costantino PD, Snyderman CH, Hirsch BF. Hydroxyapatite cement: A new method for achieving watertight closure in transtemporal surgery. Amer J Otol 1994;15:47-49.

[210] Sliindo M, Costantino P, Friedman C, Chow L. Facial skeletal augmentation using hydroxyapatite cement cranioplasty. Arch Otolaryngol Head Neck Surg 1993;119:185

[211] Kveton JF, Friedman CD, Costantino PD. Indications for hydroxyapatite cement reconstruction in lateral skull base surgery. Amer J Otol 1995;16:465-469.

[212] Noetzel J, Özer K, Reisshauer BH, Anil A, Rössler R, Neumann K, et al. Tissue responses to an experimental calcium phosphate cement and mineral trioxide aggregate as materials for furcation perforation repair, a histological study in dogs. Clin Oral Invest 2006;10:77-83.

[213] Zhang W, Walboomers XF, Jansen JA. The formation of tertiary dentin after pulp capping with a calcium phosphate cement, loaded with PLGA microparticles containing TGF-β1. J Biomed Mater Res A 2008;85:439-444.

[214] Comuzzi L, Ooms E, Jansen JA. Injectable calcium phosphate cement as a filler for bone defects around oral implants, an experimental study in goats. Clin Oral Implants Res 2002;13:304-311

[215] Chaung HM, Hong CH, Chiang CP, Lin SK, Kuo YS, Lan WH, et al. Comparison of calcium phosphate cement mixture and pure calcium hydroxide as direct pulpcapping agents. J Formos Med Assoc 1996;95:545-550.

[216] El-Ghannam A, Ahmed K, Omran M. Nanoporous delivery system to treat osteomyelitis and regenerate bone: gentamicin release kinetics and bactericidal effect. J Biomed Mater Res B: Appl Biomater 2005;73:277-284.

[217] Meraw SJ, Reeve CM, Lohse CM, Sioussat TM. Treatment of perimplant defects with combination growth factor cement. J Periodont 2000;71:8-13.

2 Preparation and characterization of brushite-forming calcium phosphate cements doped with Mg and Sr

Implanted bone tissues take benefits from the initial setting characteristics of the cements that give, in an acceptable clinical time, a suitable mechanical strength for a shorter tissue functional recovery. The major advantages of the cements include a fast setting time, excellent mouldability, injectability, and strength comparable to that of trabecular bone. The incorporation of different ions, such as magnesium (Mg) and strontium (Sr) into the structure of CPCs improves their biological responses upon implantation and might also favourably affect other properties.

Partial substitution of calcium (Ca) by Sr on β-TCP powders by an aqueous precipitation was achieved and reported in paper 2.1. The successful incorporation of Sr was proved by the observed increase of the lattice volume via XRD analysis the powders.

The main aim of the paper presented in section 2.2. was to study the influence of the setting liquid and the liquid-to-powder ratio on rheological and mechanical properties of a new Mg-substituted CPC, where the powder was obtained through aqueous precipitation.

In the paper of section 2.3, the setting behaviour of brushite-forming Sr-substituted α-TCP cements by *in situ* XRD and isothermal calorimetry techniques, is presented. The bioactivity through SBF tests was also studied and presented. SBF is a relatively easy method to simulate the environment in the human body, which has nearly the same chemical composition as blood plasma.

Combining the excellent properties of novel brushite-forming Mg- and Sr-substituted α-TCP cements (section 2.2 and 2.3) with the need of injectability to fill bone lesions and cracks to strengthen the bone, the paper in section 2.4. is focused on the study of the injectability properties of these substituted bone cements.

2.1 Formation of Strontium-Stabilized β-Tricalcium Phosphate from Calcium-Deficient Apatite

S. Kannan, S. Pina, and J. M. F. Ferreira

Dept. of Ceramics and Glass Engineering, University of Aveiro,
CICECO, 3810-193 Aveiro, Portugal.

J Amer Ceram Soc (2006) 89: 3277–3280

Abstract

A series of strontium-stabilized β-tricalcium phosphate (β-TCP) was prepared via the aqueous precipitation method, and characterized by X-ray diffraction and infrared Fourier spectrometer techniques. The general principle of preparing calcium-deficient apatite and thereby heat-treating the resultant apatite above 700ºC to form single-phase β-TCP was attempted to create strontium substituted β-TCP. The results have proved that single phase β-TCP could be formed with the substituted strontium with only an influence on the increase in lattice constants with an increase in the concentration of strontium. Further, it is also stated from the present findings that strontium has a specific role in the crystallinity of the resultant β-TCP.

Keywords: *Ca-deficient apatite, Strontium, β-TCP, Aqueous precipitation*

1. Introduction

Beta-tricalcium phosphate [β-TCP, β-$Ca_3(PO_4)_2$], which possesses stoichiometry similar to amorphous biologic precursors to bone mineral, exhibits a Ca/P molar ratio of 1.5. β-TCP has been shown to be resorbed *in vivo* [1], with new bone growth replacing the resorbed implanted β-TCP. This property represents a significant advantage of β-TCP compared with other biomedical materials that are not resorbed and replaced by natural bone. Recent years have witnessed the incorporation of strontium (Sr) into the apatite structure due to its presence in calcified bone. The essential characteristics and the role of strontium in bone mineral are: (i) it has a specific role in osteoporosis [2–4]; (ii) it has an equal share with ionic calcium in the physiological pathway [5]; and (iii) it can be deposited into the mineral structure of bone, especially into regions of high metabolic turnover [6]. As a matter of fact, the beneficial effect of low doses of stable strontium in the treatment of osteoporosis, characterized by low bone mass, fracture risk, and enhanced bone fragility, was discovered almost half a century ago [7].

Research reports have proved that strontium can be substituted in the hydroxyapatite (HA) structure prepared via different synthetic routes [8–10]. However, the research regarding the formation of single-phase strontium-substituted β-TCP has witnessed scarce documentation. A recent work reported by Bigi et al. [11] has elucidated on the formation of Sr-stabilized β-TCP through a solid-state reaction by heating β-TCP and α-$Sr_3(PO_4)_2$ for 15 h at 1000ºC. In general, a β-TCP ceramic can be prepared by a number of different routes [12–14]. The most common method is a ‘‘Wet-chemical’’ synthesis, which results in the formation of a Ca-deficient apatite (or non-stoichiometric apatite). Upon heating (calcining) to 700º – 800ºC, the Ca-deficient apatite will transform into a low-temperature polymorph of β-TCP, with the loss of water as described by Eq. (1).

$$Ca_9(HPO_4)(PO_4)_5(OH) \rightarrow 3Ca_3(PO_4)_2 + H_2O \qquad (1)$$

This methodology was adapted to prepare strontium-stabilized β-TCP by introducing a precursor of strontium into the reaction system. A series of

compositions was prepared, and the influence of Sr content on the crystallinity of β-TCP was evaluated in the present study.

2. Experimental Procedure

2.1 Powder Preparation

Reagent grade Calcium nitrate tetrahydrate [($Ca(NO_3)_2.4H_2O$, Vaz Pereira-Portugal], Strontium nitrate [$Sr(NO_3)_2$, Riedel-de-Haen] and diammonium hydrogen phosphate [$(NH_4)_2HPO_4$, Vaz Pereira-Portugal] were used as starting chemical precursors respectively for calcium, strontium and phosphorus. For the preparation of Ca-deficient apatites, a predetermined Ca/P molar ratios (concentrations of the precursors are depicted in Table 1) were set by the slow addition of $(NH_4)_2HPO_4$ solution to the continuously stirred (1000 rpm) solution of $Ca(NO_3)_2.4H_2O$. A predetermined concentration of $Sr(NO_3)_2$ was added slowly to the above solution containing calcium and phosphorus ions. The pH of the mixed solution / suspension was increased to 7.4 and maintained at this value by adding the required amounts of 8 M ammonium hydroxide (NH_4OH) solution. After the completion of addition, the reaction was performed at 90℃ for 2 hours under constant stirring conditions (1000 rpm). A Ca-deficient apatite of Ca/P molar ratio of 1.5, simultaneously without added strontium was prepared under the same conditions to compare the results. The precipitated suspension was poured out from the reactor and precipitates were separated through vacuum filtration and dried at 80℃ overnight. The dried cakes were groun d to fine powders, sieved through a mesh size of 200 μm and used for characterization studies.

Table 1: Molar concentrations of the precursors Ca, P and Mg used in the synthesis. Phosphorus precursors are same at a constant value of 0.6 M for all the reactions. (Ca+Sr)/P molar ratio of 1.5 are same for all reaction conditions

Sample code	Molar concentrations of the precursors			Wt.% of incorporated Sr
	Ca	Sr	Ca/P ratio	
Tcp	0.900	0.000	1.50	-
Sr-tcp1	0.882	0.018	1.47	1.54
Sr-tcp2	0.864	0.036	1.44	3.17
Sr-tcp3	0.846	0.054	1.41	4.76
Sr-tcp4	0.828	0.072	1.38	6.34
Sr-tcp5	0.810	0.090	1.35	7.83
Sr-tcp6	0.780	0.120	1.30	10.48
Sr-tcp7	0.720	0.180	1.20	15.72
Sr-tcp8	0.600	0.300	1.00	26.26

2.2 Powder Characterization

The as-prepared powders were calcined at different temperatures ranging from 600º to 1100ºC in a Thermolab furnace (Pt30%Rh/ Pt6%Rh-thermocouple Águeda, Portugal) at a heating rate of 5ºC/min to achieve a predetermined temperature range and a dwelling time for 2 h, and again cooled to room temperature at the rate of 5ºC/min. Phase identification of the powders before and after calcination was determined by X-ray diffraction (XRD, using a high-resolution

Rigaku Geigerflex D/Mac, C Series diffractometer, Tokyo, Japan). CuKα radiation (λ = 1.5406 nm) produced at 30 kV and 25 mA scanned the diffraction angles (2θ) between 20º and 50º with a step size of 0.02º 2θ per second. Crystallographic identification of the phases of synthesized powders was accomplished by comparing the experimental XRD patterns with standards compiled by the Joint Committee on Powder Diffraction Standards (JCPDS), which were card # 09-0169 for β-TCP. Lattice constants for β-TCP phase composition were determined by least square refinements from the well-determined positions of the most intense reflections. The reflections of the planes (1010), (214), (300), (0210), (220) and (4010) were used for calculation. The volume V of the rhombohedral unit cell was determined for each β-TCP formulation from the relation $V = 0.8660 \times a^2 \times c$. The average crystallite size of the final β-TCP composition was calculated using the Scherrer formula. The peak width of the (0 2 10) reflection of β-TCP samples were used in the calculations. Infrared spectra of the as prepared powders and powders calcined at different temperatures were obtained using an Infrared Fourier Spectrometer (FT-IR, model Mattson Galaxy S-7000, 32 scans and resolution 4 cm^{-1}). For this purpose each powder was mixed with KBr in the proportion of 1/150 (by weight) for 15 min and pressed into a pellet using a hand press. Elemental analyses for the presence of Ca, Sr and P were made using X-ray fluorescence spectroscopy (Philips PW2400 X-Ray Fluorescence Spectrometer). The vacuum of the chamber was lower than two Pascal. The error associated to each chemical element could be determined as ± 1 of the last digit of the measured values.

3.1 Results and Discussion

3.1 Formation of Sr-stabilized β-TCP

The XRD patterns of the Sr-tcp1 powder calcined at different temperatures are presented in Fig. 1. In fact all the other Sr substituted calcium deficient apatite

powders have indicated similar type of XRD and FT-IR patterns irrespective of the added strontium during the reaction.

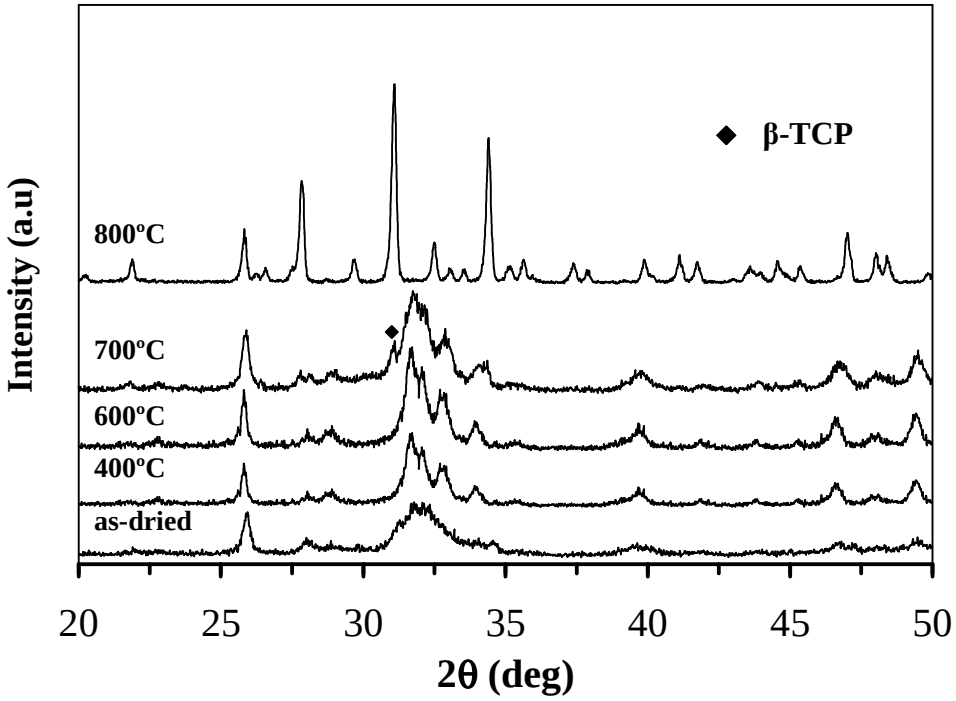

Fig. 1: Powder X-ray diffraction pattern for Sr-tcp1 powder heat treated at different temperatures. All diffraction planes at 800ºC correspond to pure β-TCP phase. Unmarked peaks at temperatures other than 800ºC corresponds to HAP phase

The as prepared powder has indicated the formation of poorly crystalline apatite phase characterized by the broad diffraction bands. It is obvious that substitution of Sr did not found to affect the diffraction pattern of as prepared powders. This results are in accordance with the previously reported results that the XRD pattern of an as-precipitated apatite powder can resemble that of HAP even though the Ca/P ratio is greater or less than the stoichiometric molar ratio of 1.67 for HAP [15,16]. The infrared spectra for the Sr-tcp1 powder heat treated at different temperatures are presented in Fig. 2.

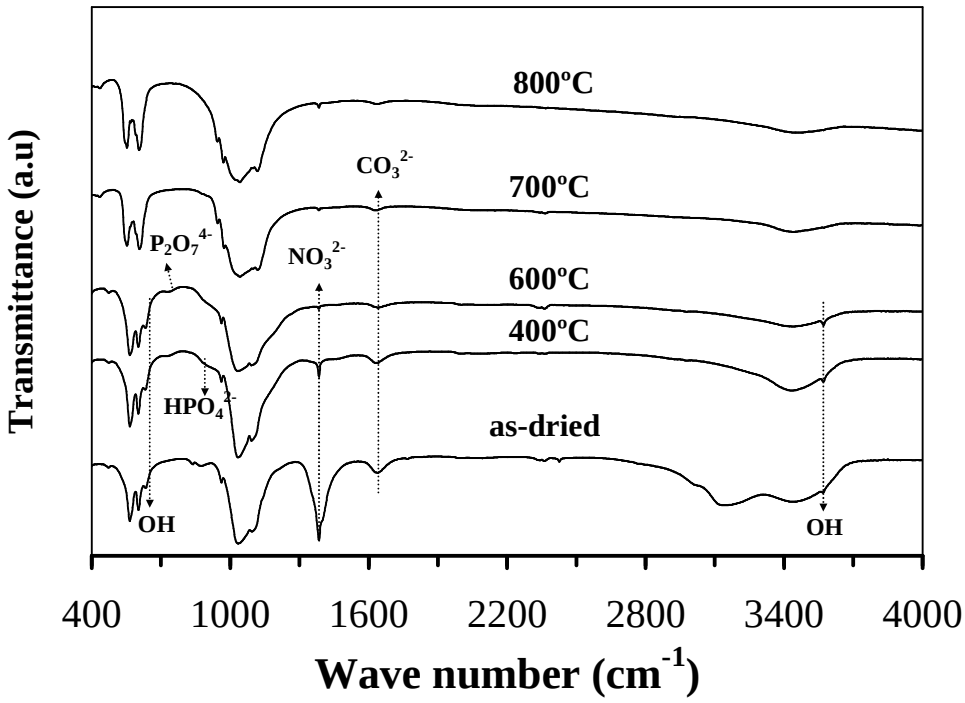

Fig. 2: FT-IR spectra for Sr-tcp1 powder heat treated at different temperatures

The spectra obtained in an as-dried condition have also confirmed the apatite phase formation with the observed fundamental vibrational modes of PO_4 group at 475, 574, 609, 966 and 1020-1120 cm^{-1}. The weak bands respective of OH group of HAP phase could also be witnessed in the infra red spectra at the region around 630 and 3570 cm^{-1} in the as-dried powder. The presence of adsorbed water (in the region around 3300-3600 cm^{-1}), carbonates (at region 1660 cm^{-1}) that is due to the adsorbed species remaining from the aqueous precipitation [17] and nitrates (1320-1480 cm^{-1}) can be confirmed in the FT-IR spectra of as-dried powders. The presence of nitrates in the as synthesized powders tends to agree with observations made in a previous study [18]. However, no sufficient information could be gained regarding the influence of Sr in the as prepared powder since the observed phases exhibit a low crystallinity leading to a lower peak definition in the XRD pattern.

Upon heat treatment, the gradual loss of adsorbed water, nitrates and carbonates from the as-dried powders are evidenced by the corresponding decrease in the FT-IR peaks resolution in the region around 1320-1480 cm^{-1}, 1660 cm^{-1} and 3400-

3600 cm^{-1} (Fig. 2) of the spectra obtained at 400ºC. The presence of both hydrogenophosphate ions (HPO_4^{2-}) at 870 cm^{-1} and OH groups [3570 cm^{-1} (stretching mode) and 630 cm^{-1} (bending mode)] has been witnessed in the infra red spectra recorded at 400ºC. XRD pattern obtained at 400ºC have also strong coincidence with FT-IR spectra. These results confirm the formation of Sr substituted calcium deficient apatite as defined by the expression (2) given below:

$$(CaSr)_{10-x}(HPO_4)_x(PO_4)_{6-x}(OH)_{2-x} \quad (2)$$

Heat treatment at 800ºC has witnessed the formation of single phase β-TCP as confirmed by the XRD pattern presented in Fig. 1. FT-IR patterns presented in Fig. 2 also confirm the disappearance of peaks for OH groups at 630 cm^{-1} (vibrational mode) and at 3570 cm^{-1} (stretching frequency). The vibrational modes of PO_4 tetrahedra of β-TCP phase and the dissappearence of CO_3 bands are evident from the FT-IR spectra after calcination above 800ºC. This fact is in good agreement with the findings of Gibson et al [19], who have reported the occurrence of a similar transformation at this temperature range for a powder prepared via aqueous precipitation method.

3.2 Influence of Strontium

Fig. 3 presents the XRD pattern of the different concentrations of Sr substituted β-TCP after heat treatment at 1100ºC. The influence of Sr can be confirmed by the observed sharp shift in the 2θ and the d-spacing values of various compositions in comparison to pure β-TCP. Data of elemental analysis reported in Table 1 also confirm the presence of Sr in all the powders. It should be noted that for all the compositions, the precursors (Ca+Sr)/P molar ratio during the course of synthesis was adjusted to 1.5 to ensure the incorporation of Sr into β-TCP.

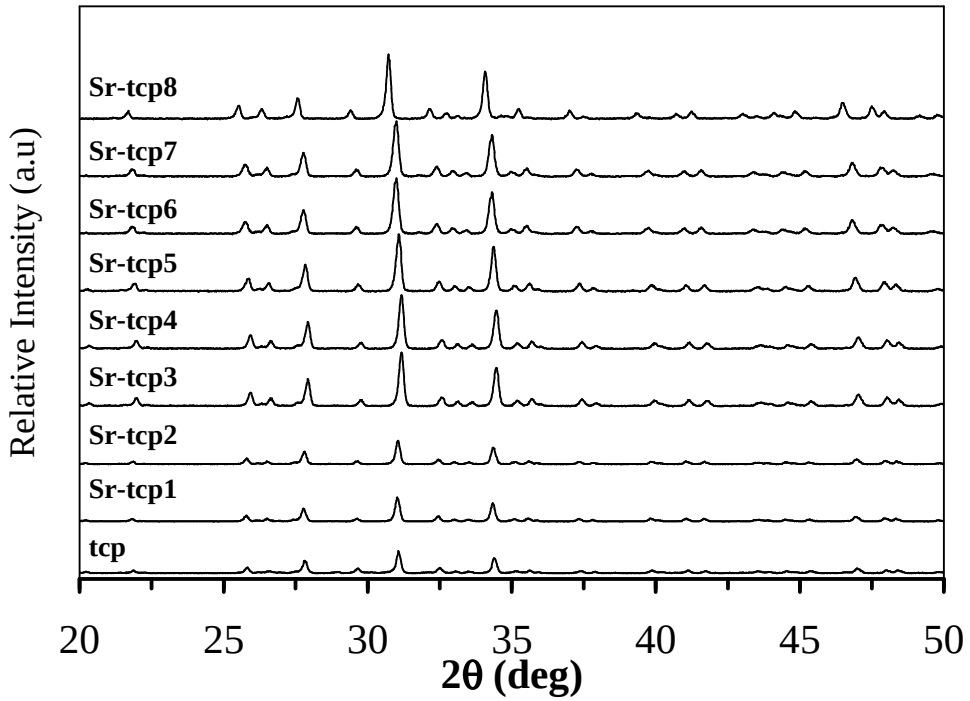

Fig. 3: XRD patterns for the different Sr substituted β-TCP powder after heat treatment at 1100ºC

Hence the role of Sr in stabilizing the β-TCP phase can be represented by equation (3) given below:

$$Ca_{9-x}Sr_x(HPO_4)(PO_4)_5(OH) \quad \rightarrow \quad 3(Ca_{3-\frac{x}{3}}Sr_{\frac{x}{3}})(PO_4)_2 \; + \; H_2O \qquad (3)$$

The graphical representation of lattice constants with the influence of Sr concentration in the β-TCP phase presented in Figs. 4 and 5 confirms the formation of rhombohedral β-TCP space group for all the compositions. From Fig. 4 it is clear that the incorporation of Sr in β-TCP has led to the significant expansion in both *a*- and *c*- axis with the increase in concentration of Sr in β-TCP. The reason is due to the greater ionic radius of strontium ion (1.13 Å) towards Ca^{2+} (0.96 Å) that has led to the expansion of unit cell. Regarding the substitution of

elements, it has been previously described that β-TCP could be stabilized by the inclusion of small cations without significant alteration in its rhombohedral structure [20,21]. In fact, Bigi et al. [11] has proved that β-TCP can host up to 80 atom % of strontium with a linear enlargement of the lattice constants, which suggests that strontium incorporation does not provoke a remarkable rearrangement of the unit cell. This fact is proved by the present results. It is also clear from the present results that substitution of Sr^{2+} ion in β-TCP structure have greater influence on the crystallinity. The small crystallite size values (Fig. 5) with the corresponding increase in the strontium concentration in the β-TCP structure is supported by this fact.

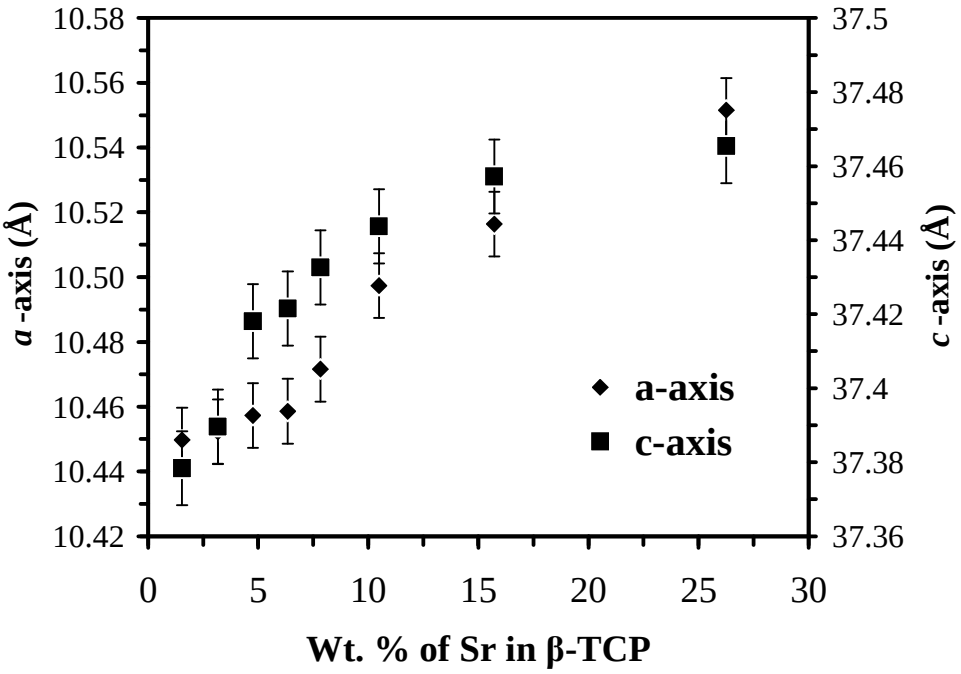

Fig. 4: Influence of lattice *a*- and *c*- axis parameters with respect to the different content of Sr in β-TCP structure. Lattice parameters for pure β-TCP (JCPDS file card no. # 09-169) (*a*=10.429, *c*= 37.38).

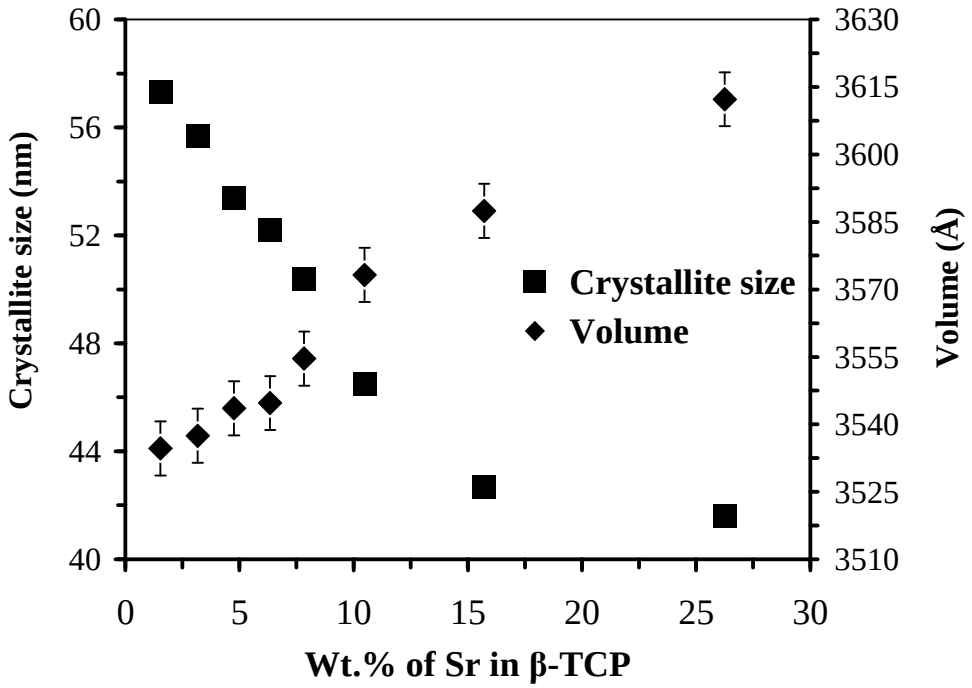

Fig. 5: Influence of unit cell volumes and crystallite sizes with respect to the different content of Sr in β-TCP structure. Cell volume for pure β-TCP (V = 3533.70).

4. Conclusion

The present study proves that a simple aqueous precipitation technique can be employed to form single phase strontium stabilized β-TCP by heating Ca-deficient apatite. The transformation mechanism that occurred at 800ºC to form single phase β-TCP with substituted Sr is similar to that of Ca-deficient apatite of Ca/P molar ratio=1.5 to form pure β-TCP without any substituted elements. The present study also confirms a linear increase in the lattice constant values (*a*-axis, *c*-axis and volume) with the increase in the concentration of strontium that is accommodated in the β-TCP structure. Additionally, the substitution of strontium has also greater influence in the crystallinity of β-TCP phase.

Acknowledgements

Thanks are due to the Portuguese Foundation for Science and Technology for the for the fellowship grants of S. Kannan (SFRH/BPD/18737/2004) and S. Pina (SFRH/BD/21761/2005).

References

[1] Gatti A.M., Zatfe D. and Poli G.P. Behaviour of tricalcium phosphate and hydroxyapatite granules in sheep bone defects. Biomaterials 1990;11:513-517.

[2] Boivin G. and Meunier P.J. The mineralization of bone tissue: a forgotten dimension in osteoporosis research. Osteoporos Int 2003;14:S19 –S24.

[3] Christoffersen J., Christoffersen M.R., Kolthoff N. and Barenholdt O. Effects of strontium ions on growth and dissolution of hydroxyapatite and on bone mineral detection. Bone 1997;20:47–54.

[4] Reginster J.Y., Deroisy R. and Jupsin I. Strontium ranelate: a new paradigm in the treatment of osteoporosis. Drugs Today 2003;39:89–101.

[5] Blake G.M., Zivanovic M.A. and Mcewan A.J. Sr-89 therapy strontium kinetics in metastatic bone disease. J Nucl Med 1986;27:1030–1035.

[6] Blake G.M., Zivanovic M.A. and Mcewan A.J. Sr-89 strontium kinetics in disseminated carcinoma of the prostate. Euro J Nucl Med 1986;2:447–451.

[7] Shorr E. and Carter A.C. The usefulness of strontium as an adjuvant to calcium in the remineralization of the skeleton in man. Bull Hosp Joint Dis Orthop Inst 1952;13: 59–63.

[8] Fowler B.O. Infrared studies of apatites. II: Preparation of normal and isotopically substituted calcium, strontium and barium hydroxyapatites and spectra-structure-composition correlations. Inorg Chem 1974;13:207-214.

[9] Sudarsanan K. and Young R.A. Structure of strontium hydroxide phosphate, $Sr_5(PO_4)_3OH$. Acta Cryst 1972;B28:3668-3670.

[10] Kim H-W., Noh Y-H., Kong Y-M., Kang J-G. and Kim, H-E. Strontium substituted calcium phosphate biphasic ceramics obtained by a powder precipitation method. J Mater Sci Mater Med 2004;15:1129-1134.

[11] Bigi A., Foresti E., Gandolfi M., Gazzano M. and Roveri N. Isomorphous substitutions in β-tricalcium phosphate: The different effects of zinc and strontium. J Inorg Biochem 1997;66:259-265.

[12] Akao M., Aoki H., Kato K. and Sato A. Dense polycrystalline β-tricalcium phosphate for prosthetic applications. J Mater Sci 1982;17:343-346.

[13] Jarcho M., Salsbury R.L., Thomas M.B. and Doremus R.H. Synthesis and fabrication of β-tricalcium phosphate (whitlockite) ceramics for potential prosthetic applications. J Mater Sci 1979;14:142-150.

[14] Famery R. and Richard P.B. Preparation of α- and β-tricalcium phosphate ceramics, with and without magnesium addition. Ceram Int 1994;20:327-336.

[15] Kannan S., Lemos I.A.F., Rocha J.H.G. and Ferreira J.M.F. Synthesis and characterization of magnesium substituted biphasic mixtures of controlled hydroxyapatite/β-tricalcium phosphate ratios. J Solid State Chem 2005;178:3190-3196.

[16] Gibson I.R., Rehman I., Best S.M. and Bonfield W. Characterization of the transformation from calcium-deficient apatite to β-tricalcium phosphate. J Mater Sci Mater Med 2000;11:799-804.

[17] Gibson I.R., Best S.M. and Bonfield W. Chemical characterization of silicon-substituted hydroxyapatite. J Biomed Mater Res 1999;44:422-428.

[18] Raynaud S., Champion E., Assollant B. and Thomas P. Calcium phosphate apatites with variable Ca/P atomic ratio. I: Synthesis, characterisation and thermal stability of powders. Biomaterials 2002;23:1065-1072.

[19] Gibson I.R., Rehman I., Best S.M. and Bonfield W. Characterization of the transformation from calcium-deficient apatite to β-tricalcium phosphate. J Mater Sci Mater Med 2000;11:799-804.

[20] Bigi A., Falini G., Foresti E., Ripamonti A., Gazzano M. and Roveri N. Rietveld structure refinement of synthetic magnesium substituted β-tricalcium phosphate. Zeitschrift fur Kristallogr 1996;211:13-16.

[21] Bigi A., Foresti E., Gazzano M., Ripamonti A. and Roveri N. J Chem Res 1986; (S)170-171.

2.2 Influence of setting liquid composition and liquid-to-powder ratio on properties of a Mg-substituted calcium phosphate cement

S. Pina[1,2], S.M. Olhero[1], S. Gheduzzi[2], A.W. Miles[2], J.M.F. Ferreira[1]

[1] University of Aveiro Department of Ceramics and Glass Engineering,CICECO, 3810-193 Aveiro, Portugal.

[2] Centre of Orthopaedic Biomechanics, Department. of Mechanical Engineering, University of Bath, Bath, United Kingdom

Acta Biomaterialia 5 (2009) 1233–1240

Abstract

The influence of four variables on various properties of a Mg-substituted calcium phosphate cement (CPC) was investigated. The variables were the heat treatment temperature of the precipitated powders, the composition of the setting liquid, the liquid-to-powder ratio (LPR), and the time over which hardened specimens were cured in air. The properties analysed were the phase composition of the starting powder, the initial setting time, the evolution of the storage shear modulus (G') and the loss shear modulus (G'') with the cement paste curing time (t), and the compressive strength. The presence of α-TCP in CPC facilitated the setting and hardening properties due to its progressive dissolution and the formation of brushite crystals. As far as the liquid composition is concerned, in cases where citric acid was used, adding a rheology modifier (10 wt.% polyethylene glycol or 0.5 wt.% hydroxyl propylmethylcellulose) to the acid led to an increase in the initial setting time, while an increase in the acid concentration led to a decrease in the initial setting time. The initial setting time showed to be very sensitive towards the LPR. The evolution of G' and G'' with curing time reflected the internal structural changes of cement pastes during the setting process. The compressive strength of the wet hardened cement specimens with and without Mg increased with curing time increasing, being slightly higher in the case of Mg-substituted CPC. The results suggest that Mg-substituted CPC holds a promise for uses in orthopaedic and trauma surgery such as for filling bone defects.

Keywords: *Magnesium; Calcium phosphate; Cement; Rheology, Setting time.*

1. Introduction

Calcium phosphate (CaP) ceramics have gained clinical acceptance for bone substitution and augmentation due to their similarities with the mineral bone composition [1-3]. Among CaPs, tricalcium phosphate (TCP, $Ca_3(PO_4)_2$), a resorbable material, and hydroxyapatite (HA, $Ca_{10}(PO_4)_6(OH)_2$), a bioactive ceramic that induces bone formation on its surface, have received particular attention [4,5]. HA-based materials have excellent osteoconductivity and bone replacement capability and do not produce toxic inflammation or foreign body responses *in vivo* [6,7]. The bioactive properties of CaP and the ability of certain compositions to undergo hydraulic reactions when mixed with a suitable liquid, such as maleic acid or citric acid, make them suitable for use as pastes that can be moulded or injected into alveolar bone defects and remain in place until tissue ingrowth occurs [8]. The predominance of HA or brushite in the hardened cements has been used as a criterion to classify the cements. The number of studies dedicated to apatite cements that set under near neutral pH region is much higher than those devoted to brushite cements [9,10]. One reason is that HA based cements exhibit better mechanical properties. However brushite cements are of special interest due to their good biocompatibility and faster resorption rate *in vivo*. Moreover, brushite is metastable in physiological conditions and brushite based calcium phosphate cements (CPCs) possess faster setting reactions.

Recent developments have focused on injectable CPCs for various applications in orthopaedics and trauma surgery, such as treating vertebral compression fractures, fractures of the femoral neck and distal radius, and filling of bone defects that have limited accessibility or narrow cavities [5]. Recently, the substitution of ions, such as Mg ions, into the structure of CaPs has been investigated [6,11-14]. Although present in low levels in natural bone (0.55 wt.%) or tooth enamel (0.44 wt.%), Mg plays an essential role in the biological process due to its significant impact on the mineralization process and also its influence on HA crystal formation and growth [6,11-14]. Furthermore, a deficiency of Mg in bone has been suggested as a possible risk factor for osteoporosis in humans [11,15,16]. Therefore, Mg-substituted CaPs are expected to produce enhanced biological and

chemical responses in the body. To date, many reports on the properties of Mg-substituted CPCs have appeared [17, and references therein]. Lilley et al. [17] have shown that the presence of magnesium had a strong effect on cement composition and strength, namely by increasing the proportion of brushite and decreasing the compressive strength. According to these authors [17], Mg could be used to adjust the composition and rate of hydration of the cement. Mg has been also reported to have a stabilising role of non-crystalline CaPs, preventing crystallisation into other more stable CaP phases [18], in good agreement with an observed decrease of the hydrolysis extent of brushite [17]. However, none of the previously reported studies have shown the effects of Mg-substitution on the structural evolution of CPCs upon hydration using rheological measurements. Therefore, the present work aims at studying the effect of Mg-substitution on the setting behaviour, as accessed by rheological and other complementary measurements, and mechanical properties of CPCs. Furthermore, the effects of four main variables on the room-temperature phase composition of the starting powder, the initial setting time of the cement paste, the evolution of the storage modulus and loss shear modulus with cement paste curing time, and the compressive strength of a Mg-substituted CPC were investigated. The variables studied were: (i) the heat treatment temperature of the precipitated powder; (ii) the composition of the liquid used to prepare the cement (setting agents used, and the presence or absence of rheology modifiers); (iii) the liquid-to-powder ratio (LPR); and (iv) the time over which hardened specimens were cured in air.

From the perspective of the clinical uses, the initial setting time of a CPC cement paste and the flow properties are of paramount importance in many applications like *in situ* fracture fixation in orthopaedics, filling root canals and sealing furcation in endodontics and vertebroplasty. CPC should not harden too fast to allow moulding or injection and not harden too slowly to allow the surgeon to close the defect shortly after cement placement. Therefore, the CPC must have an optimal setting time in order to lead to an acceptable mechanical strength after hardening and to prevent migration of cement to undesirable sites.

2. Materials and Methods

The synthesis of the Mg-substituted cement powder was carried out according to a method that has been described in detail in a previous report [6]. Briefly, the powder was obtained by aqueous precipitation from calcium nitrate tetrahydrate [$Ca(NO_3).4H_2O$, Vaz Pereira-Portugal, Sintra, Portugal], diammonium hydrogen phosphate [$(NH_4)_2HPO_4$, Vaz Pereira-Portugal, Sintra, Portugal] and magnesium nitrate hexahydrate [$Mg(NO_3)_2.6H_2O$, Merck, Darmstadt, Germany] as the starting chemical precursors, respectively for calcium, phosphorus and magnesium. The precipitate was vacuum filtrated, dried at 110ºC and then heat treated for 2 h at 800ºC, 1100ºC and 1500ºC to study the evolution of the crystalline phase.

The calcined powders were ground under dry conditions in a planetary mill, using an agate jar of 250 mL with agate balls of 10 mm and 20 mm diameter, and a weight ratio of balls to powder = 3:1, and then passed through a sieve with a mesh size of 36 μm. The powders calcined at 800ºC and 1100ºC were ground for 1 h and 2 h, respectively, while the powder calcined at 1500ºC was ground for 4 h. The separated fine fractions of the α-TCP and Mg-TCP powders calcined at 1500ºC having average volume particle sizes of 19.2 μm and 14.8 μm, respectively, were used to prepare cement pastes with liquid-to-powder ratios (LPR) varying between 0.25 and 0.50 mL g^{-1}. Different concentrations of setting agents [disodium hydrogenophosphate (Na_2HPO_4) (2.5, 5.0 and 10.0 wt.%), citric acid (5.0, 10.0 wt.%, 15.0 wt.% and 20.0 wt.%) were used. The effects of adding 10.0 wt.% poly(ethylene glycol) (PEG) (200, Sigma) or 0.5 wt.% hydroxyl propyl methylcellulose (HPMC) (3.5-5.6 mPa s at 2% by mass in water, Sigma) to the citric acid solutions as rheology modifiers were tested. The selection of these setting agents and rheology modifiers as setting liquids was due to the non-toxic nature of these additives, which are commonly used in various foods, drinks and make-up products. Citrate exists in bone mineral and is believed to play an important role in the formation and/or dissolution of bone apatite. PEG was selected due to its non-toxicity and due to the fact that it is used as plasticizer in drugs. HPMC was selected for its ability to form viscous solutions thus improving the washout resistance of the CPC. The concentration of HPMC was limited to 0.5

wt.% because preliminary studies have shown that higher concentrations retarded the CPC conversion into HA [7].

The initial setting time of the cement pastes was determined using Vicat needle technique according to the ASTM C 187-98. One minute after placing the pastes into a glass plate stored at 37ºC in 100% humidity box, the indenter (100 g in mass, 1 mm diameter of the needle) was lowered vertically onto the surface of the cement. The indentation was repeated at intervals of 30 s until no more penetration was possible. The time at this point was taken as the initial setting time.

The setting behaviour of the cement pastes was monitored through the measurement of the viscoelastic properties (storage shear modulus, G', and loss shear modulus, G'') under oscillatory shear conditions using a controlled-stress rheometer (Bohlin C-VOR 150, Bohlin Ltd., Gloucestershire, UK) equipped with a 4º / 40 mm cone-and-plate sensor system. Stress-sweep tests were performed in the range between 1 and 1000 Pa to determine the upper limit of the linear viscoelastic response (LVR) and the shear stress range of the structural breakdown of the pastes. The mechanical spectra of the investigated pastes under the conditions of LVR were measured in the frequency range from 0.1 to 100 Hz at a fixed shear stress of 20 Pa. For each test, 2 g of powder was mixed with the setting liquid at the pre-determined LPR, for 1 min to form a homogeneous suspension at room temperature. The rheological measurement started 1 minute after mixing in order to assure the same rheological history during the preparation of all the cement pastes and ended when setting was complete.

The X-ray diffraction (XRD) technique was used to identify the crystalline phases formed upon calcining the starting powder at different temperatures and after hardening of the cement pastes. For this purpose, a high-resolution Rigaku Geigerflex D/Mac, C Series diffractometer was used with Cu Kα radiation (λ= 1.5406 Å) produced at 30 kV and 25 mA scanned the diffraction angles (2θ) between 20º and 50º with a step size of 0.02º 2θ per second. The phase composition of the hardened cements was calculated by Rietveld analysis using TOPAS 3.0 software (Bruker AXS, Germany). The microstructures of the hardened cements after storage at 37ºC in a 100% humidity box for 24 h were

obtained using a scanning electron microscope (SEM) (Hitachi S4100, Tokyo, Japan).

For the compressive strength tests, the cement pastes were cast into PTFE-moulds (6 mm diameter and 12 mm height) and stored in a 37ºC, 100% humidity box for 24 h. The cement specimens were then removed from the moulds and immersed in PBS solution at 37ºC for further 12 h, 24 h and 48 h. The specimens were loaded to failure at a crosshead displacement rate of 1 mm/min using a universal materials testing machine (Instron Series IX 4301, Instron, High Wycombe, England).

Results of initial setting time and compressive strength are expressed as the mean ± standard error of the mean of triplicate determinations. Statistical analysis was performed using the SPSS 16.0 software. Comparative studies of means were performed using one-way ANOVA followed by a post hoc test (Fisher projected least-significant difference) with a statistical confidence coefficient of 0.95; therefore, p values < 0.05 were considered significant.

3. Results and Discussion

The evolution of crystalline phases with the heat treatment temperature was studied in order to select the most suitable temperature that leads to the formation of the desired α-TCP phase that exhibits hydraulic power. Fig. 1 shows the XRD patterns of the Mg-substituted (MgTCP) powder calcined at 800ºC, 1100ºC and 1500ºC. It can be seen that a low crystalline phase of β-TCP was obtained after calcination of the starting powder at 800ºC. The intensity of the XRD peaks of this phase increased considerably, with increasing the heat treatment temperature.

Calcination at 1500ºC led to the formation of mostly α-TCP phase. The presence of Mg was found preferentially incorporated into the β-TCP phase [6]. However, the peaks corresponding to Mg-substituted β-TCP did not show exact matches with those of JCPDS PDF # 09-169, which, in fact have indicated considerable shift in the 2θ and d-spacing values of maximum intensity plane (0210) towards JCPDS PDF # 1-70-0682 of phase $Ca_{2.81}Mg_{0.19}(PO_4)_2$ [6]. This is confirmed in the

present work. Although it is well documented that Mg enhances the thermal stability of β–TCP phase [19,20], the present results show that practically all the β-TCP existing at lower temperatures has been transformed into the high temperature polymorph.

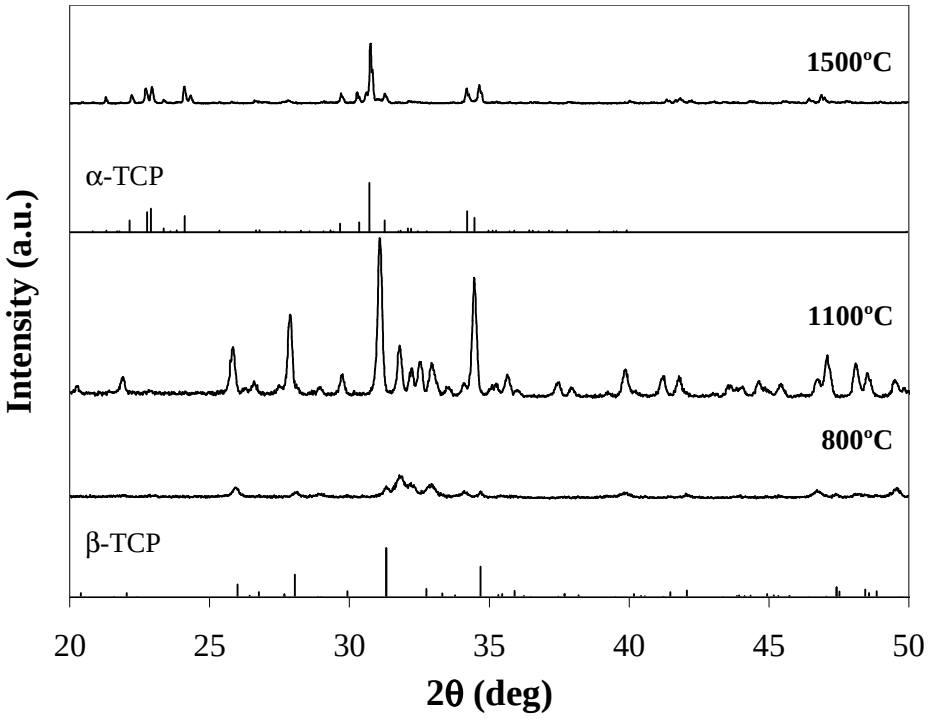

Fig. 1: XRD patterns of the Mg-substituted (MgTCP) powder heat treated at 800ºC, 1100ºC and 1500ºC. β-TCP (β-$Ca_3(PO_4)_2$, JCPDS PDF File # 1-70-682 and α-TCP (α-$Ca_3(PO_4)_2$, JCPDS PDF File # 29-359), full scale intensity = 12,000 cps.

The presence of α-TCP in bone cements facilitates the setting and hardening properties due to its progressive dissolution and the formation of an entangled network of calcium deficient HA (CDHA) crystals [6,21-25]. On the other hand, β-TCP does not cure but helps the handling time in which experiments can be conducted [24]. For this reason, it was decided to use the powder calcined at 1500ºC containing mostly the α-TCP phase. The values of the initial setting time using this powder, for various combinations of setting liquids and LPRs, are given in Table 1. Literature studies [7,25-28] on the influence of LPR on CPC properties have used a relatively wide range of LPR values (0.25-0.87 mL g^{-1}). As mentioned

in the experimental section, the values of LPR were firstly varied in the range of 0.25-0.50 mL g^{-1}. It was noted that for LPR values below 0.30 mL g^{-1} the cement paste could not be injected through a needle gauge 12 (2.2 mm inner diameter) due to its high viscosity, while good flowability was verified for LPR ≥ 0.35 mL g^{-1}. However, considering that the initial setting time of the paste was > 30 min for LPR ≥ 0.35 mL g^{-1}, the LPR range of 0.30-0.34 mL g^{-1} was selected to prepare cement pastes to proceed with further experiments.

Table 1: Influence of additives and LPRs on the setting time of the pastes.

	Initial Setting times (min)		
Additives (wt. %)	**L/P = 0.3 mLg^{-1}**	**L/P = 0.32 mLg^{-1}**	**L/P = 0.34 mLg^{-1}**
2.5 % Na_2HPO_4	>>30	>>30	>>30
5 % Na_2HPO_4	>>30	>>30	>>30
10% Na_2HPO_4	>>30	>>30	>>30
5 wt% Citric acid	4.0±0.1	8.0± 0.2	6.0±0.1
10 wt% Citric acid	3.0±0.1	5.0±0.5	4.0±0.3
15 wt% Citric acid	3.0±0.4	2.0±0.8	2.0±0.1
10 % PEG + 5 % Citric acid	6.0±0.1	9.0±0.2	10.0±0.2
10 % PEG +10 % Citric acid	4.0±0.6	8.0±0.5	6.0±0.3
10% PEG + 20 % Citric acid	3.0±0.3	6.0±0.1	3.0±0.2
0.5% HPMC+ 5% Citric acid	13.0±0.2	16.0±0.5	18.0±0.1
0.5%HPMC+10% Citric acid	12.0±0.1	15.0±0.4	16.0±0.2
0.5%HPMC+20% Citric acid	11.0±0.1	9.0±0.8	11.0±0.5

It is seen that both liquid solutions (based on Na_2HPO_4 or in citric acid) enabled workable cement pastes to be formed with the lowest LPR used (0.30 mL g^{-1}). As

expected, the initial setting time increased with increasing LPR values ($p < 0.05$). Rapid hardening of the cement paste was observed for low LPR values, resulting in short working time frame which, effectively, makes these materials unsuitable for injection. Therefore, a LPR of 0.34 mL g^{-1} was used in subsequent tests. The evolution with time of G'and G'' of the cement pastes prepared with different concentrations of Na_2HPO_4 and citric acid for the selected LPR of 0.34 mL g^{-1} is shown in Fig. 2 and 3, respectively.

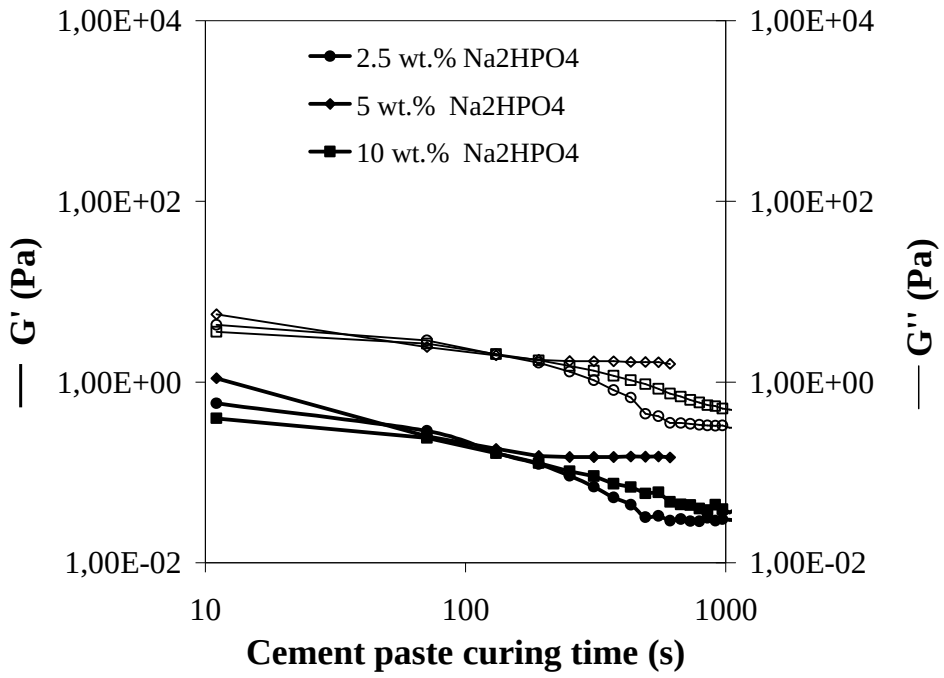

Fig. 2: Time-sweep curves of Mg-substituted (MgTCP) cement pastes prepared with different added amounts of Na_2HPO_4, (LPR = 0.34 mL g^{-1}).

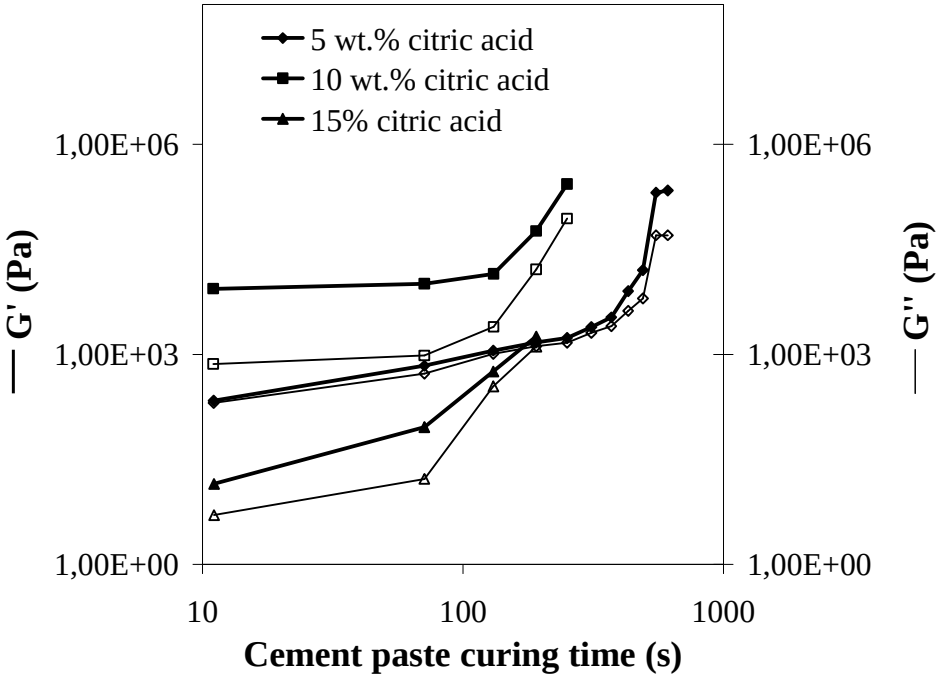

Fig. 3: Time-sweep curves of Mg-substituted (MgTCP) cement pastes prepared with different added amounts of citric acid, (LPR = 0.34 mL g^{-1}).

All the curves presented in Fig. 2 show a decreasing trend of the rheological parameters along the whole plotted time frame. Moreover, the G'' curves appear always above the G' curves, confirming the predominance of the viscous character of the pastes containing Na_2HPO_4. An opposite situation was observed with the cement pastes prepared with citric acid (Fig. 3). Both G' and G'' increase with time increasing, but the G' curves appear always above those of G'', confirming the predominance of the solid-like characteristics of the pastes. This means that the hydration reactions and the setting process are faster in the presence of citric acid. As can be seen, the main changes in the slope of the G' and G'' curves occur for shorter times as the citric acid concentration increases, resulting in a decreasing trend in the initial setting time, in close agreement with the data presented in Table 1. Both G' and G'' increased with increasing concentrations of the citric acid from 5 to 10 wt.%, followed by an opposite trend when the amount of citric acid was increased to 15 wt.% ($p = 0.002$). Increasing amounts of citric acid result in an

increase of the viscosity of the liquid and of the paste and accelerates the setting time of the cement. However, when citric acid is present in excess it appears to weaken the hardened cement structure.

While the addition of citric acid resulted in pastes that were workable within a few minutes, those made with Na_2HPO_4 remained liquid for more than 30 min for all the LPRs tested. A literature survey [28,29] about the role of Na_2HPO_4 solutions as setting liquids for CPC suggests that it can not be easily described. Using α-TCP and α-TCP + dicalcium phosphate dihydrate (DCPD) based cements systems, Khairoun et al. [28] found decreasing setting times with increasing concentrations of Na_2HPO_4. It was argued that the addition of Na_2HPO_4 increased the degree of supersaturation of Ca^{2+} and PO_4^{3-} ions in the solution during hydration, thus improving the impetus of the reaction. On the other hand, the study by Wang et al. [29], who investigated a cement based on highly reactive amorphous calcium phosphate (ACP) and brushite, reports a small delaying effect compared with water. From these reported results and those found in the present work, it seems clear that the effect of Na_2HPO_4 on the cement hardening kinetics strongly depends on the chemical and phase compositions of the CPC and eventually on the characteristics of the starting powders derived from the preparation method, or even specific powders/ liquid interactions.

In order to better understand the role of Mg in the Mg-substituted (MgTCP) cement pastes, a baseline cement based on pure α-TCP, denominated as TCP cement, was also prepared and ground under the same conditions. The aim was to include a critical comparison of the values for the properties (initial setting time, compressive strength, microstructural features) for this baseline cement to the corresponding values for the appropriate Mg-substituted cement. The magnesium content of the cement is believed to inhibit setting to calcium deficient HA [13]. To evaluate if the long setting times with sodium phosphate in the present study could be due to the presence of magnesium, cement pastes made of Mg-free α-TCP (TCP) and Mg-substituted (MgTCP) were prepared with 5 wt.% Na_2HPO_4 solution. For both cases, the results presented in Figure 4 show a first similar decreasing trend of G' and G'', with the G'' curves appearing always above the G' curves, confirming the predominance of the viscous character, like observed in Fig. 2. The

curves of the Mg-free cement paste start increasing a bit sooner (after about 11 min, in comparison to about 14 min) and appear above those of the Mg-substituted cement paste. However, the differences in setting behaviour between Mg-free and Mg-substituted cement pastes are not so remarkable. These results suggest that Na_2HPO_4 solutions are unsuitable as setting liquids for both TCP and MgTCP cement pastes. The different effectiveness of Na_2HPO_4 solutions and citric acid solutions as setting liquids might be due to their different pH values and dissolution capabilities of the CPC powders. The pH values for Na_2HPO_4 and citric acid solutions were around 5 and 1.5, respectively.

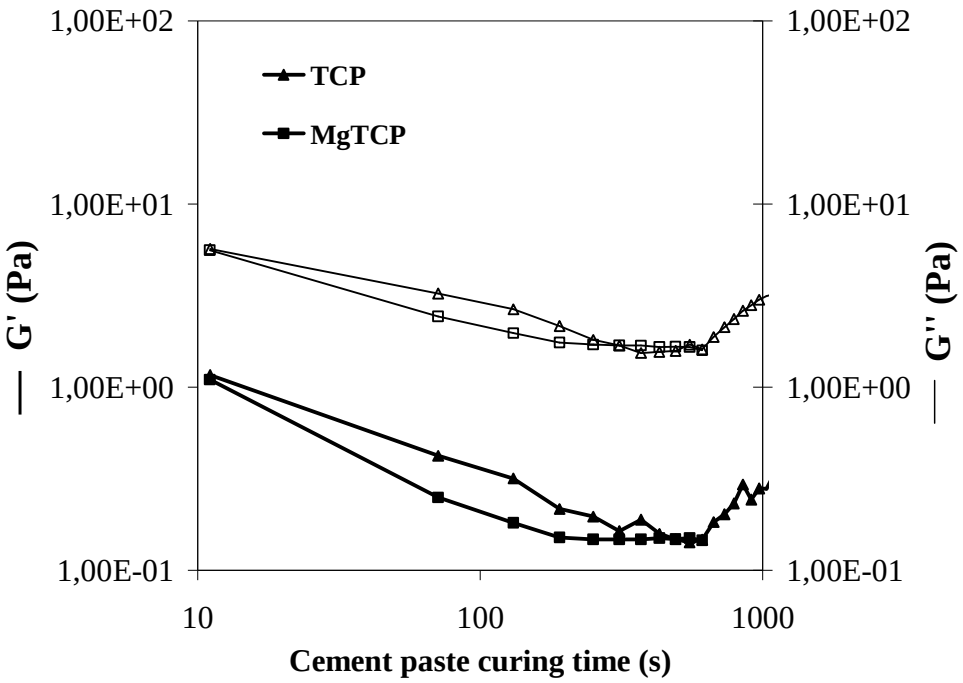

Fig. 4: Time-sweep curves of Mg-substituted (MgTCP) and Mg-free (TCP) cement pastes prepared with 5 wt.% Na_2HPO_4 (LPR = 0.34 mL g^{-1}).

The addition of rheology modifiers to the citric acid made the initial setting times to increase in comparison to the systems in which rheology modifiers are absent (Table 1). In other words, the presence of rheology modifiers enhances the flow ability and, hence, the injectability, of the cement. The delay of the setting process

is less pronounced in the case of PEG (initial setting times in the range of 6-10 min.), in comparison to HPMC. In fact, an added amount of HPMC that is 20 times less that of PEG resulted in longer initial setting times (9-18 min.). PEG and HPMC are hydrophilic polymers that form a network structure with water molecules, which become less free to spontaneously react with inorganic CaPs. Consequently, the formed network may integrate the polymer structure. This phenomenon is more emphasized when the polymer presents high molecular weight as in the case of HPMC, which could explain the decrease of setting time in the presence of this additive in comparison to the systems with added PEG. These results are important from the perspective of the clinical uses giving room to adjust the optimal setting time, since CPC should not harden too fast to allow moulding or injection and not harden too slowly to allow the surgeon to close the defect shortly after cement placement.

The evolution with cement paste curing time of G’ and G’’ of the cement pastes prepared with different concentrations of citric acid and fixed added amounts of the rheology modifiers, 10 wt.% PEG, or 0.5 wt.% HPMC, is shown in Fig. 5 and 6, respectively. The results in Fig. 5 show that the increase of citric acid concentration from 5 wt.% to 10 wt.% resulted initially in a faster setting of the pastes, but a further increment of citric acid to 20 wt.% revealed again an opposite effect, similar to the trend shown in Fig. 3 in absence of PEG. In contrast, the presence of 0.5 wt.% of HPMC inhibited the setting process for citric acid concentrations lower than 10 wt.% (Fig. 6). In this case, the setting process only took place with added 20 wt.% of citric acid after about 12 min.

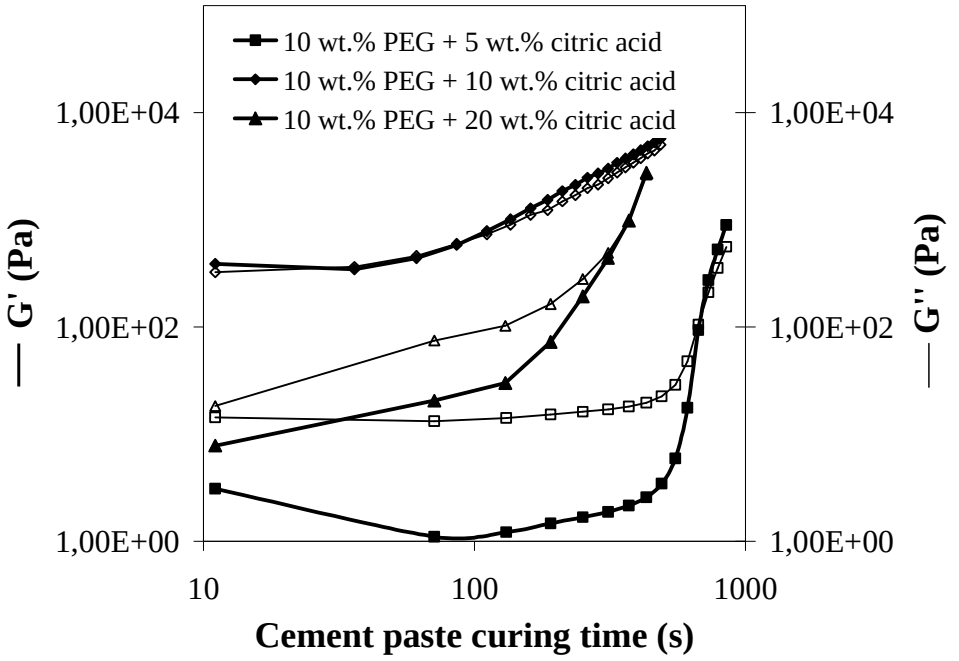

Fig. 5: Time-sweep curves of Mg-substituted (MgTCP) cement pastes prepared with 10 wt.% PEG and different added amounts of citric acid (LPR = 0.34 mL g^{-1}).

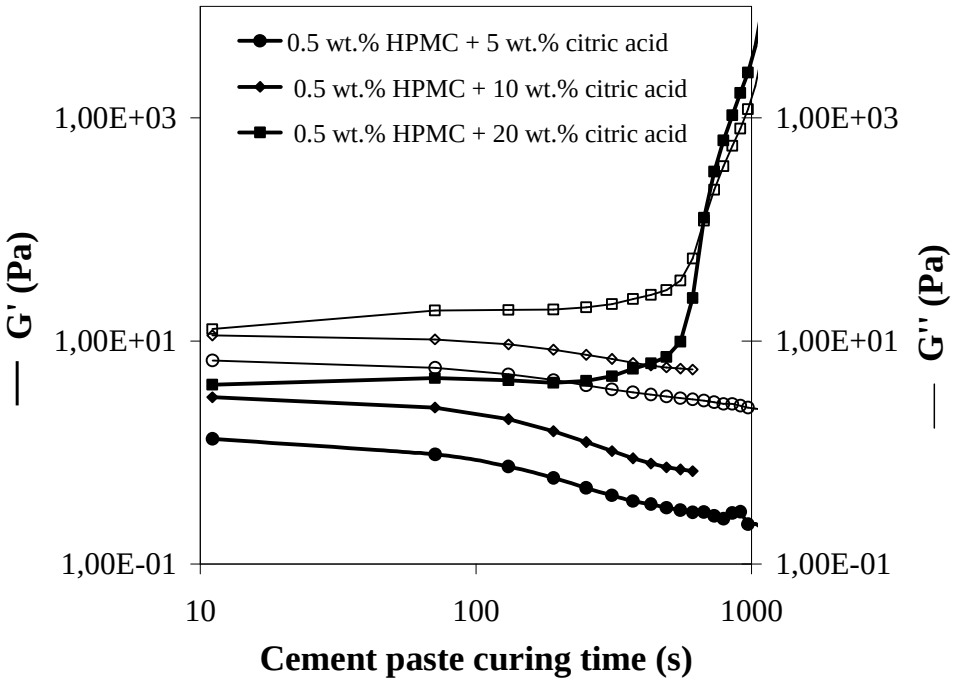

Fig. 6: Time-sweep curves of Mg-substituted (MgTCP) cement pastes prepared with 0.5 wt.% HPMC and different added amounts of citric acid (LPR = 0.34 mL g^{-1}).

Based on the results shown in Fig. 5 and 6, and considering that bone cement must be placed in the implantation site in about 6-8 min [9], the setting liquid with a composition of 10 wt.% PEG + 20 wt.% citric acid was selected for preparing CPC samples for mechanical tests. The setting behaviour of Mg-free and Mg-substituted cement pastes prepared under these conditions were also compared. Fig. 7 presents the evolution of G' and G'' with the curing time of the TCP and MgTCP cement pastes. The results show that TCP presents a faster setting and higher storage modulus along the whole hydration period in comparison to MgTCP. The results of Vicat test (not presented) for the TCP cement paste prepared with 20 wt.% of citric acid + 10 wt.% of PEG gave initial setting times in the range of 2-3 min, in close agreement with rheological tests shown in Figure 7, being shorter than those presented in Table 1 for MgTCP cement pastes. These results show that Mg incorporation delays the initial setting time. This feature can be usefully exploited in combination with the setting liquid composition to optimise the setting behaviour of Mg-containing cements and make their clinical application successful.

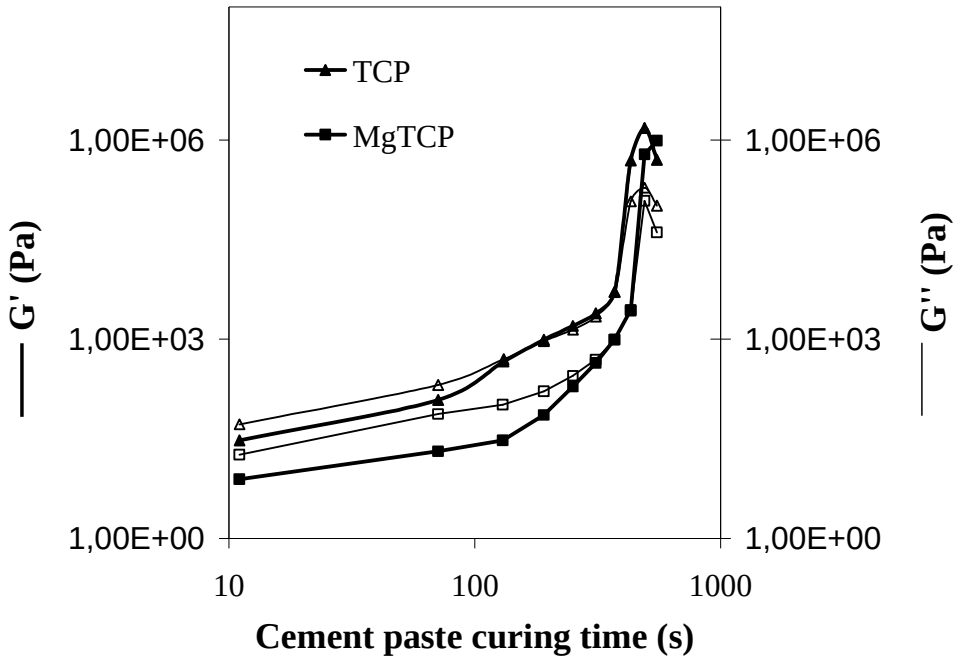

Fig. 7: Time-sweep curves of Mg-substituted (MgTCP) and Mg-free (TCP) cement pastes prepared with 10 wt.% PEG + 20 wt.% citric acid (LPR = 0.34 mL g^{-1}).

Fig. 8 compares the XRD patterns of the cements prepared using 10 wt.% PEG + 20 wt.% citric acid as setting liquid after curing for 24 h. It can be seen that the hardened cements consist of three crystalline phases. The TCP cement is constituted by 76% of α-TCP and 24% brushite, while the MgTCP cement consists of 62% α-TCP, 23% brushite and 15% β-TCP. However, the degree of crystalinity of the MgTCP cement is apparently lower in comparison to TCP cement. This can be understood considering Mg exerts a stabilising effect of the β-TCP phase [6, 11, 12] and tends to prevent the crystallisation of the most stable CaP phases upon hydration [18]. These findings are consistent with the morphological features observed in the SEM micrographs of fractures surfaces of the hardened cements after 24 h of setting at 37ºC shown in Fig. 9. Larger and better developed crystals are seen in the TCP cement. The crystals are irregular in shape and size in the case of Mg-containing cement.

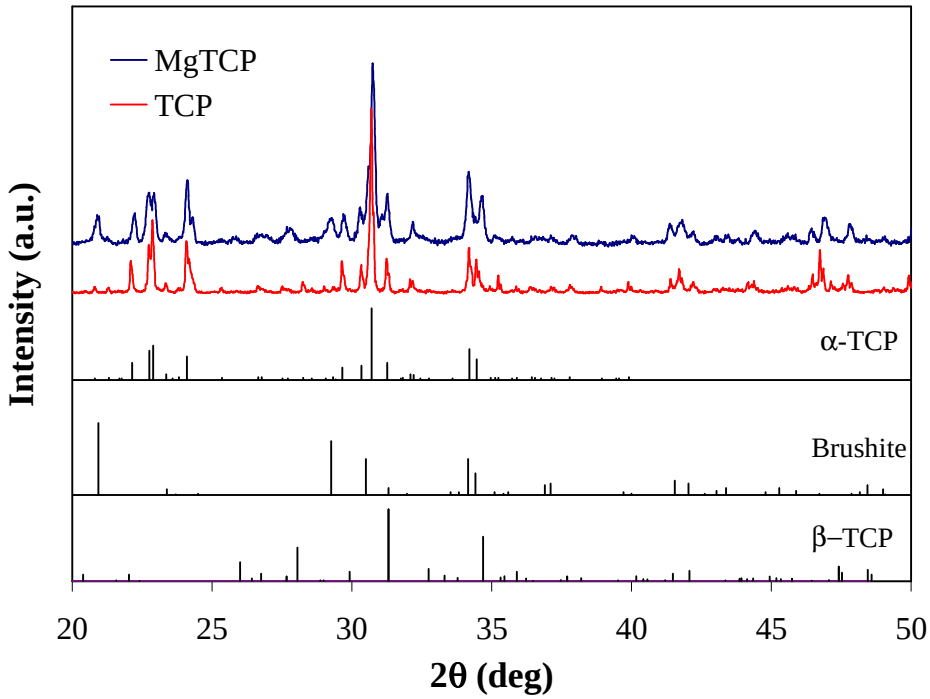

Fig. 8: XRD patterns of MgTCP and TPC cements hardened for 24 h. The pastes were prepared with 10 wt.% PEG + 20 wt.% citric acid (LPR = 0.34 mL g^{-1}). Brushite JCPDS PDF File # 9-0077); α-TCP ($Ca_3(PO_4)_2$, JCPDS PDF File # 29-359) and β-TCP (β-$Ca_3(PO_4)_2$, JCPDS PDF File # 1-70-682), full scale intensity = 4,000 cps.

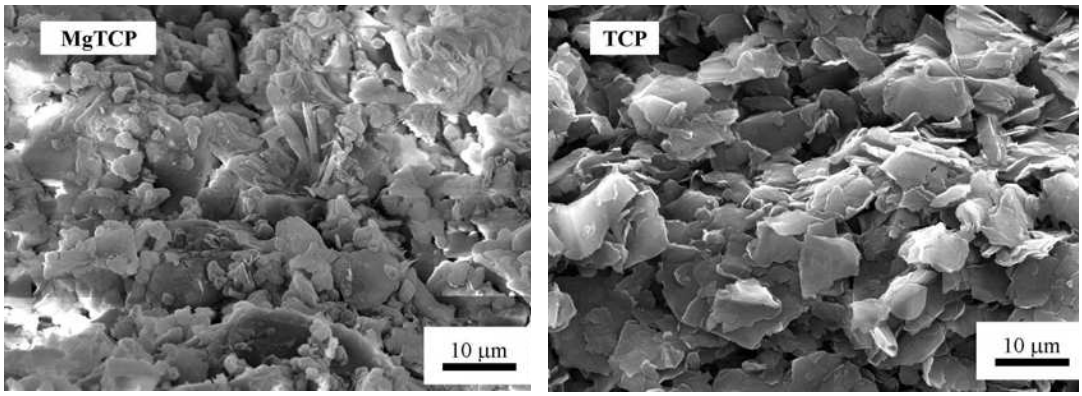

Fig. 9: Scanning electron micrographs of the MgTCP and TCP cements hardened for 24 h. The pastes were prepared with 10 wt.% PEG + 20 wt.% citric acid (LPR = 0.34 mL g^{-1}).

The compressive strength values of TCP and MgTCP cements hardened for 24 h and kept under wet conditions for further 12 h, 24 h and 48 h, before performing the measurements, are shown in Fig. 10. The decrease of the compressive strength of the hardened cement specimens after 24 h of immersion in PBS solution can be attributed to a gradual structural degradation process ($p \cong 0.004$). The measured values of the wet compressive strength after 48 h are somewhat around the lower limit of the range for cancellous bone (10-30 MPa) [30], achieving average values of about 12.4 and 9.2 MPa for the MgTCP and TCP cements, respectively. The results show that Mg-containing cement specimens exhibit slightly higher compressive strength values in comparison to cements with no Mg substitution ($p<0.05$), probably due to the different phase compositions (TCP cement is richer in α-TCP and brushite, while MgTCP cement also contains β-TCP).

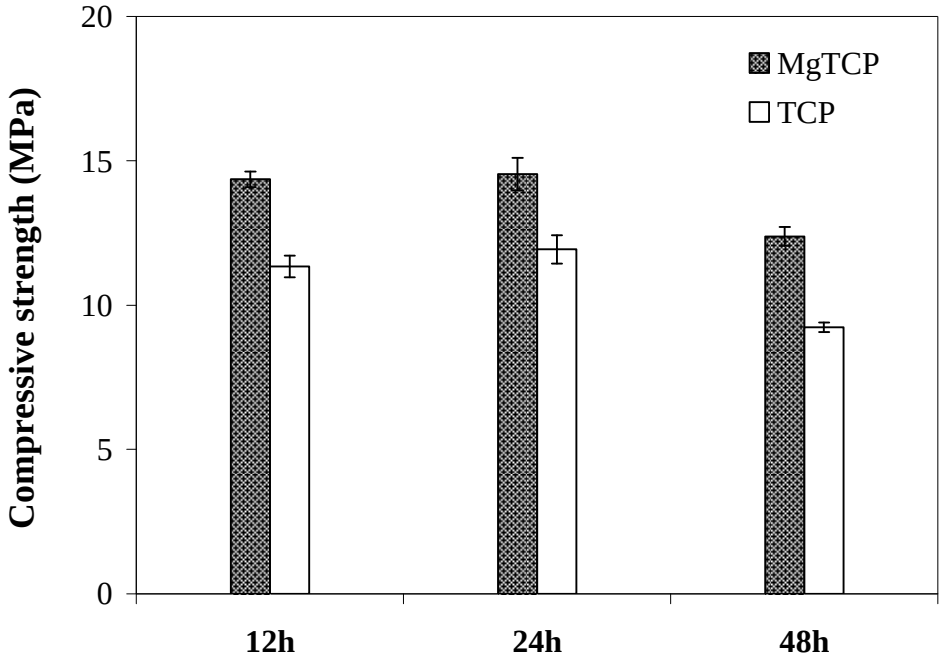

Fig. 10: Compressive strength values measured for the MgTCP and TCP cements hardened for 24 h and kept under wet conditions for further 12 h, 24 h and 48 h. The pastes were prepared with 10 wt.% PEG + 20 wt.% citric acid (LPR = 0.34 mL g^{-1}).

The overall results obtained in the present study enable to state that Mg-substituted CPC pastes prepared with a setting solution comprising citric acid and PEG have a good potential for being use in orthopaedic and trauma surgery (for example, to fill bone defects) and therefore should be considered for further experimentation aiming at exploiting other recognized beneficial effects of Mg on the biological and mineralization process.

4. Conclusions

The results presented and discussed along this work proved the usefulness of rheological measurements under oscillatory mode to access the structural

evolution of the cement pastes upon the hydration process *in situ* before setting. This is of significance concerning the moulding ability and injectability of cement pastes intended for applications in poorly accessible fracture sites such as is the case in vertebroplasty and kyphoplasty. It was demonstrated that for obtaining reactive CPC, the precipitated powders must be heat treated at a temperature of 1500ºC to favour the formation of α-TCP as the predominant phase.

The use of aqueous solutions of Na_2HPO_4 revealed to be unsuitable as setting liquids for both TCP and MgTCP cements prepared in the frame of the present work. Contrarily, aqueous citric acid solutions exhibited high reactivity towards the cement powders, firstly accelerating the setting process with increasing acid concentrations, followed by a decreasing trend in the presence of excess citric acid. The initial setting times tended to decrease in the presence of rheology modifiers (10 wt.% PEG or 0.5 wt.% HPMC) enabling to tailor the setting behaviour, the flow ability, and the workability of the cement pastes according to the surgical needs. The setting process tends to be slower in the case of MgTCP in comparison to TCP cements, a giving further room to adjust the relevant paste properties. Workable cement pastes were obtained for LPR in the range of 0.30-0.34 mL g^{-1}. The flowing ability and the initial setting times are enhanced with increasing LPR. The compressive strength of the hardened cement specimens tended to decrease for curing times longer than 24 h due to a gradual degradation effect experienced upon immersion in PBS solution. Mg-containing cement specimens appeared to be slightly stronger in comparison to Mg-free cements, probably due to a more favourable crystalline phase composition.

Acknowledgments

Thanks are due to CICECO for the support and to the Portuguese Foundation for Science and Technology for the fellowship grants of S. Pina (SFRH/BD/21761/2005) and S.M. Olhero (SFRD/BPD/27013/2006).

References

[1] Takagi, S. and Chow, L. C. Formation of macropores in calcium-phosphate cement implants. J Dent Res 1995; 74:559-559.

[2] Generosi, A., Smirnov, V. V., Rau, J. V., Albertini, Y. R., Ferro, D., and Barinov, S. M. Phase development in the hardening process of two calcium phosphate bone cements: an energy dispersive X-ray diffraction study. Mater Res Bull 2007;in press

[3] Bohner, M. Calcium orthophosphates in medicine: from ceramics to calcium phosphate cements. Injury-Inter J Care Injured 2000; 31:37-47.

[4] Bohner, M., Merkle, H. P., Landuyt, P. V., Trophardy, G., and Lemaitre, J. Effect of several additives and their admixtures on the physico-chemical properties of a calcium phosphate cement. J Mater Sc: Mater Med 1999; 11:111-116.

[5] Liu, C. S., Shao, H. F., Chen, F. Y., and Zheng, H. Y. Rheological properties of concentrated aqueous injectable calcium phosphate cement slurry. Biomaterials 2006; 27:5003-5013.

[6] Kannan, S., Lemos, I. A. F., Rocha, J. H. G., and Ferreira, J. M. F. Synthesis and characterization of magnesium substituted biphasic mixtures of controlled hydroxyapatite/beta-tricalcium phosphate ratios. J Sol St Chem 2005; 178:3190-3196.

[7] Xu, H. H. K., Carey, L. E., Simon, C. G., Takagi, S., and Chow, L. C. Premixed calcium phosphate cements: Synthesis, physical properties, and cell cytotoxicity. Dent Mater 2007; 23:433-441.

[8] LeGeros, R. Z. Calcium Phosphates in Oral Biology and Medicine. Basel, Karger 1991;

[9] Bohner, M. and Gbureck, U. Thermal reactions of brushite cements. J Biomed Mater Res Part B: Appl Biomater 2008; 84B:375-385.

[10] Bohner, M. Reactivity of calcium phosphate cements. J Mater Chem 2007; 17:3980-3986.

[11] Kannan, S., Lemos, A. F., Rocha, J. H. G., and Ferreira, J. M. F. Characterization and mechanical performance of the Mg-stabilized β-$Ca_3(PO_4)_2$ prepared from Mg-substituted Ca-deficient apatite. J Am Cer Soc 2006; 89:2757-2761.

[12] Kannan, S., Rocha, J. H. G., and Ferreira, J. M. F. Synthesis and thermal stability of sodium, magnesium co-substituted hydroxyapatites. J Mater Chem 2006; 16:286-291.

[13] Suchanek, W. L., Byrappa, K., Shuk, P., Riman, R. E., Janas, V. F., and TenHuisen, K. S. Preparation of magnesium-substituted hydroxyapatite powders by the mechanochemical-hydrothermal method. Biomaterials 2004; 25:4647-4657.

[14] Fadeev, I. V., Shvorneva, L. I., Barinov, S. M., and Orlovskii, V. P. Synthesis and structure of magnesium-substituted hydroxyapatite. Inorg Mater 2003; 39:947-950.

[15] Kannan, S. and Ferreira, J. M. F. Synthesis and thermal stability of hydroxyapatite-beta-tricalcium phosphate composites with cosubstituted sodium, magnesium, and fluorine. Chem Mater 2006;18:198-203.

[16] Suchanek, W., Byrappa, K., Shuk, P., Riman, R, Janas, V., and TenHuisen, K. S. Mechanochemical-hydrothermal synthesis of calcium phosphate powders with coupled magnesium and carbonate substitution. J Sol St Chem 2004; 177:793-799.

[17] Lilley, K.J., Gbureck, U., Farrar, D.F., Ansell, C. and Barralet, J.E. Cement from magnesium substituted hydroxyapatite. J Mater Sc: Mater Med 2005; 16: 455-460.

[18] TenHuisen, K.S. and Brown, P.W. Effects of magnesium on the formation of calcium-deficient hydroxyapatite from $CaHPO_4.2H_2O$ and $Ca_4(PO_4)_2O$. J Biomed Mater Res 1997; 36: 306-314.

[19] Mortier, A., Lemaitre, J., and Rouxhet, P. G. Temperature-Programmed Characterization of Synthetic Calcium-Deficient Phosphate Apatites. Thermochim Acta 1989; 143:265-282.

[20] Enderle R, Goetz-Neunhoeffer F Gobbels M Muller FA Greil P. Influence of magnesium doping on the phase transformation temperature of α-TCP ceramics examined by Rietveld refinement. Biomaterials 2005; 26:3379-3384.

[21] Fernandez, E., Gil, F. J., Ginebra, M. P., Driessens, F. C. M., Planell, J. A., and Best, S. M. Calcium phosphate bone cements for clinical applications - Part II: Precipitate formation during setting reactions. J Mater Sc: Mater Med 1999; 10:177-183.

[22] Fernandez, E., Gil, F. J., Ginebra, M. P., Driessens, F. C. M., Planell, J. A., and Best, S. M. Calcium phosphate bone cements for clinical applications - Part I: Solution chemistry. J Mater Sc: Mater Med 1999; 10:169-176.

[23] Nilsson, M. Injectable calcium sulphate and calcium phosphate bone substitutes. Thesis, Lund University, Faculty of Medicine, Lund, Sweden, 2003;

[24] Baroud, G., Cayer, E., and Bohner, M. Rheological characterization of concentrated aqueous □-tricalcium phosphate suspensions: The effect of liquid-to-powder ratio, milling time, and additives. Acta Biomater 2005; 1:357-363.

[25] Sarda, S., Fernandez, E., Llorens, J., Martinez, S., Nilsson, M., and Planell, J. A. Rheological properties of an apatitic bone cement during initial setting. J Mater Sc: Mater Med 2001; 12:905-909.

[26] Burguera, E. F., Xu, H. K. and Sun, L. Injectable calcium phosphate cement: effects of powder-to-liquid ratio and needle size. J Biomed Mater Res Part B: Appl Biomater 2008, 84B:493-502.

[27] Alves, H. L. R., Santos, L. A. and Bergmann, C. P. Injectability evaluation of tricalcium phosphate bone cement. J Mater Sci: Mater Med 2008, 19:2241-2246.

[28] Khairoun, I., Boltong, M. G., Driessens, F. C. M., and Planell, J. A. Some factors controlling the injectability of calcium phosphate bone cements. J Mater Sc: Mater Med 1998; 9:425-428.

[29] Wang, X. P., Ye, J. D., and Wang, H. Effects of additives on the rheological properties and injectability of a calcium phosphate bone substitute material. J Biomed Mater Res Part B: Appl Biomater 2006; 78B:259-264.

[30] Duck, F.A. Physical properties of tissue: a comprehensive reference book. Academic, London 1990.

2.3 Newly developed Sr-substituted α-TCP bone cements

S. Pina[1], P.M.C. Torres[1], F. Goetz-Neunhoeffer[2], J. Neubauer[2] and J.M.F. Ferreira[1]

[1]University of Aveiro, Department of Ceramics and Glass Engineering, CICECO, 3810-193 Aveiro, Portugal.

[2]Mineralogy, University of Erlangen-Nuremberg, 91054 Erlangen, Germany

Acta Biomaterialia (2009), doi: 10.1016/j.actbio.2009.09.001

Abstract

New bone cements made of Sr-substituted brushite-forming α-TCP were prepared and characterised in the present work. The quantitative phase analysis and structural refinement of the starting powders and of hardened cements were performed by X-ray powder diffraction and Rietveld refinement technique. Isothermal calorimetry along with setting time analysis allowed a precise tracing of the setting process of the pastes. The pastes showed exothermic reactions within the first 10-15 minutes after mixing and further release of heat after about 1 hour.

An apatitic phase formed upon immersion of the hardened cements in simulated body fluid for 15 and 30 days due to the conversion of brushite into apatite confirming their *in vitro* mineralization capability. The compressive strength of the wet cement specimens decreased with increasing curing time, being higher in the case of Sr-substituted CPC.

The results suggest that the newly developed Sr-substituted brushite-forming α-TCP cements hold an interesting promise for uses in orthopaedic and trauma surgery such as for filling bone defects.

Keywords: *strontium; brushite; bone cement; XRD, Rietveld refinement; calorimetry; in vitro tests.*

1. Introduction

Calcium phosphate (CaP) ceramics have gained clinical acceptance for bone substitution and augmentation due to their similarities with the mineral bone composition [1-3]. At present, there are two types of calcium phosphate cements (CPCs) depending on the end-product of the reaction: apatite (AP) cements and dicalcium phosphate dihydrate (DCPD or brushite) cements [4, 5]. Apatite is formed above pH 4.2, while brushite is preferentially formed in calcium phosphate cements when pH value of the paste is < 4.2 [6], although it may grow even up to pH 6.5 [6]. AP cements showed higher mechanical strength but have slow *in vivo* resorption rates that interfere with the bone regeneration process. Brushite cements have raised interest because they are resorbed *in vivo* much faster than AP cements [7,8]. Moreover, brushite is metastable in physiological conditions and brushite based cements possess faster setting reactions [6].

Recent years have witnessed the incorporation of strontium (Sr) into the CaP structure due to its presence in calcified bone. The essential characteristics and the role of Sr in bone mineral are: (i) its specific role in osteoporosis; (ii) its equal share with ionic calcium in the physiological pathway and (iii) it can be deposited into the mineral structure of bone, especially in regions of high metabolic turnover [9-11]. In addition, Sr increases osteoclast apoptosis and enhances preosteoblastic cell proliferation and collagen synthesis. Consequently, Sr ions depress bone resorption and maintain bone formation. Therefore, Sr-substituted CaPs are expected to produce enhanced biological and chemical responses in the body. The substitution of Ca by Sr has been studied in various CaP, namely brushite-forming cements [12,13]. Saint-Jean et al. [14] reported that the bioactivity of the set strontium-containing apatite cements was comparable to the bioactivity of pure calcium deficient hydroxyapatite (CDHA).

Isothermal calorimetry has proved to be a powerful tool to study the setting kinetics of CPCs, in which the thermal reactions of the cement pastes are followed at constant temperature over time [4, 15-17]. Over the years, isothermal calorimetry has been used to characterize the setting properties of many materials, such as acrylic bone cement [18-20], apatite cements [16, 21-23] and

brushite based cements [4, 5, 17]. Nevertheless, none of the previously reported studies have shown the effects of the presence of Sr in a brushite-forming α-TCP cement upon hydration using isothermal calorimeter measurements. Therefore, one of the aims of the present work is studying the setting of Sr-substituted brushite-forming α-TCP cements by the evolution of the heat release rate accompanied by *in situ* XRD analysis. The second goal of the present study aims at evaluating the bioactivity of the hardened cements through *in vitro* tests and their wet mechanical properties.

In vitro tests may not represent the real situation of an implant, since the greater is the systems complexicity, the greater is its variability. However, they can provide fast results regarding the materials interactions in biological mediums, thus helping to minimize testing on animals. *In vitro* tests have been used to evaluate the biocompatibility of materials for over two decades and they are widely used today owing to the easy availability of cell strains on the market. The *in vitro* studies on the (Ca, Sr) HA powders revealed a greater apatite deposition with Sr-containing HA, while the *in vivo* (Ca, Sr) HA cement study revealed an increase in the thickness of the bone layer formed at the interface bone-cement and a better osteointegration [15, 24, 25].

2. Materials and Methods

2.1. Preparation of powders and cement pastes

The synthesis of the Sr-substituted cement powder was carried out according to a method that has been described in detail in previous report [26]. Briefly, the powder was obtained by aqueous precipitation from calcium nitrate tetrahydrate [$Ca(NO_3)\cdot 4H_2O$, Vaz Pereira-Portugal, Sintra, Portugal], diammonium hydrogen phosphate [$(NH_4)_2HPO_4$, Vaz Pereira-Portugal, Sintra, Portugal] and strontium nitrate [$Sr(NO_3)$, Riedel-de-Haen, Seelze, Germany] as the starting chemical precursors, respectively for calcium, phosphorus and strontium. The molar ratio

(Ca + Sr)/P used was (1.32+0.18)/1, thus performing the stoichiometric ratio of 1.5 for β-TCP.

The formation of Sr-substituted β-TCP can be described by Equation (1) [26]:

$$Ca_{9-x}Sr_x(HPO_4)(PO_4)_5(OH) \quad \rightarrow \quad 3(Ca_{3-\frac{x}{3}}Sr_{\frac{x}{3}})(PO_4)_2 \quad + \quad H_2O \qquad (1)$$

The precipitate was vacuum filtrated, dried at 110ºC and then heat treated for 2 h at 1500ºC, in order to obtain the formation of the desired α-TCP phase that exhibits hydraulic power. This powder will be hereafter designated as SrCPC. The calcined powder was ground under dry conditions in a planetary mill, using an agate jar of 250 mL with agate balls of 10 mm and 20 mm diameter, and a weight ratio of balls to powder = 3:1, and then passed through a sieve with a mesh size of 36 μm. The separated fine fraction of the SrCPC powder had an average particle size of 13.4 μm measured using a light scattering instrument (Coulter LS 230, UK, Fraunhofer optical model). For comparison purposes, and a better understanding of the role of Sr in the Sr-substituted cement pastes, reference cement made of pure α-TCP, denominated as aCPC cement, was also prepared and ground under the same conditions described above. The aim was to include a critical comparison of the values for the properties (initial setting time, compressive strength, microstructural features) for the reference cement to the corresponding values for the appropriate Sr-substituted cement. The measured average particle size of aCPC powder was 17.32 μm.

From the SrCPC and aCPC powders, cement pastes were prepared using liquid-to-powder ratio (LPR) of 0.34 mL g^{-1}, which has been considered in a previous work of the same authors [27], to give a good balance between the rheological and setting behaviours. Two different mixing liquids were used: (i) 10 wt.% poly(ethylene glycol) (PEG) (200, Sigma) + 20 wt.% citric acid solution (called as Liquid P) and (ii) 0.5 wt.% hydroxyl propyl methylcellulose (HPMC) (3.5-5.6 mPa*s at 2% by mass in water, Sigma) + 10 wt.% PEG + 20 wt.% citric acid solution

(called as Liquid H). Citric acid was selected as setting liquid because its non-toxicity [28]. Citrate exists in bone mineral and is believed to play an important role in the formation and/or dissolution of bone apatite. PEG was also selected for its non-toxicity and its non-immunogenicity [29]. HPMC was selected for its ability to form viscous solutions thus improving the washout resistance of the CPC. The concentration of HPMC was limited to 0.5 wt.% because preliminary studies have shown that higher concentrations retarded the CPC conversion into HA [30].

Specific surface areas (SSA) of the starting powders and of some similarly milled hydrated cements were obtained according to the BET method using a Micromeritics Gemini 2370 V5.00 (Norcross, USA) through the gas adsorption measurements, after degassing the powders in a Micromeritics Flow prep 060 (Norcross, USA).

2.2. X-ray diffraction and structural analysis by the Rietveld refinement method

For refinement studies, the XRD of the powders was performed with a SIEMENS D5000 equipped with a diffracted beam graphite monochromator and the *in situ* XRD of the hardening cements was recorded with a SIEMENS D5000 with SolX detector. Data sets were collected from 2θ = 10-50º with a step size of 0.02º, with CuKα radiation. XRD measurements for all the investigated compositions were repeated three times in three independent samples.

The phase composition of the samples was calculated on the basis of XRD patterns by means of Rietveld analysis with TOPAS 3.0 software (Bruker AXS, Germany). Rietveld refinement was performed using the structural models (ICSD Database) of all phases listed in Table 1. Refined parameters were scale factor, sample displacement, background as Chebyshev polynomial of fifth order, crystallite size and lattice parameters. All parameters were refined simultaneously.

2.3. Isothermal calorimetry

The heat flow evolved during hydration of the cements was monitored using an isothermal calorimeter (TAM Air, Sweden), containing eight separated measuring cells, at 23ºC. The cements (4.0 g of powder) were separately mixed with two different liquids H and P, with LPR of 0.34 mL g^{-1}. The pastes were placed in closed HDPE ampoules and left in the calorimeter chamber for 20 h. At least two measurements were made for each composition. After 5 days of hydration, dried and milled powder cements were used for XRD analyses.

2.4. Setting time

The initial setting time of the cement pastes was determined using Vicat needle technique according to the ASTM C 187-98. One minute after placing the pastes into a glass plate stored at 37ºC in 100% humidity box, the indenter (100 g in mass, 1 mm diameter of the needle) was lowered vertically onto the surface of the cement. The indentation was repeated at intervals of 30 s until no more penetration was possible. The time at this point was taken as the initial setting time.

2.5. Chemical analysis

The chemical analysis of the starting SrCPC powder and of cylindrical (6 mm diameter, and 3 mm height) SrCPC (P) and SrCPC (H) cement samples (hardened for 5 days) after immersing for 2 days into 5 mL distilled water at 37ºC under constant stirring (75 rpm), as well as the Sr^{2+} and Ca^{2+} concentrations leached out from SrCPC (P) and SrCPC (H) cement samples were determined by ICP spectroscopy (Model 70 Plus, Jobin Yvon, France).

2.6. *In vitro* tests

In order to evaluate the mineralisation behaviour of the cements *in vitro*, the set cements were placed into polystyrene flasks containing simulated body fluid (SBF) with ion concentrations (Na^+ 142.0, K^+ 5.0, Ca^{2+} 2.5, Mg^{2+} 1.5, Cl- 148.8, HPO_4^- 1.0, HCO_3^{2-} 4.2, SO_4^{2-} 0.5 mM L^{-1}) nearly equivalent to those of human blood plasma, as discussed by C. Tas [31], for 15 and 30 days. The samples were left setting in PTFE-moulds (Φ 6 $\times$ 12 mm^3) in a 37ºC, 100% humidity box, for 24 h. The set samples were then immersed into SBF solution and continuously shaken at a rate of 75 r min^{-1}, at 37ºC. The liquid was refreshed after every 2 days. After the above mentioned immersion periods in SBF, the samples were washed with distilled water and allowed to dry at 37ºC for 1 day and analysed by means of Scanning Electron Microscopy (SEM) (Hitachi S4100, Tokyo, Japan) and ATR-FTIR spectrometry (FT-IR model Mattson Galaxy S-7000, 32 scans and resolution 4 cm^{-1}).

2.7. Compressive strength

For the compressive strength measurements, the cement pastes were cast into PTFE-moulds (Φ 6 $\times$ 12 mm^3) and stored in a 37ºC, 100% humidity box for 24 h. The cement specimens were then removed from the moulds and immersed in PBS solution (1.37 M NaCl, 27 mM KCl, 80.6 mM Na_2HPO_4, 19.4 mM KH_2PO_4) at 37ºC for further 6 h, 24 h and 48 h. The specimens were loaded to failure at a crosshead displacement rate of 1 mm min^{-1} using a universal materials testing machine (Shimadzu Autograph, Trapezium 2, Japan). Results of compressive strength are expressed as the mean $\pm$ standard error of the mean of triplicate determinations.

2.8. Statistical analysis

Statistical analysis was performed using the SPSS 16.0 software. Comparative studies of means were performed using one-way ANOVA followed by a post hoc test (Fisher projected least-significant difference) with a statistical confidence coefficient of 0.95; therefore, *p* values < 0.05 were considered significant.

3. Results

The chemical composition of the starting of SrCPC powder and of the hardened cement as determined by ICP spectroscopy indicated the following concentrations: 11.74 mol.% Sr^{2+} and 88.26 mol.% Ca^{2+} for the starting of SrCPC powder, which are close to the planned ones of 12 mol.% and 88 mol.%, respectively.
The evolution of crystalline phases of the starting powders without and with Sr incorporation, as well as of the respective cements hydrated for 5 days at 23ºC with the liquids P and H is shown in Figure 1 and Figure 2, respectively. It can be seen that α-TCP was the single phase identified in the starting powders. Hydration led to some consumption of α-TCP and to the formation of brushite, as a minor crystalline phase.

The quantitative Rietveld analysis of XRD patterns confirmed that the starting powders consist of 100% of α-TCP phase, whereas both hydrated cements contained predominantly α-TCP and a fraction of brushite. The cements hydrated with liquid P contained around 77.5 ± 1.0 % of α-TCP and 22.5 ± 1.0 % of brushite, whereas in the case of the cements prepared with liquid H, brushite formation was favoured, reaching values about 25.7 ± 1.0 %.

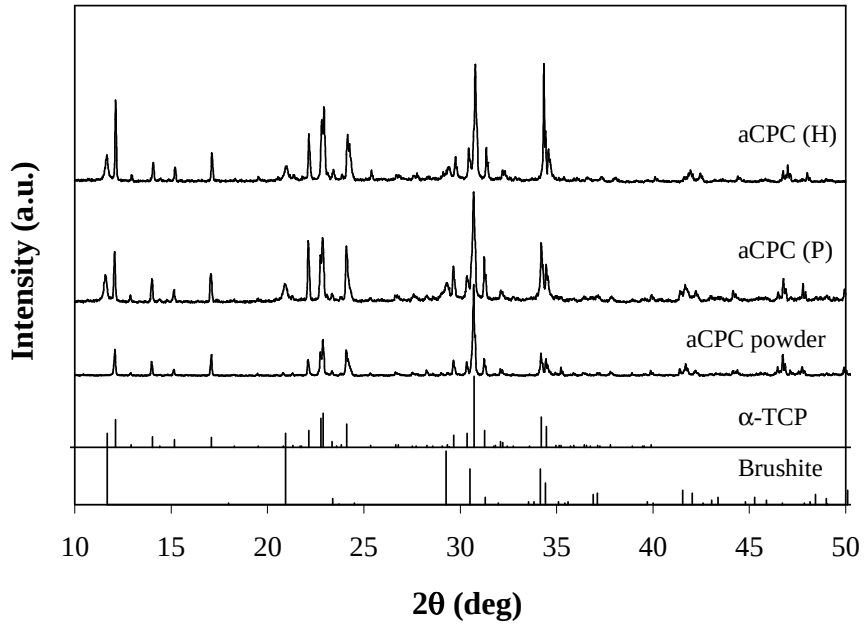

Fig. 1: XRD patterns of the starting powder aCPC, and of the cements prepared from pastes with (i) 10 wt.% PEG + 20 wt.% citric acid (Liquid P (P)) and (ii) 0.5 wt.% HPMC + 10.0 wt.% PEG + 20.0 wt.% citric acid (Liquid H (H)) after 5 days of hydration. Brushite (JCPDS PDF File # 9-0077) and α-TCP ($Ca_3(PO_4)_2$, JCPDS PDF File # 29-359), full scale intensity = 6,000 cps.

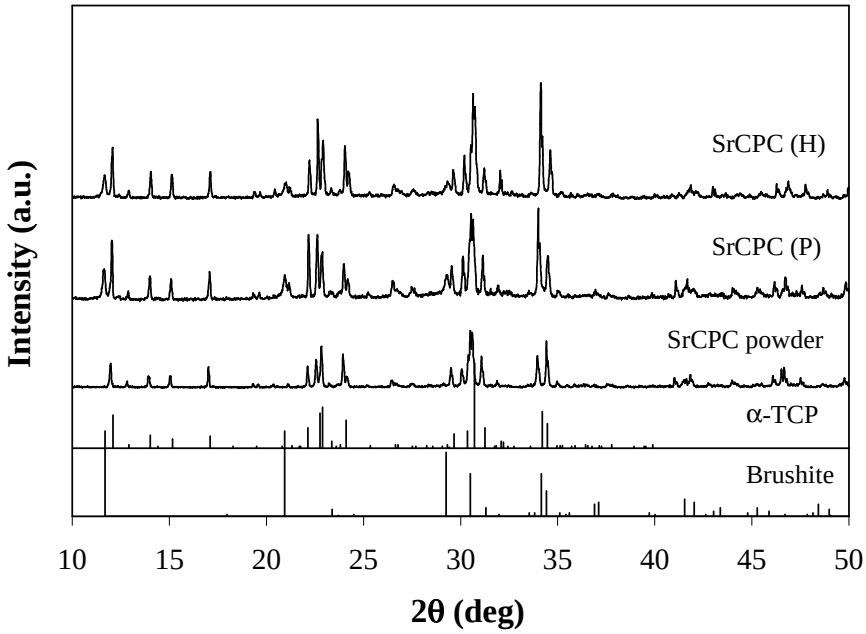

Fig. 2: XRD patterns of the starting powder doped with Sr, SrCPC, and of the cements prepared from pastes with (i) 10 wt.% PEG + 20 wt.% citric acid (Liquid P (P)) and (ii) 0.5 wt.% HPMC + 10.0 wt.% PEG + 20.0 wt.% citric acid (Liquid H (H)) after 5 days of hydration. Brushite (JCPDS PDF File # 9-0077) and α-TCP ($Ca_3(PO_4)_2$, JCPDS PDF File # 29-359), full scale intensity = 6,000 cps.

Table 2 shows the lattice parameters of the α-TCP and brushite phases determined in the cements aCPC and SrCPC after 5 days of hydration. The SrCPC presented increased lattice parameters compared to α-TCP powder, proving that Sr has been incorporated in the SrCPC crystal structure. Table 2 also shows that the lattice parameters of brushite crystals remained similar for both hydrated cements.

Table 2: Lattice parameters of α-TCP and brushite phases of aCPC and SrCPC, after 5 days of hydration.

	Lattice parameters (Å) (±0.002)							
	α-TCP				**Brushite**			
Samples	a	b	c	β	a	b	c	β
aCPC	12.885	27.285	15.221	126.2	5.807	15.189	6.237	116.4
SrCPC	12.936	27.521	15.287	126.5	5.807	15.183	6.256	116.3

For a better perspective concerning the phase's evolution with hydration time, *in situ* XRD measurements were done. Figure 3 shows the *in situ* XRD patterns for SrCPC upon hydration for a period of 12 h using 10 wt.% PEG + 20 wt.% citric acid. In view of the fact that both mixing liquids enabled similar behaviour during hydration, it was decided to present simply for one case (liquid P). It can be seen that the brushite phase started its formation after approximately 1 h of hydration and the intensity of these diffraction lines increase very intensively from 1 to 5 h of hydration. Concomitantly, the diffraction lines corresponding to α-TCP phase decreased with increasing hydration times. The *in-situ* XRD experiments with cements pastes started immediately after 2 min of mixing. We must assume that part of the α-TCP has been already dissolved after mixing with the liquid containing 10 wt.% PEG + 20 wt.% citric acid.

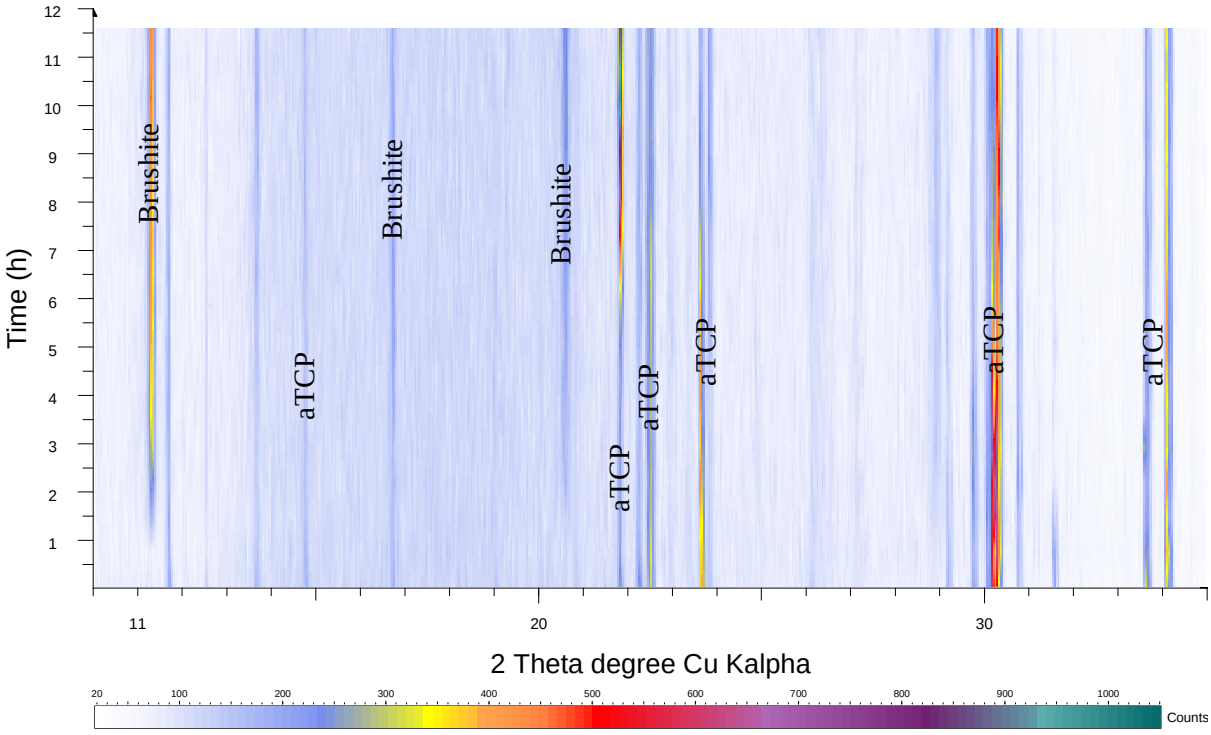

Fig. 3: *In situ* XRD patterns performed within the first 12 h of hydration of cement pastes of SrCPC prepared with 10 wt.% PEG + 20 wt.% citric acid.

Isothermal calorimetry measurements showing the heat flow and the cumulated heat of hydration released from the exothermic setting reaction as a function of reaction time for the powders aCPC and SrCPC, mixed with two different liquids, are presented in Figures 4a and 4b, respectively. For both starting powders and setting liquids, the heat flow profiles display first and main exothermic peaks with maxima centred at approximately 4 min, and the end of this main exothermic reaction occurs after 10-15 min (Fig. 4a). A second and much smaller exothermic effect appears centred at hydration times close to 1 h. These two steps of hydration are consistent with the gradual decreasing intensity of XRD lines of α-TCP and the appearance of XRD lines of brushite phase after about 1 h of hydration, as shown in Fig. 3. Such consecutive events suggest the occurrence of dissolution-precipitation and phase transformation processes.

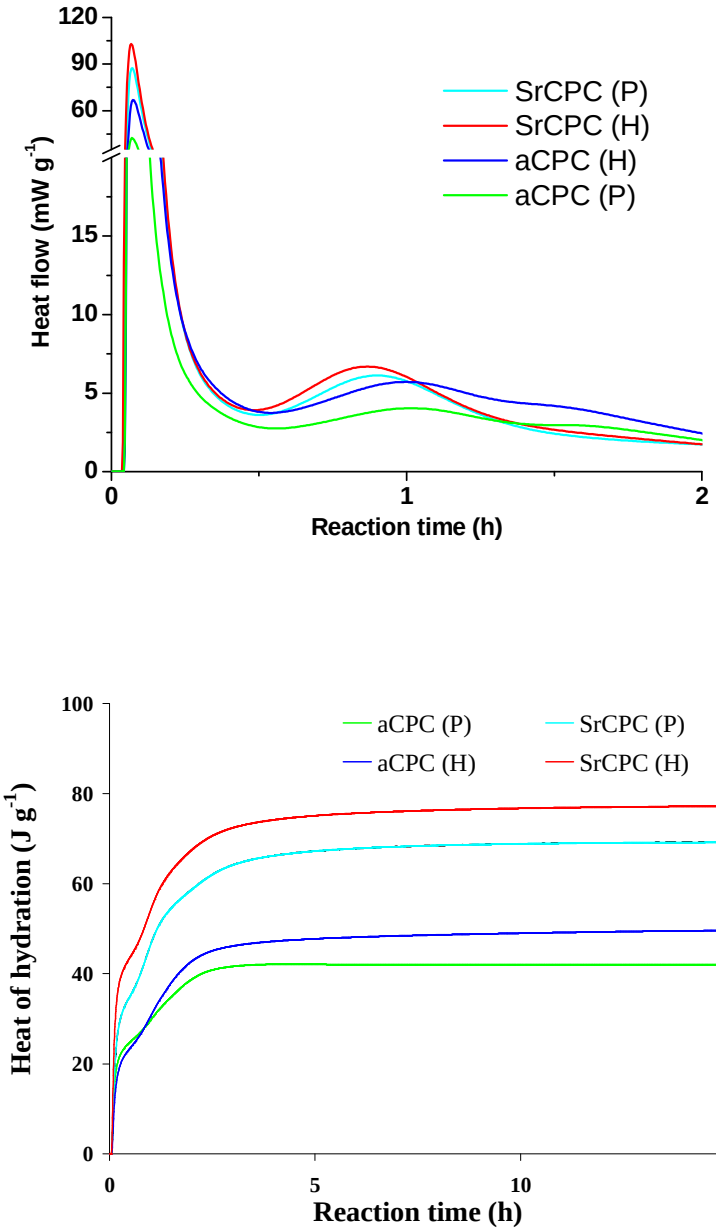

Fig. 4: (a) Heat flow, and (b) Cumulated released heat of hydration profiles as measured by isothermal calorimetry for two hardening cements prepared with (i) 10 wt.% PEG + 20 wt.% citric acid (Liquid P (P)) and (ii) 0.5 wt.% HPMC + 10.0 wt.% PEG + 20.0 wt.% citric acid (Liquid H (H)).

The first initial heat flow can be correlated to the dissolution of α-TCP directly after mixing and a possible precipitation of amorphous material, but not to the formation of any crystalline phase. After 1 h brushite, the stable phase at pH below 5, starts

to form, probably from precipitated amorphous material. This relatively slow transformation process stops after about 5 h since only little heat is produced from the reaction of the paste after that time.

The reactions are more intensive in the case of Sr-substituted cement pastes. The heat flow intensity of SrCPC cement pastes achieves values of ~88 mW g^{-1} and ~103 mW g^{-1}, for liquid P and liquid H, respectively, which compare respectively with about 43 mW g^{-1} and 68 mW g^{-1} for aCPC cement pastes (Figure 4a). The same information can be drawn from Figure 4b: within 15 h the SrCPC cement pastes released cumulated heat of hydration of ~69 J g^{-1} and ~77 J g^{-1}, for liquid P and liquid H, respectively, which compare respectively with about ~42 J g^{-1} and ~50 J g^{-1} for aCPC cement pastes. These observations are consistent with the measured average particle diameters, D_{50}, of the 17.32 μm and 10.78 μm, for aCPC and SrCPC powders, respectively and with their specific surface areas (Table 3). The results presented in Figure 4 clearly show that the thermal effects are stronger for the cement pastes prepared with liquid H.

The initial setting times of the cement pastes were measured using Vicat needle technique. The obtained results were 2 ± 0.5 min for aCPC and 3 ± 0.5 min for SrCPC the cements prepared with liquid P; and 5 ± 0.5 min for aCPC and 7 ± 0.5 min for SrCPC, when cement pastes were made with liquid H ($p<0.05$), in line with thermal results.

The BET specific surface areas of the starting powders and of the similarly milled cements aCPC and SrCPC after 5 days of hydration in the two different mixing liquids are reported in Table 3. It can be seen that, in comparison to the starting powders, the SSA of set cements is significantly higher (26-38 times for the aCPC cements and 67-71 times for the SrCPC). This suggests that the hydration product in the hardened cements might consist of intermingle brushite crystals or amorphous material (calcium citrate, amorphous calcium phosphate) with a fine porous structure.

Table 3: Comparison of the BET specific surface areas measured for the starting powders and for the similarly milled hardened cements aCPC and SrCPC prepared with liquid P and liquid H after 5 days of hydration.

	Specific surface area (m^2/g)		
	Starting powders	Milled hardened cements	
		Set in Liquid P	Set in Liquid H
aCPC	0.62 ± 0.01	16.36 ± 0.14	23.41 ± 0.17
SrCPC	0.78 ± 0.01	55.11 ± 0.5	52.15 ± 0.5

In order to predict the mineralization behaviour of the cements after implantation, the ATR-FTIR spectra of the SrCPC cement hardened for 24 h and prepared from the Sr-substituted α-TCP powder mixed with 10.0 wt.% PEG + 20.0 wt.% citric acid, taken before and after 30 days of immersion in SBF is shown in Fig. 5. Before immersion, SrCPC presents two sharp PO_4 peaks at 1060 and 540 cm^{-1} and a broad peak centred at 3330 cm^{-1} due to adsorbed H_2O. The peaks at 1590 and 1420 cm^{-1} might belong to calcium citrate. According to Hofmann et al. [5], FTIR-monitoring of a fast setting brushite bone cement revealed sharp peaks in close proximity at 1555 and 1410 cm^{-1}.

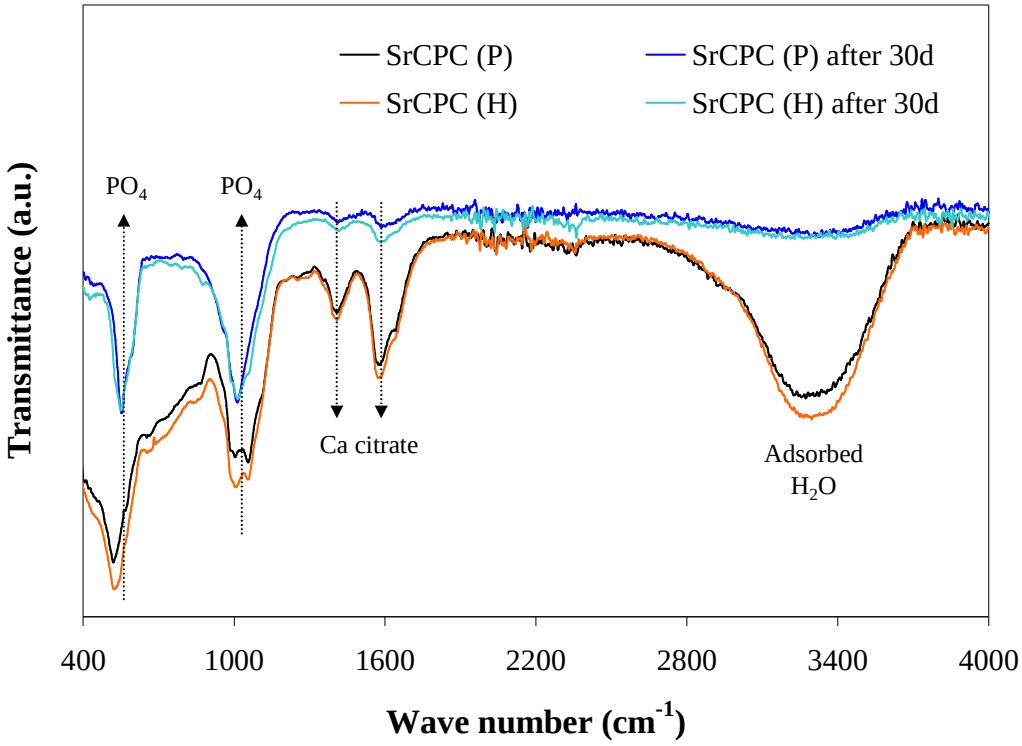

Fig. 5: ATR-FTIR spectra of the SrCPC cements prepared with (i) 10 wt.% PEG + 20 wt.% citric acid (Liquid P (P)) and (ii) 0.5 wt.% HPMC + 10.0 wt.% PEG + 20.0 wt.% citric (Liquid H (H)), before and after 30 days of immersion in SBF solution.

These peaks were consistent with the most intense peaks in the calcium citrate spectra and related with DCP formation (either DCPD or DCPA) upon hydration in the presence of citric acid solution. They were attributed to the CO_2^- symmetric and asymmetric stretching vibrations of calcium citrate intermediates in the hardened cements before immersion in SBF [5]. The immersion of the cements in SBF resulted in a sharpening of PO_4 peaks at 1060 and 540 cm^{-1} and a significant decreased intensity of the band relative to adsorbed water and of the Ca citrate peaks. The differences observed in the ATR-FTIR spectra support the dissolution of brushite and precipitation of apatite.

Figure 6 shows the morphological features of fractured surface of hardened SrCPC cements before and after immersion in SBF for 15 and 30 days. The hardened cement shows well developed dense crystals, probably belonging to the remaining α-TCP phase, and porous aggregates of the hydration product consisting of smaller crystals with irregular morphologies. These observations

support the measured SSA values reported in Table 3. After 15 days of immersion, the surface appears partially covered with a fine apatite layer. Prolonging the immersion period for further 15 days just gives rise to a more extensive deposition of the apatite layer.

The chemical composition of the cements hardened for 5 days after the leaching experiments in distilled at 37ºC for two days indicated Sr^{2+} concentrations of 11.32 mol.% and 11.15 mol.% for the SrCPC (P) and SrCPC (H), respectively, which are slightly lower in comparison to the planned concentration of 12 mol.% and 88 mol.%, respectively. On the other hand, the Sr^{2+} concentrations in the leaching liquids were 13.5 mol.% and 14.4 mol.% for the SrCPC (P) and SrCPC (H), respectively. These results suggest a somewhat preferential release of Sr^{2+} in water in comparison to Ca^{2+} ions.

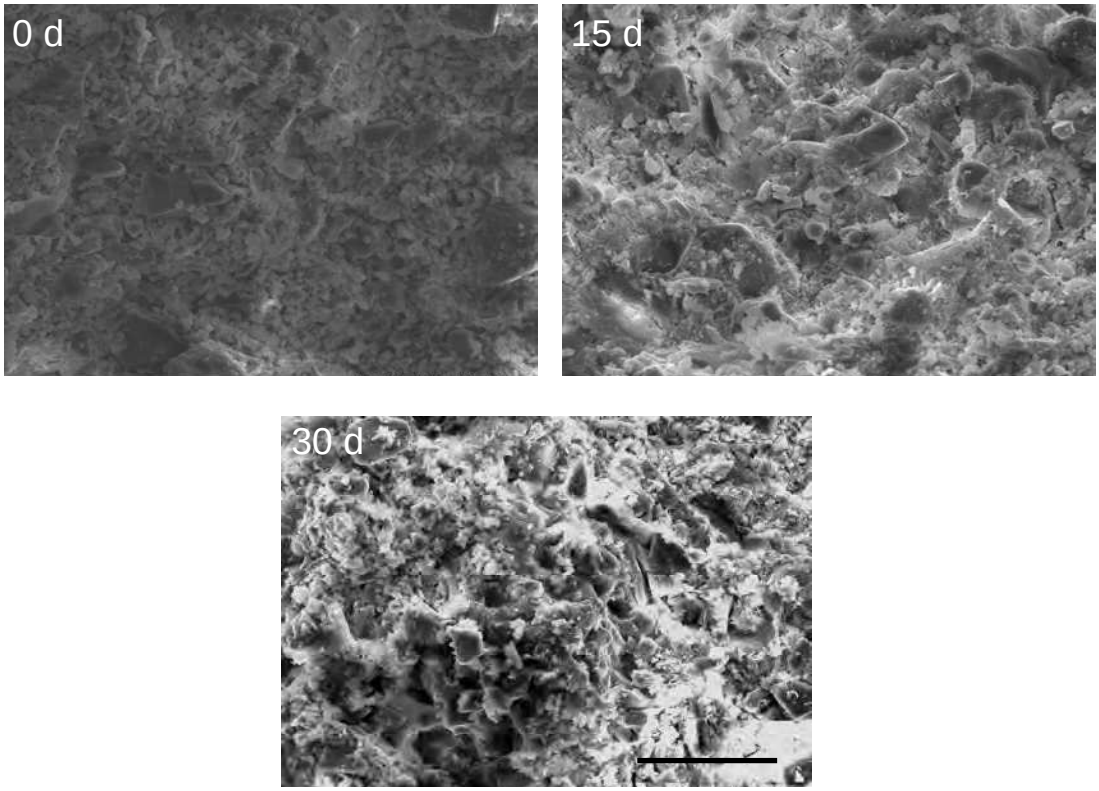

Fig. 6: Scanning electron micrographs of the SrCPC cement before (0 d), and after immersion in SBF solution for 15 days and 30 days. The pastes were prepared with 10 wt.% PEG + 20 wt.% citric acid (LPR = 0.34 mL g^{-1}). Bar 60 μm.

The compressive strength values of aCPC and SrCPC cements hardened for 24 h and kept under wet conditions for further 6 h, 24 h and 48 h, before performing the measurements, are shown in Figure 7. The compressive strength dropped with an increase of immersion time in PBS solution, which can be attributed to a gradual structural degradation process ($p \cong 0.008$). The measured values of the wet compressive strength after 48 h achieved average values of about 13.7 MPa and 9.2 MPa for the SrCPC and aCPC cements, respectively. The results show that Sr-containing cement specimens exhibit higher compressive strength values in comparison to Sr-free cements ($p<0.05$).

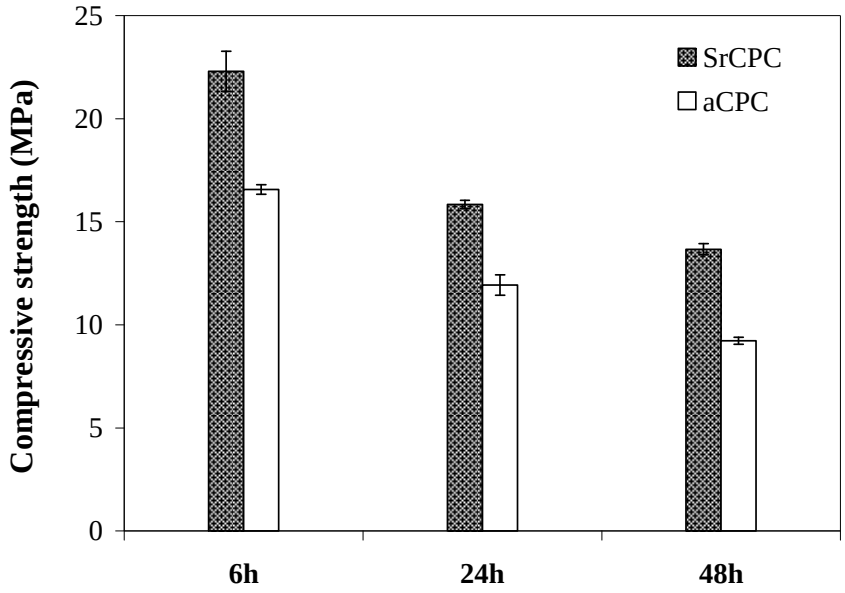

Fig. 7: Compressive strength values measured for the aCPC and SrCPC cements hardened for 24 h and kept under wet conditions for further 6 h, 24 h and 48 h. The pastes were prepared with 10 wt.% PEG + 20 wt.% citric acid (LPR = 0.34 mL g^{-1}).

4. Discussion

The results presented in this study put into evidence several beneficial effects derived from the presence of strontium in brushite-containing α-TCP cements.

The observed decrease in the intensity of the α-TCP peaks and to the formation of brushite upon the hydration reactions between the single phase α-TCP starting powders and setting liquids can be attributed to the partial dissolution of the starting powders and the precipitation of brushite as new phase. This is consistent with the isothermal calorimetry measurements. The first strong exothermic peaks with maxima centred at approximately 4 min are due to dissolution reactions.

Brushite appears in the *in-situ* XRD pattern after 1 h of reaction whereas the first heat flow maximum is reached after a few minutes, which might be the result of the higher solubility of the brushite compared to the dissolving phase α-TCP and to a possible precipitation of amorphous material (calcium citrate, amorphous calcium phosphate). The first range of *in-situ* XRD data is completed after 15 minutes of hydration and we have to take into account that some α-TCP was already dissolved immediately after mixing with the liquid. The second maximum of heat flow at 50 minutes (SrCPC) and 60 minutes (aCPC) can be correlated to a transformation of amorphous material to brushite phase. But a mass balance based on the quantitative Rietveld phase analysis of cements hydrated with e.g. liquid P (77.5 ± 1.0 % of α-TCP and 22.5 ± 1.0 % of brushite) and on the LPR = 0.34 mL g^{-1} used in the present experiments strongly suggest the occurrence of this event. As a matter of fact, neglecting the amorphous material, the mass balance could be described by Equation 2:

$$(Ca,Sr)_3(PO_4)_2 + 0.11\ C_6H_8O_7 + H_2O \rightarrow 0.11\ (Ca,Sr)_3(C_6H_5O_7)_2 + 0.775\ (Ca,Sr)_3(PO_4)_2 + 0.225\ CaHPO_4.2H_2O \quad (2)$$

However, reactants and reaction products are not balanced in terms of Ca^{2+} and Sr^{2+} cations, since we start from 3 mol of (Ca,Sr) and end up with only 2.885 mol in all reaction products. These results strongly support the hypothesis that amorphous calcium phosphate has been also formed, witch has a Ca/P ratio ranging from 1.2-2.2 [32]. The formation of amorphous calcium phosphate could not be seen in the XRD pattern because of its non-crystalline nature, but the formation of amorphous calcium citrate is also supported by the observed sharp ATR-FTIR peaks at 1590 and 1420 cm^{-1} (Figure 5).

The higher exothermicity of the cement pastes prepared with Sr-substituted powder is related to a several factors: (i) The lattice strains associated to the expansion of the lattice parameters with the incorporation of a larger ionic radius of Sr (1.21 Å) compared to Ca (1.07 Å) [33] causes the lattice to expand in both the *a* and *c* axis directions [34] are expected to favour particle size reduction during milling, as has been observed; (ii) The same lattice strains might also facilitate a faster kinetics and favourable thermodynamics of the dissolution process due to changes of the pH value in the cement pastes. M. H. Alkhraisat et al. [12] investigated the effectiveness of using Sr-substituted β-TCP as cement reactant and verified that, after mixing, the cement pH started to increase rapidly until it reached a first plateau and that lower pH values are maintained for a longer period of time by higher Sr-content in β-TCP. This interpretation is consistent with the higher values of SSA and lower average particle diameters measured for the SrCPC cements in comparison to Sr-free cements for both liquid solutions. As a matter of fact, a faster dissolution process implies a higher degree of supersaturation to be achieved, leading to higher rates of nucleation and product formation [17]. Therefore, a less ordered hydrated structure is expected to be precipitated.

The somewhat more intense heat flow and heat of hydration from the setting reaction of cements prepared with liquid H (Figure 4) suggests that the presence of HPMC is playing some role. The difference between two liquids can solely be attributed to the heat of adsorption of HPMC, probably onto the surface of the newly formed brushite nuclei. The ability of cellulose derived molecules such as CMC and HPMC to be readily adsorbed onto the surface mineral particles, including apatite-like minerals is well documented in literature [35]. The extent of adsorption increases with increasing ionic strength of the liquid, a situation that occurs in a reacting system involving dissolution [35]. It has also been reported [36] that these kinds of polymeric additives tend to adsorb onto the surface of the calcium phosphate powders, acting sometimes as dispersing agent, improving the flowability of cement pastes by keeping the particles separated from each other. The specific adsorption of the polymeric species is certainly thermodynamically driven, so that some heat of adsorption is expected to be released [36]. This would

explain the small heat flow differences observed in Figure 4 between cement pastes prepared from the two setting liquids tested.

On the other hand, the newly formed brushite nuclei and the amorphous material (calcium citrate, amorphous calcium phosphate) are expected to exhibit a high surface area. Adsorbing HPMC molecules onto the surface of these newly formed brushite and amorphous calcium phosphate nuclei species would delay the growth of brushite crystals and create favourable conditions for a continual dissolution of α-TCP phase. This is consistent with the delayed initial setting times of cement formulations prepared with liquid H (3 ± 0.5 min and 7 ± 0.5 min for aCPC and for SrCPC, respectively) in comparison to liquid P (2 ± 0.5 min and 5 ± 0.5 min, for the corresponding aCPC and for SrCPC). This would explain why the content of brushite is slightly higher in the hardened cements prepared with liquid H. As a matter of fact, the second exothermic effect centred at hydration times close to 1 h is also smaller for liquid P in comparison to liquid H. This exothermic effect can indubitably be attributed to the formation of brushite and further dissolution of α-TCP, which diffraction lines start to appear after approximately 1 h of hydration, as seen in Figure 3. As expected, the increasing intensity of the brushite diffraction lines with hydration time increasing is accompanied by a decreasing of the α-TCP phase.

It was reported [4] that the exothermic precipitation of brushite occurs rapidly compared to the formation of HA. Furthermore, the heat released in the presence of Sr was considerably higher towards Sr-free cements, reflecting the high reactivity of SrCPC cement in contrast to aCPC cement. These findings and the present results are in apparent contradiction with other results reported elsewhere [14] showing a decrease in the reactivity with increasing Sr content, but this could be different at neutral pH for apatite-forming α-TCP cements. However, this last study [14] used 2.5 wt.% Na_2HPO_4 as the setting liquid and a LPR = 1. Considering these differences and the fact that in the present work a fixed content of Sr has been used, a direct comparison of the results can not be made.

Rietveld refinement analyses performed on the starting powders and on the hardened cements confirmed the considerable increase in the lattice parameters of Sr-substituted α-TCP in both the *a* and *c* axis directions (Table 2) [33, 34]. Table

2 further shows that the lattice parameters for brushite crystals present in aCPC and SrCPC cements are similar meaning the absence of Sr in this phase.

From the perspective of the clinical uses, the setting time of a CPC cement paste is of paramount importance since it should not harden too fast to allow moulding or injection and not harden too slowly to allow the surgeon to close the defect shortly after cement placement. Therefore, the CPC must have an optimal setting time in order to lead to an acceptable mechanical strength after hardening and to prevent migration of cement to undesirable sites. To authors' knowledge there are only three calorimetry studies devoted to brushite cements suggesting that thermograms are related to the setting time [4, 17, 37]. Hoffmann et al. [17] observed that the initial and final setting time of various brushite formulations were correlated to the extent of the largest exothermic peak occurring during setting reaction, while Pittet [37] determined the change of brushite CPC temperature during setting using a thermocouple. Moreover, Bohner et al. [4] upon measuring the setting times of different pastes prepared from β-TCP + MCPM powders also suggested a linkage between setting time and first exothermic peak. These findings support the present results that also point out to a link between setting time and main exothermic peak since the first exothermic peak occurred within the same time interval as the initial setting times obtained via indentation.

The immersion tests intended to approach an *in vivo* environment upon implantation of the cement in a clinical application provide conditions for a continuous hydration of cements and to promote *in situ* deposition of apatite around the residual pores [38]. The results shown in Figures 5 and 6 confirm that an apatitic layer has been formed at the surface the Sr-substituted cements immersed in SBF, indicating its mineralization capability. ATR-FTIR spectroscopy (Figure 5) was found useful to detect the presence of brushite and apatitic groups.

Several *in vitro* and *in vivo* studies [14] showed that at low doses of Sr administration, the Sr uptake in bone might increase the bone volume by increasing the extent of bone formation sites and reducing bone resorption, without however affecting the rate of bone formation, neither altering the bone mineralization. This was attributed to the role of Sr on bone cells, inducing osteoblast activity and inhibiting osteoclast activity. Additionally, the resorption *in*

vivo was found to be inhibited by the stabilization of the bone apatite crystals upon Sr incorporation.

The wet compressive strength values of SrCPC cement are in the range of 1-24 MPa for compressive strengths reported in literature for brushite-forming cements [1] as well as in the range for cancellous bone (10-30 MPa) [39]. The results show that Sr-containing cement specimens exhibit higher compressive strength values in comparison to Sr-free cements, probably due to the lower content of brushite phase present in SrCPC cement (pure brushite cements are characterized by their low mechanical strength). It is thought possible that citric acid might have slowly diffused out of the cement during soaking in PBS, thus leading to a weaker structure. This helps explaining the decrease of compressive strength with immersion time.

5. Conclusions

The incorporation of Sr in the α-TCP crystal structure was proved by increased lattice parameters of the starting SrCPC powder in comparison to the Sr-free aCPC. The lattice strains due to Sr-substitution favoured the milling process and made the starting SrCPC powder more reactive. The isothermal calorimetry, used for the first time in Sr-substituted brushite-forming α-TCP cements, enabled a good traceability of the hydration reactions pointing out to a two-step hardening process: (i) the dissolution of the starting powders and nuclei formation of intermediate amorphous phases (calcium citrate, amorphous calcium phosphate) within the first 10-15 min after mixing; and (ii) the nucleation and growth of brushite after about 1 h. The results confirmed a close linkage between initial setting time and main exothermic peak. The precipitation of amorphous (Ca, Sr)-citrate, amorphous (Ca, Sr)-phosphate) needs to be considered in an overall mass balance of hydration reactions. After a certain time the amorphous (Ca, Sr)-phosphate is transformed into brushite. From our results we conclude that the amount of remaining α-TCP in the hydrated pastes is dependent of the amount of added citric acid. The initial setting time of the newly developed Sr-substituted brushite-forming α-TCP

cements can be extended and optimised, in comparison to Sr-free α-TCP cements, to allow the surgeon to close the defect shortly after cement placement in a better controlled manner. The presence of Sr did not hinder the conversion of brushite into apatite. The wet compressive strength of SrCPC cements are in the range of values (10-30 MPa) reported for cancellous bone even after immersion in PBS solution for 48 h. These characteristics, allied to the specific roles of Sr in osteoporosis and physiological pathway, and in the regulation of bone apposition and resorption, confer them an interesting promise for uses in orthopaedic and trauma surgery such as for filling bone defects. Such characteristics qualify the SrCPC cements for further studies *in vivo*.

Acknowledgments

Thanks are due to CICECO for the support and to the Portuguese Foundation for Science and Technology for the fellowship grant of S. Pina (SFRH/BD/21761/2005).

The authors gratefully acknowledge financial support from GRICES-DAAD. The authors also like to thank C. Stabler and D. Jansen, Institute of Mineralogy, University of Erlangen-Nuremberg, for experimental support and helpful discussions.

References

[1] Bohner M. Calcium orthophosphates in medicine: from ceramics to calcium phosphate cements. Injury-International J of the Care of the Injured 2000;31:37-47.

[2] Generosi A, Smirnov VV, Rau JV, Albertini YR, Ferro D, Barinov SM. Phase development in the hardening process of two calcium phosphate bone cements: an energy dispersive X-ray diffraction study. Mater Res Bull 2008;43:561-571.

[3] Takagi S, Chow LC. Formation of Macropores in Calcium-Phosphate Cement Implants. J Dent Res 1995;74:559-559.

[4] Bohner M, Gbureck U. Thermal reactions of brushite cements. J Biomed Mater Res: Appl Biomater 2008;84B:375-385.

[5] Hofmann MP, Young AM, Gbureck U, Nazhat SN, Barralet JE. FTIR-monitoring of a fast setting brushite bone cement: effect of intermediate phases. J Mater Chem 2006;16:3199-3206.

[6] Gbureck U, Dembski S, Thull R, Barralet JE. Factors influencing calcium phosphate cement shelf-life. Biomater 2005;26:3691-3697.

[7] Gisep A, Wieling R, Bohner M, Matter S, Schneider E, Rahn B. Resorption patterns of calcium-phosphate cements in bone. J Biomed Mater Res Part A 2003;66:532-540.

[8] Constantz BR, Barr BM, Ison IC, Fulmer MT, Baker J, McKinney LA, Goodman SB, Gunasekaren S, Delaney DC, Ross J, Poser R. Histological, chemical, and crystallographic analysis of four calcium phosphate cements in different rabbit osseous sites. J Biomed Mater Res B 1998;43B:451-461.

[9] Marie PJ, Ammann P, Boivin G, Rey C. Mechanisms of action and therapeutic potential of strontium in bone. Calcif Tissue Int 2001;69:121–129.

[10] Dahl SG, Allain P, Marie PJ, Mauras Y, Boivin G, Ammann P, Tsouderos Y, Delmas PD, Christiansen C. Incorporation and distribution of strontium in bone. Bone 2001;28:446–453.

[11] Wong CT, Lu WW, Chan WK, Cheung KMC, Luk DK, Lu DS, Rabie ABM, Deng LF, Leong JCY. *In vivo* cancellous bone remodeling on a Strontium containing hydroxyapatite (Sr-HA) bioactive cement. J Biomed Mater Res 2003;68A:513-521.

[12] Alkhraisat MH, Moseke C, Blanco L, Barralet JE, Lopez-Carbacos E, Gbureck U. Strontium modified biocements with zero order release kinetics. Biomater 2008;29:4691-4697.

[13] Alkhraisat MH, Marino FT, Rodríguez CR, Jerez LB, Lopez-Cabarcos E. Combined effect of strontium and pyrophosphates on the properties of brushite cements. Acta Biomater 2008;4:664-670.

[14] Saint-Jean SJ, Camire CL, Nevsten P, Hansen S, Ginebra MP. Study of the reactivity and in vitro bioactivity of Sr-substituted □-TCP cements. J Mater Sci: Mater Med 2005;16:993-1001.

[15] Bohner M, Malsy AK, Camire CL, Gbureck U. Combining particle size distribution and isothermal calorimetry data to determine the reaction kinetics of alpha-tricalcium phosphate-water mixtures. Acta Biomater 2006;2:343-348.

[16] TenHuisen KS, Brown PW. Formation of calcium-deficient hydroxyapatite from alpha-tricalcium phosphate. Biomater 1998;19:2209-2217.

[17] Hofmann MP, Nazhat SN, Gbureck U, Barralet JE. Real-time monitoring of the setting reaction of brushite-forming cement using isothermal differential scanning calorimetry. J Biomed Mater Res: Appl Biomater 2006;79B:360-364.

[18] Abdulghani S, Nazhat SN, Behiri JC, Deb S. Effect of triphenyl bismuth on glass transition temperature and residual monomer content of acrylic bone cements. J Biomater Sci: Pol Ed 2003;14:1229-1242.

[19] Borzacchiello A, Ambrosio L, Nicolais L, Harper EJ, Tanner KE, Bonfield W. Isothermal and non-isothermal polymerization of a new bone cement. J Mater Sci: Mater Med 1998;9:317-324.

[20] Xu JT, Wang Q, Fan ZQ. Non-isothermal crystallization kinetics of exfoliated and intercalated polyethylene/montmorillonite nanocomposites prepared by in situ polymerization. Eur Pol J 2005;41:3011-3017.

[21] Camire CL, Gbureck U, Hirsiger W, Bohner M. Correlating crystallinity and reactivity in an α-tricalcium phosphate. Biomater 2005;26:2787-2794.

[22] Brunner TJ, Bohner M, Dora C, Gerber C, Stark WJ. Comparison of amorphous TCP nanoparticles to micron-sized alpha-TCP as starting materials for calcium phosphate cements. J Biomed Mater Res: Appl Biomater 2007;83B:400-407.

[23] Brunner TJ, Grass RN, Bohner M, Stark WJ. Effect of particle size, crystal phase and crystallinity on the reactivity of tricalcium phosphate cements for bone reconstruction. J Mater Chem 2007;17:4072-4078.

[24] Wong CT, Lu WW, Chan WK, Cheung KMC, Lukl KDK, Lu DS, et al. In vivo cancellous bone remodeling on a strontium-containing hydroxyapatite (Sr-HA) bioactive cement. J Biomed Mater Res 2004;68A:513-521.

[25] Christoffersen J, Christoffersen MR, Kolthoff N, Barenholdt O. Effects of strontium ions on growth and dissolution of hydroxyapatite and on bone mineral detection. Bone 1997;20:47-54.

[26] Kannan S, Pina S, Ferreira JMF. Formation of strontium-stabilized □-tricalcium phosphate from calcium-deficient apatite. J Amer Ceram Soc 2006;89:3277-3280.

[27] Pina S, Olhero SM, Gheduzzi S, Miles AW, Ferreira JMF. Influence of setting liquid composition and liquid-to-powder ratio on properties of a Mg-substituted calcium phosphate cement. Acta Biomater 2009;5:1233-1240.

[28] Vescini F, Buffa A, La Manna G, Ciavatti A, Rizzoli E, Bottura A, Stefoni S, Caudarella R. Long-term potassium citrate therapy and bone mineral density in idiopathic calcium stone formers. J Endocrinol Inv 2005;28:218-222.

[29] www.piercenet.com/products/browse.cfm?fldID=12D97D8D-5056-8A76-4E95-9EA0D0B54BDB

[30] Xu HHK, Carey LE, Simon CG, Takagi S, Chow LC. Premixed calcium phosphate cements: Synthesis, physical properties, and cell cytotoxicity. Dent Mater 2007;23:433-441.

[31] Tas AC. Synthesis of biomimetic Ca-hydroxyapatite powders at 37 degrees C in synthetic body fluids. Biomater 2000;21:1429-1438.

[32] Dorozhkin SV. Calcium orthophosphate cements for biomedical application. J Mater Sci 2008;43:3028–3057.

[33] Shannon RD, Prewitt CT. Effective Ionic Radii in Oxides and Fluorides. Acta Crys: Struct Crys and Crys Chem 1969;25:925-946.

[34] Kim HW, Koh YH, Kong YM, Kang JG, Kim HE. Strontium substituted calcium phosphate biphasic ceramics obtained by a powder precipitation method. J Mater Sci: Mater Med 2004;15:1129-1134.

[35] Somasundaran P. Encyclopedia of Surface and Colloid Science, Vol. 1, 2nd Edition, CRC Press 2006, pp 659-662.

[36] Oudar J. Physics and chemistry of surfaces. Glasgow: Blackie, 1975

[37] Pittet C. Development and characterisation of injectable calcium phosphate cements for use in vertebroplasty. PhD Thesis. Swiss Federal Institute of Technology of Lausanne 2001.

[38] Guo DG, Xu KW, Zhao XY, Han Y. Development of a strontium-containing hydroxyapatite bone cement. Biomater 2005;26:4073-4083.

[39] Curry NA, Jones DW. Crystal structure of brushite, calcium hydrogen orthophosphate dihydrate - neutron-diffraction investigation. J Chem Soc 1971;23:3725-3729.

[40] Mathew M, Schroeder LW, Dickens B, Brown WE. Crystal structure of alpha-$Ca_3(PO_4)_2$. Acta Crys: Struct Commun 1977;33:1325-1333.

2.4 Injectability of brushite-forming Mg-substituted and Sr-substituted α-TCP bone cements

S. Pina, P.M.C. Torres and J.M.F. Ferreira

University of Aveiro, Dept. of Ceramics and Glass Engineering, CICECO,3810-193 Aveiro, Portugal.

J Mater Sci: Mater in Med DOI 10.1007/s10856-009-3890-2

Abstract

The influence of Magnesium- and Strontium-substitutions on injectability and mechanical performance of brushite-forming α-TCP cements has been evaluated in the present work. The effects of Mg- and Sr-substitutions on crystalline phase composition and lattice parameters were determined through quantitative X-ray phase analysis and structural Rietveld refinement of the starting calcium phosphate powders and of the hardened cements. A noticeable dependence of injectability on the liquid-to-powder ratio (LPR), smooth plots of extrusion force versus syringe plunger displacement and the absence of filter pressing effects were observed. For LPR values up to 0.36 mL g^{-1}, the percentage of injectability was always higher for Mg-containing cements and lower for Sr-containing cements, respectively, while all the pastes could be fully injected for LPR > 0.36 mL g^{-1}. The hardened cements exhibited relatively high wet compressive strength values (~17-25 MPa) being the Sr- and Mg-containing cements the strongest and the weakest, respectively, holding an interesting promise for uses in trauma surgery such as for filling bone defects and in minimally invasive techniques such as percutaneous vertebroplasty to fill lesions and strengthen the osteoporotic bone.

Keywords: *magnesium; strontium; brushite; bone cement; injectability; mechanical strength*

1. Introduction

The continued increase in the age of the population and the concomitant increasing incidence of bone diseases such as osteoporosis (a disease that results in a loss of normal bone density, mass and strength, leading to a condition in which bones are increasingly porous or full of small holes and vulnerable to breaking), osteomyelitis, malignant tumors, or traumatic accidents, has generated higher demands for bone grafting [1,2]. Vertebroplasty and kyphoplasty are minimally invasive procedures for vertebral compression fractures (VCF) usually caused by osteoporosis, which are fractures in vertebra, the irregular bones that make up the spinal column.

The orthopedic cements used in vertebroplasty and kyphoplasty are based on polymethylmethacrylate (PMMA) for their mechanical properties. However, this kind of cements might cause extensive necrosis due to noticeable exothermal effects upon curing [2-5]. Besides, PMMA cements have several other drawbacks, including no biologic potential to remodel or integrate into the surrounding bone, no direct bone apposition, excessive inherent stiffness, high polymerization temperature, and potential monomer toxicity. PMMA is also commonly used as bone void filler in surgery requiring the removal of bone as in bone tumours [6,7].

Calcium phosphate cements (CPC) have been in clinical use for the last 10 years. They are prepared from a powder and a liquid, forming a viscous and easy mouldable paste that after being implanted sets and hardens within the body as either a non-stoichiometric calcium deficient hydroxyapatite (CDHA) or brushite, sometimes blended with unreacted particles and other phases. They are commonly used as bone filling defects and in trauma surgeries as mouldable paste-like bone substitute materials. Their most salient features include good biocompatibility, excellent bioactivity, self-setting characteristic, low setting temperature, adequate stiffness, and easy shaping to any complicated geometry [8-16]. Nearly perfect adaptation to tissue surfaces in bone defects, a gradual bioresorption followed by new bone formation and the lack of any by-products are other distinctive advantages of CPC [6,7].

Recently, the development of injectable CPC is seen with alacrity due to their importance for minimally invasive surgical techniques such as percutaneous vertebroplasty to fill bone lesions and cracks to strengthen the bone [15,17-22]. Injectable osteoconductive CPC can fit bone defects perfectly and be used as an adjunct to internal fixation for treating selected fractures, as filling voids in metaphyseal bone, thereby reducing the need for bone graft, and improving the holding strength around metal devices in osteoporotic bone. They can easily be used by bone remodeling cells for reconstruction of damaged parts of bones [11,15]. Injectability is also important for applications with limited accessibility and narrow cavities, and when there is a need for precise placement of the paste to conform to a defect area, such as periodontal bone repair and tooth root canal fillings. However, liquid-phase separation (the so-called filter-pressing effect) provoked by the extrusion pressure applied to the cement paste after a certain injection time has often been observed in commercial formulations [4,23]. This problem has been the focus of several previous studies [4,11,15,21-26]. Habib et al. [23] concluded that high extrusion velocity, small syringe size, short cannula and high liquid-to-powder ratio (LPR) favoured injectability. Sarda et al. [21] found enhanced injectability of α-TCP-water mixtures with the addition of citrate ions. Barralet et al. [24] made similar observations for brushite and apatite cements and found improved injectability with increasing LPR. Leroux et al. [26] used sodium glycerophosphate, latic acid, glycerol and chitosan to improve injectability and measured lower extrusion forces in the presence of all these additives. However, commercial formulations still suffer from several shortcomings related to unsatisfactory levels of some properties: (i) low mechanical strength; (ii) poor injectability; (iii) ionic mismatches towards the bone composition, which includes (but is not limited to) the following cations: Na^+, K^+, Mg^{2+}, Ca^{2+}, H^+ and anions: PO_4^{3-}, HPO_4^{2-}, $H_2PO_4^-$, CO_3^{2-}, HCO_3^-, SO_4^{2-}, HSO_4^-, Cl^-, F^-, SiO_4^{4-} [4,7,11,15]. Insufficient mechanical strength and the poor injectability are interdependent properties, both affected by a number of experimental factors, such as particle size and particle size distribution of the powder, the degree of crystallinity (amorphous calcium phosphates tend to give more viscous and reactive mixtures), the presence of rheological modifiers and/or other additives with specific roles.

Usually, injectability of a cement paste varies inversely with its viscosity and with the time after starting the mixing of liquid and powder [4,7,23,26]. Enhancing the injectability of a cement paste by increasing LPR degrades the mechanical properties and cohesion of hardened cements and markedly elongates the initial and final setting times [7].

Substitution of trace elements, such as Mg and Sr ions in the apatite structure has been the subject of widespread investigation, because of their impending role in the biological process, as observed during implantation studies [27-35]. Mg is undoubtedly one of the most important bivalent ions associated with the biological apatite; Sr increases osteoclast apoptosis and enhances preosteoblastic cell proliferation and collagen synthesis [35]. However, none of the above mentioned literature reports have been focused on studying the injectability of brushite-forming Mg- and Sr-substituted α-TCP cements. Therefore, the main goal of the present study is to investigate the influence of single Mg- and Sr-substitutions on the injectability of brushite-forming α-TCP cements.

2. Materials and Methods

2.1. Preparation of powders and cement pastes

The Mg- and Sr-substituted cements with molar ratio (Ca + x)/P = (1.35 + 0.15)/1 = 1.5 (x denoting the molar content of Sr or Mg), thus performing the stoichiometric ratio of β-TCP, were used in the present study. The starting Mg- and Sr-substituted powders were prepared by aqueous precipitation as described elsewhere [36]. Briefly, calcium nitrate tetrahydrate [$Ca(NO_3)\cdot 4H_2O$, Vaz Pereira-Portugal, Sintra, Portugal], diammonium hydrogen phosphate [$(NH_4)_2HPO_4$, Vaz Pereira-Portugal, Sintra, Portugal], magnesium nitrate hexahydrate [$Mg(NO_3)_2.6H_2O$, Merck, Darmstadt, Germany] and strontium nitrate [$Sr(NO_3)$, Riedel-de-Haen, Seelze, Germany] were used as starting chemical precursors, respectively for calcium, phosphorus, magnesium and strontium. The precipitates

were filtrated, dried at 110ºC and then heat treated at 1500ºC to convert them mostly into α-TCP.

The calcined cakes were milled and passed through a 36 μm sieve and then used as starting CPC powders. Particle size distributions of the powders were determined using a light scattering instrument (Coulter LS 230, UK, Fraunhofer optical model). The particle morphology of the powders was obtained using a scanning electron microscope (SEM) (Hitachi S4100, Tokyo, Japan).

Cement pastes were prepared by mixing different proportions of the starting CPC powders with an aqueous solution consisting of 20 wt.% citric acid (Sigma) + 10 wt.% poly(ethylene glycol) (PEG) (200, Sigma) + 0.5 wt.% hydroxyl propyl methylcellulose (HPMC) (3.5-5.6 mPa s at 2% by mass in water, Sigma) in order to get liquid-to-powder ratios (LPR) of 0.34, 0.35, 0.36 and 0.38 mL g^{-1}.

These cements will be hereafter designated as Mg-BC and Sr-BC, respectively for Mg- and Sr-substituted cements. For comparison purposes and a better understanding of the effects of Mg and Sr on injectability of substituted cement pastes, pure α-TCP cement was also prepared and used as reference (Ref-BC).

2.2. X-ray diffraction and structural analysis by the Rietveld refinement method

Identification of the crystalline phases formed upon hydration of cement pastes was performed by X-ray diffraction (XRD) using a high-resolution SIEMENS D5000 with SolX detector. Data sets were collected from 2θ = 10-50º with a step size of 0.02º, with CuKα radiation. The phase composition of the samples was calculated on the basis of XRD patterns by means of Rietveld analysis with TOPAS 3.0 software (Bruker AXS, Germany). Rietveld refinement was performed using the structural models (ICSD Database) of all phases listed in Table 1.

Table 1: ICSD-Data used for Rietveld refinement and phase quantification

Phase	Structural model	
	ICSD code	Authors
α-TCP (tricalcium phosphate)	923	Mathew et al. [37]
β-TCP	97500	Yashima et al. [38]
Brushite (DCPD)	16132	Curry et al. [39]

2.3. Rheological measurements

Rheological measurements of the cement pastes were carried out with a rotational controlled-stress rheometer (Bohlin C-VOR 150, Bohlin Ltd., Gloucestershire, UK) equipped with a 4º / 40 mm cone-and-plate sensor system. Viscosity measurements were performed in the shear rates range of about 0.1 - 100 s^{-1}. For each test, 2 g of powder was mixed with the setting liquid at LPR = 0.35 mL g^{-1}, for 1 min to form a homogeneous paste at room temperature. The rheological measurement started 1 minute after mixing in order to assure the same rheological history during the preparation of all the cement pastes.

2.4. Setting times

The initial setting time of the cement pastes was determined using Vicat needle technique according to the ASTM C 187-98. One minute after placing the pastes into a glass plate stored at 37ºC in 100% humidity box, the indenter (100 g in mass, 1 mm diameter of the needle) was lowered vertically onto the surface of the cement. The indentation was repeated at intervals of 30 s until no more penetration was possible. The time at this point was taken as the initial setting time.

2.5. Injectability testing

The injectability tests were carried out with a 10 mL syringe (15 mm diameter and 80 mm in length) fitted with a cannula of 2.2 mm inner diameter and 91 mm in length, according to a procedure described in previous studies [9,14,40]. The paste (5 g of powder + the required amount of liquid) was hand-mixed for 1 min and then placed into the syringe. The syringe was placed between the compression plates of a testing machine (Shimadzu Autograph, Trapezium 2, Japan) using a home made apparatus fixture. The cement pastes were extruded at a crosshead speed of 15 mm min^{-1} up to a maximum load of 100 N. The evolution of the extrusion force was recorded against the extruding time and the percentage of extruded paste was determined as the mass of the paste that could be expelled from the syringe divided by the original mass of the paste inside the syringe [14,40]. For each experimental set of conditions, injectability measurements were repeated three times and the average values calculated.
In order to evaluate the eventual occurrence of filter-pressing effects whenever the pastes could not be totally extruded, both the extruded pastes and the pastes remaining in the syringe were examined for the LPR. For that, the weights of the pastes before and after complete drying at 120ºC for 24 h were measured.

2.6. Mechanical testing

Cement pastes were cast into PTFE-moulds (Φ 6 $\times$ 12 mm deep) and stored for 24 h in a 100% humidity box at 37ºC. The cement specimens were then removed from the moulds and immersed in PBS solution at 37ºC for additional 6 h, 24 h and 48 h. The compressive strength measurements were done using a universal materials testing machine (Shimadzu Autograph, Trapezium 2, Japan) at a crosshead displacement rate of 1 mm min^{-1}. Results of compressive strength are expressed as the mean $\pm$ standard error of the mean of triplicate determinations.

2.7 Statistical analysis

Statistical analysis of injectability and mechanical strength data was performed using the SPSS 16.0 software. Comparative studies of means were performed using one-way ANOVA followed by a post hoc test (Fisher projected least-significant difference) with a statistical confidence coefficient of 95%; therefore, *p* values < 0.05 were considered significant.

3. Results

Particle diameter distributions of the starting CPC powders after milling and sieving are depicted in Fig. 1. All size distribution curves are essentially monomodal with average particle diameters, D_{50}, of 17.32 μm, 10.78 μm, 15.97 μm, for Ref-BC, Sr-BC and Mg-BC powders, respectively. Minor populations centred at about 2 μm are also apparent, being somewhat more intense in the case of Sr-BC powder.

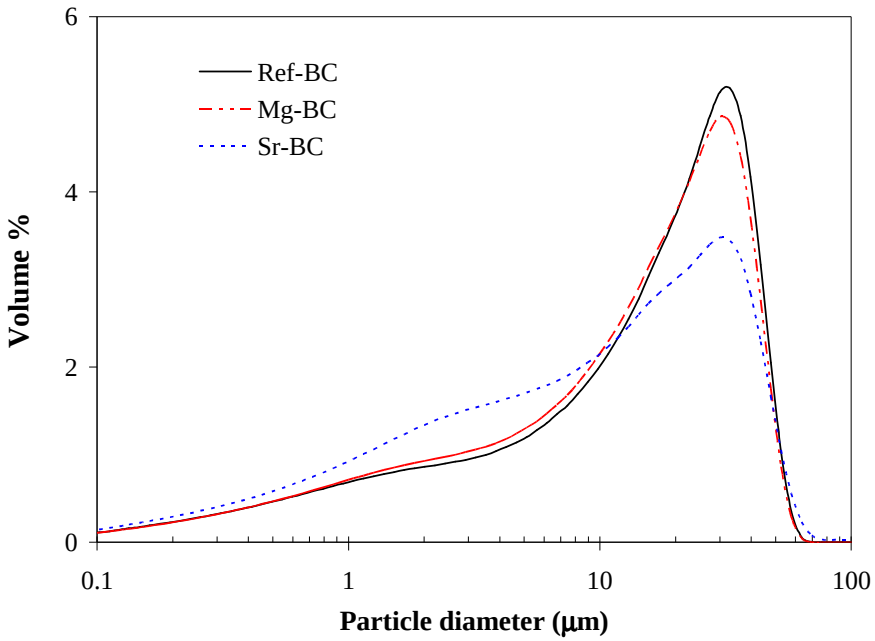

Fig. 1: Particle size distributions of the starting CPC powders after milling.

Fig. 2 presents the XRD diffraction patterns of the powdered hardened undoped and Mg- or Sr-substituted cements after 2 days of hydration. All the hydrated cements consist mostly of α-TCP, and brushite as a minor crystalline phase. The presence of β-TCP is noted only in the case of Mg-substituted cement.

Quantitative Rietveld XRD analyses of phases on the starting powders and formed upon hydration for 2 days are presented in Table 2. The reported data confirm that the starting powders are mostly constituted by α-TCP for Ref-BC and Sr-BC cements, while for Mg-BC it consists of a mixture of α-TCP as the main phase and β-TCP as minor phase. The hydrated cements consist predominantly of α-TCP and a fraction of brushite, with an additional β-TCP phase in the case of Mg-BC.

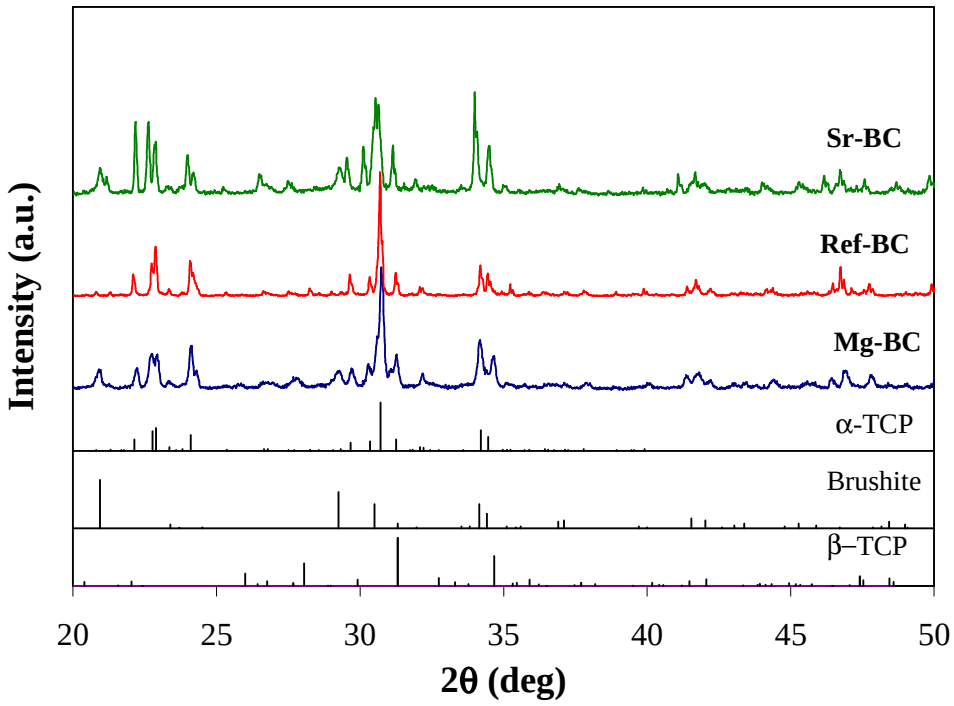

Fig. 2: XRD patterns of cements prepared from a mixing liquid with 0.5 wt.% HPMC + 10 wt.% PEG + 20 wt.% citric acid, after 2 days of hydration. α-TCP ($Ca_3(PO_4)_2$, JCPDS PDF File # 29-359), Brushite (JCPDS PDF File # 9-0077) and β-TCP (β-$Ca_3(PO_4)_2$, JCPDS PDF File # 1-70-682); full scale intensity = 6,000 cps.

Table 2: Rietveld refinement phase analysis of the starting powders and of the cements hydrated for 2 days

	Composition (%)					
	Ref-BC		**Sr-BC**		**Mg-BC**	
Phases	Powder	Hydrated	Powder	Hydrated	Powder	Hydrated
α-TCP	100.0	77.5	100.0	77.3	84.6	71.8
Brushite	-	22.5	-	22.7	-	22.8
β-TCP	-	-	-	-	15.4	5.4

The flow curves of the cement pastes with a LPR = 0.35 are presented in Fig. 3. All of them exhibit similar shear-thinning character. Although very close to each other, if ordered by decreasing viscosity at given shear rates, the curves appear as Sr-BC > Ref-BC > Mg-BC. Accordingly, the initial setting times of the cement pastes tended to increase in the same order: 5 ± 0.5 min for Ref-BC, 7 ± 0.5 min for Sr-BC and 10.0± 0.5 min for Mg-BC ($p<0.05$).

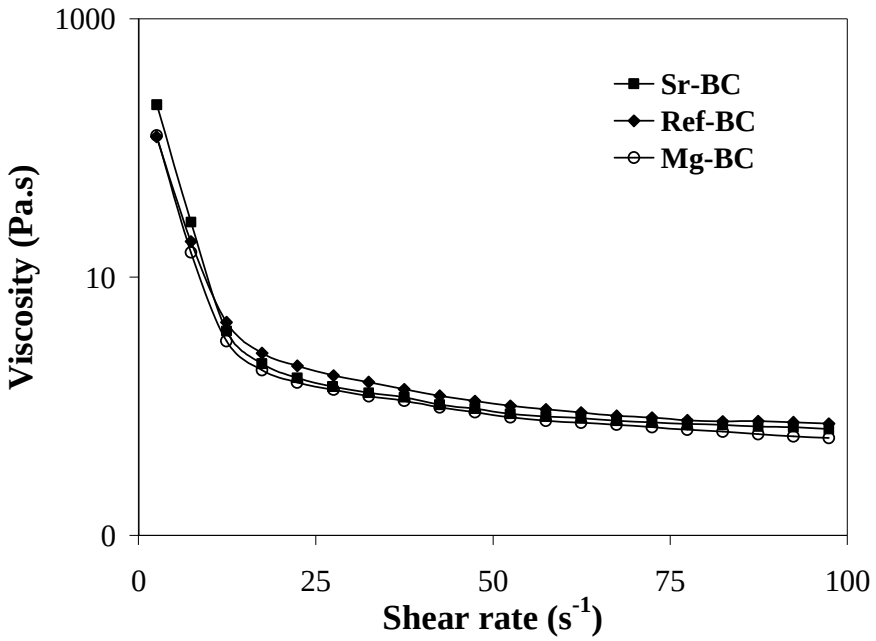

Fig. 3: Viscosity versus shear rate curves of the cement pastes prepared with LPR of 0.35 mL g^{-1}.

The forces required for extruding the pastes as a function of syringe plunger displacement are shown in Fig. 4 for two different LPR values of 0.34 and 0.38 mL g^{-1}. It can be seen that for LPR = 0.34 mL g^{-1} the extrusion force soon exceeded the pre-set maximum force after 4.3-5.1 mm of plunger travel. The higher extrusion forces demanded for the lower LPR hindered full injection under the set conditions, although higher extrusion forces could be exerted even by hand injection. For the LPR = 0.38 mL g^{-1}, the extrusion curves present a relatively long plateau followed by a fast increase. All the extrusion curves present similar behaviors with the shortest and the longest extrusion plateaux being observed for the Sr-, and the Mg-substituted cement pastes, respectively, with the Ref-BC cement paste in an intermediate position. The observed trends denote different reactivities of the starting cement powders ($p<0.05$) towards the setting liquid. None of the cements presented the filter-pressing effect during extrusion from the syringe.

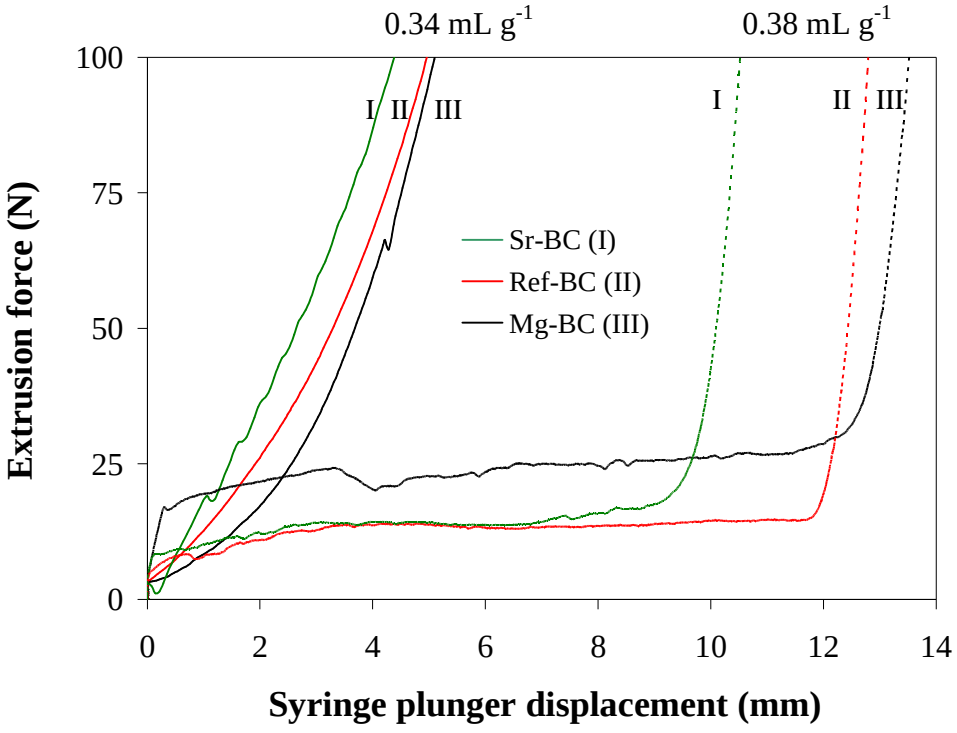

Fig. 4: Extrusion force versus syringe plunger displacement for cement pastes prepared with LPR of 0.34 mL g^{-1} (continuous lines) and of 0.38 mL g^{-1} (dashed lines).

Fig. 5 plots the dependence of the injectability of the cement pastes versus LPR in the range 0.34-0.38 mL g^{-1}, 1.5 min after starting mixing the powder with the setting liquid. It can be seen that the injectability increased with increasing LPR, due to the concomitant decrease of the viscosity of the pastes. Nearly full injectable pastes were obtained for LPR ≥ 0.38 mL g^{-1}. It is also observed that the composition of the starting powders influences the injectability. Mg-BC is the easiest injectable composition, probably due to the presence of some remaining β-TCP phase, which has a much longer handling time, and to the specific role of Mg in delaying the setting process [36].

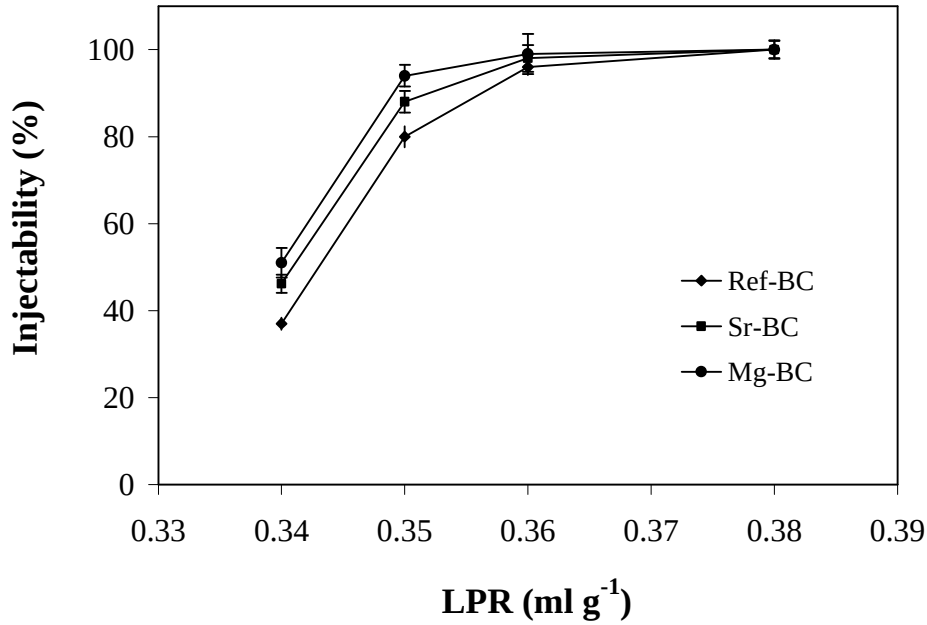

Fig. 5: Injectability of the cement pastes as function of LPR, 1.5 min after starting mixing the powder with the setting liquid.

The wet compressive strength values of the cements hardened for 24 h and kept under wet conditions for further 6 h, 24 h and 48 h, before performing the measurements, are shown in Fig. 6. As expected, the compressive strength decreased with an increase of immersion time in PBS solution, due to a gradual structural degradation process ($p < 0.05$). It can be observed that Sr-BC cement specimens exhibit the highest compressive strength values, followed by Ref-BC cements ($p \cong 0.009$), and by Mg-BC cements ($p \cong 0.012$). This can be probably due to the presence of β-TCP phase in Mg-BC.

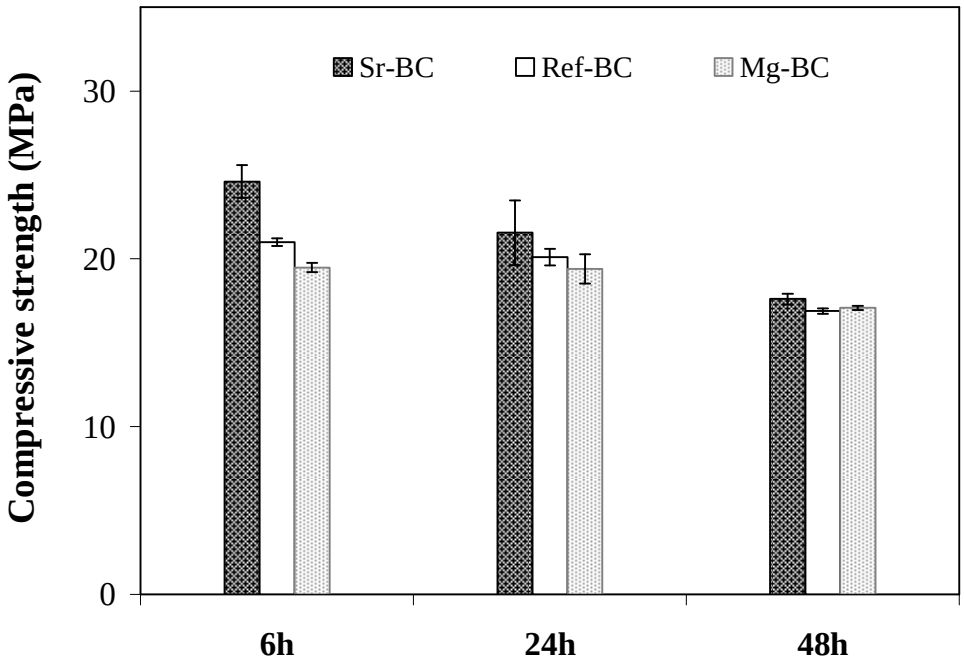

Fig. 6: Compressive strength values measured for the wet cements hydrated for 24 h and kept under wet conditions for further 6 h, 24 h and 48 h. The pastes were prepared with 0.5 wt.% HPMC + 10 wt.% PEG + 20 wt.% citric acid (LPR = 0.38 mLg^{-1}).

4. Discussion

Improving the less performing aspects of CPCs requires lowering the LPR values while keeping suitable flow properties. These requirements are not easy to conciliate, especially in reacting systems as cement pastes are. It has been shown that in non-reacting aqueous systems low viscosity suspensions of calcium phosphate powders containing unusual high solids loading (60 vol.%) could be easily prepared [41]. This solids loading corresponds to a LPR of 0.21 mL g^{-1}, much lower than those used in injectable CPC [7]. Therefore, the key to formulate strong injectable CPC is to decrease LPR while keeping a relatively low viscosity. This strategy to enhance the mechanical properties leads to a decrease of the cement porosity, which in turn will reduce the resorption kinetics. But this drawback can be coped using brushite-based CPC like the ones proposed in the

present work, which have a faster resorption than apatite CPC [4,36,42]. Injectability of CPC pastes is strongly dependent on their flow properties, which, in turn, depend on a number of factors including particle/agglomerate size and particle/agglomerate size distributions, the nature of the phases present (amorphous or crystalline), the liquid-to-powder ratio (LPR), and the presence of rheological modifiers. Injectability, the ability of the cement pastes to be extruded through relatively fine nozzles, requires a shear thinning behaviour. The presence of particle agglomerates with an open structure and sweeping large areas when the system flows tends to confer a shear thickening behaviour to the cement pastes, which, in turn, is the direct cause of the filter-pressing effect often observed in CPC pastes. Considering that the time allowed for mixing the starting CPC powders and setting liquid is short and that hand mixing is unsuitable for destroying particle agglomerates, it is essential that the starting powders have been already deagglomerated and possess a relatively wide particle size distribution [43]. This was the reason why the powders were milled / deagglomerated and passed through a 36 μm sieve before being used to prepare the cement pastes. This procedure, and probably the use of HPMC as gelling agent, fully prevented the filter-pressing phenomenon during extrusion from the syringe for all cement pastes.

The shear-thinning character revealed in Fig. 3 (LPR = 0.35) was typical of cement pastes with other LPR values. This type of rheological behaviour with viscosity decreasing as shear rate increases is very suitable for injection through narrow nozzles.

In order to check if the shear rate range adopted could well represent the injectability conditions, the maximum shear rate, τ_w, at the cannula wall was estimated based on the Hagen-Poisseuille equation for steady laminar flow [44]. The following holds for the maximum shear rate τ_w at the pipe wall:

$$\tau_w = \frac{4\dot{V}}{\pi R^3}$$

Where $\dot{V}$ is the volume flow rate [$m^3\ s^{-1}$], and R is the inside diameter of the capillary [m]. The conditions set for injectability tests correspond to a volume flow rate of about $44.2\times10^{-9}\ m^3\ s^{-1}$ and a maximum shear rate at the inner cannula wall of about 16.6 s^{-1}. Therefore, the shear rate range used to access the flow behaviour covers all the possible values for this inner diameter (2.2 mm) of the cannula even if the volume flow rate was increased by 6 times.

The plots of extrusion force as a function of syringe plunger displacement shown in Fig. 4 reveal the dependence of extrusion force on the LPR as shown by several previous studies [4,7,21,23,26]. It is worthy noting that all the extrusion curves presented in Fig. 4 are smoother that those reported for similar LPR values but non-reacting systems. Such roughness was probably due to the presence of particles agglomerates, although their destruction would be easier in a non-reacting system [14].

Concerning the effects of ionic substitutions, the sets of extrusion curves presented in Fig. 4 show the same order: the Sr-BC is always shortest and the Mg-BC is the longest. This means that Sr enhances the reactivity of the cement pastes, while Mg tends to delay the setting process of α-TCP based cements. The remaining β-TCP phase in the starting powder of this cement, which has a much longer handling time, is also expected to improve the injectability. This is according to what has been reported earlier for the influence of Sr-substituted and Mg-substituted cements [35,45]. Lilley et al. [34] showed a strong effect of Mg on setting kinetics and on the characteristics of hardened cements namely, a decreasing rate of hydration, an increased proportion of brushite formed upon setting, and a decrease in compressive strength. Mg has been also reported to have a stabilizing role of non-crystalline CaPs, preventing crystallization into other more stable CaP phases [46], in good agreement with an observed decrease of the hydrolysis extent of brushite [34]. Bone restoration studies made in rats showed that using CPC doped with low doses of Sr increased the number of bone forming sites and vertebral bone volume, while no adverse effects could be observed on mineral profile, bone mineral chemistry or bone matrix mineralization [47]. Saint-Jean et al. [48] reported comparable bioactivities for hardened Sr-containing apatite cements and calcium deficient hydroxyapatite.

The injectability results plotted in Fig. 5 are in good agreement with the extrusion curves shown in Fig. 4 and with data reported in previous studies [49]. For LPR values up to 0.36 mL g^{-1}, the percentage of injectability is always higher for the case of Mg-BC and lower for Sr-BC. For LPR > 0.36 mL g^{-1} all the pastes could be fully injected under the relatively low applied forces set in the present work.

The measured wet compressive strength values (~17-25 MPa) of the cements are in the upper limit of range of 1-25 MPa for compressive strengths reported in literature for brushite-forming cements [6] as well as in the range for cancellous bone (10-30 MPa) [50]. The results show that Sr-containing cement specimens exhibit higher compressive strength values in comparison to undoped Ref-BC followed by Mg-BC cement, probably due to the lower content of brushite phase present in Sr-BC (pure brushite cements are characterized by their low mechanical strength). Citric acid has likely diffused out slowly during soaking in PBS, thus leading to a weaker structure. This helps explaining the decrease of compressive strength with immersion time.

5. Conclusions

The present study showed that the obtained Mg- and Sr-substituted α-TCP cement pastes exhibited general good injectability characteristics even under a moderate maximum applied force of 100 N, which revealed to be dependent on the cement composition and on the LPR. Practically full injectable cement pastes were obtained for LPR $\geq$ 0.36 mL g^{-1}. The wet compressive strength of the hardened cements specimens is fairy high. Even the lower compressive strength values corresponding to the higher LPR used in the present work 0.38 mL g^{-1} are comparable to that of trabecular bone. These results shown that the brushite-forming α-TCP bone cements developed in the present work, especially the Sr-substituted one, hold an interesting promise for uses in trauma surgery such as for filling bone defects and in minimally invasive techniques such as percutaneous vertebroplasty to fill the lesions and to strengthen the osteoporotic bone.

Acknowledgments

Thanks are due to CICECO for the support and to the Portuguese Foundation for Science and Technology for the fellowship grant of S. Pina (SFRH/BD/21761/2005).

The first author is grateful to C. Stabler, from Institute of Mineralogie, University of Erlangen-Nuremberg, Germany, for his valuable help.

References

[1] Gbureck U, Vorndran E, Muller FA, Barralet JE. Low temperature direct 3D printed bioceramics and biocomposites as drug release matrices. J Control Release. 2007;122:173-180.

[2] Metallidis S, Topsis D, Nikolaidis J, Alexiadou E, Lazaraki G, Grovaris L, Theodoridou A, Nikolaidis P. Penetration of moxifloxacin and levofloxacin into cancellous and cortical bone in patients undergoing total hip arthroplasty. J Chemotherapy. 2007;19:682-687.

[3] Bohner M. Reactivity of calcium phosphate cements. J Mater Chem. 2007;17:3980-3986.

[4] Bohner M, Gbureck U, Barralet JE. Technological issues for the development of more efficient calcium phosphate bone cements: A critical assessment. Biomaterials. 2005;26:6423-6429.

[5] Fernandez E. Bioactive bone cements. Wiley Encyclopaedia of Biomedical Engineering: John Wiley & Sons, Inc.; 2006.

[6] Bohner M. Calcium orthophosphates in medicine: from ceramics to calcium phosphate cements. Inj-Intern Care Injur. 2000;31:37-47.

[7] Dorozhkin SV. Calcium orthophosphates. J Mater Sci. 2007;42:1061-1095.

[8] Brown WE, Chow LC. A New Calcium-Phosphate Setting Cement. J Dental Res. 1983;62:672-672.

[9] Wang XP, Ye JD, Wang H. Effects of additives on the rheological properties and injectability of a calcium phosphate bone substitute material. J Biomed Mater Res Appl Biomater. 2006;78:259-264.

[10] Yuan HP, Li YB, de Bruijn JD, de Groot K, Zhang XD. Tissue responses of calcium phosphate cement: a study in dogs. Biomaterials. 2000;21:1283-1290.

[11] Alves HLR, dos Santos LA, Bergmann CP. Injectability evaluation of tricalcium phosphate bone cement. J Mater Sci Mater Med. 2008;19:2241-2246.

[12] Baroud G, Cayer E, Bohner M. Rheological characterization of concentrated aqueous á-tricalcium phosphate suspensions: The effect of liquid-to-powder ratio, milling time, and additives. Acta Biomater. 2005;1:357-363.

[13] Boesel L, Reis RL. The effect of water uptake on the behaviour of hydrophilic cements in confined environments. Biomaterials. 2006;27:5627-5633.

[14] Bohner M, Baroud G. Injectability of calcium phosphate pastes. Biomaterials. 2005;26:1553-1563.

[15] Burguera EF, Xu HHK, Sun LM. Injectable calcium phosphate cement: Effects of powder-to-liquid ratio and needle size. J Biomed Mater Res Appl Biomater. 2008;84:493-502.

[16] Gauthier O, Muller R, von Stechow D, Lamy B, Weiss P, Bouler JM, Aguado E, Daculsi G. In vivo bone regeneration with injectable calcium phosphate biomaterial: A three-dimensional micro-computed tomographic, biomechanical and SEM study. Biomaterials. 2005;26:5444-5453.

[17] Baroud G, Wu JZ, Bohner M, Sponagel S, Steffen T. How to determine the permeability for cement infiltration of osteoporotic cancellous bone. Med Eng & Phys. 2003;25:283-288.

[18] Khairoun I, Boltong MG, Driessens FCM, Planell JA. Some factors controlling the injectability of calcium phosphate bone cements. J Mater Sci Mater Med. 1998;9:425-428.

[19] Bai B, Jazrawi LM, Kummer FJ, Spivak JM. The use of an injectable, biodegradable calcium phosphate bone substitute for the prophylactic augmentation of osteoporotic vertebrae and the management of vertebral compression fractures. Spine. 1999;24:1521-1526.

[20] Ginebra MP, Rilliard A, Fernandez E, Elvira C, San Roman J, Planell JA. Mechanical and rheological improvement of a calcium phosphate cement by the addition of a polymeric drug. J Biomed Mater Res. 2001;57:113-118.

[21] Sarda S, Fernandez E, Nilsson M, Balcells M, Planell JA. Kinetic study of citric acid influence on calcium phosphate bone cements as water-reducing agent. J Biomed Mater Res. 2002;61:653-659.

[22] Gbureck U, Barralet JE, Spatz K, Grover LM, Thull R. Ionic modification of calcium phosphate cement viscosity. Part I: hypodermic injection and strength improvement of apatite cement. Biomaterials. 2004;25:2187-2195.

[23] Habib M, Baroud G, Gitzhofer F, Bohner M. Mechanisms underlying the limited injectability of hydraulic calcium phosphate paste. Acta Biomater. 2008;4:1465-1471.

[24] Barralet JE, Grover LM, Gbureck U. Ionic modification of calcium phosphate cement viscosity. Part II: hypodermic injection and strength improvement of brushite cement. Biomaterials. 2004;25:2197-2203.

[25] Sarda S, Fernandez E, Llorens J, Martinez S, Nilsson M, Planell JA. Rheological properties of an apatitic bone cement during initial setting. J Mater Sci Mater Med. 2001;12:905-909.

[26] Leroux L, Hatim Z, Freche M, Lacout JL. Effects of various adjuvants (lactic acid, glycerol, and chitosan) on the injectability of a calcium phosphate cement. Bone. 1999;25:31-34.

[27] Bigi A, Foresti E, Gandolfi M, Gazzano M, Roveri N. Isomorphous substitutions in beta-tricalcium phosphate: The different effects of zinc and strontium. J Inorg Biochem. 1997;66:259-265.

[28] Kannan S, Lemos AF, Rocha JHG, Ferreira JMF. Characterization and mechanical performance of the Mg-stabilized á-Ca 3 (PO 4) 2 prepared from Mg-substituted Ca-deficient apatite. J Am Ceram Soc. 2006;89:2757-2761.

[29] Kannan S, Lemos IAF, Rocha JHG, Ferreira JMF. Synthesis and characterization of magnesium substituted biphasic mixtures of controlled hydroxyapatite/beta-tricalcium phosphate ratios. J Sol State Chem. 2005;178:3190-3196.

[30] Kannan S, Pina S, Ferreira JMF. Formation of strontium-stabilized á-tricalcium phosphate from calcium-deficient apatite. J Am Ceram Soc. 2006;89:3277-3280.

[31] Kannan S, Rocha JHG, Ferreira JMF. Synthesis and thermal stability of sodium, magnesium co-substituted hydroxyapatites. J Mater Chem. 2006;16:286-291.

[32] Fadeev IV, Shvorneva LI, Barinov SM, Orlovskii VP. Synthesis and structure of magnesium-substituted hydroxyapatite 1. Inorg Mater. 2003;39:947-950.

[33] Suchanek WL, Byrappa K, Shuk P, Riman RE, Janas VF, TenHuisen KS. Preparation of magnesium-substituted hydroxyapatite powders by the mechanochemical-hydrothermal method. Biomater. 2004;25:4647-4657.

[34] Lilley KJ, Gbureck U, Knowles JC, Farrar DF, Barralet JE. Cement from magnesium substituted hydroxyapatite. J Mater Sci Mater Med. 2005;16:455-460.

[35] Rokita E, Hermes C, Nolting HF, Ryczek J. Substitution of Calcium by Strontium within Selected Calcium Phosphates. J Cryst Growth. 1993;130:543-552.

[36] Pina S, Olhero SM, Gheduzzi S, Miles AW, Ferreira JMF. Influence of setting liquid composition and liquid-to-powder ratio on properties of a Mg-substituted calcium phosphate cement. Acta Biomater. 2009;5:1233-1240.

[37] Mathew M, Schroeder LW, Dickens B, Brown WE. Crystal structure of alpha-$Ca_3(PO_4)_2$. Acta Crys: Struct Commun 1977;33:1325-1333.

[38] Yashima M, Sakai A, Kamiyama T, Hoshikawa A. Crystal structure analysis of beta-tricalcium phosphate Ca-3(PO4)(2) by neutron powder diffraction. J Sol St Chem 2003;175:272-277.

[39] Curry NA, Jones DW. Crystal structure of brushite, calcium hydrogen orthophosphate dihydrate - neutron-diffraction investigation. J Chem Soc 1971;23:3725-3729.

[40] Xu HHK, Weir MD, Burguera EF, Fraser AM. Injectable and macroporous calcium phosphate cement scaffold. Biomaterials. 2006;27:4279-4287.

[41] Lemos AF, Ferreira JMF. Combining foaming and starch consolidation methods to develop macroporous hydroxyapatite implants. Bioceram. 16 2004;254:1041-1044.

[42] Bohner M, Gbureck U. Thermal reactions of brushite cements. J Biomed Mater Res Appl Biomater. 2008;84:375-385.

[43] Olhero SM, Ferreira JMF. Influence of particle size distribution on rheology and particle packing of silica-based suspensions. Powder Techn. 2004;139:69-75.

[44] Mezger TG. The rheology handbook: for users of rotational and oscillation rheometers. Hannover: Vicentz Verlag; 2002.

[45] Alkhralsat MH, Marino FT, Rodriguez CR, Jerez LB, Cabarcos EL. Combined effect of strontium and pyrophosphate on the properties of brushite cements. Acta Biomater. 2008;4:664-670.

[46] TenHuisen KS, Brown PW. Effects of magnesium on the formation of calcium-deficient hydroxyapatite from $CaHPO_4.2H_2O$ and $Ca_4(PO4)_2O$. J Biomed Mater Res. 1997;36:306-314.

[47] Grynpas MD, Hamilton E, Cheung R, Tsouderos Y, Deloffre P, Hott M, Marie PJ. Strontium increases vertebral bone volume in rats at a low dose that does not induce detectable mineralization defect. Bone. 1996;18:253-259.

[48] Saint-Jean SJ, Camire CL, Nevsten P, Hansen S, Ginebra MP. Study of the reactivity and in vitro bioactivity of Sr-substituted α-TCP cements. J Mater Sci Mater Med. 2005;16:993-1001.

[49] Khairoun I, Driessens FCM, Boltong MG, Planell JA, Wenz R. Addition of cohesion promoters to calcium phosphate cements. Biomaterials. 1999;20:393-398.

[50] Duck FA. Physical properties of tissue: a comprehensive reference book. London: Academic Press Limited; 1990.

3 *In vitro* and *in vivo* behaviour of brushite-forming calcium phosphate cements doped with Sr and Zn

Biocompatibility, resorption and replacement of bone substitutes are required for good fracture repair. Therefore, the evaluation of cytotoxicity, resorption and new bone formation of the brushite-forming CPCs in a body environment were studied *in vitro* (using MG63 and MC3T3-E1 cell lines) and *in vivo* by injecting pastes of the cements studied in paper 3.1 and 3.2 into trabecular bone defects in a pig model.

Zn and Sr are essential trace elements with stimulatory effects on bone formation having a direct specific proliferative effect on osteoblastic cells *in vitro*, hence the effects of Zn and Sr incorporation into the structure of starting powders on the properties with of the CPCs were also evaluated.

3.1 *In vitro* performance assessment of new brushite-forming Zn- and ZnSr-substituted β-TCP bone cements

S. Pina[1*], S.I. Vieira[2*], P.M.C. Torres[1], F. Goetz-Neunhoeffer[3], J. Neubauer[3], O.A.B. da Cruz e Silva[2], E.F. da Cruz e Silva[4], J.M.F. Ferreira[1]

[1]University of Aveiro, Dept. of Ceramics and Glass Engineering, CICECO, 3810-193 Aveiro, Portugal

[2]University of Aveiro, Health Sciences Dept., Centro de Biologia Celular, 3810-193 Aveiro, Portugal

[3]Mineralogy, University of Erlangen-Nuremberg, 91054 Erlangen, Germany

[4]University of Aveiro, Dept. of Biology, Centro de Biologia Celular, 3810-193 Aveiro, Portugal

[*]Both authors contributed equally to this work

Submitted to J Biomed Mater Res, Part B: Applied Biomaterials

Abstract

The present study investigated the *in vitro* performance of brushite-forming Zn- and ZnSr-substituted β-TCP cements bone cements in terms of wet mechanical strength and biological response. Quantitative phase analysis and structural refinement of the powdered samples were performed by X-ray powder diffraction and Rietveld refinement technique. Initial and final setting times of the cement pastes, measured using Gilmore needles technique, showed that ZnSrCPC sets faster than ZnCPC. The measured values of the wet strength after 48 h of immersion in PBS solution at 37ºC showed that ZnSrCPC cements are stronger than ZnCPC cements. Human osteosarcoma derived MG63 cell line proved the non-toxicity of the cement powders, using the resazurin metabolic assay.

Keywords: *Zinc; Strontium; Brushite Cement; Setting time, Mechanical strength, Cytotoxicity*

1. Introduction

During the last three decades, there has been a growing interest in calcium phosphate cements (CPC). CPC are excellent bone substitutes due to their good biocompatibility, excellent bioactivity, self-setting characteristics, low setting temperature, adequate stiffness, and easy shaping for any complicated geometry [1-9].

According to the end-product of the setting reaction, hydraulic CPCs can be classified into apatite (AP) cements and brushite (dicalcium phosphate dihydrate, DCPD) cements [10, 11]. Recently, brushite cements have been considered with increasing enthusiasm because brushite is metastable in physiological conditions and can be resorbed *in vivo* much faster than AP cements [12, 13].

The biocompatibility of brushite based cements has been tested in various *in vitro* experimental applications and *in vivo* [12-16]. The results showed that brushite cements are generally well tolerated by the bone and soft tissue environment *in vivo*, such that cement resorption was closely followed by new bone formation.

In recent years, ionic substitutions in calcium phosphate ceramics, such as strontium (Sr) and zinc (Zn), have been the subject of massive interest owing to the critical roles these ions play in the biological process after implantation [16-23]. Zn is an essential trace element with stimulatory effects on bone formation, having a direct specific proliferative effect on osteoblastic cells *in vitro* and thought to possess a potent and selective inhibitory effect on osteoclastic bone resorption *in vivo* [16, 22]. The Zn^{2+} ion is involved in many metallo-enzymes and proteins including alkaline phosphatase (ALP). Sr increases osteoclast apoptosis and enhances preosteoblastic cell proliferation and collagen synthesis [23]. Consequently, Sr ions depress bone resorption and maintain bone formation. Therefore, Sr- and/or Zn-substituted CaPs are expected to produce enhanced biological and chemical responses in the body.

Among various calcium phosphate phases, β-TCP is greatly biocompatible and resorbable in bone tissue. Furthermore, β-TCP is an adequate Zn carrier with low release rate. For example, Ito et al. [24] found that a slow Zn^{2+} release from a biphasic ZnTCP/AP ceramics containing Zn doped β-TCP implanted in rabbit

femora stimulated bone formation. Based on a histological and histomorphometrical study using femora of rabbits, Kawamura et al. [25] reported that 51% of new bone has grown around ZnTCP/AP implants.

The present study investigated the setting times, compressive and diametral tensile strengths, and the cytotoxicity for osteoblast-like cells (MG63 cell line) in *in vitro* culture of new brushite-forming Zn- and ZnSr-substituted β-TCP cements. The release of Zn and Sr ions from the cements into distilled water and the *in vitro* bioactivity tests through immersion in SBF were also determined.

2. Materials and Methods

2.1. Cements preparation

Brushite cement pastes were produced by mixing 55 wt.% of Zn- or ZnSr-substituted β-tricalcium phosphate (β-TCP) powder with 45 wt.% of monocalcium phosphate monohydrate (MCPM, Sigma-Aldrich, Germany) using liquid-to-powder ratio (LPR) of 0.34 mL g^{-1}. According to a previous study of the same authors [26], a LPR of 0.34 mL g^{-1} yielded an optimal balance between the rheological and setting behaviors. The mixing liquid used was 10 wt.% poly(ethylene glycol) (PEG) (200, Sigma) + 15 wt.% citric acid solution. The cements setting occurs via the reaction as follows:

$$\beta\text{-}Ca_3(PO_4)_2 + Ca(H_2PO_4)_2.H_2O + 7H_2O \rightarrow 4CaHPO_4.2H_2O$$

Zn- and ZnSr-substituted β-TCP powders were synthesized by aqueous precipitation as described in detail in previous reports [27-29]. The precipitates were vacuum filtrated, dried at 110ºC, heat treated for 2 h at 1100ºC and grounded under dry conditions in a planetary mill. The powders containing Zn, or Zn + Sr were designated, respectively, as ZnCPC and ZnSrCPC. The milled powders were passed through a sieve with a mesh size of 36 μm and the separated fine fractions of the ZnCPC and ZnSrCPC powders had an average particle size of 1.37 and

1.53 μm, respectively, measured using a light scattering instrument (Coulter LS 230, UK, Fraunhofer optical model).

2.2. XRD and Rietveld refinement evaluation

The incorporation of doping elements into the β-TCP structure was assessed by Rietveld refinement studies. The X-ray diffraction (XRD) analysis of the powders was performed with a SIEMENS D5000 equipped with a diffracted beam graphite monochromator and the XRD of the hardened cements was recorded with a SIEMENS D5000 with SolX detector. Data sets were collected from 2θ = 10-70º with a step size of 0.02º and counting time of 6 s with CuKα radiation. XRD measurements for all the investigated compositions were performed by preparing and measuring them three times independently. The phase composition of the samples was calculated on the basis of XRD patterns by means of Rietveld analysis with TOPAS 3.0 software (Bruker AXS, Germany). Rietveld refinement of the starting β-TCP powders and of the hydrated cements was performed using the structural models (ICSD Database) of all phases listed in Table 1. Refined parameters were scale factor, sample displacement, background as Chebyshev polynomial of fifth order, crystallite size and lattice parameters. All parameters were refined simultaneously.

Table 1: ICSD-Data used for Rietveld refinement and quantification

Phase	Structural model	
	ICSD code	Authors
β-TCP (tricalcium phosphate)	97500	Yashima et al. [30]
Brushite (DCPD)	16132	Curry et al. [31]

2.3. Determination of setting times

The setting times of the cements were assessed using an automated Gilmore needle apparatus (imeter, MSB Breitwieser, Augsburg, Germany). To test the setting time, a freshly prepared cement paste was automatically lifted against a needle weighing 212 g with a diameter of 0.692 mm connected to an analytical balance. For each indentation the weight reduction of the needle and the corresponding penetration depth was recorded. From these values the so-called “imeter-hardness” was calculated from the relation strength per penetration depth standardized by the diameter of the used needle [32]. The indentation was repeated at intervals of 30 s until the cement was completely set. Applying the dimensions and weights of the needles given in ASTM C266 the values for the static pressure acting on the specimen at the initial and final setting time were calculated. In accordance with the standard the initial and final setting times are defined when the light and the heavy needles, respectively, failed to make an appreciable indentation. A depth of 0.08 mm of the resulting, barely visible indentation, leads to an ‘imeter-hardness’ of 3.94 MPa mm^{-1} or 63.0 MPa mm^{-1} matching the criteria for the initial or final setting times. Therefore, initial and final setting times were obtained when these characteristic values were reached in the course of the measurement. The setting times of the cements were measured at 37ºC and >60% humidity. Each measurement was performed three times and the average value was calculated.

2.4. Mechanical testing

The mechanical strengths of the cements were evaluated in terms of compressive strength (CS) and of diametral tensile strength (DTS), as illustrated in previous reports [33,34]. Therefore, for CS and DTS measurements, the cement pastes were cast into PTFE cylindrical moulds (Ø 6 x 12 mm^3) and (Ø 6 x 3 mm^3), respectively, and stored in a 37ºC, 100% humidity box for 24 h. The cement specimens were then removed from the moulds and immersed in PBS solution (1.37 M NaCl, 27 mM KCl, 80.6 mM Na_2HPO_4, 19.4 mM KH_2PO_4) at 37ºC for

further 48 h. The specimens were loaded to failure at a crosshead displacement rate of 1 mm min^{-1} and 10 mm min^{-1}, for CS and DTS, respectively, using a universal materials testing machine (Shimadzu Autograph, Trapezium 2, Japan). For DTS tests, the samples were compressed diametrically and DTS (MPa) was calculated by $\frac{2F_{Max}}{\pi \times d \times l}$, where $d =$ diameter, $l =$ length and F_{Max} is the failure load. Results of CS and DTS are expressed as the mean ± standard error of the mean of triplicate determinations.

2.5. Release of ionic species from cements

The chemical compositions of the starting ZnCPC and ZnSrCPC powders and of the cylindrical (Ø 6 x 3 mm^3) cement samples (hardened for 5 days) after immersing for 1, 3 and 7 days into 5 mL of SBF at 37ºC under constant stirring (75 rpm), as well as, the amounts of Zn^{2+}, Sr^{2+} and Ca^{2+} released from ZnCPC and ZnSrCPC cements were determined by ICP spectroscopy (Model 70 Plus, Jobin Yvon, France).

2.6. Mineralization tests in SBF

The cement samples were left setting in PTFE-moulds (∅ 6 × 12 mm^3) in a 37ºC, 100% humidity box, for 24 h. In order to evaluate the biomineralization activity of the cements *in vitro* before cell cultures, the set cements were immersed for 30 days into polystyrene flasks containing simulated body fluid (SBF) with ionic concentrations (Na^+ 142.0, K^+ 5.0, Ca^{2+} 2.5, Mg^{2+} 1.5, Cl- 148.8, HPO_4^- 1.0, HCO_3^{2-} 4.2, SO_4^{2-} 0.5 mM L^{-1}) nearly equivalent to those of human blood plasma [35] and continuously shaken at a rate of 75 rpm, at 37ºC. Then, the samples were washed with distilled water and allowed to dry at 37ºC for 1 day and analyzed by means of Scanning Electron Microscopy (SEM) (Hitachi S4100, Tokyo, Japan) and elemental chemical analysis by EDS (Rontec EDS System).

2.7. Cytotoxicity assays using MG63 cells

The powdered cements were sterilized by γ-radiation prior testing them in cell cultures. The human osteosarcoma derived MG63 cell line (ATCC CRL-1427) was used to determine the cement powders cytotoxicity through the resazurin metabolism assay [36]. MG63 cells were maintained at 37ºC in a humidified atmosphere of 5% CO_2 in air, in Eagle's Minimum Medium in EBSS (Eagle's Balanced Salt Solution) supplemented with 1% NEAA and 2 mM L-Glutamine (Gibco BRL, Invitrogen), supplemented with 10% (v/v) fetal bovine serum (FBS, Gibco BRL, Invitrogen), 1% (v/v) of a 100 U mL^{-1} penicillin and 100 mg mL^{-1} streptomycin solution (Gibco BRL, Invitrogen) and 3.7 g L^{-1} $NaHCO_3$. First, the sensitivity and the range of linearity between resazurin reduction to resorufin and the density of MG63 viable cells were determined in a cell curve assay. Cells were seeded in 35 mm plates at 1 x 10^3 cells cm^{-2}. For 11 days, each 24 h growth medium was removed by aspiration and replaced with fresh medium containing 10% of a resazurin (Sigma Aldrich) solution (0.1 mg mL^{-1} resazurin in PBS [Pierce, Perbio]). Cells were further incubated for 4 h at 37ºC in the dark and resazurin reduction was measured spectrophotometrically (Cary 50 BIO, Varian) at 570 and 600 nm. Cells were subsequently ressuspended with 0.25% trypsin/EDTA (Gibco BRL, Invitrogen) and the number of viable cells determined using a 0.4% solution of the Trypan blue dye (Sigma Aldrich) and a hemocytometer. For each day, a final resazurin value ($O.D._F$) was calculated as the ratio O.D. 570/O.D. 600 nm minus the O.D. 570/O.D. 600 nm ratio of a negative control (resazurin media incubated for 4 h in the absence of cells) and the $O.D._F$ was plotted against cells density.

To determine cell viability when exposed to the cement powders, cells were seeded at 1 x 10^4 cells cm^{-2} onto 35 mm plates, and cultured in cell media supplemented with 0, 0.01, 0.1 or 1 mg mL^{-1} of ZnCPC or ZnSrCPC cement powders. This range of cement concentrations were chosen as 1 mg mL^{-1} already resulted in a saturated solution. Following 24 h, 48 h and 72 h of incubation at 37ºC in a humidified 5% CO_2 and 95% air atmosphere, growth medium was removed by aspiration and replaced with fresh medium containing 10% of the 0.1

mg mL^{-1} resazurin solution. After 4 h incubation as described above, 1 mL of the medium was collected and cell viability was determined by measuring O.D. at 570 and 600 nm. For each time point, the $O.D._F$ levels of cells incubated with 0 mg mL^{-1} cement powder were taken as 100% and cell viability calculated as a percentage of these control values. All experiments were carried out in triplicate and expressed as the mean ± standard error of the mean.

2.8. Statistical analyses

Statistical analyses were performed for setting times, CS and DTS measurements and cell viability tests using the SPSS 16.0 software. Comparative studies of means were performed using one-way ANOVA followed by a post hoc test (Fisher projected least-significant difference) with a statistical confidence coefficient of 0.95; therefore, *p* values < 0.05 were considered significant.

3. Results

The evolution of crystalline phases of the cements hydrated for 2 days with Sr and/or Zn incorporation is presented in Fig. 2.

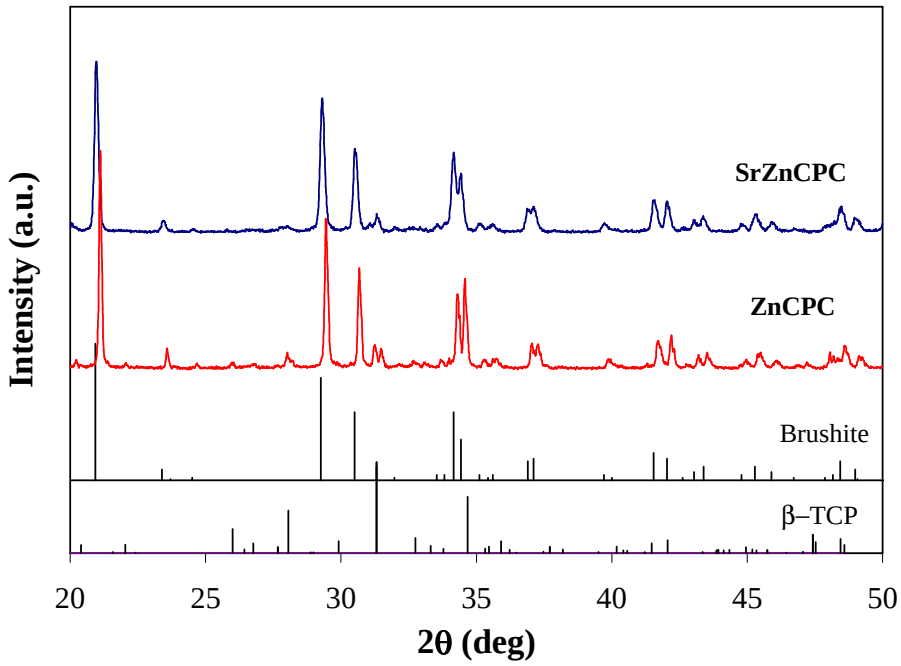

Fig. 2: XRD patterns of the ZnTCP and ZnSrTCP cements after 2 days of hydration. Brushite (JCPDS PDF File # 9-0077) and β-TCP ($Ca_3(PO_4)_2$, JCPDS PDF File # 1-70-682), full scale intensity = 6,000 cps.

It can be seen that the main product of the setting reaction in both cements is brushite, with some remaining β–TCP phase. The quantitative Rietveld analysis of XRD patterns confirmed that the starting powders consisted of 100% of β–TCP phase, while the cements contained around 90% of brushite and about 10% of β–TCP. Table 2 shows the lattice parameters of the β–TCP of the starting powders and of the brushite phase determined in the cements after 2 days of hydration. It can be seen that the lattice parameters of β–TCP phase decreased with the incorporation of Zn and Zn+Sr ions in the crystal structure. The decrease is more accentuated in the Zn-substituted β–TCP. Table 2 also shows that the lattice parameters of the formed brushite crystals were not noticeably affected by the incorporation of Sr or Zn, although an unexpected slightly increasing trend is apparent.

Table 2: Lattice parameters of β-TCP in the starting powders and of brushite phase in the hardened cements after 2 days of hydration

Lattice parameters (Å)						
	β-TCP (starting powder)		Brushite (hydrated cement)			
Samples	**a**	**c**	**a**	**b**	**c**	**β**
Pure phase	10.435	37.409	5.812	15.180	6.239	116.43
ZnCPC	10.413	37.337	5.816	15.193	6.246	116.38
ZnSrCPC	10.428	37.372	5.822	15.206	6.252	116.38

Setting times and wet mechanical, CS and DTS, results are presented in Table 3. The presence of Sr in the cement ZnSrCPC led to a faster setting in comparison to the ZnCPC cement.

The measured values of the wet strengths, CS and DTS, after 48 h immersion in PBS solution at 37ºC show that the tensile strength is around 5 times lower than compressive strength, in good agreement with other findings reported elsewhere [34]. Besides, ZnSrCPC cement exhibit higher CS and DTS values, in comparison to ZnCPC cements ($p<0.05$).

Table 3: Setting time and wet mechanical strengths, after 48 h, of the cements

	Setting time (min)		Compressive strength (CS) (MPa)	Diametral tensile strength (DTS) (MPa)
	IST	**FST**		
ZnCPC	13.2 ± 0.4	23.9 ± 0.3	16.3 ± 0.5	3.4 ± 0.4
ZnSrCPC	11.1 ± 0.3	20.8 ± 0.2	18.2 ± 0.5	3.7 ± 0.5

The chemical composition of the starting ZnCPC and ZnSrCPC powders and of the hardened cements as determined by ICP spectroscopy indicated the following concentrations: 2.43 mol.% Zn^{2+} and 97.57 mol.% Ca^{2+} for the starting ZnCPC sample, and 2.33 mol.% Zn^{2+}, 2.12 mol.% Sr^{2+} and 95.55 mol.% Ca^{2+} for the

starting ZnSrCPC sample, which are close to the planned ones of 2.22 mol% Zn and 2.22 mol% Sr respectively. The concentrations of Zn and Sr released from the hardened cements after the leaching experiments in distilled water at 37ºC for 1, 3 and 7 days are plotted in Fig. 2.

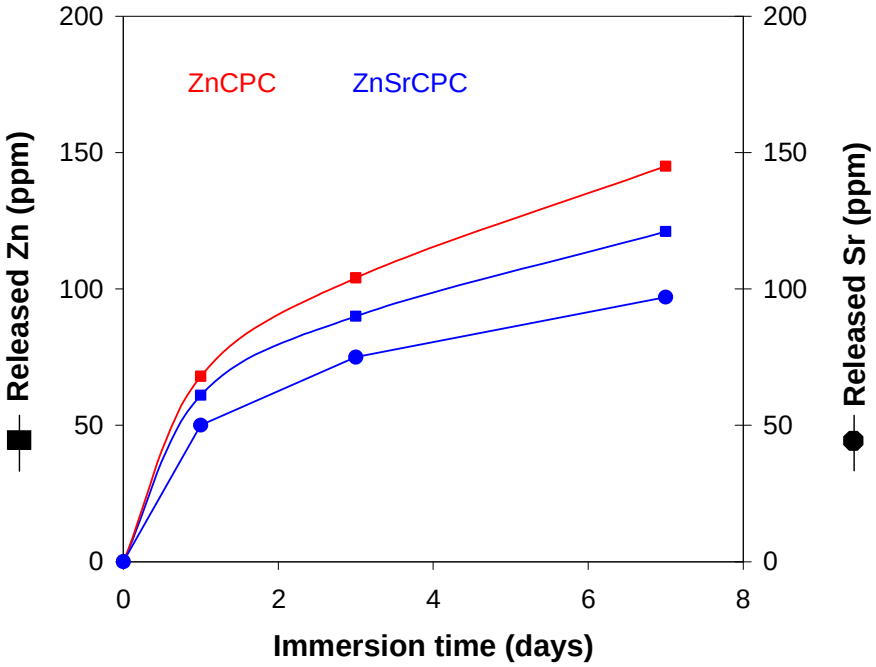

Fig. 2: Concentration of Zn^{2+} and Sr^{2+} released from ZnCPC and ZnSrCPC cements, after 1, 3 and 7 days of immersion in SBF.

It can be seen that both cement compositions, ZnCPC and ZnSrCPC show a gradual increase of the amounts of Zn^{2+} and Sr^{2+} released along the time period of immersion in SBF. The results suggest that there seems to be a certain preference for the release of Zn^{2+} in comparison to Sr^{2+}.

The morphological features of fractured surfaces of hardened ZnCPC and ZnSrCPC cements after immersion in SBF for 30 days are shown in Fig. 3. The cements show well developed porous spherulites made of intermingling lamellar crystals of apatite, as confirmed by EDS (data not shown), due to the conversion of brushite into apatite.

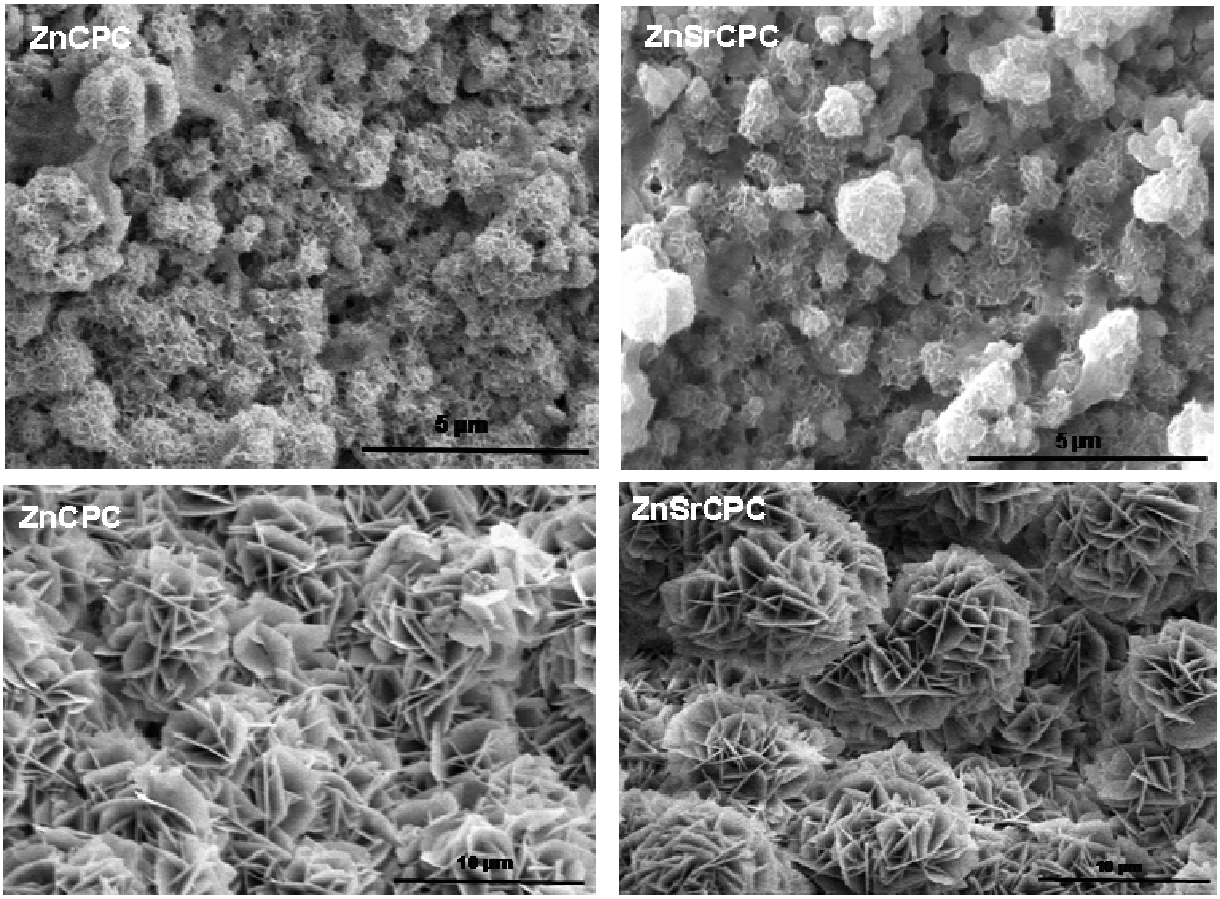

Fig. 3: Scanning electron micrographs of the ZnCPC and ZnSrCPC cements after immersion in SBF solution for 30 days.

Cell viability of MG63 osteoblastic-like cells cultured on the cement powders and under control conditions was evaluated by the non-destructive and non-toxic resazurin metabolism assay (Fig. 4). In the resazurin reduction test, viable cells reduce this non-toxic blue-colored probe dye to pink resorufin. The usefulness of the resazurin assay as a measure of cell proliferation and viability was first tested in a MG63 cell proliferation assay (Fig. 4a), and a linear response could be observed between 1 and 7 x 10^4 cells cm^{-2}. Cells were then seeded at 1 x 10^4 cells cm^{-2} in the presence of different cement powder concentrations and the percentage of cell viability determined (Fig. 4b). The levels of resazurin reduction by cells seeded with increasing concentrations of both cement powders was similar and non-significantly different from control conditions (0 mg mL^{-1} powder cements). Of note, MG63 cell morphology did not show any alterations in the

presence of the powders (data not shown). Hence, ZnCPC and ZnSrCPC cements were not cytotoxic to MG63 osteoblastic-like cells at the concentrations tested, being both viable for further *in vivo* tests of their physiological properties.

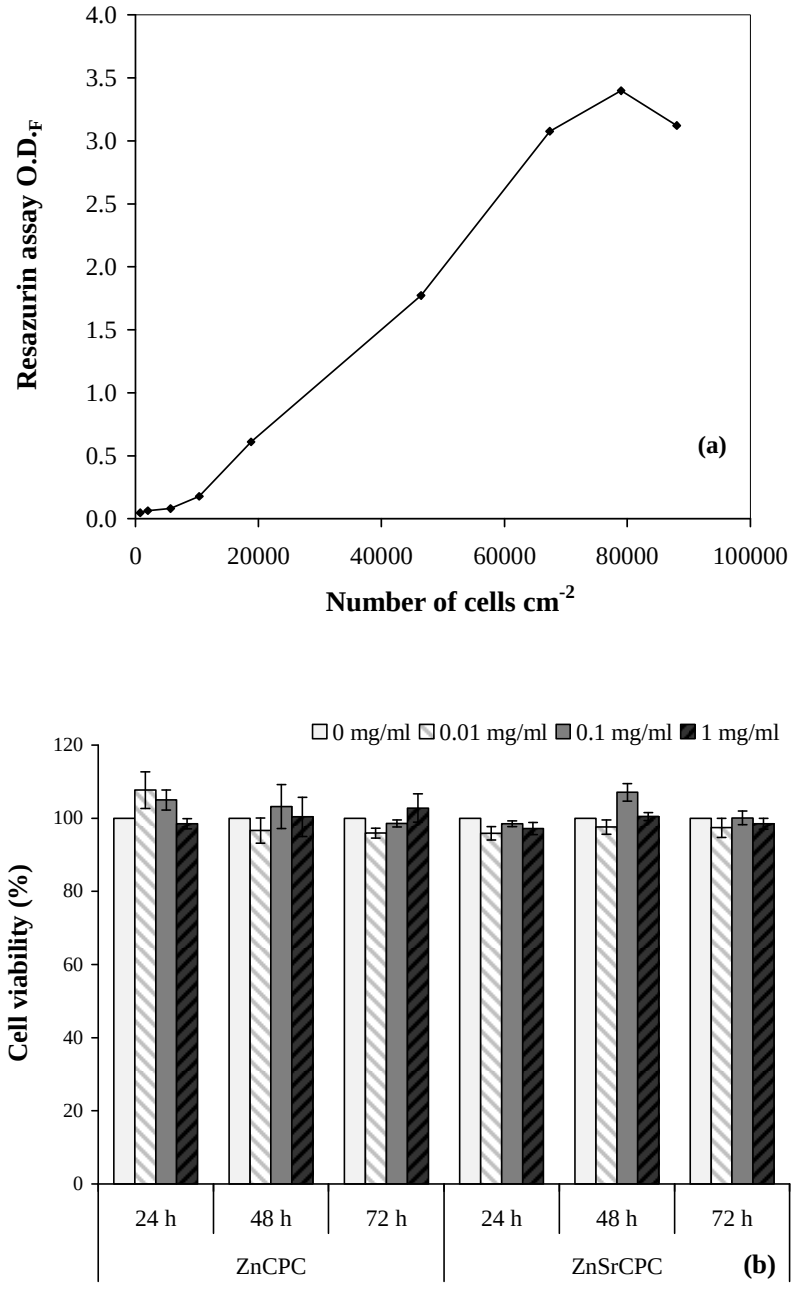

Fig. 4: Cell viability assays of MG63 osteoblastic-like cells exposed to ZnTCP and ZnSrTCP cement powders: (a) relation between the resazurin assay and MG63 cellular density, demonstrating a zone of linearity between measured O.D. and cell proliferation; and (b) cell viability of cells cultured with increasing concentrations of ZnCPC and ZnSrCPC cement powders.

4. Discussion

Bone fractures and diseases such as osteoporosis are common throughout an individual's life and at more advanced ages, and both result in bone breakdown and in the need for bone regeneration. Ceramic biomaterials have been shown to exhibit osteoconductive properties, and ionic substitution in ceramic biomaterials can modify their properties like crystallinity, solubility, and biological performance. Among other ions, strontium and zinc are beneficial due to their excellent properties on stimulating bone formation, as investigated in the present study after their incorporation in a brushite-forming β-TCP.

Rietveld refinement analyses performed on the cements hydrated for 2 days confirmed that no significant changes in the lattice parameters of the newly formed brushite phase occurred with the partial replacement of Ca by Zn and Sr (Table 2). The incorporation of Sr and Zn ions in the crystal structure of the starting β-TCP powders were proved by the resulting changes in the lattice parameters. As a matter of fact, the observed variations can be understood considering the ionic radii of the relevant elements (Zn = 0.74 Å; Ca = 0.99 Å; Sr= 1.12 Å) [37,38]. Therefore, the structure is expected to shrink more when the smaller Zn ion replaces Ca. On the other hand, the average size of Zn + Sr [(0.74 Å+1.12 Å)/2 = 0.93 Å] is somewhat smaller that the size of Ca ion, justifying the smaller decrease the lattice parameters. However, the same reasoning does not seem to be applicable to the formed brushite phase in which a slightly opposite trend is apparent. The different behaviors of these two crystalline phases need to be better investigated in the future.

The setting time of a CPC cement paste is of vital importance since it should not harden too fast, to allow molding or injection, nor too slowly, to allow the surgeon to close the defect shortly after cement placement. The setting times of brushite cements are usually too fast, and for the case of β-TCP + MCPM mixtures, setting can occur in a few seconds [39]. The use of additives, such as gelling agents that exert a retarding effect, enable to keep the setting reaction under control. Accordingly, the obtained initial and final setting times (Table 3) in the present study are somewhat higher than the ones reported elsewhere [40], possibly due to

the presence of PEG, a gelling agent, that slows down the dissolution of the starting powders, and the nucleation and precipitation processes of the resulting brushite phase while improving the handling and cohesive properties of the cements. Another reason for the longer setting times obtained might be the relatively high amount of β-TCP (55%), since β-TCP alone does not cure and tends to prevent the crystallization of brushite phase upon hydration. Moreover, the presence of Sr in the ZnSrCPC cement led to a faster setting than for the ZnCPC cement. This is according to the higher reactivity of brushite-forming SrCPC cement in comparison to undoped or Mg-doped β-TCP cements reported elsewhere [41].

The measured wet mechanical strength values (Table 3) are comprised within the ranges reported for brushite (1-24 MPa) [42] and for trabecular bone (10-30 MPa) [43]. Besides, the presence of Sr in ZnSrCPC cement led to higher CS and DTS values, in comparison to ZnCPC cements ($p<0.05$). The beneficial effect of Sr on the CS has been also reported for brushite forming β-TCP bone cements [44].

The observed slow increase of released Zn^{2+} and Sr^{2+} along the time of immersion in SBF (Fig. 2) of both cement compositions, ZnCPC and ZnSrCPC, is not surprising considering that this medium is supersaturated towards HA. The present results of *in vitro* mineralization tests after 30 days of cements immersion in SBF showed that Zn ions released from ZnCPC and ZnSrCPC did not inhibit the formation and growth of an apatite layer as confirmed by EDS and SEM analysis (Fig. 3). It was reported that the release of Zn from Zn-containing TCP was partially inhibited by the precipitation of HA on ZnTCP particles during immersion in SBF [22]. Therefore, it was suggested that the rates of Zn release *in vitro* depend on the solution calcium and phosphate concentrations, meaning that ZnTCP is an “intelligent material” with self-release regulating ability [22].

Considering that ZnCPC and ZnSrCPC cements were able to release the physiological relevant Zn and Sr ions and to transform into apatite under simulated physiological conditions, these biomaterials were qualified for *in vitro* cytotoxicity assays using human osteosarcoma derived MG63 cells. The results obtained revealed that both ZnCPC and ZnSrCPC cement powders are biocompatible up to concentrations reaching saturation in cell media.

5. Conclusions

The results presented and discussed along this work enabled to conclude that Zn and Sr elements could effectively replace partially Ca in the structure of starting β-TCP powders. The observed decreases in the lattice parameters are proportional to the size of single or combined substituted ions. The incorporation levels are close to the planned ones suggesting the suitability of the method used to prepare the powders. The retention of substituted ions in the hardened cements was also proved by their slow release in SBF. This feature is promising to grant the continuous presence of low concentrations of these ions to play their specific roles in osteoporosis and physiological pathways in the regulation of bone apposition and resorption *in vivo*. Further, the presence of zinc and strontium in brushite-forming cements did not inhibit the convertion into apatite under simulated physiological conditions. Moreover, the ZnCPC and ZnSrCPC cements were found to be non-toxic to human osteosarcoma-derived MG63 cells. The wet mechanical properties of cements are comprised within the ranges reported for brushite and for trabecular bone, qualifying them for further *in vivo* experiments.

Acknowledgments

Thanks are due to CICECO for the support and to the Portuguese Foundation for Science and Technology for project REEQ/1023/BIO/2005 and for the fellowship grants of S.P. (SFRH/BD/21761/2005), S.I.V. (SFRH/BPD/19515/2004) and P.M.C.T. (SFRH/BD/62021/2009).

References

[1] Brown WE, Chow LC. A New Calcium-Phosphate Setting Cement. J Dental Res 1983;62:672-672.

[2] Wang XP, Ye JD, Wang H. Effects of additives on the rheological properties and injectability of a calcium phosphate bone substitute material. J Biomed Mater Res Part B 2006;78:259-264.

[3] Yuan HP, Li YB, de Bruijn JD, de Groot K, Zhang XD. Tissue responses of calcium phosphate cement: a study in dogs. Biomaterials 2000;21:1283-1290.

[4] Alves HLR, dos Santos LA, Bergmann CP. Injectability evaluation of tricalcium phosphate bone cement. J Mater Sci - Mater in Med 2008;19:2241-2246.

[5] Baroud G, Cayer E, Bohner M. Rheological characterization of concentrated aqueous alpha-tricalcium phosphate suspensions: The effect of liquid-to-powder ratio, milling time, and additives. Acta Biomater 2005;1:357-363.

[6] Boesel L, Reis RL. The effect of water uptake on the behaviour of hydrophilic cements in confined environments. Biomaterials 2006;27:5627-5633.

[7] Bohner M, Baroud G. Injectability of calcium phosphate pastes. Biomaterials 2005;26:1553-1563.

[8] Burguera EF, Xu HHK, Sun LM. Injectable calcium phosphate cement: Effects of powder-to-liquid ratio and needle size 9. J Biomed Mater Res Part B 2008;84:493-502.

[9] Gauthier O, Muller R, von Stechow D, Lamy B, Weiss P, Bouler JM, et al. In vivo bone regeneration with injectable calcium phosphate biomaterial: A three-dimensional micro-computed tomographic, biomechanical and SEM study. Biomaterials 2005;26:5444-5453.

[10] Bohner M, Gbureck U. Thermal reactions of brushite cements. J Biomed Mater Res Part B 2008;84:375-385.

[11] Hofmann MP, Young AM, Gbureck U, Nazhat SN, Barralet JE. FTIR-monitoring of a fast setting brushite bone cement: effect of intermediate phases. J Mater Chem 2006;16:3199-3206.

[12] Constantz BR, Ison IC, Fulmer MT, Baker J, McKinney LA, Goodman SB, et al. Histological, chemical, and crystallographic analysis of four calcium phosphate cements in different rabbit osseous sites. J Biomed Mater Res Part B 1998;43:451-461.

[13] Gisep A, Wieling R, Bohner M, Matter S, Schneider E. Resorption patterns of calcium-phosphate cements in bone. J Biomed Mater Res Part A 2003;66:532-540.

[14] Bohner M, Theiss F, Apelt D, Hirsiger W, Houriet R, Rizzoli G, et al. Compositional changes of a dicalcium phosphate dihydrate cement after implantation in sheep. Biomaterials 2003;24:3463-3474.

[15] Tamimi F, Torres J, Lopez-Cabarcos E, Bassett D, Habibovic P, Luceron E, et al. Minimally invasive maxillofacial vertical bone augmentation using brushite based cements. Biomaterials 2009;30:208-216.

[16] Li X, Sogo Y, Ito A, Mutsuzaki H, Ochiai N, Kobayashi T, et al. The optimum zinc content in set calcium phosphate cement for promoting bone formation in vivo. Mater Sci and Eng 2008.

[17] Marie P, Ammann P, Boivin G, Rey C. Mechanisms of action and therapeutic potential of strontium in bone. Calcif Tissue Int 2001;69:121-129.

[18] Dahl S, Allain P, Marie P, Mauras Y, Boivin G, Ammann P, et al. Incorporation and distribution of strontium in bone. Bone 2001;28:446-453.

[19] Wong CT, Lu WW, Chan WK, Cheung KMC, Lukl KDK, Lu DS, et al. In vivo cancellous bone remodeling on a strontium-containing hydroxyapatite (Sr-HA) bioactive cement. J Biomed Mater Res Part A 2004;68:513-521.

[20] Ishikawa K, Miyamoto Y, Yuasa T, Ito A, Nagayama M, Suzuki K. Fabrication of Zn containing apatite cement and its initial evaluation using human osteoblastic cells. Biomaterials 2002;23:423-428.

[21] Kannan S, Goetz-Neunhoeffer F, Neubauer J, Ferreira JMF. Synthesis and structure refinement of zinc-doped □-tricalcium phosphate powders. J Amer Ceram Soc 2009;92:1592-1595.

[22] Otsuka M, Marunaka S, Matsuda Y, Ito A, Layrolle P, Naito H, et al. Calcium level-responsive in vitro zinc release from zinc containing tricalcium phosphate (ZnTCP). J Biomed Mater Res 2000;52:819-824.

[23] Rokita E, Hermes C, Nolting HF, Ryczek J. Substitution of Calcium by Strontium within Selected Calcium Phosphates. Journal of Crystal Growth 1993;130:543-552.

[24] Ito A, Ojima K, Naito H, Ichinose N, Tateishi T. Preparation, solubility, and cytocompatibility of zinc-releasing calcium phosphate ceramics. J Biomed Mater Res 2000;50:178-183.

[25] Kawamura H, Ito A, Miyakawa S, Layrolle P, Ojima K, Ichinose N, et al. Stimulatory effect of zinc-releasing calcium phosphate implant on bone formation in rabbit femora. J Biomed Mater Res 2000;50:184-190.

[26] Pina S, Olhero SM, Gheduzzi S, Miles AW, Ferreira JMF. Influence of setting liquid composition and liquid-to-powder ratio on properties of a Mg-substituted calcium phosphate cement. Acta Biomater 2009;5:1233-1240 .

[27] Kannan S, Ferreira JMF. Synthesis and thermal stability of hydroxyapatite-beta-tricalcium phosphate composites with cosubstituted sodium, magnesium, and fluorine. Chem Mater 2006;18:198-203.

[28] Kannan S, Goetz-Neunhoeffer F, Neubauer J, Ferreira JMF. Ionic substitutions in biphasic hydroxyapatite and beta-tricalcium phosphate mixtures: Structural analysis by rietveld refinement. J Amer Ceram Soc 2008;91:1-12.

[29] Kannan S, Pina S, Ferreira JMF. Formation of strontium-stabilized á-tricalcium phosphate from calcium-deficient apatite. J Amer Ceram Soc 2006;89:3277-3280.

[30] Yashima M, Sakai A, Kamiyama T, Hoshikawa A. Crystal structure analysis of beta-tricalcium phosphate Ca-3(PO4)(2) by neutron powder diffraction. J Sol St Chem 2003;175:272-277.

[31] Curry NA, Jones DW. Crystal structure of brushite, calcium hydrogen orthophosphate dihydrate - neutron-diffraction investigation. J Chem Soc 1971;23:3725.

[32] Berger. New characterization of setting times of alkali containing calcium phosphate cements by using an automatically working device according to Gillmore needle test. Key Eng Mat 2006;309-311:825-828.

[33] Chow LC, Hirayama S, Takagi S, Parry E. Diametral tensile strength and compressive strength of a calcium phosphate cement: Effect of applied pressure. J Biomed Mater Res 2000;53:511-517.

[34] Gbureck U, Grolms O, Barralet JE, Grover LM, Thull R. Mechanical activation and cement formation of alpha-tricalcium phosphate. Biomaterials 2003;24:4123-4131.

[35] Tas AC. Synthesis of biomimetic Ca-hydroxyapatite powders at 37 degrees C in synthetic body fluids 1. Biomaterials 2000;21(14):1429-1438.

[36] Ueno A, Miwa Y, Miyoshi K, Horiguchi T, Inoue H, Ruspita I, et al. Constitutive expression of thrombospondin 1 in MC3T3-E1 osteoblastic cells inhibits mineralization. J Cell Phys 2006;209:322-332.

[37] Kannan S, Goetz-Neunhoeffer F, Neubauer J, Ferreira JMF. Synthesis and Structure Refinement of Zinc-Doped beta-Tricalcium Phosphate Powders. J Amer Ceram Soc 2009;92:1592-1595.

[38] Kannan S, Goetz-Neunhoeffer F, Neubauer J, Rebelo AHS, Valério P, Ferreira JMF. Rietveld Structure and In Vitro Analysis on the Influence of Magnesium in Biphasic (Hydroxyapatite and □-Tricalcium Phosphate) Mixtures. J Biomed Mater Res Part B: Appl Biomater 2009;90:404-411.

[39] Bohner M. Calcium orthophosphates in medicine: from ceramics to calcium phosphate cements. Injury-Inter J Care Inj 2000;31:37-47.

[40] Gbureck U, Barralet JE, Spatz K, Grover LM, Thull R. Ionic modification of calcium phosphate cement viscosity. Part I: hypodermic injection and strength improvement of apatite cement. Biomaterials 2004;25:2187-2195.

[41] Pina S, Torres PMC, Ferreira JMF. Injectability of brushite-forming Mg-substituted and Sr-substituted α-TCP bone cements J Mater Sci - Mater Med *DOI 101007/s10856-009-3890-2* 2009.

[42] Gbureck U, Barralet JE, Spatz K, Grover LM, Thull R. Ionic modification of calcium phosphate cement viscosity. Part I: hypodermic injection and strength improvement of apatite cement. Biomaterials 2004;25:2187-2195.

[43] Duck FA. Physical properties of tissue: a comprehensive reference book. London: Academic Press Limited, 1990.

[44] Pina S, Torres PMC, Goetz-Neunhoeffer F, Neubauer J, Ferreira JMF. Newly developed Sr-substituted α-TCP bone cements Acta Biomater *doi:101016/jactbio200909001* 2009.

3.2 Osteoconductive properties of brushite-forming Zn- and ZnSr-substituted β-TCP bone cements

S. Pina[1*], S.I. Vieira[2*], P. Rego[3], P.M.C. Torres[1], O.A.B. da Cruz e Silva[2], E.F. da Cruz e Silva[4], J.M.F. Ferreira[1]

[1]University of Aveiro, Dept. of Ceramics and Glass Engineering, CICECO, 3810-193 Aveiro, Portugal

[2]University of Aveiro, Health Sciences Dept., Centro de Biologia Celular, 3810-193 Aveiro, Portugal

[3]University of Lisbon, Orthopaedic Clinic, Medicine Faculty, 1600-190 Lisbon, Portugal

[4]University of Aveiro, Dept. of Biology, Centro de Biologia Celular, 3810-193 Aveiro, Portugal

[*]Both authors contributed equally to this work

To be submitted to Biomaterials

Abstract

The core aim of this study was to investigate the *in vivo* performance of brushite-forming Zn- and ZnSr-substituted β-TCP cements injected into trabecular bone cylindrical defects in pigs.

In vitro proliferation and differentiation responses of osteoblastic-like cells (MC3T3-E1 cell line) to bone cements, at cellular and molecular levels, were also studied. Presence of zinc and strontium in brushite-forming cements was found to stimulate pre-osteoblastic proliferation, activity and maturation. MC3T3-E1 osteoblastic-like cells exposed to the powdered cements showed higher adhesiveness capacities and higher ALP activity, in comparison with control cells. Furthermore, they presented higher Type-I collagen secretion and fiber formation. Proliferative and collagen extracellular matrix deposition properties were more evident for cells grown in cements doped with Sr.

In vivo assays of the ZnCPC and ZnSrCPC osteoconductive properties were carried out, using carbonated apatite cement (Norian SRS) as control. There was no evidence of adverse foreign body reaction. Histological and histomorphometric analyses were performed at 1 and 2 months, after implantation. Results indicate that the investigated ZnCPC and ZnSrCPC cements are biocompatible, osteoconductive, and good candidate materials to use as bone substitutes. The presence of Sr enhanced the rate of new bone formation. The new ZnCPC and ZnSrCPC cements revealed better *in vivo* performance in comparison to the control carbonated apatite cement.

Keywords: *zinc; strontium; brushite cement; proliferation; ALP; cell adhesion; Type-I collagen; resorption*

1. Introduction

Calcium phosphate cements (CPC) have unique characteristics for bone substitution compared with other biomaterials. Their excellence relies on good biocompatibility, excellent bioactivity, self-setting characteristic, low setting temperature, adequate stiffness, and easy shaping for any complicated geometry [1-9]. In addition, CPC have such compositional resemblance to bone mineral that they induce a biological response similar to the one generated during bone remodelling. Calcium phosphate biomaterials are successfully used in cranio-maxillofacial, dental, and orthopedic surgery [10-13].

Among the different biocompatible calcium phosphate (CaP) phases present in human bone, brushite (dicalcium phosphate dihydrate, DCPD) has a higher solubility than hydroxyapatite (HA) at physiological pH, and an ideal *in vivo* resorption rate [14-16]. Brushite based bone cements are generally well tolerated by the bone and soft tissue environment *in vivo*, such that cement resorption is closely followed by new bone formation. Furthermore, brushite cements are known to be biocompatible, osteoconductive and bioresorbable, having a potential interest for bone regeneration procedures.

From a cellular and molecular perspective, it has been shown that some biomaterials are able to directly modify the osteoblastic proliferation rate and some of their functions, such as the synthesis of alkaline phosphatase (ALP) [17-19]. The ionic composition of such biomaterials is a key factor in their bioactivity, and ionic incorporation into TCP structure, such as zinc (Zn) and strontium (Sr) ions, have been proved to be traces elements with stimulatory outcomes on bone formation, having a direct specific proliferative effect on osteoblastic cells *in vitro* and a potent and selective inhibitory effect on osteoclastic bone resorption *in vivo* [20, 21]. Moreover, Zn is involved in many metallo-enzymes and proteins, including ALP, whereas Sr enhances collagen synthesis and has beneficial effects in the treatment of osteoporosis due to the prevention of bone loss by a mechanism that depresses bone resorption [22-25]. Osteoblasts are cells found on bone surface, being directly responsible for bone formation. As osteoblasts differentiate from their precursors they begin to secrete bone matrix proteins, such

as Type-I collagen that represents about 90% of the organic matrix. The network of Type-I collagen fibres provides the structure on which bone mineral is deposited. Type-I collagen and brushite particles are both predominant in fracture callus [26, 27], with the main structural framework of a human fracture callus consisting of disordered, mineralized collagen fibrils containing CaP crystals. Brushite particles are found in the noncollagenous organic matter around nonmineralized, ordered collagen fibrils, and it is believed that these particles serve as the reservoir of calcium and phosphate ions for subsequent mineralization [28].

There is still little knowledge concerning the *in vivo* behaviour of brushite-forming cements with Zn and Sr co-substituted in β-TCP. The main aim of the present study was to examine and compare the *in vivo* response of two new brushite-forming Zn and ZnSr-containing CPCs and a commercial apatite CPC, after implantation in trabecular bone in pigs. Additionally, the *in vitro* proliferation and differentiation responses of osteoblast-like cells (MC3T3-E1 cell line) to the bone cements were studied. Various cellular and molecular responses to the biomaterials were assayed, including cell viability determinations by the resazurin assay, photometric evaluation of ALP activity after enzymatic cleavage of p-nitrophenyl phosphate, and time-dependent Type-I collagen production.

2. Materials and Methods

2.1. Cement preparation

Brushite cements were prepared as described in the previous study [29]. Briefly, the cement pastes were prepared by mixing 55 wt.% of Zn- or ZnSr-substituted β-tricalcium phosphate (β-TCP) powder with 45 wt.% of monocalcium phosphate monohydrate (MCPM, Sigma-Aldrich, Germany) using liquid-to-powder ratio (LPR) of 0.34 mL g^{-1}. The aqueous solution used was 10 wt.% poly(ethylene glycol) (PEG) (200, Sigma) + 15 wt.% citric acid solution.

Zn- and ZnSr-substituted β-TCP powders were synthesized by aqueous precipitation as described in detail in previous reports [30-32]. The precipitates were vacuum filtrated, dried at 110ºC, heat treated for 2 h at 1100ºC and grounded under dry conditions in a planetary mill, and finally passed through a sieve with a mesh size of 36 μm.

The Zn- and ZnSr-substituted β-TCP cements were designated as ZnCPC and ZnSrCPC, respectively.

2.2. MC3T3-E1 cell culture

The osteoblastic cell line MC3T3-E1 (ATCC CRL-2593) was maintained at 37ºC in a humidified atmosphere of 5% CO2 in air, in 2mM Glutamine-containing Minimum Essential α-Medium in EBSS (Eagle's Balanced Salt Solution) supplemented with 10% (v/v) fetal bovine serum (FBS), 1% (v/v) of a 100 U mL^{-1} penicillin and 100 mg mL^{-1} streptomycin solution (Gibco BRL, Invitrogen) and 3.7 g L^{-1} $NaHCO_3$. Sub-confluent cultures (80-90% confluency) were splitted 1:5 using a 0.25% trypsin/EDTA (Gibco BRL, Invitrogen) solution at 5% CO_2, 37ºC.

2.3. Cytotoxicity and cell proliferation assays in cement blocks and powders

The resazurin metabolic assay [33] was used to determine the cements cytotoxicity/biocompatibility to MC3T3-E1 cells. The sensitivity and the range of linearity between resazurin reduction to resorufin and the density of MC3T3-E1 viable cells were first determined in a cell curve assay, as previously [33]. Briefly, cells were seeded in 35 mm plates at 1 x 10^3 cells cm^{-2} and, at the indicated time points, cells were incubated for 4 h with fresh medium containing 10% of a resazurin (Sigma Aldrich) solution (0.1 mg mL^{-1} resazurin in PBS [Pierce, Perbio]). Resazurin reduction was thereafter measured spectrophotometrically (Cary 50 BIO, Varian) at 570 and 600 nm. The number of viable cells was further counted using a 0.4% solution of the Trypan blue dye (Sigma Aldrich) and a

hemocytometer. For each day, a final resazurin value ($O.D._F$) was calculated as the ratio O.D. 570/O.D. 600 nm minus the O.D. 570/O.D. 600 nm ratio of a negative control (resazurin media incubated for 4 h in the absence of cells), and the $O.D._F$ was plotted against cells density.

To determine dose-dependent cell viability and proliferation when exposed to the cement powders, 1 x 10^5 cells were seeded in 35 mm wells (density of 1 x 10^4 cells cm^{-2}), and cultured in cell media supplemented with 0, 0.01, 0.1 or 1 mg mL^{-1} of ZnCPC or ZnSrCPC cement powders. This range of cement concentrations were chosen as 1 mg mL^{-1} already resulted in a saturated solution. Following 24 h, 48 h and 72 h of incubation at 37ºC in a humidified 5% CO_2 and 95% air atmosphere, growth medium was removed by aspiration and replaced with fresh medium containing 10% of the 0.1 mg mL^{-1} resazurin solution. After 4 h of incubation, 1 mL of the medium was collected and cell viability was determined by measuring O.D. at 570 and 600 nm, as described above. For each time point, the $O.D._F$ levels of cells incubated with 0 mg mL^{-1} cement powder were taken as 100% and cell viability calculated as a percentage of these control values. Upon 72 h, cells morphology was evaluated by phase contrast (PhC) microscopy in an inverted Olympus IX81 epifluorescence microscope, and microphotographs were taken at 18ºC with a Digital CCD monochrome camera F-View II (Soft Imaging System).

For the cement blocks assay of cellular viability and proliferation with time in culture, ZnCPC and ZnSrCPC blocks (∅ 6 × 3 mm^3, set at 37ºC, for 24 h) in 24-wells were pre-incubated with media for 2 days, after what were washed with phosphate buffer saline (PBS) solution. Cells were seeded at 2.5x10^4 cells cm^{-2} onto the surface of the blocks and incubated for 20 days, with media being substituted by resazurin-containing media at days 2, 5, 8, 10 and 20. After 4 h of incubation, cell viability was determined as described for the powdered samples. Cells were re-incubated with fresh media at each experimental day and at day 15 in culture, between experimental days 10 and 20.

Prior to cell experiments, cement samples were sterilized by γ-radiation. All experiments were carried out in triplicate and expressed as the mean ± standard error of the mean.

2.4. Determination of alkaline phosphatase (ALP) activity

MC3T3-E1 cells were seeded at 1 x 10^4 cells cm^{-2} in 35 mm wells and cultured on 1 mg mL^{-1} ZnCPC and ZnSrCPC powders. At day 3 in culture, achievement of cells confluency was visually confirmed. ALP activity of exposed cells was evaluated at 0, 1, 3, 6, 14 and 21 days post-confluency (DPC). After removal of the culture medium, cells were washed with PBS and harvested in 1 mL universal ALP buffer (100 mM citric acid, 100 mM KH_2PO_4, 100 mM sodium tetraborate.$10H_2O$, 100 mM Tris, 100 mM KCl; pH 11) with a disposable cell scraper.

Cells with or without cement were sonicated twice for 20 sec and centrifuged for 5 min at 2000 rpm at room temperature. The supernatant was used for determinating ALP activity following addition of the substrate p-nitrophenyl phosphate (Fluka). The production of p-nitrophenol was determined spectrophotometrically at 420 nm, after 2 and 5 min of reaction at 37ºC. The ALP activity was expressed as the increase in p-nitrophenol aborbance per min per microgram of protein ($\Delta OD.min^{-1}.mg^{-1}$), upon subtraction of the blank O.D. (1mL universal buffer plus substrate). To determine protein mass, parallel samples were harvested with 1% SDS, and total protein content measured using a BCA kit (Pierce).

2.5. ZnCPC and ZnSrCPC time-dependent cell adhesion assays

The altered capacity of cells to adhere to a plastic support was measured upon cells exposure to the cement powders for increasing time periods. Post-exposition adhesion assays were performed at 0, 3, 14 and 21 days post-confluency (DPC), upon cells plating as described above for the ALP assay (day 0 = 3 days post-seeding). Cells media was changed every other ~3-5 days in culture. At each experimental day, cells were washed with PBS, incubated with Trypsin-EDTA solution for 5 min at 37ºC, and ressuspended in 3 ml fresh media. Cells were counted using the Trypan blue dye, 1x10^5 cells were seeded into 24-well plates

with 1 mL fresh media (final volume), and left to adhere for 1 h in an atmosphere of 5% CO_2 at 37ºC. Quantification of adherent cells was perf ormed indirectly by measuring the amount of non-adherent ressuspended cells in the media. For that, cells media were homogeneized and collected, ressuspended cells counted using the Trypan blue dye, and the percentage of adherent cells was calculated taken the seeded $1x10^5$ cells as 100%. Three independent experiments were performed.

2.6. Type-I collagen time-dependent protein expression and cellular localization

MC3T3-E1 cells were treated as described for the ALP assays and subjected to immunoblot analyses to determine the profile of Type-I procollagen and collagen protein expression and medium secretion with time of exposition to 1 mg/ml cement powders (days in post-confluency, DPC, cultures). Type-I collagen cellular distribution was further analyzed by immunocytochemistry procedures at 3 DPC (confluency was achieved at 3 days in vitro).

2.6.1. Antibodies

Primary antibody used was anti-Collagen Type-I (Novus Biologicals, Germany), which recognizes Type-I procollagen (monomeric α1(I) and α2(I) chains, β chains corresponding to α/α dimmers, trimeric γ chains) and various collagen forms (tropocollagen, the mature trimeric γ chains, microfibrils, fibrils and fibers). Secondary antibodies used were FITC-conjugated anti-rabbit IgGs (Calbiochem) for immunocytochemistry analyses, and horseradish peroxidase-linked anti-rabbit IgGs for enhanced chemiluminescence (ECL) detection (GE Healthcare).

2.6.2. Immunoblot analyses of Type-I collagen protein expression and media secretion

At the indicated days in post-confluency (DPC) cultures, cells conditioned media (1 ml) were collected into 10% SDS-containing microtubes and cells were harvested with a 1% SDS boiling solution. Samples were boiled for 10 min and sonicated, and total mass content determined using the BCA kit (Pierce). Mass-normalized cell lysates and media samples (60 µg) were subjected to reducing 6.5% SDS-PAGE in Tris-Glycine buffer, and electrophoretically transferred onto nitrocellulose membranes. Precision Plus Dual Color (Bio-Rad) were used as protein standards. Immunoblotting of the transferred proteins was performed by incubating membranes O/N with the anti-Collagen Type-I primary antibody, after blocking non-specific binding sites with non-fat dry milk in TBS-T (10 mM Tris-HCl at pH 8.0, 150 mM NaCl, 0.5% Tween). Detection was achieved using a horseradish peroxidase-linked secondary antibody and an ECL kit (GE Healthcare).

2.6.3. Confocal microcopy analyses of Type-I collagen protein distribution

Cells treated as above (section 2.8.2) were grown on 35 mm plates-containing pre-treated coverslips and fixed with a 4% paraformaldehyde PBS solution at 3 DPC. Cells were methanol-permeabilized, non-specific sites blocked by 1 h incubation with a 3% BSA PBS solution, and coverslips submitted to immunocytochemistry procedures using the anti-Collagen Type-I antibody diluted in 3% BSA PBS. Upon three washes with PBS, cells were incubated with the FITC-conjugated secondary antibody. Coverslips were mounted on microscope slides with DAPI-containing Vectashield antifading reagent (Vector). Images were acquired in a LSM 510 META confocal microscope (Zeiss) using an Argon laser line of 488 nm (FITC channel), and a Diode 405-430 laser (DAPI channel).

2.7. Animal model and implantation procedure

Animal studies were performed at Hospital Santa Maria, Lisbon, Portugal, according to European regulations and following permission granted by the Ethical Committee. Owing to ethical and economic reasons, only two animals were used for implantation procedures. Two mature male pigs weighting between 40 and 50 kg were used as experimental animals, for observation periods of 1 and 2 months for each animal. Injection sites were shaved and cleaned with Betadine (10% povidone-iodine). The animals were operated under general anesthesia performed with intravenous injection of ketamine (Ketalar, Pfizer, Porto Salvo, Portugal) and xylazine hydrochloride (Rompun 2%, Bayer, Germany) under aseptic conditions. To implant the cement pastes, a longitudinal incision on the outer surface of the foot was made until expose the tarsal bone and three circular holes drilled perpendicular to the long axis of the bone with a drill bit of Ø 3.5 mm (Synthes, USA) in each animal (see Fig. 1). The CPCs to be implanted were prepared by hand mixing for 1 min and then injected in the cavities with a 5 mL syringe. The holes were filled, respectively, with ZnSrCPC, ZnCPC and reference apatite cement (Norian SRS®, Norian Corp., Synthes, USA). In each hole, one marker (skin stapler) was placed into the cement paste, during setting, for localization of the implant position at the end of the implantation period. Setting time of 11 ± 2 min after filling the holes was granted for the cements, ZnSrCPC and ZnCPC, before closing. Norian SRS was mixed and applied according to the specifications of the producer. Subcutaneous tissues were closed using resorbable Dafilon 2/0 sutures (Braun, Queluz de Baixo, Portugal), whereas skin was closed with a skin stapler. Both animals recovered from the operative procedure without incident. Postoperative pain killer, Tramadol (Medinfar, Amadora, Portugal) and antibiotic cefazolina (Labesfal, Campo de Besteiros, Portugal) were administered for 3 days. By the second postoperative day, the pigs began to walk freely with access to food and water. At the end of the predetermined period of implantation (1 and 2 months), the animals where operated according to the same protocol. Removal of the implants and some surrounding bone was performed using a hollow drill bit of Ø 6.5 mm (Synthes, USA).

Fig. 1: Photograph showing the surgical procedure of drilling holes for posterior cement pastes implantation.

2.7.1. Histological and histomorphometric analyses

The specimens containing the defects with the cements were fixed in 4% formaldehyde, decalcified in nitric acid and embedded in paraffin. For histological and histomorphometric analysis, cross-sections of 5 µm thicknesses were cut (Leica RM 2145 saw microtome). The sections were taken from the middle of the specimens and stained with hematoxylin/eosin (H&E), which allows detection of newly formed bone. Histological and histomorphometric analyses were performed using a laser scanning confocal fluorescence microscope (Zeiss LSM 510 META), equipped with a 561 nm DPSS laser. To quantitatively determine the amount of newly formed bone, the histological sections were analyzed after both implantation time periods (1 month and 2 months). At least twelve H&E stained histological sections were randomly chosen for every condition, and each section was observed under a confocal laser scanning microscope at Plan-Neofluar 10x/0.3 magnification (histological and histomorphometrical analyses) and Plan-Apochromat 100x/1.4 Oil (histological analyses). The removed cylindrical specimen (Ø 6.5 mm) contained old trabecular bone at the periphery (~1.5 mm at each side). Hence, images of newly formed bone and matrix were taken at the middle and periphery of the removed implant (defect area). A total of 25

microphotographs were taken and analyzed for every condition. The Zeiss LSM 510 4.0 image analysis software was used to determine the areas occupied by organic material positive for the protein-staining Hematoxylin dye. The areas occupied specifically by newly formed bone, organic matrix and 'empty spaces' (non-protein) were also determined, with data being presented as mean ± standard error of the mean. The intensity of the fluorescent organic material was also recorded as a measure of density, as microphotographs were taken with the same laser and gain settings. For the ZnSrCPC implants, low magnified (10x) and zoomed (4x) or highly magnified images (100x) were taken along the z-axis (z-stack), projected into one image and used to create a 3D volume image further displayed as a video (supplemental figures).

2.8. Statistical analysis

Statistical significance analysis was conducted using the SPSS 16.0 software, by one way analysis of variance ANOVA, followed by a post hoc test, with the level of statistical significance set at $p<0.05$. Data are expressed as means ± standard error of the mean of at least three independent experiments. In order to the low number of experimental animals, statistical analyses were not performed for the histological and histomorphometric analyses.

3. Results

Dose-dependent cell viability and proliferation of MC3T3-E1 osteoblastic-like cells cultured on the ZnCPC and ZnSrCPC cements for 24, 48, and 72 h was evaluated by the non-destructive and non-toxic resazurin metabolism assay (Fig. 2). The usefulness of the resazurin assay as a measure of cell proliferation and viability was first tested in a MC3T3-E1 cell proliferation assay (Fig. 2a), and a linear response could be observed between 1 and 4 x 10^4 cells cm^{-2}, being this cell density interval used in the following proliferation assays.

Cells were seeded at 1 x 10^4 cells cm^{-2} in the presence of different cement powder concentrations and the percentage of cell viability determined (Fig. 2b and 2c). No cytotoxic effects were observed for any of the cement powders doses used, and cells O.D. increased with time in culture for all conditions. For ZnCPC (Fig. 3b), small increases in cellular proliferation were observed for 0.1 and 1.0 mg mL^{-1} (fold-increases of 1.10-1.30 over control conditions, 0 mg mL^{-1} powder cements). Exposition to 0.1 and 1.0 mg mL^{-1} ZnSrCPC (Fig. 2c) induced higher dose-dependent increases in cellular proliferation, resulting in fold-increases of 1.30-1.50 (for 1.0 mg mL^{-1}) over control levels. Noteworthy, at day 3 in culture cells confluency was achieved, as visually confirmed. The pH range indicator on cells media (phenol red) revealed no alterations to the physiological pH 7.4, as confirmed by pH media measurements (Basic Meter PB-11, Sartorius).

Cytotoxicity and proliferation assays in cement blocks (Fig. 3d) revealed that MC3T3-E1 cell viability was decreased relatively to control conditions (cells plated directly onto the plastic bottom). Results also showed that cell viability increased until 8-10 days in culture and slight decreased further on, for all conditions tested. Again, cells grown in the presence of ZnSrCPC showed higher levels of proliferation for all time points tested than for ZnCPC ($p<0.05$). Media pH acidification was visually detected in the first days of culture in ZnCPC and ZnSrCPC blocks. The alteration in media colour corresponded to pH decreases to 5.5-6.5, but pH in cement blocks-containing wells increased to physiological levels of ~7.4 following day 2 in culture.

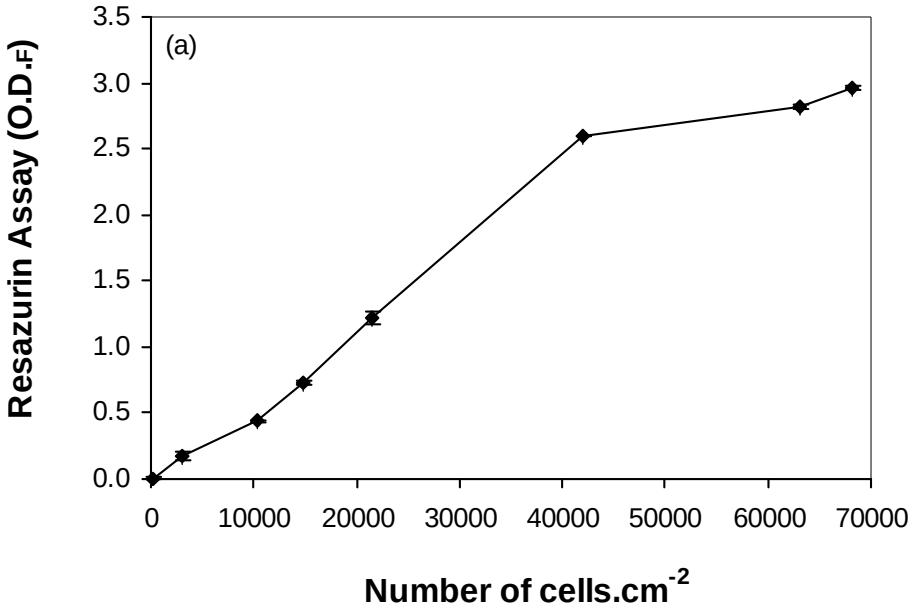
(a)
Resazurin Assay (O.D.F)
3.5
3.0
2.5
2.0
1.5
1.0
0.5
0.0
0
10000
20000
30000
40000
50000
60000
70000
Number of cells.cm-2

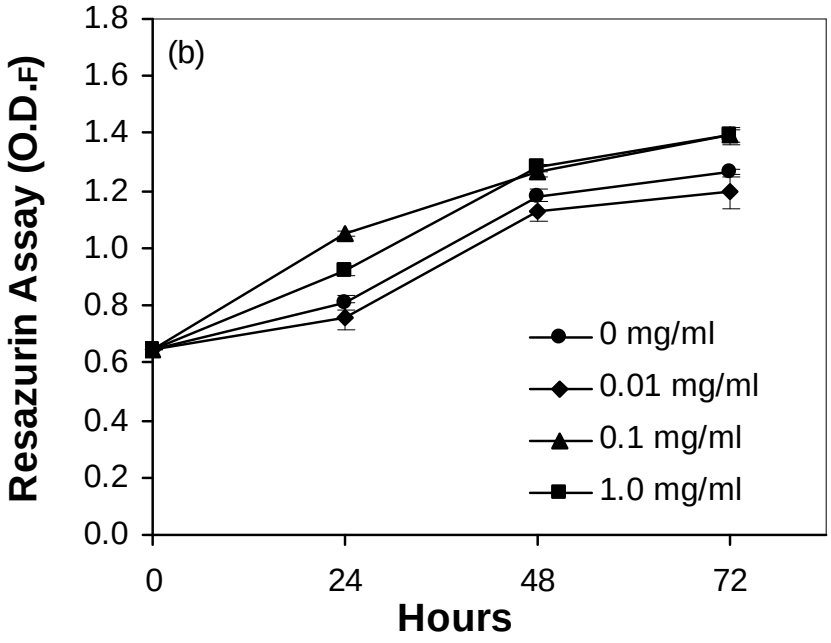
(b)
Resazurin Assay (O.D.F)
1.8
1.6
1.4
1.2
1.0
0.8
0.6
0.4
0.2
0.0
0
24
48
72
Hours
0 mg/ml
0.01 mg/ml
0.1 mg/ml
1.0 mg/ml

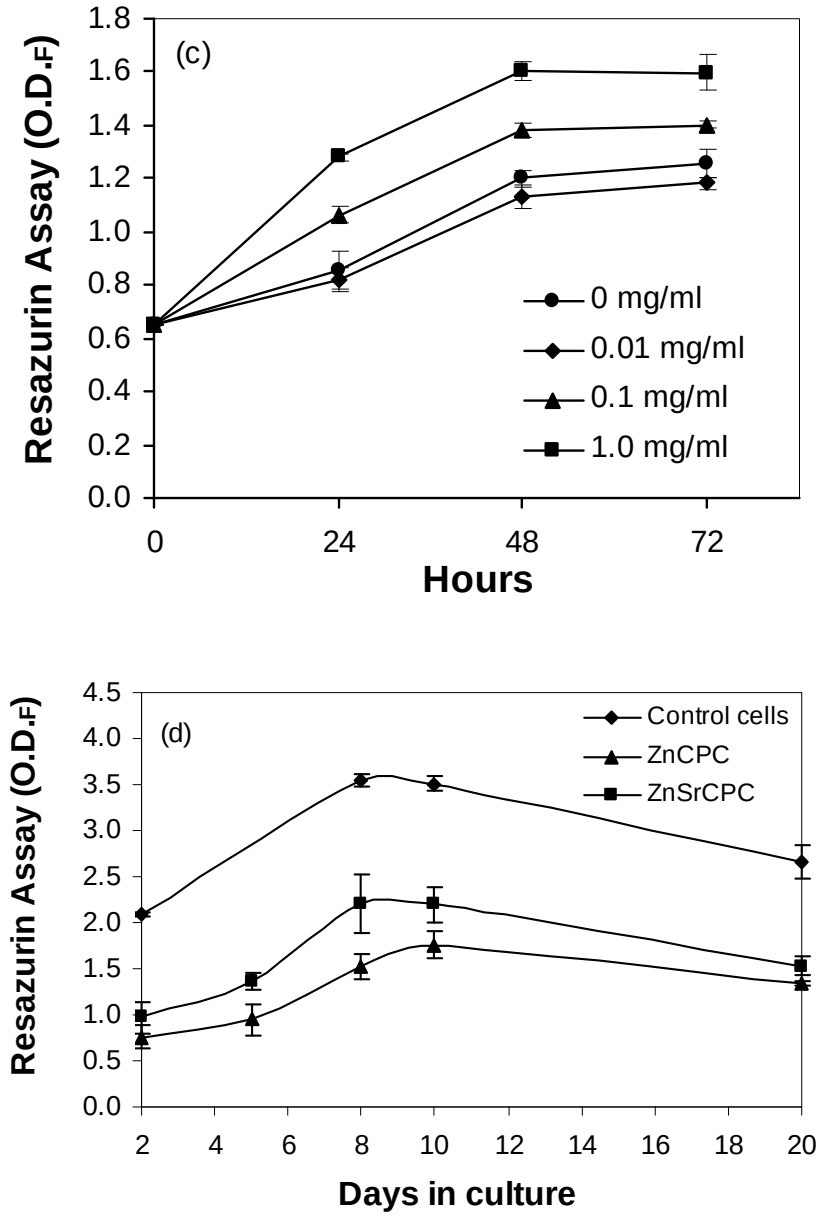

Fig. 2: Cell viability assays of MC3T3-E1 osteoblastic-like cells exposed to ZnCPC and ZnSrCPC cement powders: (a) relation between the resazurin assay and MC3T3-E1 cellular density, demonstrating a zone of linearity between measured O.D. and cell proliferation; (b) cell viability of cells cultured with increasing concentrations of ZnCPC and (c) ZnSrCPC cement powders for 24, 48 and 72 h; (d) cell viability of cells cultured onto ZnCPC and ZnSrCPC blocks. Results presented are the mean ± SE of at least three independent experiments.

Morphological analyses of MC3T3-E1 cells exposed for 72 h to 1 mg mL^{-1} of ZnCPC and ZnCPC cement powders revealed some observable differences (Fig. 3). Phase contrast microphotographs reveal that cells in contact with cements (arrows) appear to possess a more irregular cell shape, especially for ZnCPC, with increased number of plasma membrane protuberances. A decrease in cellular volume and nucleus (N) size is especially evident for ZnSrCPC-exposed cells, what correlates with its observed higher rate of cellular proliferation (Fig. 2c). Of note, the higher cellular densities of ZnSrCPC-exposed cultures can be depicted in Fig. 3 microphotographs that show a higher number of cells (and respective nuclei) and less intercellular space.

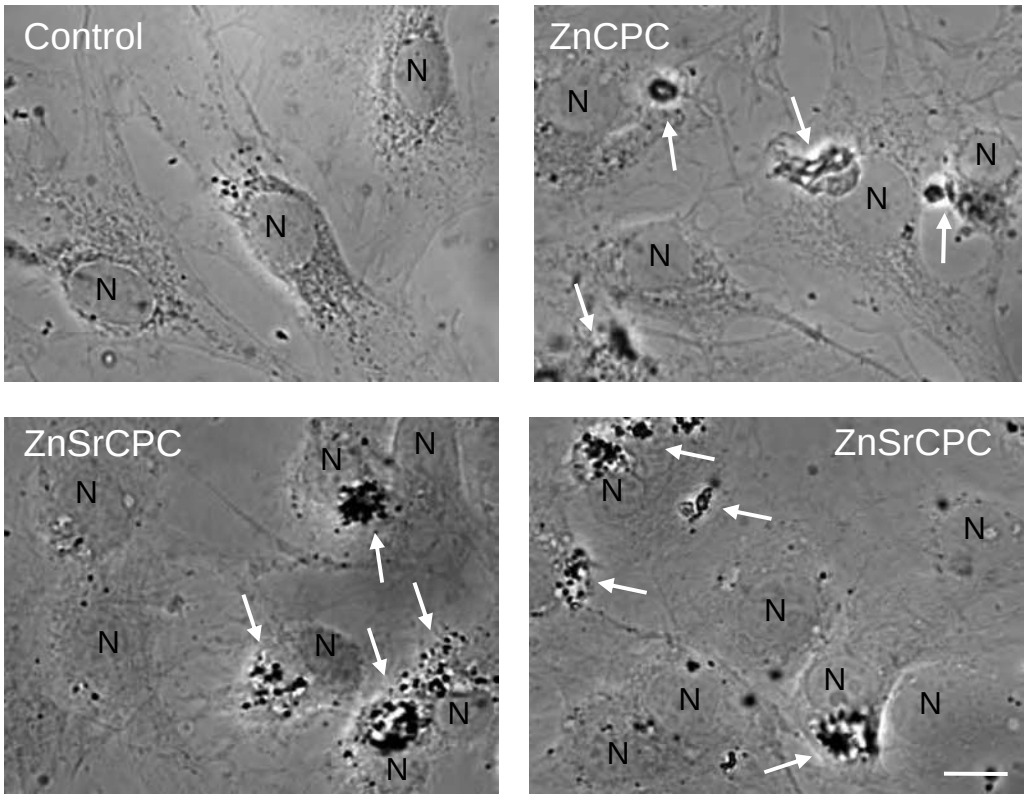

Fig. 3: Phase contrast microphotographs of MC3T3-E1 cells exposed to 1 mg mL^{-1} of cement powders (ZnCPC and ZnSrCPC) for 72 h. N: cells nuclei. Arrows: visible aggregates of cement powders. Bar 10 µm.

ALP assays indicated that MC3T3-E1 cells not only maintain their capability to express active ALP enzymes on powdered cements, but even increase it with time in culture (Fig. 4). For all conditions tested, ALP activity was similarly maintained and slightly increased until two weeks in post-confluency culture, after what it rapidly increased until the last time point (28th day). From days 21 to 28, a known period of cell differentiation, ALP activity of cells incubated with ZnCPC and ZnSrCPC cement powders significantly increased over control levels ($p<0.05$). Of note, crude ALP activity of powdered cements exposed cells increased significantly over control levels starting from day 6 in post-confluency culture, but until day 21 this increase resulted from their higher induction of cell proliferation.

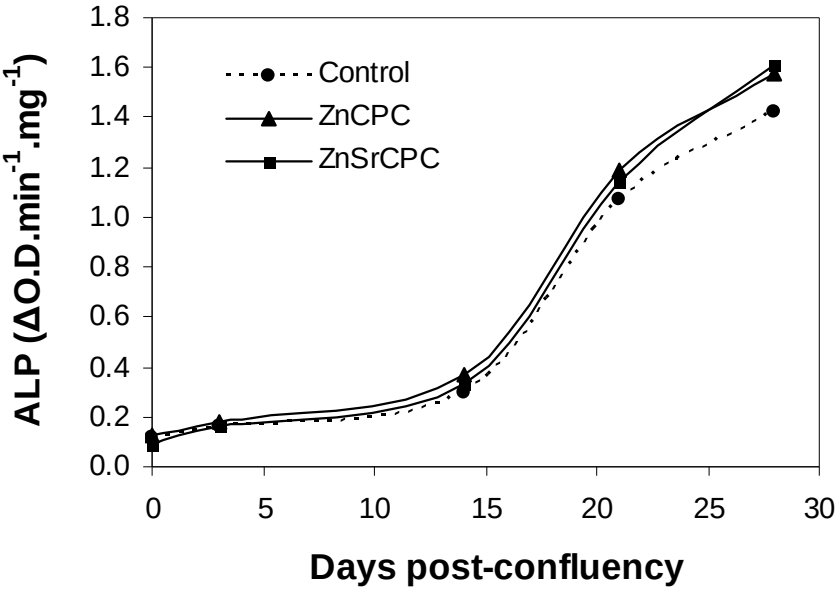

Fig. 4: Alkaline phosphatase (ALP) activity of MC3T3-E1 cells cultured on 1 mg mL^{-1} ZnCPC and ZnSrCPC powdered cements for several days (0, 1, 3, 6, 14 and 21) post-confluency achievement. The ALP activity was expressed as the increase in p-nitrophenol aborbance per min per microgram of protein ($\Delta OD.min^{-1}.mg^{-1}$). Results presented are the mean of two independent experiments.

This effect was annulled when data was presented per mg of total protein content, therefore excluding the proliferation variable, with results mainly reflecting variations in the state of cell maturation leading to differential ALP activities.

When collecting cells lysates for analysis of their ALP activity, it was noted that non-exposed control cells were more easily detached from the plastic than cells

exposed to ZnCPC and ZnSrCPC, suggesting that they may exhibited alterations in adhesive capacities. Hence, further studies assayed differential adhesion capacities of MC3T3-E1 cells exposed to the cements powders.

Upon 0, 3, and 14 DPC cell culture, a time-dependent increase in the capacity of MC3T3-E1 cells to adhere to a plastic support was observed (Fig. 5), further decreasing until day 21. Both ZnCPC and ZnSrCPC cement powders were able to increase the cells adherence properties, in comparison with non-exposed control cells. Powdered ZnCPC was even slightly more effective, with the ZnSrCPC cement appearing to behave in an intermediate position between control and ZnCPC exposed cells at days 0 and 3, what may relate to the higher number of ZnSrCPC proliferating cells, known to be less adhesive.

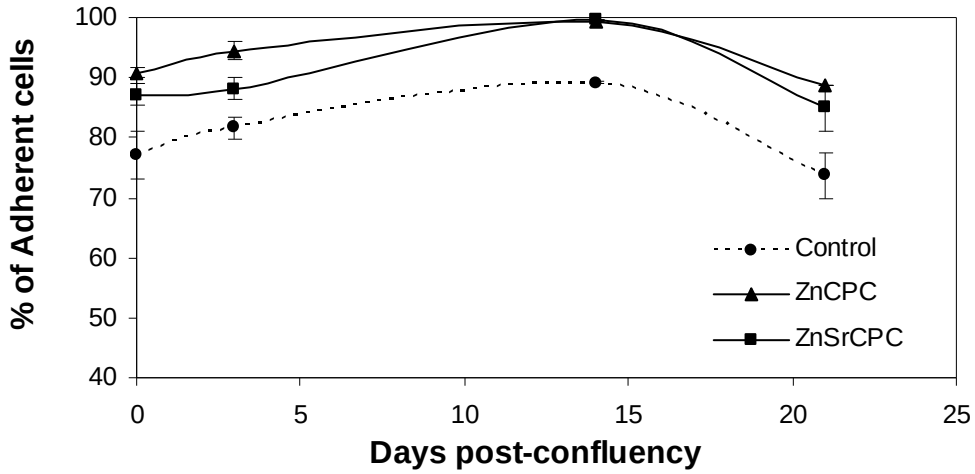

Fig.5: ZnCPC and ZnSrCPC-dependent MC3T3-E1 cells adhesion capacities. The capacity of cells to adhere to a plastic support for 1 h was measured following cells exposure to the cement powders for 0, 3, 14 and 21 days post-confluency. At each experimental day, $1x10^5$ cells were seeded into 24-well plates and left to adhere for 1 h at 37ºC. Media was further collected and the number of non-adherent ressuspended cells counted (x). The percentage of adherent cells was calculated ($1x10^5$ - x), taking the initial $1x10^5$ cells as 100%. Results presented are the mean ± SE of three independent experiments.

The effect of the powdered cements on collagen protein synthesis, secretion and fibrillar deposition was studied by immunoblot and immunocytochemistry analyses.

In terms of immunoblot bands profile, collagen is somewhat complex (Fig. 6). Monomeric Type-I procollagen consists of α1 (~140KDa) and α2 (~130KDa) chains, which are intracellular processed (signal peptide cleavage, hydroxylation of proline and lysine residues, glycosylation of lysine residues). Alpha chains can intracellularly associate into dimers (~270KDa) and trimers (~400KDa; triple helix consisting of two α1 and one α2 chains). There is some covalent cross-linking already within these forms, which are not breakable by SDS-PAGE denaturing conditions [34]. All these cell-associated Type-I pro-collagen forms were present in all samples and a time-dependent profile for the various cellular procollagen forms could be observed (Fig. 6A.I). Between 0, 3 (proliferation period) and 14, 21 (maturation period) DPC, a high increase (3-4 fold-increase) in the levels of cellular pro-collagen is noted, especially for the dimeric β(I) and trimeric γ(I) forms. Levels of cell-associated Type-I pro-collagen go in the following order: Control > ZnSrCPC > ZnCPC, except at 3 DPC. Nonetheless, these levels were much more similar at 14 and 21 DPC following extensive samples sonication, which permits the visualization of cell layer-associated fibrils and its breakdown products (Fig. 6A.II). Further, this allowed detecting an increase in the formation of collagen fibrils for ZnSrCPC at 3 DPC, observable in all triplicate determinations. Remarkably, there were ZnSrCPC-induced alterations in the electrophoretic migration of all procollagen monomer and dimeric bands (Fig. 6A "*"), revealing higher levels of post-translational procollagen modifications. This also occurred at lower extent for β chains in ZnCPC samples.

Intracellular procollagen is shipped to the trans-Golgi network (TGN) to be medium secreted. Extracellularly, γ chains are enzymatically processed into tropocollagen, promoting their aggregation into cell layer-associated collagen microfibrils and fibrils [35]. Hence, the levels of medium soluble procollagen were also analysed (Fig. 6B). It could be observed that procollagen secretion (peaking at 3 DPC) precedes as expected, trimeric procollagen, tropocollagen and fibrils formation (abundant from 14 DPC onward). Figure 6B shows higher procollagen secretion for ZnCPC and ZnSrCPC-exposed cells at 3 DPC, and lower from 14 DPC onward, suggesting higher depletion of intracellular collagen at 3 DPC.

In order to confirm the immunoblot observations at 3 DPC, and as collagen antibodies exhibit its higher degree of specificity under non-denaturing native conditions, cells were subject to microscopy analysis of Type-I collagen cellular distribution (Fig. 7). Similarly to the immunoblot results of Fig. 6, the overall levels of intracellular collagen were in the following order: ZnSrCPC ≈ Control > ZnCPC, but differently distributed. While for control cells, procollagen was accumulated inside intracellular granule-like densities, for ZnCPC and ZnSrCPC-exposed cells the intracellular procollagen-containing vesicles were smaller and more numerous. These results suggest the occurrence of CPC-induced alterations in collagen secretion, from regulated to more constitutive-like. Further and more remarkably, the extracellular cell-associated collagen fibers were generally longer and denser for the ZnSrCPC, confirming an earlier/enhanced aggregation of tropocollagen into fibrils and fibers. Control and ZnCPC presented similar collagen extracellular fibers.

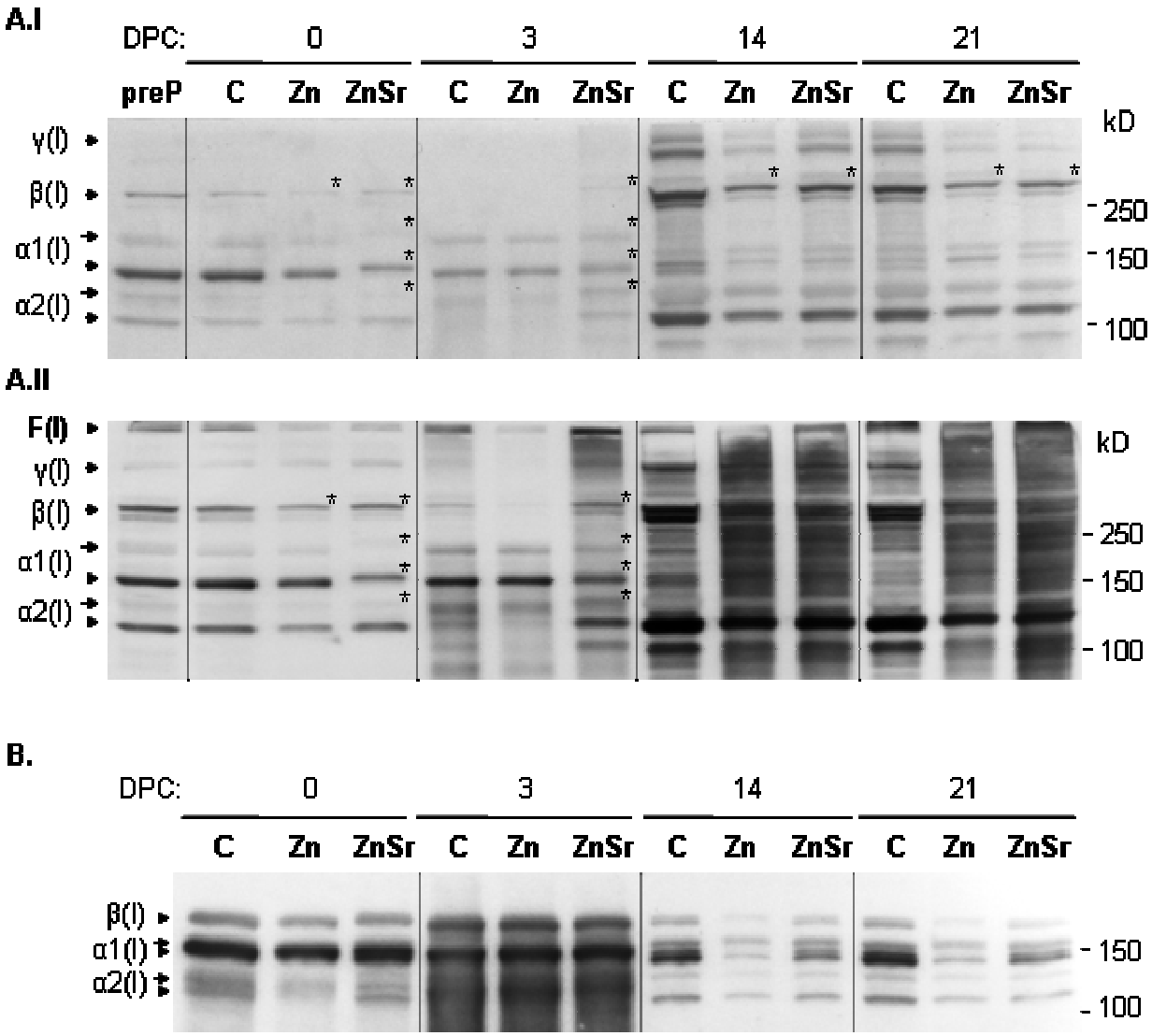

Fig. 6: Immunoblot analysis of cell-associated and medium secreted Type-I collagen with time in post-confluency culture. MC3T3-E1 cells lysates (A) and conditioned media (B) were collected at days 0, 3, 14 and 21 of post-confluency culture (DPC). Samples were resolved under reducing conditions and Type-I collagen was immunodetected. Once several insoluble fibers could be denoted in the samples microtubes, to detect higher collagen aggregates (fibrils and fibers), cells lysates were further sonicated for partial fibers breakdown (A, lower blot). Note that collagen proteins profiles and levels are equal in pre-plated (prepP, cells initially plated) and control 0DPC cells, as expected. α1(I) and α1(II), procollagen monomeric chains, unprocessed (arrowhead) and processed (arrow); β, procollagen dimeric forms; γ, procollagen trimeric forms; F, collagen fibers. Migration of molecular weight markers is indicated to the right.

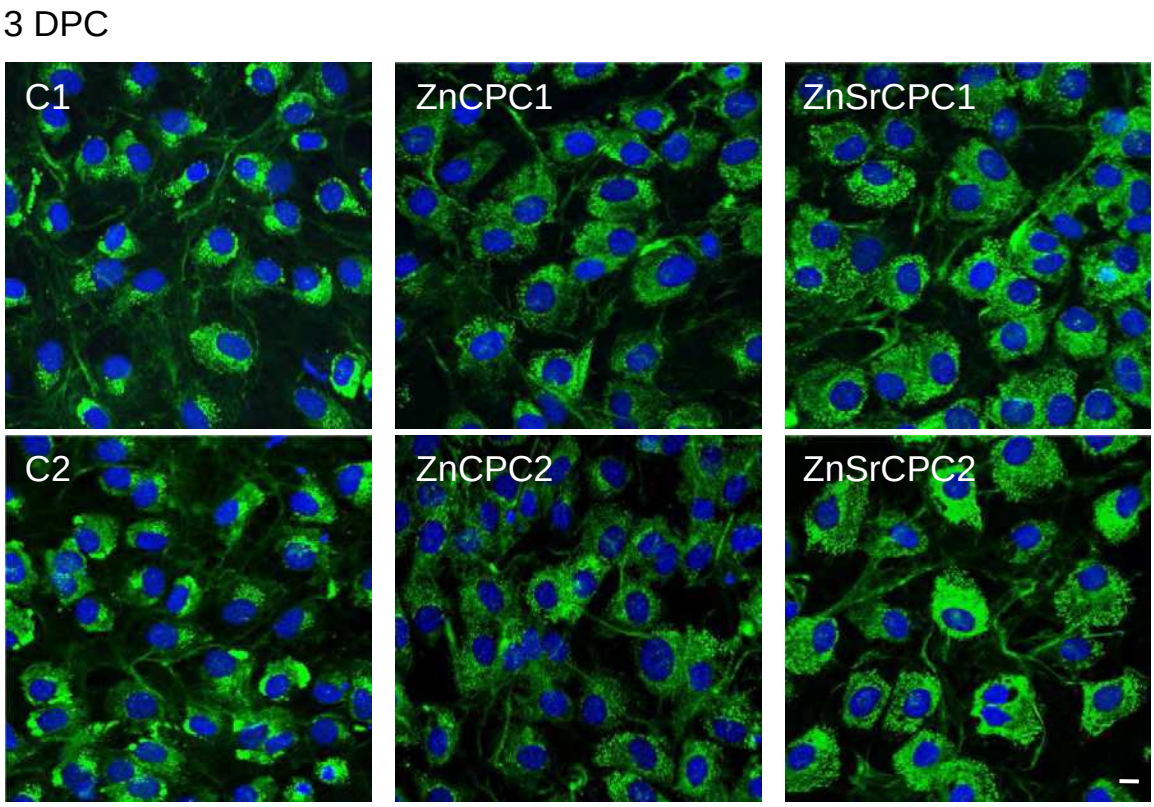

Fig.7: Confocal microscopy analysis of intra and extracellular Type-I collagen at 3 days post-confluency (DPC). Cells exposed or not (C) to 1mg/ml ZnCPC and ZnSrCPC for 3 days in post-confluency cultures (a total of 6 days of exposition) were subject to immunocytochemistry procedures to analyze type I collagen distribution (green fluorescence) by confocal microscopy. Two representative microphotographs for each condition are presented. DAPI (blue fluorescence), nuclear marker. Bar, 10 µm.

Histological analysis demonstrated that the studied CPC cements were both osteoconductive and biocompatible. Taking advantage of the fluorescent properties of hemotoxylin [36], and as confocal microscopy can bring higher sensitivity than wide field microscopy, histological and histomorphometric analyses of *in vivo* cements implants were conducted using a confocal laser scanning microscope. Hemotoxylin is an acidic basophilic dye that stains intracellular and extracellular proteins (but not nuclei or lipids), with fluorescence emissions in

green and red. Hence, in fluorescent microscopy, the organic protein material appears red (or alternatively green) and the nuclei and lipids appear black.

Microphotographs of implant cross-sections revealed that newly formed bone (NB) was growing from the periphery inwards (Fig. 8), being deposited into the old bone, circumscribing the bone defect. Further, organic protein-containing matrix (Mx) was also observed (Fig. 8), although at higher amounts at 1 month of implantation and less after 2 months.

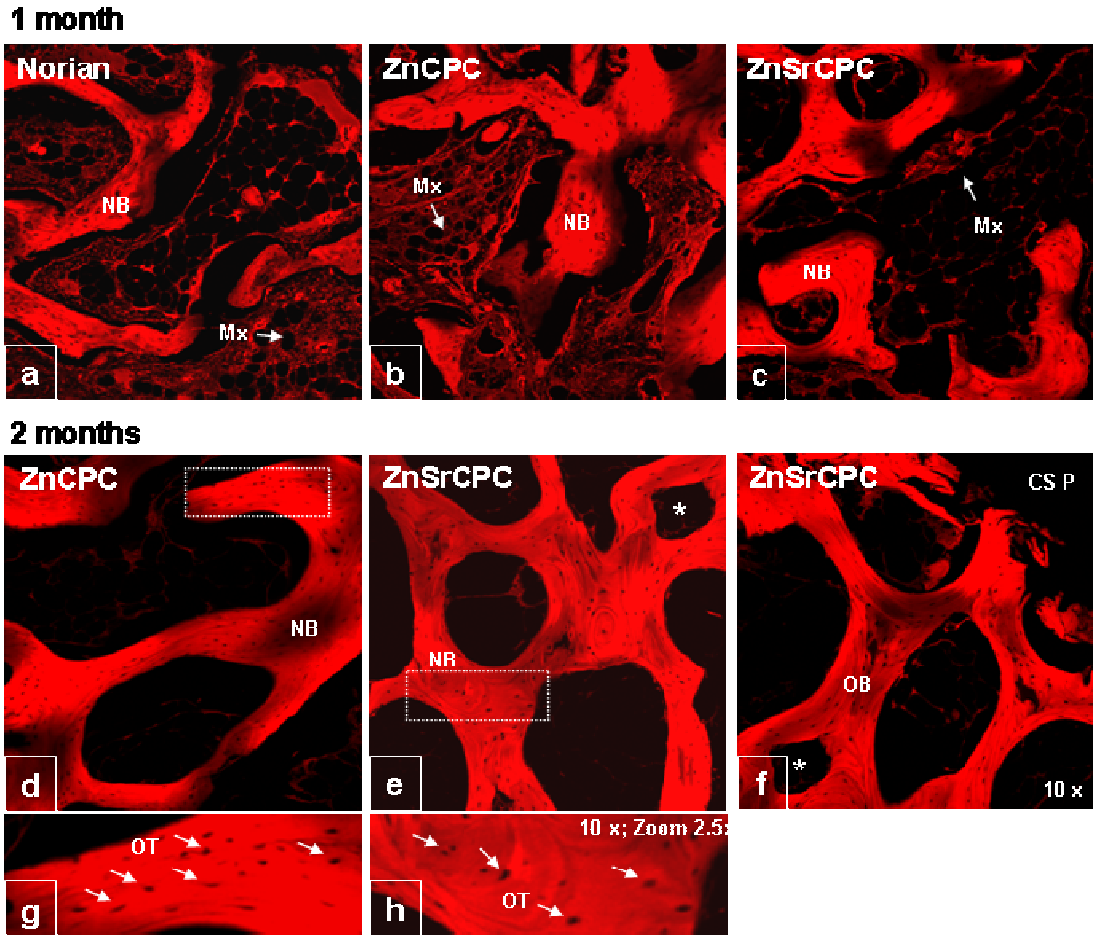

Fig. 8: Confocal fluorescent micrographs of histological H&E stained sections, showing the tissue osteogenic response to Norian SRS® (a), ZnCPC (b,d,g) and ZnSrCPC (c,e,f,h) cements after 1 (a-c) and 2 (d-h) months of implantation. NB: new bone; Mx: protein matrix; OTB: old trabecular bone; CS P: cross-section periphery; OT: osteocytes; arrows/OT in g,h: osteoclast-like cells.

Three different osteogenic profiles were denoted for Norian, ZnCPC, and ZnSrCPC cements. For Norian and ZnCPC cements at 1 month of implantation, new bone was found at higher amounts in the more peripheral areas than in the center (Fig. 8 a, b). The central zones of the section had black areas and areas filled with unorganized matrix enriched in cells, probably being active remodeling areas of cement and bone callus (Fig. 8 a, b). These areas were almost absent in the ZnSrCPC 1 month implants, where osteoclasts could only be found sparsely and at lower cell densities, around old or newly formed bone, and throughout the cross-sections. The differences observed suggest that ZnSr cement resorption had occurred at a higher rate during the first month of implantation, accompanied by bone formation. Further, bone deposition appeared to be increasing in organization in the following order: Norian < ZnCPC < ZnSrCPC. In the latter, new bone was mainly found in trabeculae-like concentric structures and crossing the section, while for ZnCPC similar structures could also be found, although mainly at the periphery of the implant and with larger 'empty' cavities within. For Norian, the new bone was mainly deposited in less circular and lengthy structures (Fig. 8 a-c). Following 2 months of implantation, the concentric lamellae deposition into trabecular bone becomes obvious (Fig. 8 d,e) and closed circular trabeculae are the main structures found, especially in the ZnSrCPC implants. At this time period, at the periphery of the cross-sections it was not possible to distinguish new bone from host bone (old trabecular bone). The continuity between new and old bone and within the newly formed trabeculae was notorious for the ZnSrCPC and is highlighted (Fig. 8 e, f; * marks the same structure in contiguous microphotographs; see also supplemental Fig. S1). Fig. 8 g and h show magnified structures of Fig. 8 d and e, where arrows indicate osteocytes' (OT) black nuclei. These are mature osteoblasts that are trapped inside bone, occupying small cavities known as lacunae at the junctions of the lamellae, visible in all photos of new formed bone. The layers of deposited lamellae are also visible.

Several histological features can be observed in Fig. 9. Osteoclast-like cells are found within areas of unorganized matrix, mainly at the center of the section (Norian and ZnCPC), but also at the periphery (ZnSrCPC). These probably

correspond to active areas of osteoid secretion by osteoblasts, and of cement, mineral and bone callus resorption by osteoclasts (Fig. 9 a, indicated by arrows). For all implants, rows of cuboid epithelial cells could be found at the periphery of several sections, possibly denoting mesenchymal pre-osteoblastic cells (Fig. 9 b). Ossification centers (nuclei of calcification and new bone formation) could be found especially for both ZnCPC and ZnSrCPC cements (Fig. 9 c). For ZnCPC, and especially for ZnSrCPC, osteoblast-like cells (OB, arrowheads) could be observed producing and mineralizing organized matrix that lays foundation for new bone formation (Fig. 9 d). This matrix is found in very close relation with the new bone being formed, before osteoblasts became imprisoned in the latter and differentiate into osteocytes.

The percentage of area occupied by new protein-containing organic material was determined and presented in Fig. 10. Several differences were found, in correlation with the previous histological observations. At 1 month of cement implantation, total protein area increased as following: Norian < ZnSrCPC < ZnCPC. Detailed analysis clarified that while for ZnSrCPC this proteinaceous organic material was almost exclusively new bone, for ZnCPC this equally corresponded to new bone and matrix. From 1 to 2 months of implantation, the percentage of matrix in the implant decreased as osteogenesis continued, although more evident for ZnSrCPC, with a notorious increase in the amount of new bone. The latter reached 50.0 ± 5.1% of total area, while ZnCPC reached 34.7 ± 8.7%. The area of ZnSrCPC ‘empty spaces’ also decreased as new bone formation increased reinforcing that, with time of implantation, cement was being resorbed as new-bone formed. Concomitantly, fluorescence intensity of the organic material filling the implant was also determined and used as an indirect measure of protein density. As it can be observed from the microphotographs (Fig. 8), the intensity of newly formed bone is much higher than of the surrounding matrix, due to its much higher density and volume. New bone fluorescence intensity increased for both ZnCPC and ZnSrCPC cements between 1 and 2 months of implantation, as expected. This indicates an increase in bone average density, probably due to remodeling activity. The concomitant decreases in matrix

average intensity may be related to resorption of initially unorganized protein matrix and bone callus, which contributed to the formation of new trabecular bone.

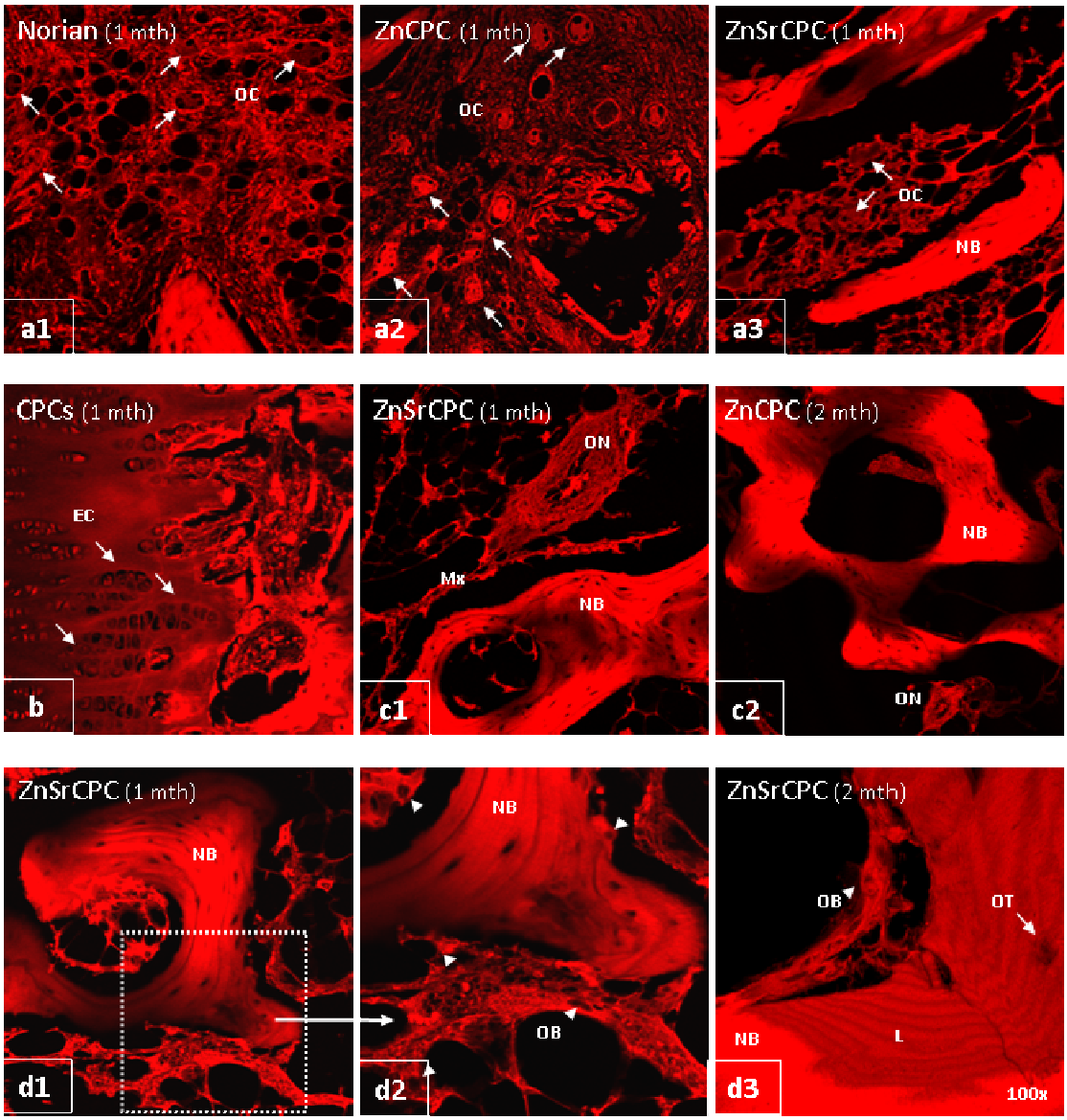

Fig. 9: Confocal fluorescent micrographs of H&E stained sections, showing histological details of the tissue osteogenic response to Norian SRS®(a1), ZnCPC (a2,c2) and ZnSrCPC (a3,c1,d) cements after 1 and 2 months of implantation. mth: month; CPC: representative of all three cements; OC: osteoclast-like cells, easily indentified by their multiple nuclei and highly proteinaceous cytoplasm (arrows); NB: new bone; EC: epithelial cells; Mx: matrix; ON: ossification nucleus; OB: osteoblast-like cells; OT: osteocytes; L: lamellae. Images from ***a*** to ***d2*** were taken with a 10x objective and zoomed 1.5-2x, except ***d2*** that was zoomed 4x; ***d3*** represents a image projection of a z-stack, taken with a 100x objective.

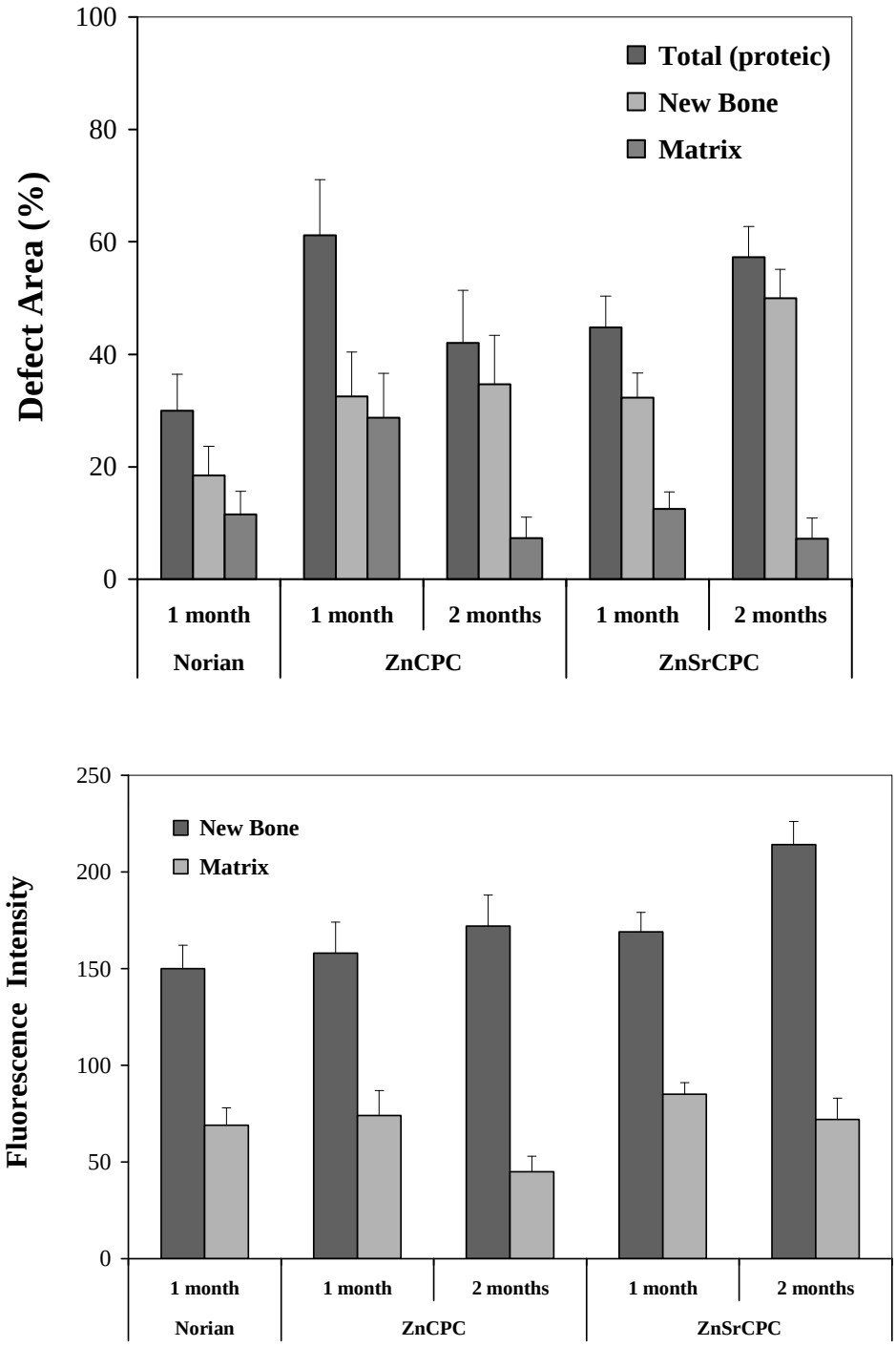

Fig. 10: Histomorphometric analysis of H&E stained sections of ZnCPC, ZnSrCPC and Norian SRS® cements for 1 and 2 months of implantation: (a) defect area (%) of new bone formed, the matrix and the total areas and (b) fluorescence intensity of new bone and matrix areas.

4. Discussion

The present study examined and compared the *in vivo* response of two brushite-forming Zn and ZnSr-containing CPCs and a commercial apatite CPC, after implantation in trabecular bone in pigs. Additionally, the *in vitro* proliferation and differentiation responses of osteoblastic cells (MC3T3-E1 cell line) to the cements were also evaluated. Osteoblasts play a central inhibitory role in the pathophysiology of osteoporosis where reduced bone mass and deterioration in bone microarchitecture lead to enhanced skeletal fragility. Osteoporosis results from a negative balance between the bone-forming activities of osteoblasts and the resorptive activities of osteoclasts. Inadequate osteoblast activity may result from a relative deficiency in proliferation or differentiation of osteoprogenitors, or excessive apoptosis.

The osteoblastic MC3T3-E1 cell line was used for *in vitro* studies. This cell line has been established from C57BL/6 mouse calvaria and selected on the basis of high ALP activity in the resting state. Cells have the capacity to differentiate into osteoblasts and osteocytes and have been demonstrated to secrete collagen and to form calcified bone tissue *in vitro*, being adequate to study the cellular and molecular responses to the biomaterials tested.

Dose-dependent cell viability and proliferation of MC3T3-E1 osteoblastic-like cells cultured on both ZnCPC and ZnSrCPC cement samples confirmed their biocompatibility and capability of induction of cellular proliferation under physiological pH (Fig. 2). These results are consistent with previous studies, where it has been reported that the zinc-releasing CPC significantly promoted osteoblastic MC3T3-E1 cell proliferation *in vitro* at zinc content of 1.20 wt % [37, 38]. Furthermore, exposition to ZnSrCPC powder led to the highest dose-dependent levels of proliferation (Fig. 2c), and cells grown in the presence of ZnSrCPC blocks showed higher levels of proliferation, than for ZnCPC ($p<0.05$) (Fig. 2d). These data reveals that Sr is a good osteoblastic proliferation inducer, what was visually confirmed by the higher cellular density of ZnSrCPC cultures (phase contrast microphotographs of Fig. 3), and is in agreement with previous studies indicating that Sr-containing ionic cements are more osteoconductive than

Zn-containing ionic cements [39]. Noteworthy, the differences observed relatively to control non-exposed cells depending the type of cement samples (powder or block) used for cell culture tests most probably reflect initial variations of the cells media pH. While for powdered cements media pH did not change and cement-exposed cells had increased O.D. levels over control levels, the presence of cement blocks initially lead to a decrease in pH and concomitantly decreased initial cell viability. Nonetheless, when pH increased and stabilized around 7.4 following the 2nd day in culture after media substitution, the cellular proliferation profiles of control cells and ZnSrCPC were not only similar but ZnSrCPC even exhibited a higher proliferation rate (2.3 vs 1.7 fold-increases for control cells and ZnSrCPC between days 2 and 8). Further results implicated ZnCPC and ZnSrCPC in osteoblastic differentiation processes. The cements were able to increase MC3T3-E1 cells ALP activity over control levels at later periods in culture (Fig. 4), which strongly indicate a higher maturation state for these cells. Similarly, Otsuka et al. [40] have observed that MC3T3-E1 cells ALP activity is lower in the first 1-2 weeks in culture and further increases until day 35, and related this increase with the cells maturation state. MC3T3-E1 cells maturation is reached following ~14 days in culture [41, 42], being previously found at a more proliferative state. Further, ALP is used as an indicator of cells differentiation acquisition [43]. The present results indicated that MC3T3-E1 cells differentiation start/strongly occurs around the 14th day in culture, when ALP activity increases (Fig. 4). Further, as it can be depicted from the resazurin studies (Fig. 2d), cells proliferated into ~10 days when exposed to cement blocks, and the results on protein content (determined for ALP assays, data not shown) showed an increase in total protein content until 14 days in culture, and further decrease until the last day tested (28th DPC). Results also proved that both ZnCPC and ZnSrCPC cements increase osteoblastic cells differentiation in terms of ALP activity, especially from the 21st DPC culture on. Further, as ZnCPC and ZnSrCPC results are virtually equal, as expected Zn ions appear to be the relevant inducers of ALP activity, which is a Zn-dependent enzyme present in most mammalian tissues [25].

ZnCPC and ZnSrCPC cements proved to induce other physiological relevant property, which may underlie their observed high *in vivo* osteogenic capacities.

These cements were observed to be able to increase osteoblasts intrinsic cell-to-matrix adhesion capacities (Fig. 5). This was first observed visually when collecting cells lysates for ALP determination, where cells grew in biofilms attached more tightly to the plastic support for ZnCPC and ZnSrCPC exposed cells, suggesting higher expression of extracellular matrix and/or adhesion proteins. Confirmation arrived from the cell adhesion assays, with cells previously exposed to the cement powders exhibiting higher adhesive capacities, either intrinsic (non-depending on their secreted extracellular matrix, ECM) or due to ECM secretion (Fig. 5). Of note, during the proliferative period (until two weeks post-confluency), the ZnSrCPC-exposed cells adhesiveness were slightly lower than for the ZnCPC cells. This perfectly correlates to its higher induction of cells division and with the fact that cells in division are more loosely connected to the support than interphase cells. Further, the higher number of cell membranar protuberances observed for ZnCPC cells (Fig. 3) suggests a high number of focal adhesion points. Interestingly, all three cultures exhibited a decrease in their adhesive capacities from the 14^{th} to the 21^{st} DPC in culture, when cells started their differentiation process. At these later periods, decreased intrinsic adhesive properties may correlate with increased dependence on an extracellular matrix. Indeed, this corresponds to the period of higher deposition of extracellular collageneous matrix, as observed in Fig. 6A. Immunoblot and immunocytochemistry methods revealed cements-induced alteration MC3T3-E1 collagen production, secretion and extracellular fibers formation. In synthesis, cements enhance collagen secretion in the pre-differentiation period (3 DPC, Fig. 6B), which correlates well with their subsequent higher collagen fiber formation in the differentiation period (14 and 21 DPC, Fig. 6A.II). Further, ZnSrCPC induces a higher rate of collagen aggregation into fibers already at 3 DPC, as confirmed by both immunoblot and immunocytochemistry analyses (Fig. 6A.II and 7). Indeed, in ZnSrCPC exposed cells, Type-I collagen fibers were observed to be longer and denser suggesting an earlier/enhanced aggregation of tropocollagen into fibrils and fibers. This may be related with the delayed SDS-PAGE migration profiles of procollagen in ZnSrCPC cell lysates, which reflects its higher level of procollagen post-translational modifications (hydroxylation and subsequent glycosylation of

hydroxylysine). Indeed, hydroxyproline and hydroxylysine, derived from proline and lysine hydroxylation, respectively, occur at the RER and are necessary for the formation and stabilization of collagen, playing key roles in collagen stability [44]. Hence, ZnSrCPC appears to induce overhydroxylation of proline and/or lysine amino acids, potentially accelerating collagen cross-linking and fiber formation, and explaining results at 3 DPC.

Type-I collagen is the most abundant type of collagen in bone, being the most abundant protein component in the ECM. Given that ZnSrCPC induces Type-I collagen deposition into the ECM and increases the number of collagen-secreting osteoblasts, and as the first stage for bone formation by osteoblasts is collagen secretion.

Implants were performed in trabecular bone due to its higher metabolic rate per unit of volume, when compared to cortical bone. Further, rates of change in bone density are likely to be greater at sites that are predominantly trabecular [45]. Moreover, it has been observed that trabecular bone density decreases faster than that of compact bone as osteoporosis progresses [46]. Of note, no inflammation or other complications associated with the implanted materials were observed throughout the observational time periods.

Histological and histomorphometrical analyses revealed that, with increased implantation periods, new bone regenerated and gradually penetrated into the implant. The pattern of trabecular bone that was formed in the implantation area was qualitatively similar to the adjacent old trabecular bone in the sections' periphery. New bone grew towards the implant centre, replacing fluorescent-black spaces and suggesting that cement was being first resorbed in the implantation periphery. This is expected, as it is the site of contact between the implant and old bone, mesenchymal cells, and macrophages that ultimately differentiate into osteoclasts. Reduction of protein-containing organic matrix from 1 to 2 months, along with increased new bone formation to relative high levels (Fig. 8 and 9) also reflects that ZnCPC and ZnSrCPC were good osteoconductive biomaterials. Zn and Sr proved to be good inductors of osteoprogenitor cell proliferation and differentiation, as upon 1 month intensive bone remodeling was undergoing in the adjacent bone matrix of the original drill hole. Further, results indicated that Sr is a

more potent inhibitor of osteoclastic activity than Zn, as much fewer osteoclast-like cells could be found in ZnSrCPC implants. Partial substitution of Zn ions by Sr ions in ZnSrCPC revealed to be beneficial, as cement resorption and organized bone formation were faster and higher for this cement. Constantz et al. [15] have observed that cement resorption is due to macrophages and macrophage-derived osteoclastic cells, after the complete transformation of brushite into carbonated apatite. Indeed, for ZnCPC at 1 month of implantation, we could find dispersed areas of cell-mediated resorption and remodeling, such as osteoclast-driven resorption and osteoblast-mediated osteoid formation. These areas were found central to the implant and relatively distant to the zones of new bone deposition, as previously noted by other authors [47]. Similar qualitative results were obtained for Norian (Fig. 8 and 9), also suggesting that cement and primary matrix were still being resorbed at those zones at 1 month of implantation, although at much less extension (Fig. 8). Moreover, there was a higher amount of ‘empty space’ (which includes cement) for Norian than for ZnCPC, reinforcing that Norian cement was by far being resorbed at lower rate than ZnCPC. For ZnSrCPC however, cement resorption was rapid, as at 1 month of implantation few areas of remodeling activity of ‘empty spaces’ and unorganized matrix could be observed. Of note, the larger solubility of brushite compared to apatite is one essential reason for the faster resorption of the brushite matrix. While apatite cements, such as Norian, remain almost unchanged throughout study periods of 6 months, brushite cements are resorbed at a rate between 60% and 90% amid 2-6 months of study periods [47].

In osteogenic terms, for the ZnCPC cement a high percentage of new bone is found at the periphery of the implant but not at the centre after 1 month of implantation. For ZnSrCPC cement, however, new bone was found evenly distributed throughout the implant, which included several trabeculae-like structures already crossing the entire histological sections. Upon 2 months of implantation, high levels of bone regeneration could be noted for ZnCPC and especially for ZnSrCPC, where contiguous trabeculae crossing the histological sections could be found, suggesting the completion of the osteoregenerative process mediated by brushite conversion into apatite.

5. Conclusions

The biocompatibility and *in vivo* performance of brushite-forming Zn- and ZnSr-substituted β-TCP cements injected into trabecular bone cylindrical defects in pigs was successfully demonstrated.

MC3T3-E1 osteoblastic-like cells exposed to the powdered cements proliferated more, showed higher adhesiveness capacities and higher ALP activity, in comparison with control cells. Furthermore, they presented higher Type-I collagen secretion and fiber formation, at pre-differentiation and differentiation periods, respectively. Proliferative and collagen ECM deposition properties were more evident for cells grown in ZnSrCPC than in ZnCPC.

In vivo assays of the ZnCPC and ZnSrCPC osteogenic regenerative properties were carried out, using carbonated apatite cement (Norian SRS) as a control. Results indicate that the investigated ZnCPC and ZnSrCPC cements are biocompatible, osteoconductive, and good candidate materials to use as bone substitutes. Moreover, the presence of Sr has enhanced the rate of cement resorption and new bone formation. The new ZnCPC and ZnSrCPC cements revealed better *in vivo* performance in comparison to the control carbonated apatite cement.

Acknowledgments

Thanks are due to CICECO for the support and to the Portuguese Foundation for Science and Technology for the project REEQ/1023/BIO/2005 and the fellowship grants of S.P. (SFRH/BD/21761/2005) and S.I.V. (SFRH/BPD/19515/2004).

The authors are also very grateful to Prof. Doutor Henrique Bicha Castelo, Director of the Service of Medicine and Experimental Surgery, Hospital of Santa Maria, Lisbon, for the facilities supply in experimental animal studies, according to European regulations and following permission granted by the Ethical Committee.

In addition, the authors are thankful to A. Pinto, Institute of Molecular Medicine, Lisbon, for the preparation of the sections for histological and histomorphometric analysis.

References

[1] Brown WE, Chow LC. A New Calcium-Phosphate Setting Cement. J Dent Res 1983;62:672-672.

[2] Wang XP, Ye JD, Wang H. Effects of additives on the rheological properties and injectability of a calcium phosphate bone substitute material. Journal of Biomedical Materials Research Part B-Applied Biomaterials 2006;78B(2):259-264.

[3] Yuan HP, Li YB, de Bruijn JD, de Groot K, Zhang XD. Tissue responses of calcium phosphate cement: a study in dogs. Biomaterials 2000 Jun;21(12):1283-1290.

[4] Alves HLR, dos Santos LA, Bergmann CP. Injectability evaluation of tricalcium phosphate bone cement. Journal of Materials Science-Materials in Medicine 2008 May;19(5):2241-2246.

[5] Baroud G, Cayer E, Bohner M. Rheological characterization of concentrated aqueous á-tricalcium phosphate suspensions: The effect of liquid-to-powder ratio, milling time, and additives. Acta Biomater 2005;1(3):357-363.

[6] Boesel L, Reis RL. The effect of water uptake on the behaviour of hydrophilic cements in confined environments. Biomaterials 2006;27:5627-5633.

[7] Bohner M, Baroud G. Injectability of calcium phosphate pastes. Biomaterials 2005;26(13):1553-1563.

[8] Burguera EF, Xu HHK, Sun LM. Injectable calcium phosphate cement: Effects of powder-to-liquid ratio and needle size 9. Journal of Biomedical Materials Research Part B-Applied Biomaterials 2008;84B(2):493-502.

[9] Gauthier O, Muller R, von Stechow D, Lamy B, Weiss P, Bouler JM, et al. In vivo bone regeneration with injectable calcium phosphate biomaterial: A three-dimensional micro-computed tomographic, biomechanical and SEM study. Biomaterials 2005;26(27):5444-5453.

[10] Noetzel J, Özer K, Reisshauer BH, Anil A, Rössler R, Neumann K, et al. Tissue responses to an experimental calcium phosphate cement and mineral trioxide aggregate as materials for furcation perforation repair, a histological study in dogs. Clin Oral Invest 2006;10:77-83.

[11] Kamerer DB, Friedman CD, Costantino PD, Snyderman CH, Hirsch BF. Hydroxyapatite cement: A new method for achieving watertight closure in transtemporal surgery. Amer J Otol 1994;15:47-49.

[12] Bohner M. Physical and chemical aspects of calcium phosphates used in spinal surgery Eur Spine J 2001;10 114-121.

[13] Turner TM, Urban RM, Singh K, Hall DJ, Renner SM, Lim TH, et al. Vertebroplasty comparing injectable calcium phosphate cement compared with polymethylmethacrylate in a unique canine vertebral body large defect model. Spine Journal 2008 May-Jun;8(3):482-487.

[14] Bohner M, Theiss F, Apelt D, Hirsiger W, Houriet R, Rizzoli G, et al. Compositional changes of a dicalcium phosphate dihydrate cement after implantation in sheep. Biomaterials 2003 Sep;24(20):3463-3474.

[15] Constantz BR BB, Ison IC, Fulmer MT, Baker J, McKinney LA, Goodman SB, Gunasekaren S, Delaney DC, Ross J, Poser R. Histological, chemical, and crystallographic analysis of four calcium phosphate cements in different rabbit osseous sites. J Biomed Mater Res Part B 1998;43:451-461.

[16] Gisep A, Wieling R, Bohner M, Matter S, Schneider E, B R. Resorption patterns of calcium-phosphate cements in bone. J Biomed Mater Res Part A 2003;66:532-540.

[17] Naji A, Harmand M. Cytocompatibility of two coating materials, amorphous alumina and silicon carbide, using human differentiated cell cultures. Biomaterials 1991;12:690-694.

[18] Malik M, Puleo D, Bizios R, Doremus R. Osteoblasts on hydroxyapatite, alumina and bone surfaces in vitro: morphology during the first 2 hours of attachment. Biomaterials 1992;13:123-128.

[19] Puleo D, Preston K, Shaffer J, Bizios R. Examination of osteoblast-orthopaedic biomaterial interactions using molecular techniques. Biomaterials 1993;14:111-000.

[20] Li X, Sogo Y, Ito A, Mutsuzaki H, Ochiai N, Kobayashi T, et al. The optimum zinc content in set calcium phosphate cement for promoting bone formation in vivo. Mater Sci and Eng 2008.

[21] Otsuka M, Marunaka S, Matsuda Y, Ito A, Layrolle P, Naito H, et al. Calcium level-responsive in vitro zinc release from zinc containing tricalcium phosphate (ZnTCP). J Biomed Mater Res 2000;52:819-824.

[22] Rokita E, Hermes C, Nolting HF, Ryczek J. Substitution of Calcium by Strontium within Selected Calcium Phosphates. Journal of Crystal Growth 1993 Jun;130(3-4):543-552.

[23] Dahl S, Allain P, Marie P, Mauras Y, Boivin G, Ammann P, et al. Incorporation and distribution of strontium in bone. Bone 2001;28:446-453.

[24] Marie P, Ammann P, Boivin G, Rey C. Mechanisms of action and therapeutic potential of strontium in bone. Calcif Tissue Int 2001;69:121-129.

[25] McComb R, Bowers G, Posen S. Alkaline Phosphatase. Plenum, New York, 1979.

[26] Kurdy NM, Bowles S, Marsh DR, Davies A, France M. Serology of collagen types I and III in normal healing of tibial shaft fractures. J Orthop Trauma 1998;12:122-126.

[27] Lenart G, Bidlo G, Pinter J. Some Basic Problems in Examination of Calcium Hydrogen Phosphates of Bone. Clinical Orthop Rel Res 1972(83):263-272.

[28] Wen HB, Cui FZ, Feng QL, Li HD, Zhu XD. Microstructural Investigation of the Early External Callus after Diaphyseal Fractures of Human Long-Bone. Journal of Structural Biology 1995 Mar-Apr;114(2):115-122.

[29] Pina S, Vieira SI, Torres PMC, Goetz-Neunhoeffer F, Neubauer J, da Cruz e Silva OAB, da Cruz e Silva EF, Ferreira JMF. *In vitro* performance assessment of new brushite-forming Zn- and ZnSr-substituted β-TCP bone cements. J Biomed Mater Res, B (submitted) 2009.

[30] Kannan S, Goetz-Neunhoeffer F, Neubauer J, Ferreira JMF. Ionic substitutions in biphasic hydroxyapatite and beta-tricalcium phosphate mixtures: Structural analysis by rietveld refinement. Journal of the American Ceramic Society 2008 Jan;91(1):1-12.

[31] Kannan S, Pina S, Ferreira JMF. Formation of strontium-stabilized á-tricalcium phosphate from calcium-deficient apatite. Journal of the American Ceramic Society 2006;89(10):3277-3280.

[32] Kannan S, Goetz-Neunhoeffer F, Neubauer J, Ferreira JMF. Synthesis and Structure Refinement of Zinc-Doped beta-Tricalcium Phosphate Powders. J Amer Ceram Soc 2009;92:1592-1595.

[33] Ueno A, Miwa Y, Miyoshi K, Horiguchi T, Inoue H, Ruspita I, et al. Constitutive expression of thrombospondin 1 in MC3T3-E1 osteoblastic cells inhibits mineralization. J Cell Phys 2006;209:322-332.

[34] Lareu R. R., Arsianti I. et al. In Vitro Augmentation of Collagen Matrix Formation — Applications in Tissue Engineering. 3rd Kuala Lumpur International Conference on Biomedical Engineering 2006, Vol. 15.

[35] Sweeney S., Orgel J. et al. Candidate cell and matrix interaction domains on the collagen fibril, the predominant protein of vertebrates. J Biol Chem 2008;283:21187-21197.

[36] Fua CY, Dinishb US, Nga BK, Murukeshanb VM, Seahb LK, Lim-Tanc SK. Fluorescence Lifetime Imaging of Haematoxylin and Eosin-stained Cervical Tissue. Biomed Pharm Eng 2006.

[37] Ito A, Ojima K, Naito H, Ichinose N, Tateishi T. Preparation, solubility, and cytocompatibility of zinc-releasing calcium phosphate ceramics. Journal of Biomedical Materials Research 2000 May;50(2):178-183.

[38] Kawamura H, Ito A, Miyakawa S, Layrolle P, Ojima K, Ichinose N, et al. Stimulatory effect of zinc-releasing calcium phosphate implant on bone

formation in rabbit femora. Journal of Biomedical Materials Research 2000 May;50(2):184-190.

[39] Johal KK, Hill RG, Brook IM. In vivo response of strontium and zinc based ionomeric cement implants in bone. J Mater Sci - Mater Med 2002;13:543-552.

[40] Otsuka M, Ohshita Y, Marunaka S, Matsuda Y, Ito A, Ichinose N, et al. Effect of controlled zinc release on bone mineral density from injectable Zn-containing beta-tricalcium phosphate suspension in zinc-deficient diseased rats. J Biomed Mater Res Part A 2004 Jun 1;69A(3):552-560.

[41] Owen TA, Aronow M, Shalhoub V, Barone LM, Wilming L, Tassinari MS, et al. Progressive development of the rat osteoblast phenotype in vitro: reciprocal relationships in expression of genes associated with osteoblast proliferation and differentiation during formation of the bone extracellular matrix. J Cell Phys 1990;143:420-430.

[42] Stein GS, Lian JB, Gerstenfeld LG, Shalhoub V, Aronow M, Owen TA, et al. The onset and progression of osteoblast differentiation is functionally related to cellular proliferation. Connect Tissue Res 1989;20:3-13.

[43] Lecoeur L, Ouhayoun JP. In vitro induction of osteogenic differentiation fkom non-osteogenic mesenchymal cells. Biomaterials 1997;18:989-993.

[44] Nelson D. L. and Cox M. M.. Lehninger's Principles of Biochemistry. W. H. Freeman and Company, New York 2005.

[45] Dempster DW. Bone remodeling. Disorders of bone and mineral metabolism: New York, Raven Press, 1992. p. 355-380.

[46] Seeman E, Young N, Szmukler G, Tsalamandris C, Hopper JL. Risk-Factors for Osteoporosis. Osteoporosis Int 1993;3:S40-S43.

[47] Apelt D, Theiss F, El-Warrak AO, Zlinszky K, Bettschart-Wolfisberger R, Bohner M, et al. In vivo behavior of three different injectable hydraulic calcium phosphate cements. Biomaterials 2004;25:1439-1451.

Annexes

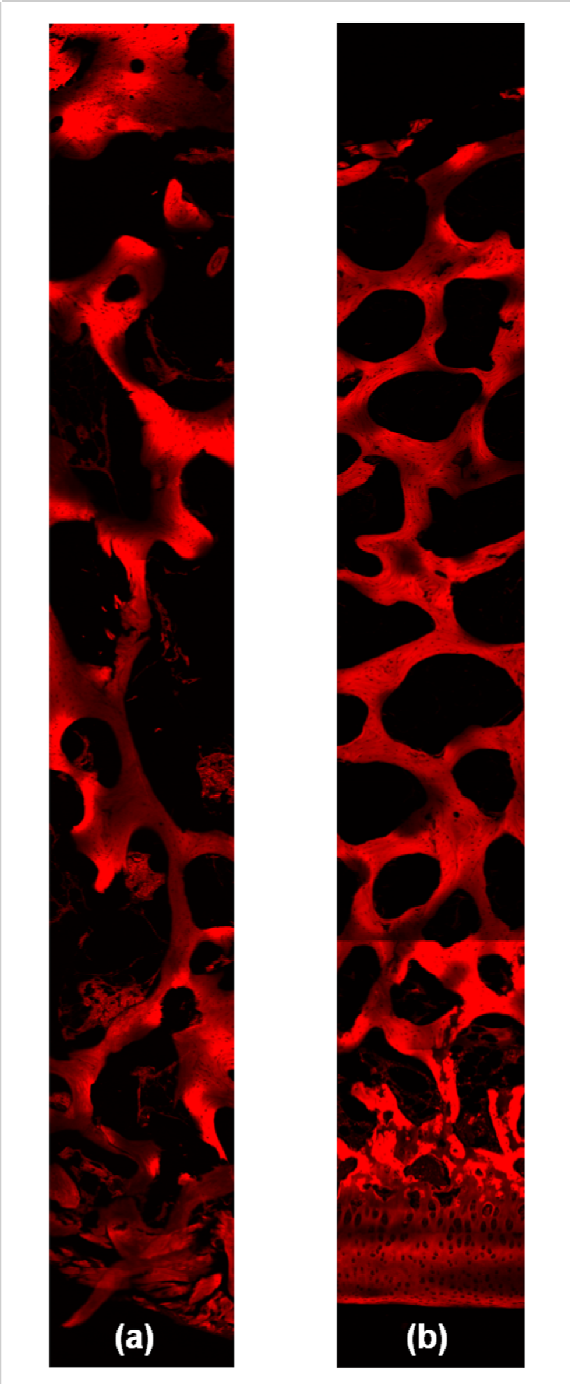

Fig. S1: Several epifluorescent microphotographs were taken of contiguous sections of **(a)** ZnCPC and **(b)** ZnSrCPC cements after 2 months of implantation. (microscope Zeiss LSM 510 META)

4 Conclusions

The present work aimed at developing ionic-substituted calcium phosphate bone cements to better mimic the elemental composition of the mineral part of the bone and evaluating the effects of the ionic substitutions in all the relevant properties. The partial replacement of calcium by magnesium, strontium and zinc was investigated in more detail due to their reported beneficial effects on stimulating bone formation with a direct proliferative effect on osteoblastic cells *in vitro*. The results obtained revealed that Sr-substituted cements exhibited an overall better performance in all relevant properties.

The results obtained prove that aqueous precipitation is a suitable technique to prepare several single phase ionic-substituted (Mg, Sr, Zn) β-TCP by heating doped Ca-deficient apatite compositions at temperatures of about 800ºC. The incorporation of the doping elements into in the β-TCP structure was confirmed by changes in the lattice constant values (*a*-axis, *c*-axis and volume) that can be correlated to the ionic sizes of the doping elements relative to that of the element that has been replaced and to their incorporated amounts.

The degree of lattice disturbance by the substituted ions revealed to have implications in terms of thermal stability of the β-TCP phase and, therefore, in the ease and extent of β-TCP → α-TCP phase transformation at higher temperatures (1450-1550ºC). Moreover, the lattice strains due to incorporation of larger size cations, such as Sr, favoured the milling process and made the starting SrCPC powder more reactive towards the setting liquid in comparison to undoped α-TCP or doped with other cations.

Aqueous solutions of citric acid with added rheological modifiers (PEG or HPMC) were shown to be suitable liquids for preparing cement pastes from the studied materials with good moulding ability, flow behaviour and setting properties. Initial setting time increased with increasing liquid-to-powder ratio (LPR) and in the presence of rheological modifiers due to their specific roles at the solid/liquid interface. Rheological measurements under oscillatory mode revealed a useful tool to assess the structural evolution along the setting process, complementing the information given by other techniques such as Vicat and Gilmore needles. Flow measurements enabled selecting the experimental conditions for workable cement pastes (LPR in the range of 0.30-0.34 mL g^{-1}) and for good injectability even under a relatively low maximum applied force of 100 N. The cement pastes could be fully injected for LPR > 0.36 mL g^{-1} without any filter pressing effects.

Isothermal calorimetry enabled the identification of a two-step hardening process: (i) the dissolution of the starting powders and nuclei formation of intermediate amorphous phases; and (ii) the nucleation and growth of brushite crystals.

Wet compressive strength of the cement specimens (after immersion in PBS solution for 48 h) was in the range of values reported for trabecular bone (10-30 MPa).

Cell cultures revealed that bone cements are non toxic, bioactive and biocompatible and stimulate osteoblastic-like cells proliferation. In addition, they presented higher adhesiveness capacities, ALP activity, Type-I collagen secretion

and fiber formation, in comparison with control cells. The osteogenic regenerative properties studies using a pig model showed that the implanted cements are biocompatible, osteoconductive, and stimulate new bone formation.

All these properties make the newly developed brushite-forming CPCs good candidates for applications in repair of bony and periodontal defects, and as bone substitutes/fillers.

Future perspectives

The results obtained so far form a stable base from which minor modifications should provide improved functional bone substitutes. The main shortcoming of the developed cements is still related to the insufficient mechanical properties, especially for load bearing clinical applications. Therefore, further studies will be required to upgrade the CPCs for applications in vertebroplasty and kyphoplasty.
Complementary studies could also be performed aiming at:

- Evaluating the effects of other ionic species existing as trace elements in bone composition;
- Implementation of various methods of cement mixing, such as vacuum mixing, centrifugation and mechanical mixing in order to improve workability/injectability at lower LPR. Due to time and equipment limitations, only manual mixing at atmospheric pressure was employed in this study;
- Detection of influence of the most relevant experimental variables in cement preparation on cell adhesion and growth-related factors (e.g. collagen, laminin);
- Evaluation of the suitability of CPCs as drug delivery systems for an array of pharmacological agents, cytokines and growth factors, which stimulate reparative bone formation.